

Imprinted Polymers for Affinity based Extractions of a Peptidic Biomarker from Protein Digests

A thesis presented to the Department of Chemistry and
Chemical Biology at the Technical University of Dortmund
for the degree of

Doctor of Philosophy in Chemistry
(Dr. phil.)

By

Abed Abdel Qader

Supervisors:

Prof. Dr. Börje Sellergren

Prof. Dr. Ralf Weberskirch

Dortmund 2014

Imprinted Polymers for Affinity based Extractions of a Peptidic Biomarker from Protein Digests

Dissertation

zur Erlangung des akademischen Grades

Doktor der Naturwissenschaften

(Dr. rer. nat.)

der Fakultät für Chemie und Chemische Biologie der
Technischen Universität Dortmund

vorgelegt von

Dipl.-Chem. Abed Abdel Qader

aus Amman, Jordananin

Dortmund 2014

Die vorliegende Doktorarbeit wurde am Institut für Umweltforschung angefertigt und eingereicht an der Fakultät für Chemie und Chemische Biologie der Technischen Universität Dortmund.

der Fakultät für Chemie und Chemische Biologie

Gutachter der Dissertation:

1. Gutachter: Prof. Dr. Börje Sellergren
2. Gutachter: Prof. Dr. Ralf Weberskirch

Tag des öffentlichen Promotionskolloquiums:

Erklärung

Hiermit erkläre ich, dass ich die vorliegende Dissertation selbständig und nur mit den angegebenen Hilfsmitteln angefertigt habe. Die Arbeit wurde bisher in gleicher oder ähnlicher Form keiner anderen Prüfungskommission vorgelegt und auch nicht veröffentlicht.

Dortmund, den date

Abdel Abdel Qader

Acknowledgment

I take this opportunity to thank all who by the grace of Allah have supported me and helped to complete my work successfully.

First and foremost, I would like to express my deep sense of gratitude to my supervisor Prof. Dr. Börje Sellergren for giving me a footing to pursue a doctoral study on a highly interesting topic in his group. I am grateful to him for readily sharing his experience with no time constraint. I am very thankful to him for his inspiring guidance, creative ideas and constant support during my study.

I thank Prof Dr. Ralf Weberskirch for so kindly agreeing to be the second evaluator for my PhD defense.

I extend the same to Prof. Dr. Dr. h.c. Michael Spiteller for providing support and opportunity to work in the INFU.

I also would like to thanks for the successful collaboration with Prof. Dr. Léon Reubsæet from department of pharmaceutical chemistry, University of Oslo, Norway.

I also gratefully acknowledge all my colleagues (past and present) at AK Sellergren for being always supportive and friendly, for providing a nice and international working environment, in particular: Reza Mohammadi, Javier Urraca, Porkodi Kadhivel, Mahadeo Halhalli, Melanie Berghaus, Patrick Lindemann, Carla Aureliano, Eric Schillinger, Sudhir Shinde, Annabel Tenboll, Emelie Fritz, Robert Sulc, Mohamad Wasim Almozaik, Malak Boutrus, Deepak Chandrasekaran, Ricarda Wagner, Marc Lamshöft and Ulrich Schoppe.

I remember to thank Monika Meuris at the BCI, TU Dortmund for the SEM measurements, and our IT expert Jürgen Jünemann for the help extended in computer simulations.

I am very thankful to Melanie, for reading parts of my dissertation and providing me with helpful comments and for being always nice colleagues and million thanks for helping me to contact the German embassy in Amman to solve my wife's visa problem. I also like to thank Patrick for resolving bureaucratic issues and Annabel for the summary translation in German language.

My special thanks to Porkodi Kadhivel for helping me with her literature survey expertise and accompanying in socializing activities.

I owe my sincere gratitude to my colleague Reza Mohammadi for his unconditional support and for helping me to solve some of my personal and work problems also for providing me literature that was a great help during my thesis. Thank you Reza for your willing to do

anything to be helpful to others, for being modest, caring, and knowledgeable- May Allah bless you and your family.

I would like to thank my friend Zhualaden Balarbi for giving me a brotherly support from Nigeria.

A sincere thanks to my friend Hussein Kalo who kept me informed through calls and emails when I came to Dortmund and helping me to get some papers, thank you so much my brother.

My heartfelt thanks to my friend Nabil Taki for the weekend get together providing delicious Moroccan food. May Allah bless you and your family!

I also owe a huge debt of gratitude to my friend Said Sghouri, someone who was always there for me whenever I needed any help, thank you so much for being with me during my sickness, for your support and your encouragement, may Allah help you.

Also I would like to thank Frau Altermann-Köster from Referat Internationales, TU Dortmund, for her help and solving some bureaucratic problems and for their financial assistance (STIBET III-Matching Funds-Stipendien des DAAD). I am grateful for their support during this process.

I would like to thank Dr. Markus Schürmann from TU Dortmund for understanding my situation and solving my problem during writing my thesis.

It is time to thank my parents; I humbly extend my most heartfelt appreciation to my parents who taught me to achieve my goal with patience and untiring effort. I remember my father Yousef, to whom I dedicate this work. I miss your call every Sundays, your support, and your encouragement. How I wish he was alive to see this moment. This work would have never been a success had it not been the constant prayers of my dear mother Moyasser. Thank you for lending a supporting hand throughout my career.

I thank my sisters (Hayfa, Manar, Sana, Hadil) and my brothers (Mossa, Issa, Mohammed, Ahmad, Nabil, Wasam) for their words of encouragement and love.

In due respect I thank my wife Banan, for her love and support during the writing of this thesis, for continuous encouragement and being so patient, for your hard work preparing the documents and studying German language to get a visa to be with me. Ich liebe dich! And our coming daughter Tuqa who is going to be born in February, thank you Baba for your patience and thoughtful behavior while writing my thesis, I am yearning to see you in my defense!

I am indebted to you all. Thank you!

Table of Contents

Abbreviations list.....	11
List of Tables.....	13
List of Figures.....	15
Summary.....	20
Zusammenfassung.....	21
Chapter 1: Introduction-State of the art	25
1.1 Lung cancer.....	25
1.2 Biomarker for lung cancer	28
1.3 Proteomic techniques	31
1.3.1 Two-dimensional gel electrophoresis.....	32
1.3.2 Mass spectrometry.....	32
1.4 Literature survey of ProGRP determination with mass spectrometry.....	33
1.5 Molecular recognition	36
1.6 Molecularly imprinted polymers.....	37
1.7 Molecularly imprinted receptors for peptides.....	41
1.7.1 Hierarchical imprinting.....	44
1.7.2 Epitope imprinting method	45
1.7.3 One monomer molecularly imprinted polymers method (OMNiMIPs)	47
1.8 Optimization and rational design of MIP	51
1.8.1 Computational approach	51
1.8.2 Combinatorial imprinting	51
Bibliography.....	54
Chapter 2: Characterization techniques.....	59
2.1 Morphology, physical and chemical polymer characterization	59
2.1.1 Elemental analysis	59
2.1.2 Fourier-Transform infrared spectrometer	60
2.1.3 Thermoporometry.....	60
2.1.3.1 Pore diameter.....	60
2.1.3.2 Pore volume measurement	60
2.1.3.3 Surface area	61
2.1.4 Scanning electron microscopy (SEM).....	61
2.1.5 Thermogravimetric analysis.....	61
2.1.6 Nitrogen adsorption	62

2.2 Chromatographic conditions for the analysis	62
2.2.1 HPLC-UV	62
2.2.2 LC-MS/MS analysis	62
2.3 Binding experiments.....	63
2.3.1 Single point rebinding	63
2.3.2 Determination of the binding capacity	64
Bibliography.....	66
Chapter 3:Mini-molecularly imprinted polymers libraries for targeting NLLGLIEAK	67
3.1 Abstract.....	67
3.2 Introduction.....	68
3.3 Methodology of polymer design	68
3.4 Template, monomer, and crosslinker	70
3.5 High Throughput Screening.....	76
3.6 Design and synthesis	78
3.6.1 Library 1	78
3.6.2 Library 2	79
3.6.3 Library 3	80
3.7 Results and Discussion	82
3.7.1 Library 1	82
3.7.1.1 Rebinding results	82
3.7.2 Library 2	86
3.7.2.1 Rebinding in dependence of the pH.....	86
3.7.2.2 Molecularly imprinted solid phase extraction (MISPE)	91
3.7.2.3 Thermoporometry	91
3.7.2.4 Microscopy SEM.....	93
3.7.3 Library 3	94
3.7.3.1 Rebinding results	94
3.7.3.2 Molecularly imprinted solid phase extraction (MISPE)	95
3.7.3.3 Selectivity test	95
3.7.4 Polymers morphology: TFMAA as a model.....	98
3.8 Experimental.....	102
3.8.1 Chemical and reagents.....	102
3.8.2 Apparatus	103
3.8.3 Synthesis	103

3.8.3.1 Library 1.....	103
3.8.3.2 Library 2.....	104
3.8.3.3 Library 3.....	105
3.8.4 Template extraction.....	106
3.8.5 Single point rebinding.....	107
3.8.6 Molecularly imprinted solid phase extraction (MISPE).....	107
3.8.7 Selectivity test.....	108
Bibliography.....	109
Chapter 4: Scaling up MIP for selective extraction of NLLGLIEAK from digestion of ProGRP in biological samples.....	111
4.1 Abstract.....	111
4.2 Introduction.....	112
4.3 Results and Discussion.....	119
4.3.1 Polymer synthesis.....	119
4.3.2 Morphology, physical and chemical polymer characterization.....	120
4.3.2.1 Elemental analysis.....	120
4.3.2.2 Infrared spectroscopy.....	120
4.3.2.3 Microscopy SEM.....	121
4.3.2.4 Thermoporometry.....	122
4.3.2.5 Thermogravimetric analysis.....	123
4.3.2.6 Determination of binding site distributions and affinities.....	124
4.3.3 Optimization of MISPE procedure.....	125
4.3.4 Analysis spiked serum sample.....	131
4.4 Experimental.....	133
4.4.1 Chemicals.....	133
4.4.2 Polymer preparation.....	133
4.4.3 Adsorption isotherms.....	134
4.4.4 MISPE method development and optimization.....	134
4.4.5 Digestion of ProGRP.....	136
Bibliography.....	137
Chapter 5: Grafted Peptide imprinted films, design and development.....	139
5.1 Abstract.....	139
5.2 Introduction.....	139
5.3 Scope of the work and chemicals used.....	140

5.3.1	Templates and monomers	140
5.3.2	RAFT mechanism.....	141
5.4	Silica support and modification	143
5.4.1	Immobilization of RAFT agent	143
5.4.2	Polymer synthesis	144
5.5	Results and Discussion	146
5.5.1	Characterisation.....	146
5.5.1.1	Elemental analysis	146
5.5.1.2	Thermogravimetric analysis TGA	146
5.5.1.3	Microscopy SEM.....	148
5.5.2	Molecularly imprinted solid phase extraction (MISPE).....	149
5.5.3	Determination of the binding capacity of the polymers	150
5.5.4	MISPE and NISPE of a digested ProGRP sample	152
5.6	Experimental.....	154
5.6.1	Chemicals.....	154
5.6.2	Silica surface activation	155
5.6.3	Amino modified silica surface	155
5.6.4	Immobilization of RAFT agent	156
5.6.5	Preparation procedure.....	157
5.6.6	Adsorption isotherms.....	158
5.6.7	Optimization of MISPE Procedure.....	158
5.6.8	MISPE protocol for NLLGLIEA[K- ¹³ C ₆ ¹⁵ N ₂]	158
	Bibliography.....	159
	Chapter 6: Conclusions	161
	Bibliography.....	165
	Curriculum Vitae	166

Abbreviations list

A β	Beta amyloid peptide
ABDV	Azo-bis-dimethylvaleronitrile
ACN	Acetonitrile
APTS	3- Aminopropyltriethoxysilane
S _A	Surface area
BET	Brunauer-Emmett-Teller
BJH	Barrett - Joyner - Halenda
CL	Crosslinker
2-D GE	Two-dimensional gel electrophoresis
DEAEMA	Diethylaminoethyl methacrylate
DTG	Differential thermogravimetry
DMF	Dimethylformamide
DMSO	Dimethylsulphoxide
D _P	Pore diameter
D _s	Surface density
DSC	Differential scanning calorimeter
2D SDS- PAGE	Two-dimensional sodium dodecyl sulfate-polyacrylamide gel electrophoresis
DVB	Divinylbenzene
EA	Elemental analysis
EAMA	N-(2-aminoethyl) methacrylamide hydrochloride
EDMA	Ethylene glycol dimethacrylate
ELISA	Enzyme linked immunosorbent assay
FT-IR	Fourier transform infrared spectroscopy
FM	Functional monomer
GRP	Gastrin-releasing peptide
HEMA	2-Hydroxyethyl methacrylate
HEPES	N-2-hydroxyethylpiperazine-N'-2-ethanesulfonic acid
HPLC	High performance liquid chromatography
HTS	High throughput screening
IF	Imprinting factor
LC-MS	Liquid chromatography-mass spectroscopy
LOD	Limits of detection
LOQ	Limits of quantification
MAA	Methacrylic acid
MeOH	Methanol
mini-MIPs	mini-Molecularly imprinted polymers
MIP	Molecularly imprinted polymer
MISPE	Molecularly imprinted solid phase extraction
NIP	Non-imprinted polymer
NOBE	N, O-bismethacryloyl ethanolamine
NSCLC	Non-small cell lung cancer
OMNiMIPs	One monomer molecularly imprinted polymers
PETRA	Pentaerythritol triacrylate
pI	Isoelectric point
PMP	Pentamethyl piperidine
ProGRP	Pro-gastrin-releasing peptide
Q	Absorption capacity
RAFT	Reversible addition fragmentation chain transfer polymerization

RP-HPLC	Reversed phase HPLC
RSD	Relative standard deviation
RT	Room temperature
SCLC	Small cell lung cancer
SEM	Scanning electron microscopy
SPE	Solid phase extraction
T	Template
TFA	Trifluoroacetic acid
TFMAA	Trifluoromethacrylic acid
TFU	N-3, 5-bis (trifluoromethyl)-phenyl-N'-4-vinylphenylurea
TGA	Thermogravimetric analysis
THF	Tetrahydrofuran
UV	Ultraviolet
V _p	Pore volume
4-Vpy	4-Vinylpyridine

Table 1.1: Amino Acid (AA) sequences of ProGRP isoforms	29
Table 1.2: Example of MIPs synthesized for recognition of peptides in aqueous media	43
Table 3.1: The templates used in the libraries of imprinted polymers for the peptide NLLGLIEAK	71
Table 3.2: Templates solubility tests.	72
Table 3.3: Design of the library 1	79
Table 3.4: Design of the library 2	80
Table 3.5: Design of the library 3	81
Table 3.6: Binding percentage for library 1 in HEPES buffer (0.1 M, pH 7.5) with NLLGLIEAK.	83
Table 3.7: Capacity scale based on uptake data in Table 3.6.....	83
Table 3.8: Rebinding test for library 2. A: Binding percentage at pH 7, B: Capacity scale at pH 7 (HEPES buffer (0.1 M), C: Binding percentage at pH 10, D: Capacity scale at pH 10 (NH ₄ Cl, NH ₄ OH buffer) with NLLGLIEAK.....	88
Table 3.9: Physical properties of imprinted and non-imprinted polymers. The DSC average pore diameter (D _p), specific pore volume (V _p), and specific surface area (S _A), were determined.....	93
Table 3.10: Peptide property functions.....	96
Table 3.11: Selected TFMAA polymer form library 1 and library 2 for morphology study...98	
Table 3.12: Stock solution preparation for template, functional monomers, initiator, and crosslinkers for library 1.	104
Table 3.13: Stock solution for template, functional monomer, initiator, and crosslinker for library 2.....	105
Table 3.14: Stock solution for template, functional monomer, initiator, and crosslinker for and volumes used for the preparation of the polymers library 3 in each well (μL).	106
Table 4.1: Selected application example of MISPE technique	114
Table 4.2: Elemental analysis of MIP, NIP and theoretical values	120
Table 4.3: Properties of MIP and NIP measured by Thermoporometry.....	123
Table 4.4: Freundlich fitting parameters, obtained with the experimental binding data of target peptide towards the imprinted (MIP) and non-imprinted polymer (NIP).....	125
Table 4.5: Optimised MISPE protocol for extraction of NLLGLIEAK from aqueous samples.	130
Table 4.6: Analytical parameters of MISPE cartridge.....	130
Table 5.1: Physical characterization of composites materials	144

Table 5.2: Composition of the polymers synthesized.....	145
Table 5.3: Elemental composition of the prepared polymers	146
Table 5.4: Mass loss and calculated film thickness.....	147
Table 5.5: Freundlich fitting parameters, obtained with the experimental binding data of NLLGLIEAK towards the P _{T2} and P _{NIP} . Each data represents the average of two replicate measurements with a coefficient of variation in the range of 0-0.3%.....	151

Figure 1.1: The most common causes of death from cancer worldwide, 2008, estimate. (World Health Organization)	26
Figure 1.2: Incidence and mortality rates in Germany, 1999 – 2010.....	26
Figure 1.3: Five-year Relative Survival Rates (%) for selected cancers in Germany between 1995 and 1999	27
Figure 1.4: Proteomics Workflow.....	31
Figure 1.5: Molecular recognition. Examples include antibody-antigen interactions, receptors binding to hormones, virus, bacteria, lectin, and enzymes binding to inhibitors	36
Figure 1.6: Schematic representation of the molecular imprinting process	38
Figure 1.7: Left the pop singer Michael Jackson who passed away after a high deadly dose of propofol. Right the chemical structure of propofol.	39
Figure 1.8: a) the chemical reaction of quinonechloroimide with propafol, and b) the working principle of molecular imprinting: b-1) the target molecule is absorbed by the MIP film, while non-target molecules cannot be adsorbed, b-2) corresponds to the washed sample, only remains target molecules adsorbed by the MIP film, b-3) target molecules adsorbed by the MIP film are released and color reagent is injected, occurring color reaction with the reagent.	40
Figure 1.9: Top: Concept of Hierarchical Imprinting (adapted from [102]). Below scanning electron microscopic images of a silica microsphere (left) and its inverse-replicated (right) ..	45
Figure 1.10: Schematic representation of the epitope approach	46
Figure 1.11: (a) Recovery of the C-terminal epitopes of A β 33-40 and A β 33-42 in the elution fractions after SPE of peptide-spiked blood serum samples (2.5 μ g/mL) on the two complementary MIPs and the NIP. The analysis was performed in triplicate with the RSD indicated. (b) Stained gel from urea-SDS-PAGE/ immunoblot analysis of elution fractions from SPE of a blood serum sample spiked with A β 1-40 (5 ng/mL) and A β 1-42 (1 ng/mL). (c) Recoveries estimated from spot intensities of the gel in (b) and the associated RSDs.	47
Figure 1.12: Uptake of Boc-Leu-enkephalin (circle) and Pyr-Leu-enkephalin (square) by the imprinted polymer and the non-imprinted polymer. The initial concentration of the peptide derivatives was 15 mM.	48
Figure 1.13: Structures of molecules discussed in the main text.	50
Figure 1.14: Structures of molecules discussed in the main text.	53
Figure 3.1: Chemical structures of the target peptide (NLLGLIEAK).	70
Figure 3.2: Chemical structures of the functional monomers used in the libraries of imprinted polymers for the NLLGLIEAK.....	73

Figure 3.3: Chemical structures of the crosslinking agents used in the libraries of imprinted polymers for the NLLGLIEAK.....	75
Figure 3.4: Schematic representation of the mini-MIPs library synthesis and evaluation	76
Figure 3.5: Left Top: Photograph showing the 96-well plate before washing. Right Top: Photograph showing filter plate after washing. Bottom: Photograph illustrating grinding the polymer and transferred to filter plate.	77
Figure 3.6: Binding capacity (A) and imprinting factors (B) for library 1	85
Figure 3.7: Binding capacity (A) and imprinting factors (B) for library 2 at pH 7	89
Figure 3.8: Binding capacity (A) and imprinting factors (B) for library 2 at pH 10.....	90
Figure 3.9: Recovery of NLLGLIEAK after loading 1 mL of an aqueous sample of the peptide (24 mg/L) in HEPES buffer (0.1 M, pH 7.5) onto T1 imprinted polymers (20 mg) selected from L2. The loading equilibration time was one hour. The elution was performed by percolating 0.5 mL of MeOH/TFA (98:2).	91
Figure 3.10: DSC curves for the melting of acetonitrile in the DEAEMA-DVB, EAMA-DVB, and TFMAA-HEMA-DVB polymers. The polymers were frozen by rapidly quenching to -60 °C and the heating curves shows pore melt and excess melt.	93
Figure 3.11: Scanning electron micrographs of imprinted and non-imprinted polymers. 2000 X magnification.	93
Figure 3.12: Binding capacity of library 3. HEPES buffer (0.1 M, pH 7.5) with NLLGLIEAK.	94
Figure 3.13: Recovery of NLLGLIEAK in the fractions collected after loading 1 mL of an aqueous sample of the peptide (25 mg/L) in HEPES buffer (0.1 M, pH 7.5) on Library 3 through P9-P12 polymers followed by percolation of 0.5 mL of ACN/H ₂ O wash solutions as indicated and elution in 0.5 mL of MeOH/TFA (98:2). The loading equilibration time was one hour.....	96
Figure 3.14: Peptide recoveries in the fractions collected after loading 1 mL of an aqueous sample of the indicated peptides (25 mg/L in HEPES buffer (0.1 M, pH 7.5) on P11 (A) and P12 (B) followed by percolation of 0.5 mL of wash solutions as indicated and elution in 0.5 mL of MeOH/TFA (98:2).The loading equilibration time was one hour.....	97
Figure 3.15: Scanning electron microscopy of TFMAA polymers, more detailed see (Table 3.11).....	100
Figure 4.1: Pentamidine.....	112
Figure 4.2: Original papers on MISPE application published since 2004. The numbers of paper were obtained from Scopus database during 2004-2013, searched by using	

“Molecularly Imprinting Polymer AND Solid Phase Extraction” as keywords (A) and then 2012 manually selected according to the MISPE application to the real samples (B).....	113
Figure 4.3: Chemical structures of analytes and template used in the MISPE protocols reported in Table 4.1.....	116
Figure 4.4: Photograph of large scaling of polymer synthesis. Before polymerization (A), after polymerization (B), and synthetic procedure for MIP preparation and hypothetical structure of the imprinted binding site (C).....	119
Figure 4.5: FT-IR spectra of (A) MIP and (B) NIP	121
Figure 4.6: Scanning electron microscopy (SEM) picture of MIP and NIP (particle size: 25-36 μm) at different magnifications.	121
Figure 4.7: DSC curves for the melting of acetonitrile in (A) MIP and (B) NIP. The sample was frozen by rapidly quenching to $-60\text{ }^{\circ}\text{C}$. The heating curves shows pore melt and excess melt.	122
Figure 4.8: TGA and DTG curves of MIP (a, b), NIP (c, d).	123
Figure 4.9: Equilibrium binding isotherms for the uptake of NLLGLIEAK by MIPs (blue line) and NIP (red line) in HEPES (0.1M, pH 7)/ACN(95:5). Free = concentration of the free solute, Bound = specific amount of bound solute.	125
Figure 4.10: Recoveries obtained on the MIP after percolation of 1 mL of 25 mg/L NLLGLIEAK (HEPES, 0.1 M, pH 7.5), using 0.5 mL of different elution solvent.	127
Figure 4.11: Recovery of NLLGLIEAK in the fractions collected after loading 1 mL of an aqueous sample of the peptide (25 mg/L) in HEPES buffer (0.1M, pH 7.5) on MIP and NIP followed by percolation of 0.5 mL of ACN/H ₂ O wash solutions as indicated and elution in 0.5 mL 0.5 mL of MeOH/TFA (98:2). The loading equilibration time was one hour.Columns represent three replicated and the error bars show the standard deviation	128
Figure 4.12: Recovery of NLLGLIEAK in each fraction using MIP and NIP, after percolation of 1 mL of 25 mg/L NLLGLIEAK (HEPES, 0.1 M, pH 7.5), washing with 0.5 mL of H ₂ O/ACN (95:5) and elution with 0.5 mL of MeOH/TFA (98:2). Columns represent three replicated and the error bars show the standard deviation.....	129
Figure 4.13: Chromatograms of loading, washing, and eluting fractions of spiked sample from MIP (a,c,e, respectively) and NIP (b,d,f, respectively) SPE cartridges. after percolation of 1 mL of 25 mg/L NLLGLIEAK (HEPES, 0.1 M, pH 7.5), washing with 0.5 mL of H ₂ O/ACN (95:5) and elution with 0.5 mL of MeOH/TFA (98:2).	129

Figure 4.14: MS-extracted chromatogram of NLLGLIEAK (transition m/z 485.8→630.3, 743.4) and LSAPGSQR (transition m/z 408.2→282.6, 544.4) in an aquatic ProGRP digest sample.	132
Figure 4.15: Recovery of NLLGLIEAK and LSAPGSQR in the fractions collected after loading 1 mL of 211 $\mu\text{g/L}$ digested ProGRP (ABC buffer (0.05M, pH 7.0) on MIP and NIP followed by percolation of 0.5 mL of $\text{H}_2\text{O}/\text{ACN}$ (95:5) and elution in 0.5 mL MeOH/TFA (98:2). The loading equilibration time was one hour	132
Figure 4.16: Flow chart for analysis ProGRP sample.	132
Figure 4.17: Examples of SPE cartridges (A), Peristaltic pump (B).....	135
Figure 5.1: Generic structures of RAFT chain transfer agent.....	141
Figure 5.2: Reaction scheme of RAFT polymerization.....	142
Figure 5.3: Reaction mechanism for the synthesis of functionalized RAFT.....	144
Figure 5.4: Procedure for preparation of MIP via RAFT modified silica for binding the T1 or T2, and hypothetical structure of the imprinted binding site.	145
Figure 5.5: TGA curves of Si-RAFT (a), P_{T1} (b), P_{T2} (c), P_{NIP} (d).....	147
Figure 5.6: Scanning electron microscopy (SEM) picture of P_{T1} , P_{T2} and P_{NIP} at different magnifications.	148
Figure 5.7: Recoveries obtained on the P_{T1} , P_{T2} and P_{NIP} after percolation of 1 mL of 10 mg/L NLLGLIEAK (HEPES, 0.1 M, pH 7.5), using 0.5 mL of different washing solvent and elution with 0.5 mL of MeOH/TFA (98:2).	149
Figure 5.8: Freundlich fitting isotherm for P_{T2} and P_{NIP} . Each data represents the average of two replicate measurements with a coefficient of variation in the range of 0-0.3%.....	151
Figure 5.9: Recovery of NLLGLIEA[$\text{K}_-^{13}\text{C}_6^{15}\text{N}_2$] in each fraction using P_{T2} and P_{NIP} , after percolation of 0.5 mL of 1 nM of NLLGLIEA[$\text{K}_-^{13}\text{C}_6^{15}\text{N}_2$] (ABC buffer, 0.04M, pH 7.0), washing with 3x 0.5 mL of $\text{H}_2\text{O}/\text{ACN}$ (7.5:92.5) and elution with 0.5 mL of $\text{ACN}/\text{H}_2\text{O}/\text{FA}$ (80:17:3). Columns represent two duplicated and the error bars show the standard deviation.	152
Figure 5.10: Recovery of digested of ProGRP in each fraction using P_{T2} and P_{NIP} , after percolation of 1.0 mL of 1 digestion buffer (ABC buffer, 0.04M, pH 7.0), washing with 3x 0.5 mL of $\text{H}_2\text{O}/\text{ACN}$ (7.5:92.5) and elution with 0.5 mL of $\text{ACN}/\text{H}_2\text{O}/\text{FA}$ (80:17:3). Columns represent two duplicated and the error bars show the standard deviation.	153
Figure 5.11: Rehydroxylation of siloxane groups.....	155
Figure 5.12: Functionalisation of silica surface with APTS.....	156
Figure 5.13: Immobilization of RAFT agent on silica surface.	157

Figure 5.14: Photograph of RAFT polymer synthesis. Before polymerization (A), after polymerization (B), and after washing and drying (C).....157

The following three-letter code and one-letter code abbreviations were used for amino acids:

Ala	A	Alanine	Met	M	Methionine
Cys	C	Cysteine	Asn	N	Asparagine
Asp	D	Aspartic acid	Pro	P	Proline
Glu	E	Glutamic acid	Gln	Q	Glutamine
Phe	F	Phenylalanine	Arg	R	Arginine
Gly	G	Glycine	Ser	S	Serine
His	H	Histidine	Thr	T	Threonine
Ile	I	Isoleucine	Val	V	Valine
Lys	K	Lysine	Trp	W	Tryptophan
Leu	L	Leucine	Tyr	Y	Tyrosine

Summary

Affinity based diagnostics depend on biologically derived affinity reagents (e.g. antibodies or antibody fragments, receptors or aptamers) due to their ability to effectively recognize and bind specific biomarkers in competitive media for assay, sensor or LC-MS based readout of the biomarker concentrations. In spite of these benefits these binders can be either hard to get due to high costs or poor availability, or they may not be compatible with denaturing conditions required during the sample pretreatment. Such problems are partly hampering the development of diagnostic methods of neurodegenerative disorders and cancer.

The aim is to prepare molecularly imprinted polymers (MIPs) capable of recognizing peptidic biomarkers in nonphysiological media e.g. acetonitrile-buffer mixtures or in denaturing media. The peptide MIPs will be used as capture phase for solid phase extraction of biological samples.

Derivatives of a diagnostic nonapeptide biomarker NLLGLIEAK resulting from tryptic digestion of the well established protein biomarker for small cell lung cancer ProGRP, were used as templates. With the objective of finding a polymer that, as stationary phase, would retain and rebind the NLLGLIEAK from the matrix components and quantitatively elute it in a small volume, a combinatorial MIP library has been synthesized. The combinatorial MIP libraries for NLLGLIEAK have been prepared by using high-throughput synthesis of MIPs at a reduced scale (mini-MIPs), to rapidly generate 96 imprinted and their corresponding non-imprinted polymers by bulk polymerization. A careful optimization of the synthesis molecularly imprinted polymers has been achieved. The parameters which have been screened and modified are templates functional monomers, crosslinkers, percentage of crosslinking, and porogen.

To test these polymers, a rebinding step was performed, by comparing the amount of target peptide which was bound in imprinted polymer and a blank nonimprinted polymer, the polymer which gave high imprinting factor was scaled up for separation application.

The MIPs developed in this work were proven potent receptors for their target biomarkers. The MIPs targeting the ProGRP signaling peptides were capable of selectively capturing the peptide from tryptic digests promising to significantly reduce the detection limit in the LC-MS-based assay.

Various parameters affecting the extraction efficiency of the polymer have been evaluated to achieve the selective preconcentration of the NLLGLIEAK from aqueous samples and to reduce nonspecific interactions. The imprinted polymer was evaluated for use as a SPE sorbent, in tests with aqueous standards; by comparing recovery data obtained using the

imprinted form of the polymer and a non-imprinted form (NIP). Extraction from the aqueous solutions resulted in more than 80 % recovery. A range of linearity for NLLGLIEAK between 1.5 and 50 mg/mL was obtained by loading 1 mL aqueous sample spiked with NLLGLIEAK at different concentrations in HEPES buffer of pH 7.0. The intra-day coefficient of variation (CV) and inter-day CV was below 7%.

In the end the bulk format was transferred to grafting of MIP films which showed excellent affinity and selectivity to NLLGLIEAK and was therefore suitable for the application in SPE. A working protocol for the development of MIPs targeting biomarker peptides compatible with denaturing conditions and organic solvents i.e. common protein analysis conditions, have been developed. This promises to significantly expand the scope of the technology in proteomics and diagnostics.

Zusammenfassung

Affinitätsbasierte Diagnostik ist abhängig von biologischen Reagenzien (z. B. Antikörpern, Antikörperfragmenten, Rezeptoren oder Aptameren). Diese affinitätsbasierten biologischen Reagenzien sind extrem effektiv, da sie Biomarker aus komplexen Medien, z.B. aus Assays oder LC-MS Analysen, erkennen und binden können. Neben den genannten Vorteilen haben diese Reagenzien die Nachteile, erstens schwer verfügbar und zweitens sehr teuer zu sein. Ein weiteres Problem stellt die mögliche Denaturierung der Reagenzien während der Probenvorbereitung dar. Solche Probleme behindern die Entwicklung von diagnostischen Methoden zur Erforschung von neurodegenerativen Erkrankungen und Krebs. Ziel ist es, molekular geprägte Polymere (MIPs) zu entwickeln, die in der Lage sind, Peptid-Biomarker aus nicht-physiologischen Medien (z.B. Acetonitril-Puffergemische oder denaturierende Medien) zu selektieren. Die Peptid-MIPs werden als Aufnehmerphase für die Festphasenextraktion (SPE) von biologischen Proben verwendet.

Derivate eines diagnostischen Nonapeptid-Biomarkers, mit der Biomarkersequenz NLLGLIEAK, welche aus dem Verdau eines Proteins des kleinzelligen Lungenkrebs ProGRP resultiert, wurde als Templat verwendet. Das Ziel war es ein Polymer zu finden, welches als stationäre Phase dienen kann und somit den Biomarker NLLGLIEAK aus den Matrixkomponenten bindet und aufkonzentriert. Dazu wurde eine kombinatorische Polymerbibliothek synthetisiert. Diese kombinatorische Bibliothek für das MIP NLLGLIEAK wurde mittels high-throughput-synthesis von MIPs auf verkleinertem Maßstab (mini- MIPs) generiert. Mittels dieser Methode können insgesamt 96 Polymere hergestellt werden. Diese bestehen aus MIPs (molekular geprägte Polymere) und NIPs (nicht geprägte Polymere). Eine sorgfältige Optimierung der Synthese molekular geprägter Polymere wurde gestartet. Die optimierten Parameter sind unter anderem die Auswahl der templat-funktionalisierten Monomere, Vernetzer, Prozentsatz der Vernetzung und Porogen.

Um diese Polymere zu testen, wurde als erstes ein Bindungstest mit einer definierten Peptidmenge durchgeführt. Das MIP und das NIP wurden verglichen und das Polymer mit dem größtem „imprinting Faktor“ zum „scale-up“ mittels „bulk“- Polymerization verwendet. Die in dieser Arbeit entwickelten MIPs bewährten sich als Rezeptoren für die Zielbiomarker. Die MIPs konnten das ProGRP Signalpeptid selektiv aus dem Verdauen des Proteins herausfiltern, was zur Folge hat, dass die Nachweisgrenze in einem LC-MS- basierten Assay reduziert werden konnte.

Verschiedene Parameter die die Effektivität der Extraktion des Polymers steigern sollten wurden ausgewertet, um die selektive Anreicherung des NLLGLIEAK aus wässrigen Proben zu testen und unspezifische Wechselwirkungen zu reduzieren. Das MIP und das NIP wurden für den Gebrauch als SPE-Sorptionsmittel evaluiert. Es konnten mehr als 80% des Peptids aus einer wässrigen Lösung zurückgewonnen werden. Es konnte ein Linearitätsbereich für NLLGLIEAK zwischen 1,5 und 50 mg/mL durch die Beladung mit 1 mL wässrige Probe erhalten werden (in HEPES-Puffer; pH 7,0). Der Intraday-Variationskoeffizient (CV) und der Interday CV lagen unter 7% .

Am Ende wurde das „bulk“-Format der MIPs auf ein „grafting“-Format zur Herstellung von dünnen MIP-Filmen übertragen. Diese Filme zeigten eine hervorragende Affinität und Selektivität gegenüber NLLGLIEAK und waren daher geeignet für die Anwendung in SPE. Eine Arbeitsanweisung zur Entwicklung von MIPs für Biomarkerpeptide ist entstanden. Diese erläutert wie MIPs, welche das Arbeiten unter denaturierenden Bedingungen und in organischen Lösungsmitteln erlauben, hergestellt werden können. Dies verspricht einen Ausbau der Anwendungsbereiche in der Technologie, in der Proteomik und in der Diagnostik.

Chapter 1

Introduction-State of the art

1.1 Lung cancer

Lung cancer is one of the most common cancers we have and a large number of people die of this disease every year. More than 1 in 10 of all cancers diagnosed in men is lung cancers. An estimated 1.6 million new cases occurred in 2008, accounting for about 13% of total cancer diagnoses (Figure 1.1) [1] [2]. Incidence trends over the past ten years in Germany are shown in Figure 1.2. Between 1999 and 2010 the incidence of German male decreased by (23%) from 75.1 to 57.9 per 100.000 inhabitants. However, the trends of incidence rate among German women run contrary to those among men which started the period at 18.7 and finished at 24.2 per 100.000 inhabitants [3]. The same trends can be observed in other European industrialized countries. The differences in incidence trends between men and women are attributed to changes in smoking habits and it is expected that the gender difference will narrow further and will have disappeared by 2020 [4]. The change in incidence of lung cancer reflects the changing smoking habits in men and women in Germany during the 20th century. Smoking is the most important risk factor for cancer causing 22% of global cancer deaths and 71% of global lung cancer deaths, according to the World Health Organization (WHO). Today around 33 % men and 22% women of the German population smoke and the proportions are increasing and roughly equal for both sexes [5]. Other most important risk factors are industrial exposure to asbestos, and environmental cause's exposure to radon, arsenic, chromium, nickel, vinyl chloride and ionizing radiation [6] [7].

There are two major types of lung cancer: non-small cell lung cancer (NSCLC) and small cell lung cancer (SCLC). Non-small cell lung cancer is much more common and accounts for 80 percent of all lung cancer cases it usually spreads to different parts of the body more slowly than small cell lung cancer.

Small cell lung cancer accounts for 20 % of all lung cancers and this type of lung cancer grows more quickly and is more likely to spread to other organs in the body. It often starts in the bronchi and towards the center of the lungs.

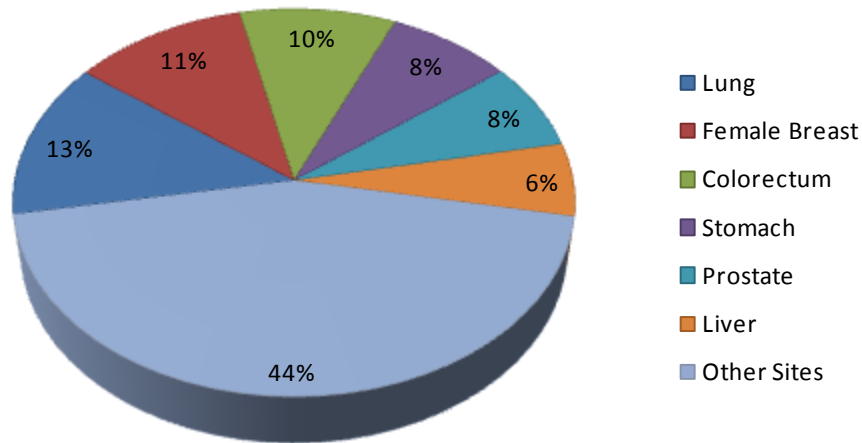


Figure 1.1: The most common causes of death from cancer worldwide, 2008, estimate. (World Health Organization) [2].

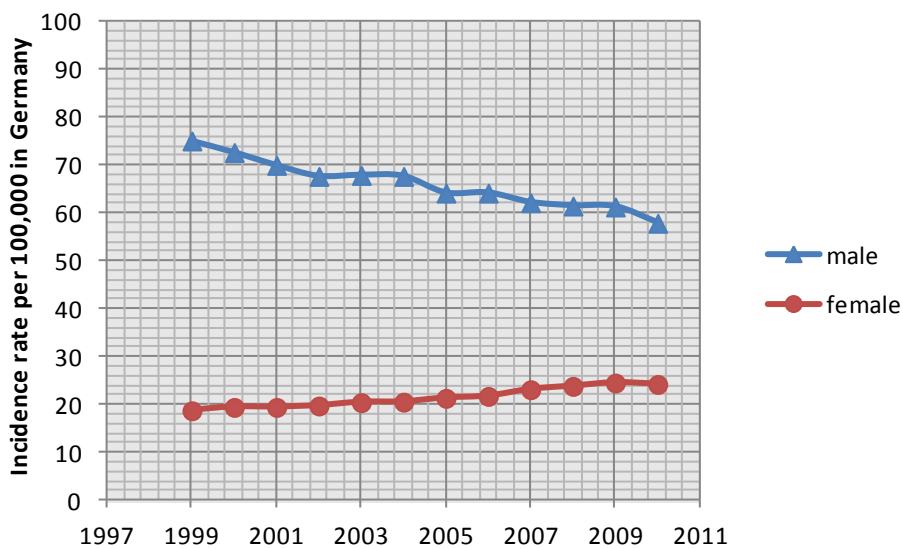


Figure 1.2: Incidence and mortality rates in Germany, 1999 – 2010 [8].

Survival rates for lung cancer tend to be much lower than those of most other common cancers. The 5-year survival rate for all patients where lung cancer is diagnosed is 13.2 %,

compared to 78.3 % for breast cancer, 57.5 % for colon cancer, 27.5% for stomach cancer, and 81.6 % for prostate cancer, while the lowest survival rate was 8 % for liver cancer as shown in Figure 1.3. However, lung cancer survival rates tend to increase when the disease is caught in an early stage. Unfortunately, most lung cancers are not identified until later stages. This is one important reason why it is so critical that research on identifying lung cancer early be expanded [1].

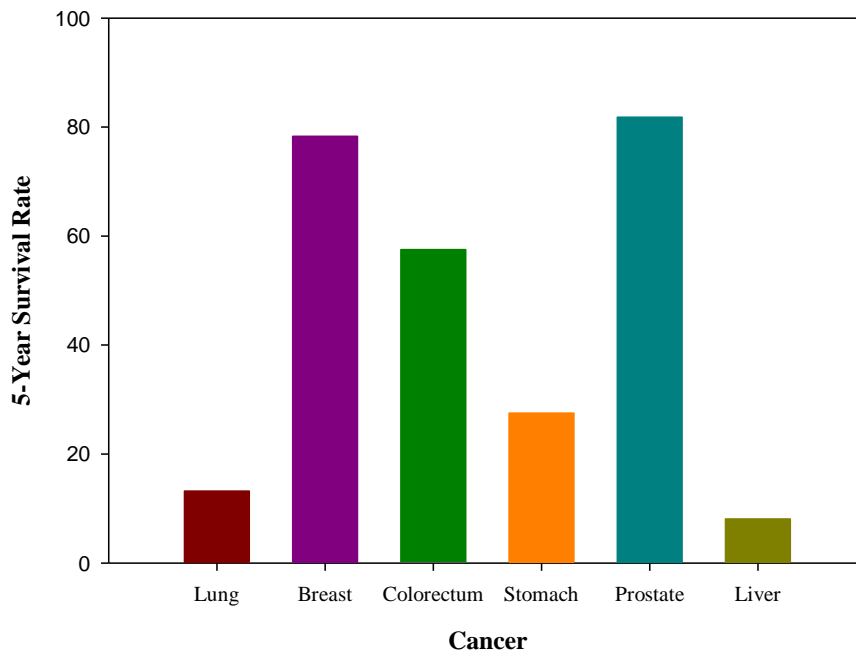


Figure 1.3: Five-year Relative Survival Rates (%) for selected cancers in Germany between 1995 and 1999 [1].

The earlier cancers can be detected, the better the chances of a cure. Researchers are now working to develop several technologies for earlier diagnosis of lung cancer, including cytology of the sputum [9] [10], circulating tumor biomarkers [11] [12], blood proteomic [13], chest tomography [14], nuclear magnetic resonance (NMR) [15], and other techniques. Each approach has limited diagnostic specificity so that depending on one technique may cause high risk for false identifying of lung cancer until researchers manage to develop a method that can be used in routine clinical analysis.

In this research we are going to focus on proteomics-based diagnostics. After surveying the literature for lung cancer diagnostics, I came across a number of contributions that use a proteomic approach in the search of SCLC lung cancer. I have chosen a number of such publications, which give a reasonable indication of the potential of the technology, its advantages and drawbacks in the search for cancer.

Proteomics is the large-scale study of proteins, particularly their structure and functions, including, identification, detection, measurement of their concentration and characterization [16].

The first step in proteomics approach is proteins separation. The target of the separation is to fractionate protein mixture from a biological sample in such a way that all the individual proteins or at least some groups of them can be identified and analyzed further. The separation is based on the chemical and physical difference of proteins that cause them to behave differently when being exposed to different environments.

Proteins can be a biomarker in cancer diagnostic. A biomarker refers to a substance or process that is indicative of the presence of cancer in the body. The United Nations' World Health Organization (WHO) defines a biomarker as "any substance, structure or process that can be measured in the body or its products and influences or predicts the incidence of outcome or disease" [17]. The NIH's National Cancer Institute (NCI) [18], describes biomarkers in its dictionary of cancer terms as "A biological molecule found in blood, other body fluids, or tissues that is a sign of a normal or abnormal process, or of a condition or disease. A biomarker may be used to see how well the body responds to a treatment for a disease or condition. Biomarkers are also called molecular marker and signature molecules".

Many biomarkers are used to monitor chronic diseases such as cancer (e.g., carcinoembryonic antigen (CEA), and diabetes (Hemoglobin-A1c 4).

1.2 Biomarker for lung cancer

Biomarkers have been extensively studied in lung cancer, but no specific marker is known for this malignancy. Carcinoembryonic antigen (CEA), squamous cell carcinoma SCC, and cytokeratins have been the most extensively studied in non small cell lung cancer (NSCLC) and neuron-specific enolase (NSE) in small cell lung cancer (SCLC) [19] [20] [21]. None of these markers is specific for lung cancer. Abnormal levels are found in other malignancies [22]. Another problem is their poor sensitivity. Often two or three tumor markers must be combined to obtain acceptable sensitivity.

NSE has become the tumor marker of choice in SCLC, just because there has been nothing better to use. However, due to its low sensitivity it must often be combined with other less specific tumor markers such as CEA.

Pro-gastrin-releasing peptide (ProGRP) a precursor of GRP is a promising marker for SCLC. Gastrin-releasing peptide (GRP) is a hormone originally isolated from porcine stomach that is widely distributed throughout the mammalian nervous system and gastrointestinal and pulmonary tract. Several researchers have noticed that GRP is produced by cells of SCLC and may, therefore, be helpful in monitoring the patients. Nonetheless, it is difficult to determine GRP in serum because of its instability in blood (half-life: 2 min) [23]. Therefore, immunoassays have been developed for the precursor GRP, ProGRP, which has a longer half life in the blood.

ProGRP is a peptide that, physiologically, is found in low concentrations in the blood of every human. Hence, it is not a tumor-specific protein, as is the case with the majority of tumor markers. ProGRP serum concentrations between 2 and 50 pg/mL are considered normal [24]. In summary, abnormal ProGRP levels are mainly found in lung cancer, with the highest concentrations in SCLC. ProGRP serum levels 150 pg/mL are indicative of SCLC.

ProGRP exists as isoforms 1, 2, and 3 and these are made up of 148, 141, and 138 amino acids, respectively, while GRP has a peptide chain of 27 amino acids [25] [26] ProGRP (31–98) is a region common to three types of ProGRP (Table 1.1).

There are sensitive immunoassays for ProGRP on the market, such as those produced by Abbott Diagnostics (ARCHITECT ProGRP assay) and Fujirebio Diagnostics, Inc. (ProGRP EIA). They provide good sensitivity, efficiency, and simplicity but are unable to distinguish between isoforms [27].

Table 1.1: Amino Acid (AA) sequences of ProGRP isoforms[§]

Isoform 1	10	20	30	40	50	60
	MRGRELPLVL	LALVLCLAPR	GRAVPLPAGG	GTVLTKMYPR	GNHWAVGHLM	GKKSTGESSS
	70	80	90	100	110	120
	VSERGSLKQQ	LREYIRWEEA	ARNLLGLIEA	KENRNHQPPQ	PKALGNQQPS	WSEDSSNFK
	130	140				
	DVGSKGKVGR	LSAPGSQREG	RNPQLNQQ			
Isoform 2	10	20	30	40	50	60
	MRGRELPLVL	LALVLCLAPR	GRAVPLPAGG	GTVLTKMYPR	GNHWAVGHLM	GKKSTGESSS
	70	80	90	100	110	120
	VSERGSLKQQ	LREYIRWEEA	ARNLLGLIEA	KENRNHQPPQ	PKALGNQQPS	WSEDSSNFK
	130	140				
	DVGSKGKGSQ	REGRNPQLNQ	Q			
Isoform 3	10	20	30	40	50	60
	MRGRELPLVL	LALVLCLAPR	GRAVPLPAGG	GTVLTKMYPR	GNHWAVGHLM	GKKSTGESSS
	70	80	90	100	110	120
	VSERGSLKQQ	LREYIRWEEA	ARNLLGLIEA	KENRNHQPPQ	PKALGNQQPS	WSEDSSNFK
	130					
	DLVDSLLQVL	NVKEGTPS				

[§]The underlined AAs are the differing part of the isoform, and the AAs in bold are signature peptides.

The analysis of proteins as biomarkers in blood, serum or plasma, has become possible with the advent of proteomics technologies and have been employed in several proteomic studies. However, these samples are very difficult to analyze with usual proteomics approaches, due to the very large number of proteins present in the sample and the huge dynamic range of 10–12 orders of magnitude [28].

For blood and its derivatives, the 20 most abundant proteins represent about 97% of the total protein content. The remaining 3% is a complex mixture in which low abundance proteins, and among them biologically and clinically important biomarkers, that are difficult to detect even with the most advanced mass spectrometric techniques [29].

Biomarkers discovered so far have typical concentrations below 1000 pg/mL, and this means that a relatively large amount of sample (at least 500 μ L for whole serum) should be analyzed to have a sufficient concentration for low abundance protein detection, but in this way the total protein content (about 50 mg) is over the maximum input for mass spectrometry (MS) applications [30].

To overcome this difficulty a pretreatment of the sample is necessary and several strategies have been proposed for the selective removal of high abundance proteins and enrichment of low abundance ones. These strategies include: precipitation using organic solvents [31], ultrafiltration [32] [33], solid phase extraction [34] [35], mesoporous silica extraction [36], magnetic bead extraction [37], electrophoresis [38], immunoaffinity depletion of the most abundant proteins [39] [40] [41], peptide library beads [42], dual size exclusion-affinity hydrogel nanoparticles [43] [44].

1.3 Proteomic techniques

The separation approaches of proteomic samples are generally based on electrophoretic and chromatographic techniques [45]. Several proteomics approaches have been used to identify novel biomarkers. These are described in detail in Figure 1.4.

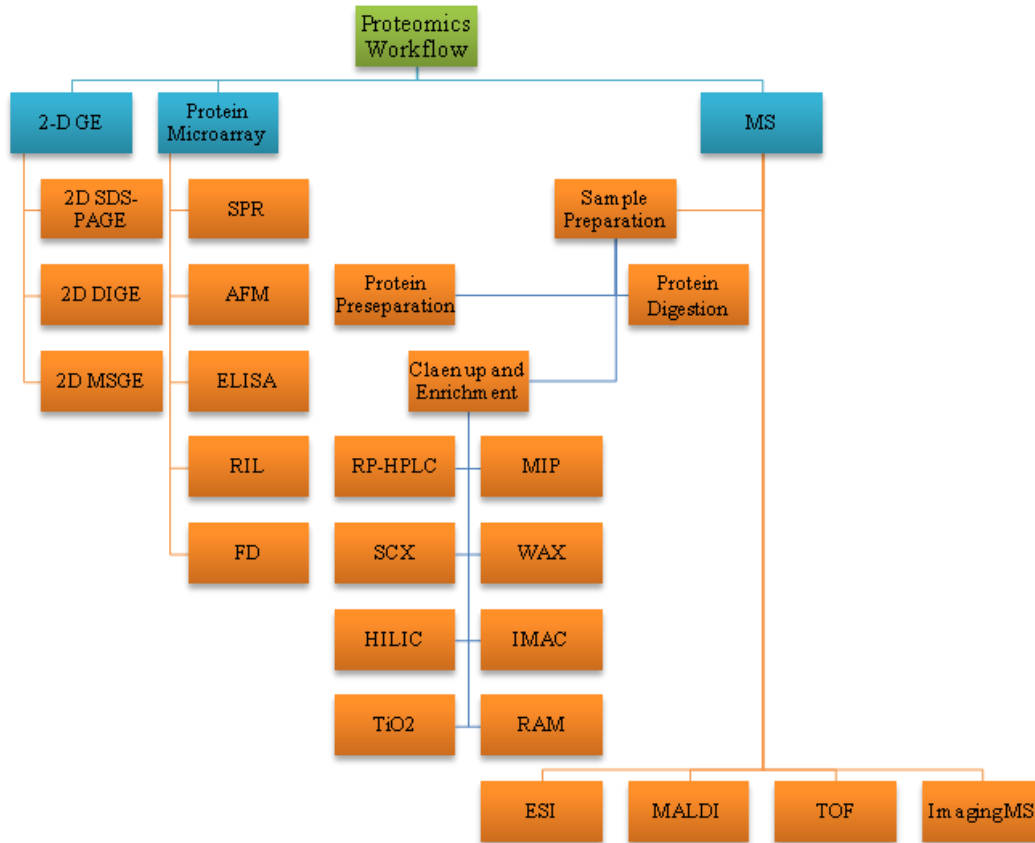


Figure 1.4: Proteomics Workflow. AFM: Atomic Force Microscopy, 2-D GE: Two-Dimensional Gel Electrophoresis, 2D SDS-PAGE: Two-Dimensional Sodium Dodecyl Sulfate Polyacrylamide Gel Electrophoresis, 2D DIGE: Two-Dimensional Differential In Gel Electrophoresis, 2D MSGE: Two-Dimensional Mass Spectrometry Gel Electrophoresis, ELISA: Enzyme-Linked Immunosorbent Assay, ESI: Electrospray ionization, FD: Fluorescence Detection, HILIC: Hydrophilic interaction, IMAC: Immobilized metal affinity, MALDI: Matrix-assisted laser desorption, MIP: Molecularly Imprinted Polymer, MS: Mass Spectrometry, RAM: Restricted Access Material, RIL: Radio Isotope Labeling, RP-HPLC: Ion-pairing reversed phase, SCX: Strong cation exchange, SPR: Surface Plasmon Resonance, TiO₂: Titanium dioxide, TOF: Time-of-flight, WAX: Weak anion exchange.

There are many challenges within translating new biomarkers into clinical laboratory tests. Only 10% of the proteins in human serum can be detected with currently available approaches, this indicates the potential for further discovery of biomarkers [46].

Classical proteomic techniques for the identification of cancer biomarkers can be categorized into two classes:

1.3.1 Two-dimensional gel electrophoresis

Two-dimensional gel electrophoresis (2-D GE) separates proteins in the first dimension on the basis of their charge and in the second dimension on the basis of their molecular mass. Since its introduction over 30 years ago has development in three generations. A first generation called 2D SDS-PAGE (Two-dimensional sodium dodecyl sulfate-polyacrylamide gel electrophoresis) the proteins are separated in two dimensions: the first dimension is isoelectric focusing (IEF), in which proteins are separated according to their isoelectric points (pI), the second dimension is sodium dodecyl sulfate-polyacrylamide gel electrophoresis (SDS-PAGE), which separates proteins according to their molecular mass. The combination of these two orthogonal separation techniques in 2-DE resolves proteins into spots (each spot being a protein isoform with specific pI and MW as its coordinates), and this map of protein spots can be considered the “protein fingerprint” of that sample. By reference to the databases, individual proteins on the map can be identified as the product of genes that have been sequenced. A second generation of 2D GE called differential in gel electrophoresis (DIGE) involves labeling the samples with different fluorescent cyanine dyes (Cy2, Cy3 and Cy5) prior to PAGE. The DIGE technique allows multiple samples e.g., one standard, one control, and one treated to be simultaneously separated under identical conditions in a single 2D gel. These fluorescent dyes bind covalently to part of the lysine (minimal labeling) or all cysteine (saturation labeling) residues of the sample proteins. By scanning the gel using lasers of different wavelength, multiple images of the samples are captured. The images are then superimposed, and quantitative differences between them determined [47].

The advantages of this method compared to conventional 2D SDS-PAGE are shorter analyses times, higher reproducibility, and relatively less sample volume need. The third generation and possibly the most significant development is the increasing use of mass spectrometry in the characterization of the separated proteins.

In general one of the main advantages of 2-D GE is robustness, and the main drawbacks are difficulty in separation of hydrophobic proteins and narrow dynamic range [46] [48].

1.3.2 Mass spectrometry

The proteins in most chromatographic approaches are digested into peptides prior to separation. The advantage is that peptides are more soluble in a broad variety of solvents and hence easier to separate than the whole proteins. The disadvantage is a tremendous increment in the number of components within such a mixture, which have to be fractionated prior to

entering the mass spectrometer. To address the question of efficient fractionation of complex peptide digests prior to their detection, a number of research groups have proposed various method with combinations of mass spectrometry (MS).

Originally MS is not a quantitative method, as the absolute signal intensity of a peptide ion measured in the MS run does not necessarily reflect the abundance of the peptide present in the analyzed sample. Therefore in order to normalize quantitative variations between MS measurements, a reliable internal standard is needed. The best internal standard for a peptide would be a peptide of identical sequence but labeled with different stable isotopes, therefore several MS-based quantitative proteomic technologies via incorporation of stable isotopes in vitro and in vivo have been developed [49].

Without going into too many details at this point which have been described in a number of recent reviews [46] [48]. Instead, I shall discuss in some detail a number of specific publications, which will give the reader a reasonable feel for the capability and future potential of mass spectrometry for the detection and quantification of ProGRP. This potential will be better illustrated by considering a number of applications of this technology in the area of biomarkers discovery.

1.4 Literature survey of ProGRP determination with mass spectrometry

Determining biomarkers with LC-MS is challenging due to complexity of the serum and plasma and huge differences in the concentration of proteins. Determination was achieved by tryptic digestion of the sample and then subsequently monitoring peptide(s) specific for the proteins to be determined. A single specific tryptic peptide will then be sufficient to determine the equimolar amount of protein it originates from assuming reproducible digestion. Such a specific tryptic peptide is defined as a signature peptide [50].

Due to the sample complexity, the reference value for ProGRP in human serum is 60 pg/mL [51] extensive sample pretreatment is required in order to obtain practical results in LC-MS-based diagnosis.

Winther and Reubsaet [52] developed an LC-MS method for the detection and quantification of ProGRP using specific tryptic digestion products from the recombinant peptide ProGRP (31–98), a sequence common to three isoforms of ProGRP. The conditions for enzymatic cleavage were optimized and MS compatibility was obtained. The digestion peptide product

NLLGLIEAK proved to be the preferable candidate to monitor ProGRP due to signal intensity, column retention, and peptide specificity.

An extensive evaluation of sample preparation and enrichment of digested ProGRP was done by the same group [53]. Sample pretreatment was carried out using ACN precipitation to decrease the sample complexity. Although ProGRP (31–98) standards were soluble in 99% ACN, it showed that optimal signal intensities were obtained by adding ACN to the serum in a 1:1 ratio v/v. A simplified tryptic digest protocol was carried out using 100 mM triethanolamine buffer to ensure pH stability during the whole procedure. And because digested spiked serum samples showed an overwhelming amount of peptide products, which were directly separated on the analytical Biobasic-C8 column, the authors used restricted access material (RAM) column technique, first to clean-up the samples from macromolecules, hydrophilic serum components and undigested proteins and peptides, second to enrichment signature peptide NLLGLIEAK. The protein precipitation-RAM (PPT-RAM) method was successfully used for clean up of the samples but couldn't be used to for sensitive detection of NLLGLIEAK due to signal suppression during electrospray ionization. The lowest amount of ProGRP (31–98) detectable in serum samples was approximated to be 1.5 ng/mL.

Winther *et al.* [54] carried out extensive work to find an optimal sample preparation for the LC-MS/MS determination of total ProGRP by introducing immunocapture on microtiter plates. The procedure is based on immuno-capture of ProGRP in 96-wells microtiter plates coated with the monoclonal antibody (mAb) E146. After immuno-capture and thorough rinse, trypsin was added for in-well digestion. Subsequently the signature peptide was enriched by SPE and determined by LC-MS/MS. The evaluation showed good repeatability (RSD, 11.9–17.5%), accuracy (3.0–6.6%), and linearity ($r^2 = 0.995$) in the tested range (0.5–50 ng/mL). Limit of detection (LOD) and limit of quantification (LOQ) were in the pg/mL area (0.20 and 0.33 ng/mL, respectively). The LOD improved with a factor of 7.5 comparing to PPT-RAM method but is still far from reference value for the biomarker 50 pg/mL.

Same group [50] validates PPT-RAM method by using signature peptide NLLGLIEAKacENR as internal standard (IS). To test this method and compare it against an established immunoassay routinely performed at Medical Centre. With IS was chosen for the quantification of ProGRP, two samples with unknown ProGRP (31–98) concentration were measured applying both methods and the results were evaluated. Using the PPT-RAM-IS method, the ProGRP (31–98) concentration was calculated to 13.9 ± 1.2 ng/mL ($n = 3$) and

69.9 ± 3.8 ng/mL ($n = 3$), whereas the immunoassay yielded 8.1 ng/mL ($n = 1$) and 56.0 ng/mL ($n=1$) respectively. As can be seen from the above values, the PPT-RAM-IS method yields elevated values compared to the immunoassay. This might be explained by the fact that the immunoassay method is more susceptible to be influenced by biomarker degradation, by assuming that degradation may affect the immunoreactivity without changing the NLLGLIEAK sequence, higher ProGRP (31–98) concentrations could potentially be observed using LC–MS/MS compared to immunoassay.

Reubsaet and his colleagues [55] recently published a method for differentiate of ProGRP isoforms. In this paper, the immunoaffinity ProGRP beads were prepared by immobilized anti-ProGRP on magnetic beads. Immunocapture was then performed by adding anti-ProGRP magnetic beads to serum sample in an Eppendorf vial. The vial was rotated and shaken to facilitate antigen–antibody interaction. The beads were then washed with a series of solutions and the last step to digest the sample. Reversed-phase liquid chromatography (RP-LC), and tandem MS are combined and utilized to detect, differentiate, and determine the three isoforms of ProGRP, NLLGLIEAK (total ProGRP), LSAPGSQR (ProGRP isoform 1), and DLVDSLLQVLNVK (ProGRP isoform 3) (See Table 1.1). Differentiation between these isoforms could be of clinical value, as well as offering insight into SCLC biology.

1.5 Molecular recognition

Molecular recognition is the underlying principle of many biological processes. Living cells and organisms need to be able to strongly and specifically bind to a particular molecular structure and distinguish between good and evil, friend and foe, food and poison molecule. The phenomenon of recognition occurs on large scale of our daily life. For example, the ability to recognize a person or place is practical happened in our daily life by receptor in nervous system [56]. One of the examples of the cell communication is presented in Figure 1.5.

The term molecular recognition refers to specific interaction between a host molecule and a guest molecule. The interactions involved through noncovalent bonding such as hydrogen bonding, metal coordination, hydrophobic forces, van der Waals forces, π - π interactions, halogen bonding and electrostatic.

There are many cells and molecules in our body, and all of them are cooperatively working in an enormously ordered fashion. Without such mutual understanding and cooperation, we cannot survive. For example, the receptors on the surface of cell membranes bind hormones and are responsible for cell-to-cell communication. When the receptor binds a hormone, its conformation is changed and the message of the hormone (e.g., lack of glucose in the body) is passed to the cell in terms of this conformational change. Now that this cell knows what is required in the body at that moment, it promotes (or suppresses) the corresponding bioreaction (s) to respond to this requirement appropriately. In the above example, glycogen is hydrolyzed and glucose is supplied to the body [57].

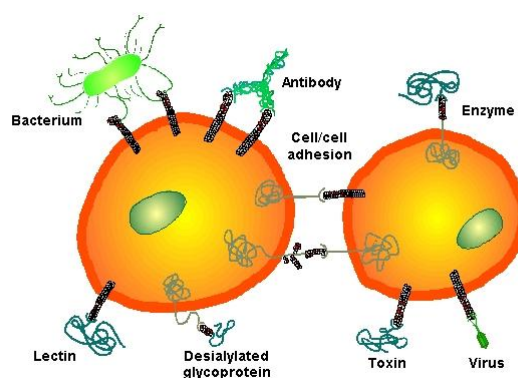


Figure 1.5: Molecular recognition. Examples include antibody-antigen interactions, receptors binding to hormones, virus, bacteria, lectin, and enzymes binding to inhibitors [58].

1.6 Molecularly imprinted polymers

Molecularly Imprinted polymers (MIP) has been developed as a method for preparation of synthetic receptors by polymerization of a self assembled complex, formed by functional monomers and template in the prepolymerization mixture with an excess of a crosslinking agent in the presence of a porogenic solvent, to produce rigid porous polymers as described in Figure 1.6. After the synthesis, the template is removed by an extraction process, leaving behind imprinted binding sites (cavities) within the polymer network that are tailored in size, shape and chemical functionality to the template. Under appropriate conditions, these cavities are able to rebind with the template molecule or structurally related compounds in a strong and selective manner when they are reintroduced to the polymer.

The synthesis of MIPs usually involves a parallel process involving synthesis of a non-imprinted polymer (NIP) under conditions identical to those of the MIP except that the template is absent. In principle, the NIP is entirely analogous to the MIP except that any binding sites within its porous structure are nonselective. The NIP can therefore be used as a benchmark for assessing the selectivity of the MIP such as recovery and breakthrough as reported in published papers [59][60].

In order to introduce functionality into these recognition sites two main approaches can be taken into account, the covalent and the non-covalent imprinting.

Covalent imprinting, reported the first time in 1972, developed by the groups of Wulff [61]. In this approach (Figure 1.6A), the functional monomer and template are bound to each other by reversible covalent bond prior to polymerization. Extraction of the template and subsequent rebinding steps will both involve on cleaving and re-establishment of these covalent bonds, which is the limitation of the method.

In non-covalent imprinting the interactions between functional monomer and template are based on interactions such as H-bonding (Figure 1.6D) or ion-pairing (Figure 1.6C). This method was established by Mosbach and his coworkers [62]. In this method the interactions between functional monomer and template during polymerization are the same as those between polymer and template in the rebinding step. Here template molecules are fixed within the polymeric matrix by non-covalent interactions with monomer to form template-monomer complexes; followed polymerization in presence of crosslinking monomer, a polymer network is formed. Subsequent removal of template by simple solvent extraction leaves behind the cavities whose size and shape are complimentary to the template molecule. Thereby a suitable imprinting effect is obtained; the template, or analogues, may then be selectively rebound by

the polymer. To date the most successful non-covalent imprinting systems using acidic monomer, methacrylic acid (MAA), basic monomer 4-vinylpyridine (4-Vpy), or a neutral monomer 2-hydroxyethyl methacrylate (HEMA) which can be used when the template are insoluble in nonpolar organic solvents or made the backbone of polymer more hydrophilic to decrease the non specific interaction [63]. The most commonly used monomer: template ratio is 4:1. Ethylene glycol dimethacrylate (EDMA) is the most common crosslinker for MIP applications, in large amounts, typically over 80% of the total monomer amount. At present, this approach is the most widely applied technique to produce imprinted polymers.

A variety of other combinations can be used for the preparation of imprinted polymers, such as semi-covalent approach first reported in 1990 by Sellergren and Andersson [64] (Figure 1.6B) is a hybrid of the non-covalent and the covalent methods, where the template is bound covalently to a functional monomer during polymerization as in the covalent approach, but the template rebinding is only based on non-covalent interactions [65].

A metal-ion imprinting can be used for the preparation of imprinted polymers (Figure 1.6E); the complex used for imprinting generally consists of polymerizable ligand(s) to complex the metal ion (generally a transition metal ion) through the donation of electrons from the heteroatom of ligand to the unfilled orbitals of the outer coordination sphere of the metal which in turn coordinates to the template [66].

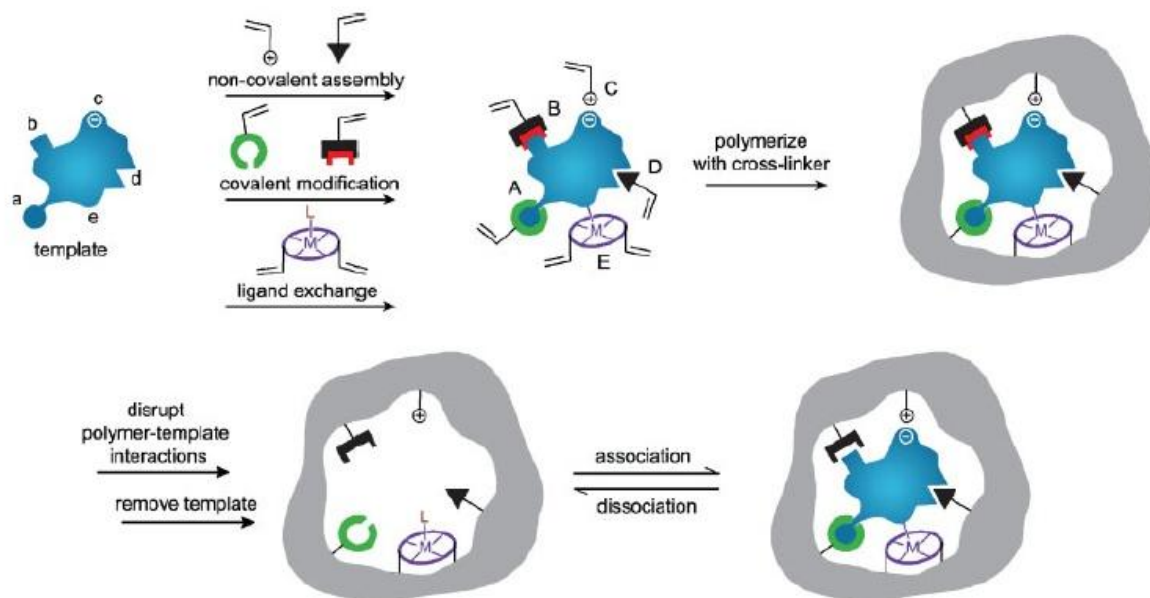


Figure 1.6: Schematic representation of the molecular imprinting process: Type of interactions: (A) reversible covalent bond(s), (B) semi-covalent bond(s), (C) electrostatic interactions, (D) hydrogen bonds, hydrophobic or van der Waals interactions or (E) co-ordination with a metal centre. Polymerization in the presence of crosslinker, results in the formation of a polymer. Template is then removed through disruption of polymer-

template interactions, and extraction from the matrix. The template, or analogues, may then be selectively rebound by the polymer [66].

Molecular imprinting played an important role in recent years, for creating synthetic receptors capable of selectively recognizing specific target molecules. One practical example is propofol.

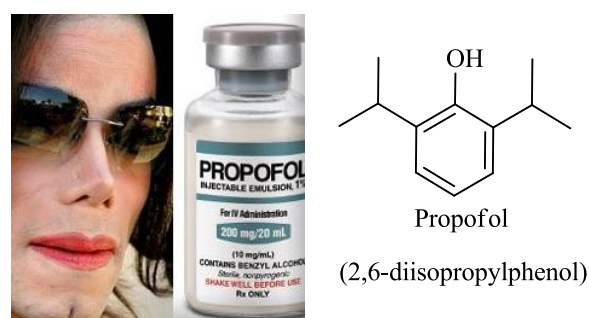


Figure 1.7: Left the pop singer Michael Jackson who passed away after a high deadly dose of propofol [67]. Right the chemical structure of propofol.

On June 25, 2009, the whole world was shocked on news that Michael Jackson had passed away. The investigators found a high deadly dose of the anesthetic drug propofol in his blood (Figure 1.7). Propofol (2, 6-diisopropylphenol) is an intravenous anesthetic widely used for the induction of anesthesia [68]. Although concentration of propofol in blood can be detected by different analytical methods, these methods are time-consuming and not easy for access [68]. One year later Hong and coworkers [68] [69] have developed a compact, fast, low cost, and disposable microfluidic biochip with on-chip MIP-based recognition. A MIP membrane was made of propofol: MAA: EDMA: ABCN (1, 1-Azo-bis (cyclohexane carbonitrile)) upon the molar ratio of 1:4:30:0.41.

The detection mechanism is based on the reaction of the propofol which is retained in the MIP film with the Gibbs reagent (quinonechloroimide) which will change to quinoneimine molecules in alkaline solution. Quinoneimine molecules will then react with propofol to form indophenol and the released product is optically monitored at 655 nm (Figure 1.8).

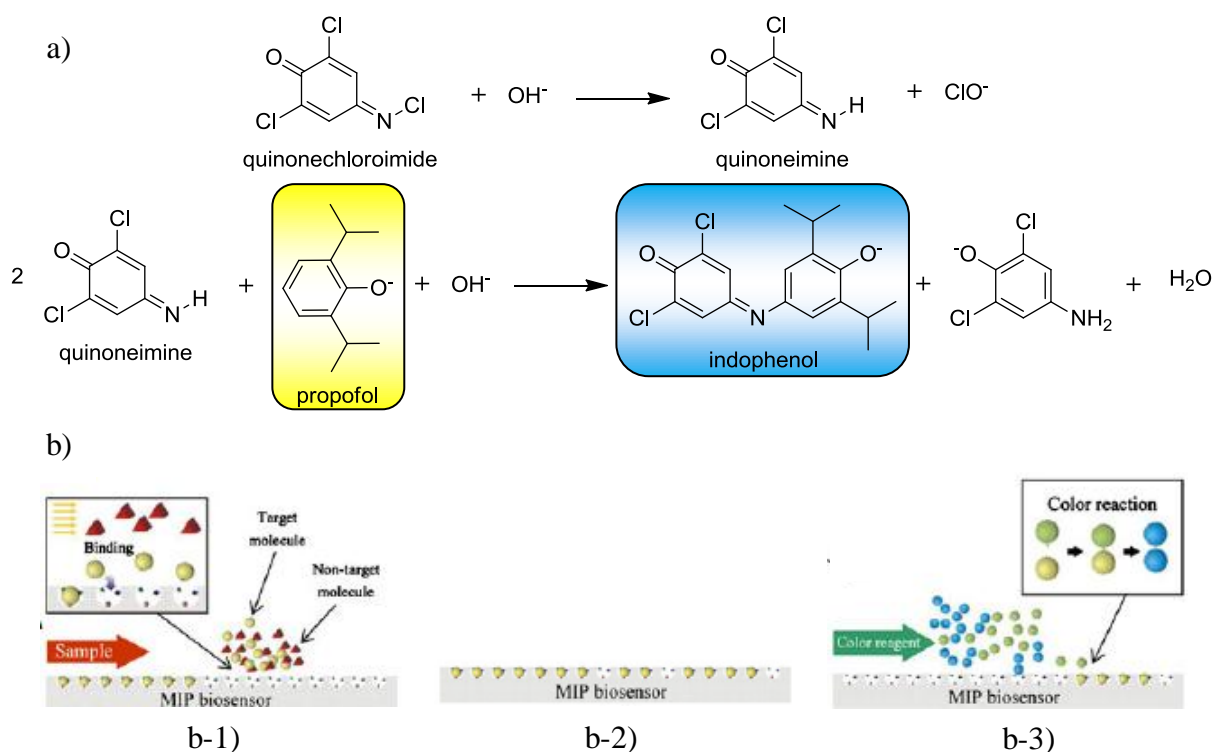


Figure 1.8: a) the chemical reaction of quinonechloroimide with propofol, and b) the working principle of molecular imprinting: b-1) the target molecule is absorbed by the MIP film, while non-target molecules cannot be adsorbed, b-2) corresponds to the washed sample, only remains target molecules adsorbed by the MIP film, b-3) target molecules adsorbed by the MIP film are released and color reagent is injected, occurring color reaction with the reagent (adapted from [68]).

The experimental results showed that the developed biomimetic chip could successfully detect propofol in the 0.25–10 mg/L range with a limit of detection of 0.25 mg/L. The authors claimed that the new platform compared well with chromatographic methods usually applied to the detection of this drug, although no comparative data were included in the study [68] [69].

The theory of imprinting polymerization and practical aspects of MIP application are covered in several reviews [70] [71] [72] [73] [74]. Despite significant development within the MIP technology, the majority of polymers prepared so far have been done by low template molecular weight and in organic solvents. For biological sample like proteins and peptides, many parameters need to be taken into account in order to create molecularly imprinted polymers capable of mimicking biological processes.

Furthermore, some more general drawbacks may need to be addressed are [75]:

- ☒ Poor recognition in water
 - Binding too weak (solvent competition)
 - Nonspecific hydrophobically driven binding

- ☒ Lack of general imprinting strategies for:
 - Hydrophilic targets
 - Biological macromolecules
 - Nonpolar poorly functionalised targets
- ☒ Binding site heterogeneity
- ☒ Poor mass transfer properties
- ☒ Low saturation capacity
- ☒ Template bleeding or leaking
- ☒ A template is needed

1.7 Molecularly imprinted receptors for peptides

Peptides and proteins are essential to life. As an example, neuropeptides are released and used as chemical messengers by different neurons for signal communication. Such biological peptides are commonly used as biomarkers to study brain function and disease processes [76].

Studies of these molecules have been dependent on our ability to selectively capture these molecules from complex biological mixtures. Therefore, it is important to be able to extract these target biomolecules from complex samples, and utilizing MIPs with high selectivity might be a good solution.

As tailor-made molecular recognition materials, a large number of MIPs have been successfully used as affinity adsorbents for the separation of low molecular weight organic compounds. In contrast, the use of MIPs for the separation and analysis of biological peptides has been limited to a few examples [77] [78] [79] [80] [81] [82] [83]. The main difficulty is that peptides are not soluble in common organic solvents that are suitable for preparing high fidelity MIPs. Although chemically modified peptides have in the past been used as templates to prepare MIPs in organic solvents, the polymers obtained often display poor binding performance for unmodified peptides under aqueous conditions, and therefore are not suitable for direct peptide separation [84] [85] [86] [87]. Besides these limitations, most of the peptide-imprinted polymers are obtained as irregular particles by repetitive grinding and sieving operations, which are very time consuming and difficult to use for preparing large quantities of MIPs [88].

The advantages of aqueous MIPs could be used as the solid phase for chromatographic analysis as well as for the purification of peptides and proteins [89], for use in biosensors [90], or for the development of biomedical diagnostics and clinical analysis [91].

However, due to their structural complexity and incompatibility of these targets with organic solvents which are typically used for imprinting. On the other hand, peptides and protein, unlike small templates, contain a large number of potential recognition sites like amine or carboxylic groups, over a relatively large surface area. Factors like thermodynamic and steric hinder the successful preparation of peptide or protein-imprinted polymers, making the preparation of such imprinted polymers a challenging task [92].

The most of MIPs to date is synthesized in organic solvents which show selectivity for relatively low molecular weight molecules. Synthesis in aqueous media of chemically and mechanically stable MIPs that demonstrate specific recognition of biomolecules continues to be a significant challenge, as aqueous solutions significantly reduce the binding strength of the non covalent template–monomer interactions that are essential to the production of an imprinting effect [93].

It has also largely been shown that MIPs only demonstrate their selectivity when rebinding template in the organic solvent in which they were synthesized [94]. For instance, MIPs which can selectively recognize given proteins or peptide sequences in aqueous media have the potential to be used as substrates in medical diagnostic applications and clinical analysis. Currently, there are a number of strategies which can be applied to prepare peptide imprinting polymer. After surveying the literature I came across a number of works that use peptide as template. I shall discuss in some detail a number of specific works, which will give the reader a reasonable feel for the capability and future potential of the MIP technology, its advantages and drawbacks in peptide imprinting.

In this review, we will discuss some of the advances that have been made in the imprinting of biological macromolecules in aqueous solutions. A number of studies in which MIPs are used for selective peptide recognition applications in aqueous systems are outlined in Table 1.2.

Table 1.2: Example of MIPs synthesized for recognition of peptides in aqueous media

Template	Analyte	Functional monomers	Crosslinker	Porogen	Molar ratio	Ref.	
Tyr-Pro-Leu-Gly	Tyr-Pro-Leu-Gly Oxytocin	MAA	EDMA	ACN	1:20:80	[92]	
					1:20:100		
				ACN:Isooctane (95:5)	1:20:60		
					1:25:100		
					1:20:80		
	1:15:60				1:12.5:50		
Boc-Leu-enkephalin	Pyr-Leu-enkephalin	—	NOBE	ACN	1:16	[88]	
Lys-Trp-Asp	Lys-Trp-Asp Arg-Trp-Asp Leu-Trp-Asp Gln-Trp-Asp Lys-Phe-Asp Lys-Trp-Glu Lys-Trp Lys-Phe Lys-Val	2-Vpy	DVB	ACN	1:5:44	[87]	
Z-L-Tyr-OH	Z-D-Tyr-OH	2-Vpy:MAA 2-Vpy MAA	EDMA	ACN	1:8:8:40 1:4:20 1:4:20	[95]	
Z-Thr-Ala-Ala-OMe	Z-Thr-Ile-Leu-OMe	MAA	TRIM PETRA	ACN	1:8:8	[96]	
					1:8:35		
					1:8:8		
					1:8:35		
Melittin	Melittin	AAc:TBAm AAm:AAc:TBAm	BIS	H ₂ O	0.03:5:40	[97]	
					0.03:5:5:40		
Boc-L-Phe-OH	Boc-D-Phe-OH	MAA	EDMA	CHCl ₃	1:4:20	[80]	
Z-L-Phe-OH	Z-D-Phe-OH	MAA	EDMA	CHCl ₃	1:4:20		
Z-L-Asp-OH	Z-D-Asp-OH	4-Vpy	EDMA	THF	1:12:60		
Z-L-Glu-OH	Z-D-Glu-OH	4-Vpy	EDMA	THF	1:12:60		
Z-L-Ala-L-Ala-OMe	Z-D-Ala-D-Ala-OMe	MAA	TRIM	CHCl ₃	1:6:6		
Z-L-Ala-Gly-L-Phe-OMe	Z-D-Ala-Gly-D-Phe-OMe	MAA	TRIM	CHCl ₃	1:8:8		
N-Ac-L-Phe-L-Trp-OMe	N-Ac-L-Phe-L-Trp-OMe	MAA	EDMA	CHCl ₃	1:5:15		[81]
Tyr-Pro-Leu-Gly	Oxytocin	MAA	EDMA	ACN	1:5:15		[98]
Z-Oxytocin	Oxytocin	MAA	EDMA	ACN	1:32:32	[83]	
			TRIM	ACN	1:32:162		
Leu⁵-enkephalin				DMSO	1:12:48	[77]	
Leu⁵-enkephalin anilide	Leu ⁵ -enkephalin	MAA	EDMA	ACN	1:18:72		
Boc-Leu⁵-enkephalin				CHCl ₃	1:12:48		
Boc-Met⁵-enkephalin				CHCl ₃	1:12:48		
Angiotensin I	Angiotensin I	6-AAm-β-CyD	MBAAm	50 mM Tris, pH 8	1:4:24	[90]	
Angiotensin II	Angiotensin II						
[Val⁵]-Angiotensin I	[Val ⁵]-Angiotensin I						
[Val⁵]-Angiotensin II	[Val ⁵]-Angiotensin II						

AAc:acrylic acid; **Ac**: acetyl; **AAm**:acrylamide; **6-AAm- β -CyD**:mono-6-(*N*-acrylamido)-6-deoxy- β -CyD; **BIS**:*N,N'*-methylenebisacrylamide; **Boc**: di-*t*-butyl dicarbonate; **DMSO**:dimethylsulphoxide; **DVB**:1,4-divinylbenzene; **EDMA**: ethylene glycol dimethylacrylate; **NOBE**: N, O-bismethacryloyl ethanolamine; **MAA**:methacrylic acid; **MBAAm**: *N,N'*-methylenebis(acrylamide); **PETRA**:pentaerythritol triacrylate; **TBA**m:*N*-*t*-butylacrylamide; **THF**: tetrahydrofuran; **TRIM**: trimethylolpropane trimethacrylate; **Tris**: 2-Amino-2-hydroxymethyl-propane-1,3-diol; **2-Vpy**: 2 vinylpyridine; **Z**:Benzyloxycarbonyl

Angiotensin I: Asp-Arg-Val-Tyr-Ile-His-Pro-Phe-His-Leu

Angiotensin II: Asp-Arg-Val-Tyr-Ile-His-Pro-Phe

[Val⁵]- **Angiotensin I**: Asp-Arg-Val-Tyr-Val-His-Pro-Phe-His-Leu

[Val⁵]- **Angiotensin II**: Asp-Arg-Val-Tyr-Val-His-Pro-Phe

Leu⁵-enkephalin: Tyr-Gly-Gly-Phe-Leu

Melittin: Gly-Ile-Gly-Ala-Val-Leu-Lys-Val-Leu-Thr-Thr-Gly-Leu-Pro-Ala-Leu-Ile-Ser-Trp-Ile -Lys-Arg-Lys-Arg-Gln-Gln

Leu⁵-enkephalin: Tyr-Gly-Gly-Phe-Leu

Oxytocin: Cys-Tyr-Ile-Gln-Asn-Cys-Pro-Leu-Gly

1.7.1 Hierarchical imprinting

The method of hierarchical imprinting was used for the first time in order to synthesize polymers with a high affinity for Theophylline (1) [100] and for Adenine (2) [101] (Figure 1.13a). Earlier studies on the imprinting of small molecules *via* hierarchical polymerization showed the potential of the method, which has been transferred to the recognition of larger target analytes, by creating surface exposed sites. The hierarchical epitope imprinting approach was developed by Sellergren and his co-worker [101].

The concept is demonstrated by first immobilizing the peptide template on the surface of a porous silica support. This small peptide may be representing a smaller peptide the terminal amino acid sequence of a target protein or large peptide. The pores of the silica beads were filled with a pre-polymerization mixture of monomers/initiator and polymerized. In the final step, the silica is dissolved and removed. The resulting polymer particles exhibit a structure and morphology similar to the “mirror image” of the original silica templates, which are capable of recognizing larger molecules with the same immobilized template, as described in Figure 1.9.

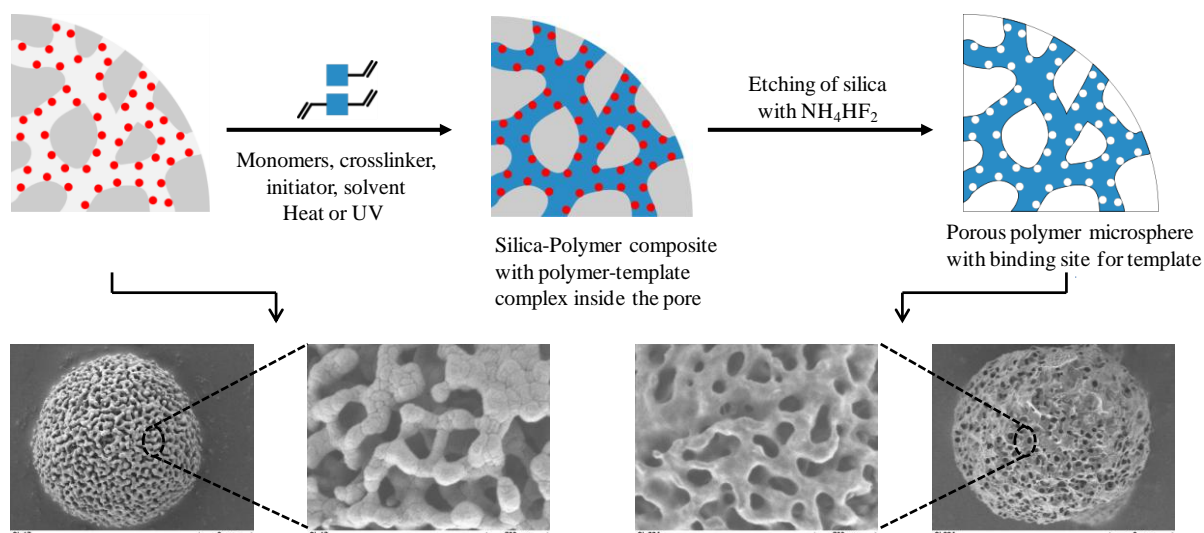


Figure 1.9: Top: Concept of Hierarchical Imprinting (adapted from [102]). Below scanning electron microscopic images of a silica microsphere (left) and its inverse-replicated (right) (adapted from [103])

1.7.2 Epitope imprinting method

Minoura and coworkers were the first to demonstrate the epitope approach for protein recognition, and the polymer they synthesized recognized not only the template but also larger peptides with the same C-terminal [104] [105]. In this technique, if a short peptide from the larger protein target molecule is used to create the imprint, then the resulting molecularly imprinted polymer should also be able to retain the whole protein molecule Figure 1.10.

Nevertheless, several parameters can be tuned for the optimization of this method, like the use of specifically designed monomers, as the urea monomers, which have been applied for the imprinting of phosphorylated peptides [106]. Only a small amount of peptide template is required in this approach, and polymer preparation is much easier than when protein is used as the template [92].

Traditionally, an epitope refers to the small active site located within the larger protein structure on an antigen, which combines with the antigen-binding site on an antibody or lymphocyte receptor [107].

To explore the epitope approach, Minoura and coworkers [78] [104] chose the neurohypophyseal hormone, oxytocin. Oxytocin (3) (Figure 1.13b) is a nonapeptide (Cys-Tyr-Ile-Gln-Asn-Cys-Pro-Leu-Gly- NH_2). The tetrapeptide, Tyr-Pro-Leu-Gly (4) (Figure 1.13b) has been chosen as the template for the preparation of the MIP. Both compounds possess the same three amino acid C-terminal sequence, Pro-Leu-Gly- NH_2 . The Tyr residue in the peptide Tyr-Pro-Leu-Gly was chosen to facilitate UV and fluorescence detection.

In this study, synthesis of the MIP was performed in an organic environment, but subsequent rebinding experiments were performed using chromatographic methods in both aqueous rich and aqueous-poor mobile phases. In the aqueous-poor mobile phase, hydrogen bonds and ionic interactions are the dominating factor in creating selective recognition sites. In the aqueous-rich phase, ionic and hydrophobic interactions provide the dominant binding interaction.

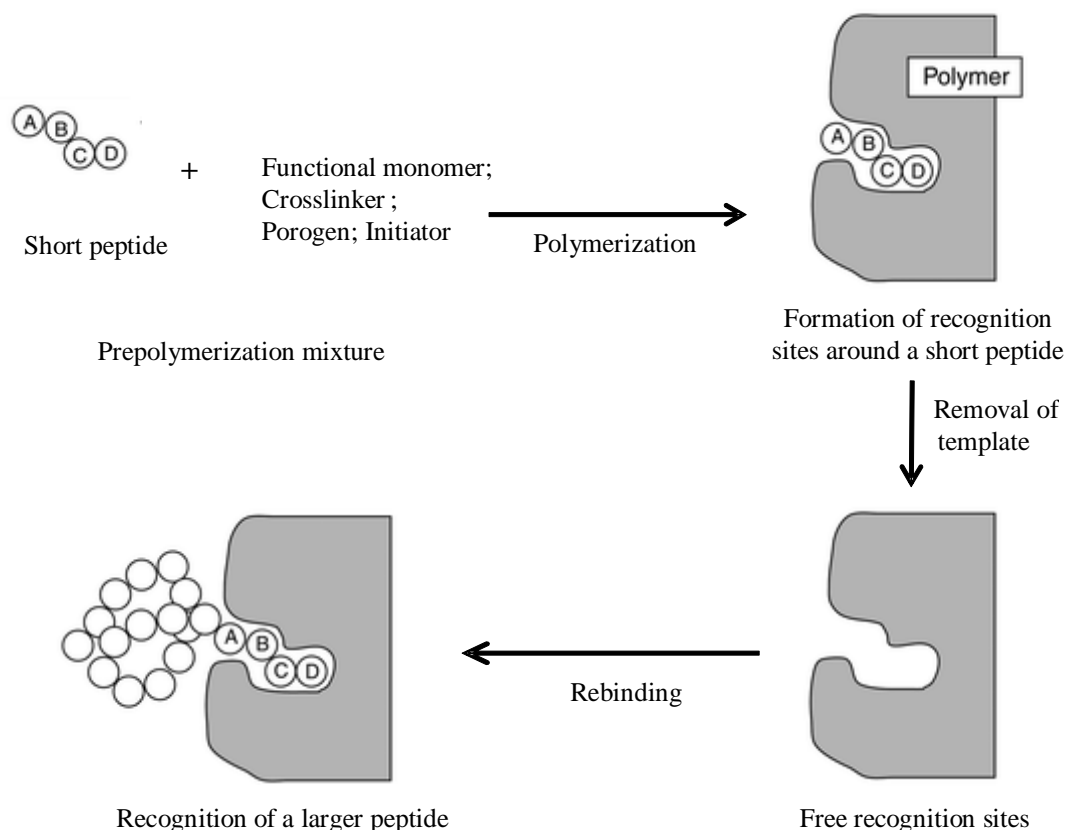


Figure 1.10: Schematic representation of the epitope approach (adapted from [78])

In contrast to previously published examples involving hydrophilic peptide sequences as templates, the imprinting of the hydrophobic peptides have posed new challenges. Sellergren and co-worker [108], they selected N-acetylated C-terminal hexapeptide sequences as epitope template Ace-Gly-Gly-Val-Val-Ile-Ala (5) and Acetyl-Met-Val-Gly-Gly-Val-Val (6) (Figure 1.13c) to prepare MIPs for discrimination of the two C-terminals of A β 1-42 and A β 1-40 respectively.

The composition of each MIP was: template (0.0142 μ mol); N-3, 5-bis (trifluoromethyl)-phenyl-N'-4-vinylphenylurea (7) (0.0142 μ mol); and the HCl salt of N- (2-aminoethyl) methacrylamide hydrochloride functional monomer (8) (1.42 mmol); DVB (7.14 mmol);

initiator (ABDV) (0.047 mmol) and ACN/DMSO (65:35) (1300 μ L). Nonimprinted polymers (NIPs) were prepared leaving out the template.

This resulted in a method capable of quantitatively and selectively enriching a shorter C-terminal peptide corresponding to the sequences A β 33-40 (Gly-Met-Leu-Val-Gly-Gly-Val-Val) and A β 33-42 (Gly-Met-Leu-Val-Gly-Gly-Val-Val-Ile-Ala) as well as the full-length sequence A β 1-40 and A β 1-42 from serum sample (Figure 1.11).

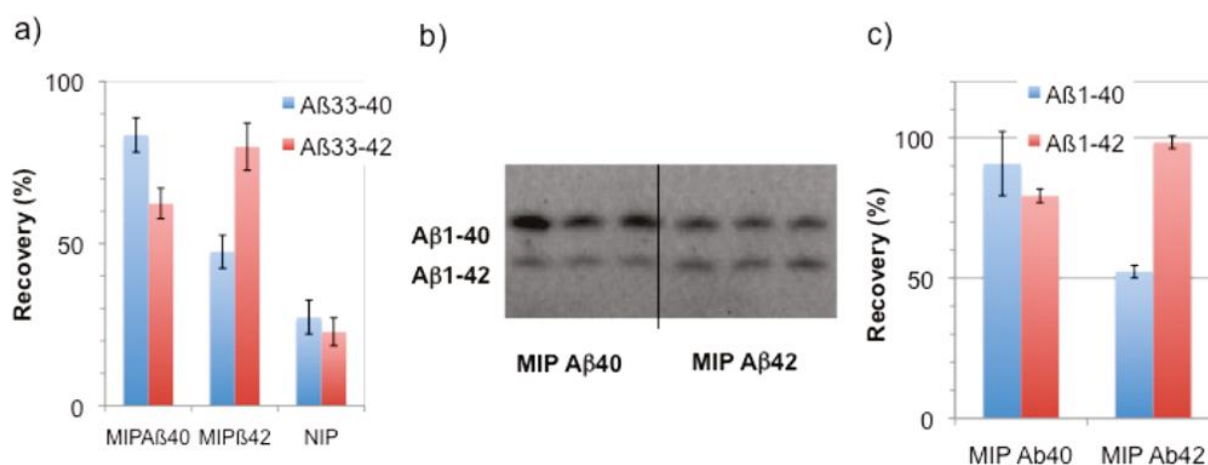


Figure 1.11: (a) Recovery of the C-terminal epitopes of A β 33-40 and A β 33-42 in the elution fractions after SPE of peptide-spiked blood serum samples (2.5 μ g/mL) on the two complementary MIPs and the NIP. The analysis was performed in triplicate with the RSD indicated. (b) Stained gel from urea-SDS-PAGE/ immunoblot analysis of elution fractions from SPE of a blood serum sample spiked with A β 1-40 (5 ng/mL) and A β 1-42 (1 ng/mL). (c) Recoveries estimated from spot intensities of the gel in (b) and the associated RSDs [108].

1.7.3 One monomer molecularly imprinted polymers method (OMNiMIPs)

The other strategy is the use of a single bi-functional monomer, N,O-bismethacryloyl ethanolamine (NOBE) (9) (Figure 1.13d), to replace the traditional combination of functional monomer and crosslinker to form high fidelity binding sites [109]. These methods are referred to as “OMNiMIPs”, which is an acronym for one-monomer molecularly imprinted polymers. This method has made optimization of the traditional bulk MIPs much more straightforward, only one monomer is used, which acts as both the functional monomer and the crosslinking monomer. This eliminates the need to optimize the ratio of functional monomer to crosslinker, which is determined empirically and has been particularly successful in imprinting against small organic templates containing free carboxyl or hydroxyl functional groups [109].

David A. Spivak and co-worker tried to find out if NOBE can be used to prepare spherical MIPs for larger and more flexible peptides that contain similar free carboxyl or hydroxyl

functionalities [110]. Two templates of N-terminal protected neuropeptides, Boc-Leu-enkephalin (10) and Pyr-Leu-enkephalin (11) (Figure 1.13d) were used to prepare MIP in the precipitation polymerization method. The MIP microspheres obtained were characterized by equilibrium binding analysis to assess their molecular recognition properties.

The imprinted polymer beads were tested for their specific binding for the original template. Boc-Leu-enkephalin and Pyr-Leu-enkephalin were incubated with different amounts of polymers in acetonitrile. As shown in Figure 1.12, the imprinted polymer bound much more the template than the non-imprinted polymer, indicating that MIP has apparently much higher affinity for the peptide because of the imprinted binding sites. At a polymer concentration of 5 mg/mL, the uptake of template by the imprinted polymer (46%) was almost 6 times that of the nonimprinted polymer [88].

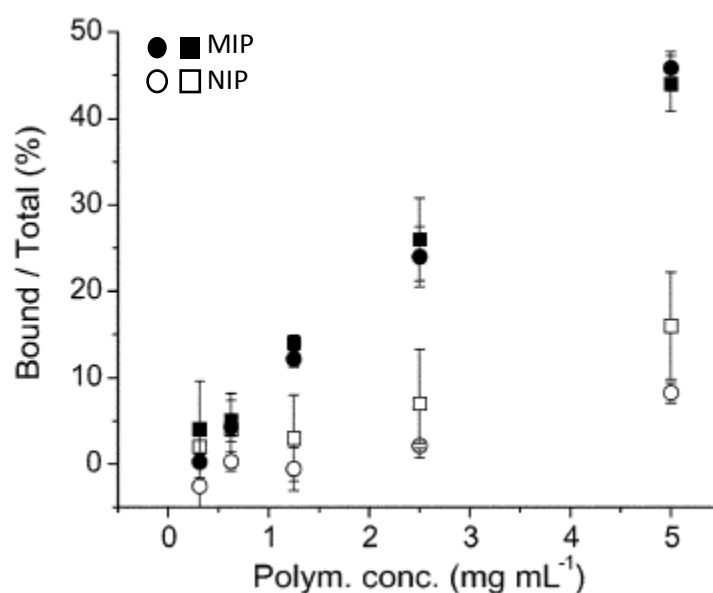
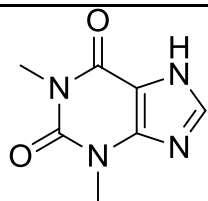
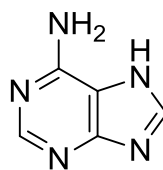


Figure 1.12: Uptake of Boc-Leu-enkephalin (circle) and Pyr-Leu-enkephalin (square) by the imprinted polymer and the non-imprinted polymer. The initial concentration of the peptide derivatives was 15 mM.

(a)

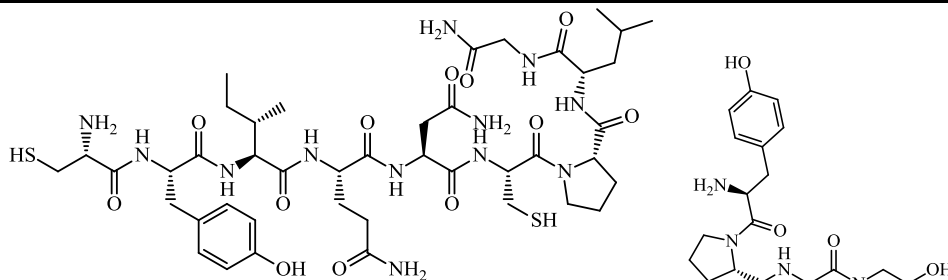


1, Theophylline



2, Adenine

(b)

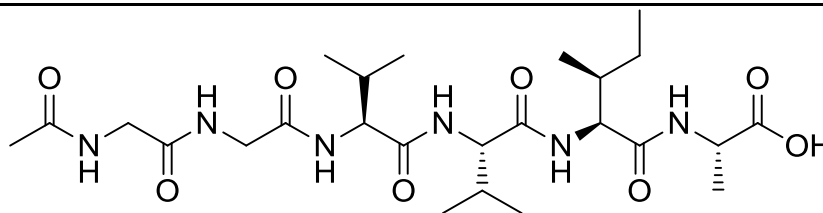


3, Oxytocin

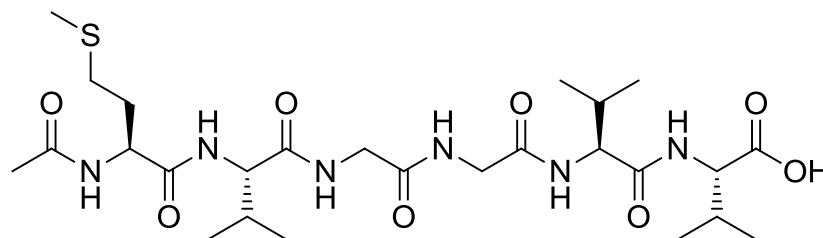
Cys- Tyr- Ile- Gln-Asn- Cys- Pro- Leu- Gly

4, Tyr-Pro-Leu-Gly

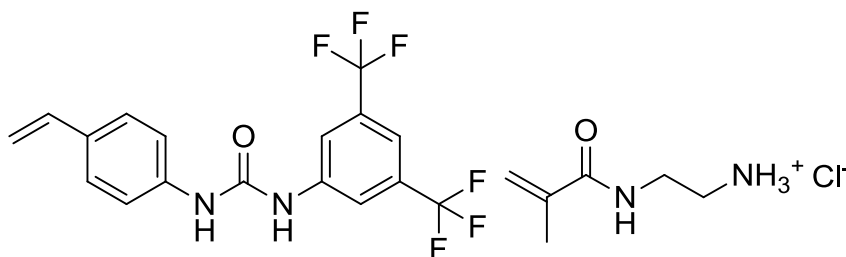
(c)



5, Acetyl-Gly-Gly-Val-Val-Ile-Ala



6, Acetyl-Met-Val-Gly-Gly-Val-Val



7, TFU

8, EAMA

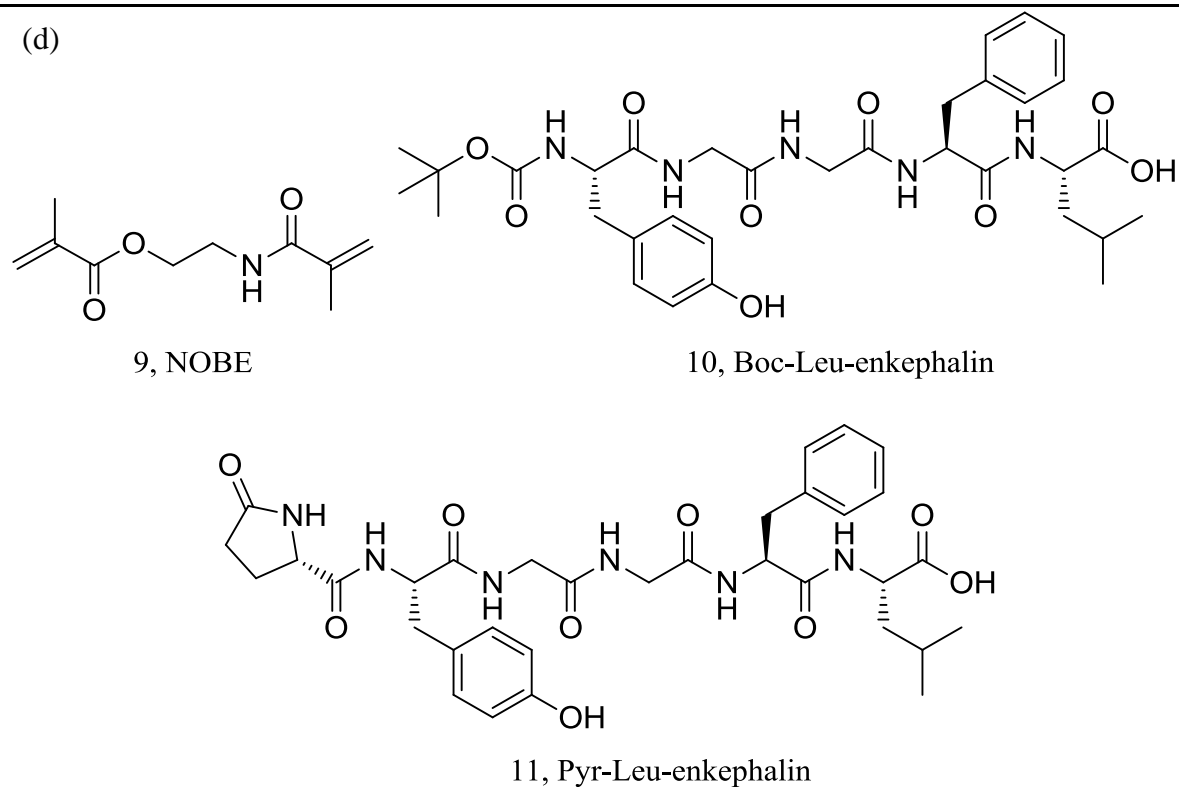


Figure 1.13: Structures of molecules discussed in the main text. (a) Theophylline and Adenine first molecules used by hierarchical imprinting method. (b) Epitope peptide Tyr-Pro-Leu-Gly used to explore epitope method by Minoura et al [104]. (c) Imprinted hydrophobic peptides for targeting β -amyloid used by Sellergren et al [108]. (d) OMNiMIPs approach was used to develop selective MIPs for the molecules shown.

1.8 Optimization and rational design of MIP

As mentioned above, the non-covalent approach is the most widely used for the preparation of MIPs, the procedure of preparation of MIPs is straightforward (mix and bake) and the post polymerization processing (crush, and sieve) does not need particular skills. However, in parallel, such flexibility is also the origin of some of the drawbacks attributed to MIPs. There are several variables of the imprinting process influence the selectivity and capacity of a MIP such as type and amount of monomer or nature of crosslinker, solvent, and temperature. Thus, the development of optimum imprinting protocol has often involved a few trial-and-error experiments using different formulations. Therefore, some attempts dealing with the optimisation of MIP formulations in a simple, fast and rational way for the obtainment of MIPs with improved molecular recognition capabilities have been proposed.

1.8.1 Computational approach

Piletsky et al. have used a computational approach to design MIPs [111]. This approach uses molecular modeling software to design and screen a virtual library of monomers against the desired template. Generally, by measuring of binding energies of template–functional monomer complexes the optimal functional monomer could be obtained [111] [112] [113].

The advantage of the strategy was demonstrated by Subrahmanyam *et al.* [111]. A virtual library of functional monomers was assigned and screened against the target molecule, Creatinine (13, Figure 1.14), using molecular modeling software, since MIPs created using traditional methods were unable to differentiate between Creatine (12) and Creatinine (13) (Figure 1.14) . The result of this simulation gave an optimised MIP composition. When this MIP was synthesized in the laboratory, it demonstrated superior selectivity in comparison to the polymer prepared using traditional approach.

It is necessary to point out that this approach is relatively new and thus, before being routinely used, it is still necessary to prepare and evaluate the best polymers (also for the worst ones it would be desirable) to confirm the trueness of the computational prediction [114].

1.8.2 Combinatorial imprinting

This method was proposed independently by the groups of Sellergren and co-worker [115] and Takeuchi et al. [116] for Triazine (14) and Sulphonylurea (15) (Figure 1.14) targeted MIPs, respectively. The method consisted of the preparation of a quite large number of polymers directly in HPLC vials in small-scale (mini-MIPs, 50 mg) to determine an optimal

MIP formulation for the template. Then, the obtained mini-MIPs was subjected to two screening steps. The ‘instant first screening’ quantified the amount of free template desorbed from the MIPs after porogen incubation, enabling a rough estimation of the affinity of the template to the MIP. The second ‘regular screening’ step involved a more systematic batch rebinding study by comparing the template capacity on the imprinted polymer with that on similar non-imprinted, blank polymers, made in the absence of template [116].

Most application of this technique has been aimed at finding suitable monomers for a given template or target analyte, also been used to find optimum monomer ratios and porogens with improving molecular recognition and suppression of nonspecific binding of analyte.

Although this combinatorial approach provided an improved method over the conventional trial-and-error approach in developing selective MIPs, one of the main drawbacks is the limited range of methodologies for the screening of mini-MIPs, being restricted to rebinding experiments in equilibrium [114]. In addition, the researcher noted that because of the slow HPLC for the binding studies, the process was still time consuming and did not allow for the development of a high throughput combinatorial library [117]. To solve this problem, Takeuchi et al. [118] developed a faster screening method that would allow evaluation of binding capacity by fluorescence measurements using a microplate reader. But the drawback of this method needs a non-volatile porogen and a fluorescent analyte.

Lanza et al. [119] demonstrated a limitation for using combinatorial approach. They concluded that small-scale rebinding results obtained at equilibrium cannot always be used to predict selectivity of MIPs in the dynamic HPLC mode formulation.

Despite these limitations, this methodology has been successfully employed in the rapid evaluation and selection of the best MIP for different analytes, triazines (14) [120], drug E (Primary alcohol, 16) [121], folic acid (17) [122], beta amyloid peptides (5, 6Figure 1.13) [108], and sulphonylurea herbicides [123] (Figure 1.14).

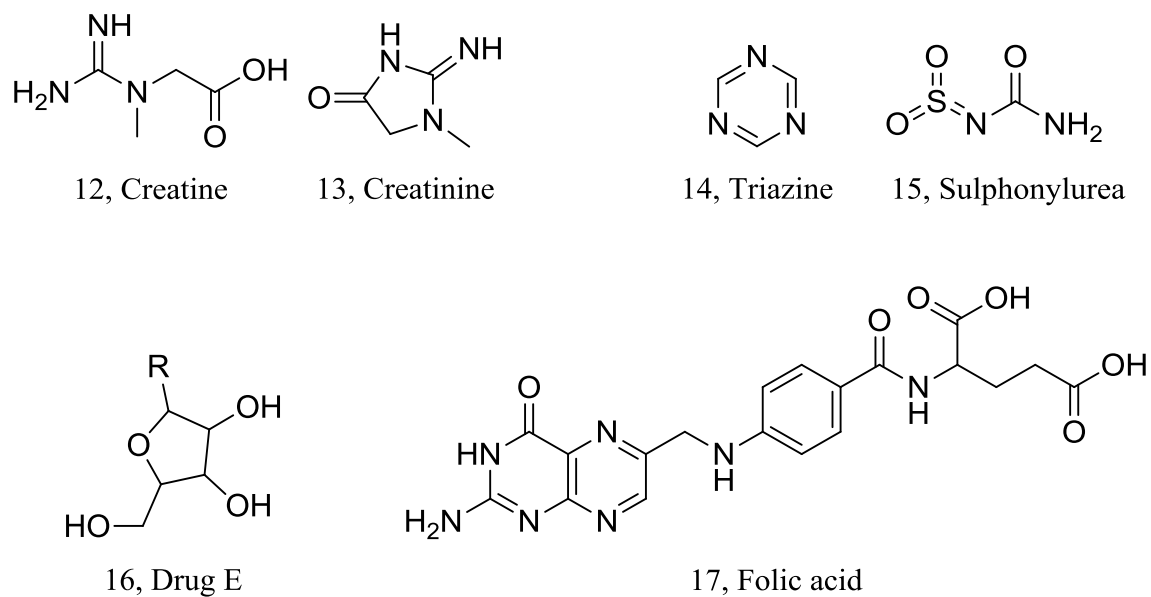


Figure 1.14: Structures of molecules discussed in the main text. A computational approach was used to develop selective MIPs for Creatine and Creatinine and a combinatorial approach was used to develop selective MIPs for Triazine, Sulphonylurea, Drug E (as shown in reference 121), and Folic acid.

Bibliography

- [1] "The GEKID Atlas – 2012," [Online]. Available: <http://www.gekid.de>. [Accessed 22 07 2012].
- [2] Husmann.G., Kaatsch.P., Katalinic.A., Bertz.J. and Kraywinkel.K, "Cancer in Germany 2005/2006 Incidence and Trends," Robert Koch Institute, Berlin, 2010.
- [3] World.Health.Organization, "WHO Report the Global TOBA CCO epidemic,2008:The MPOWER package.," World Health Organization, Geneva, 2008.
- [4] Hammond.E.C., Selikoff.I.J. and Seidman.H., *Ann N Y Acad Sci*, vol. 330, pp. 473-90, 1979.
- [5] Gilliland.F.D., Hunt.W.C., Pardilla.M. and Key.C.R, *J Occup Environ Med*, vol. 42, pp. 278-83, 2000.
- [6] "World Health Organization," 2008. [Online]. Available: <http://who.com>.
- [7] Gesundheitsberichterstattung.des.Bundes, "Krebs in Deutschland 2007/2008," Robert Koch-Institut, Berlin, 2012.
- [8] "Global Cancer Facts & Figures," American Cancer Society, Atlanta, 2nd Edition.2011.
- [9] Johnson.F.L., Turic.B., Kemp.R., Palcic.B., Sussman.R., Voelker.K.G. and Robinette.E, *Chest*, vol. 125, p. 157S, 2004.
- [10] Varella-Garcia.M., Kittelson.J., Schulte.A.P., Vu.K.O., Wolf.H.J., Zeng.C., Hirsch.F.R., Byers.T., Kennedy.T., Miller.Y.E., Keith.R.L. and Franklin.W.A, *Cancer Detect Prev*, vol. 28, p. 244, 2004.
- [11] Helmig.S. and Schneider.J, *Expert Rev. Mol. Diagn*, vol. 7, p. 555, 2007.
- [12] Yildiz.P.B., Shyr.Y., Rahman.J.S., Wardwell.N.R., Zimmerman.L.J. and et.al, *J.Thorac. Oncol*, vol. 2, p. 893, 2007.
- [13] Maciel.C.M., Junqueira.M., Paschoal.M.E., Kawamura.M.T., Duarte.R.L., Carvalho. M. G. and Domont.G.B, *J. Exp. Ther. Oncol*, vol. 5, p. 31, 2005.
- [14] Kikuchi.T. and Carbone.D.P, *Respirology*, vol. 12, p. 22, 2007.
- [15] Lichy.M.P., Aschoff.P., Plathow.C., Stemmer.A., Horger.W. and Mueller-Horvat.C, *Invest.Radiol*, vol. 42, p. 605, 2007.
- [16] Xiao.G., Recker.R. and Deng.H-W, *Clinical Medicine: Oncology*, vol. 2, pp. 63-72, 2008.
- [17] "World Health Organization," [Online]. Available: <http://www.inchem.org/documents/ehc/ehc/ehc222.htm>. [Accessed 25 06 2013].
- [18] "National Cancer Institute," [Online]. Available: <http://www.cancer.gov/dictionary/?CdrID=45618>. [Accessed 25 06 2013].
- [19] Molina.R., Filella.X., Augé.J.M., Fuentes.R., Bover.I., Rifa.J., Moreno.V., Canals.E., Viñolas.N., Marquez.A., Barreiro.E., Borrás.J. and Viladiu.P, *Tumor Biol*, vol. 24, pp. 209-18, 2003.
- [20] Foa.P., Fornier.M., Miceli.R. and et.al, *Anticancer Res*, vol. 19, pp. 3613-8, 1999.
- [21] Jorgensen.L.G., Hansen.H.H. and Cooper.E.H, *Eur J Cancer Clin Oncol*, vol. 25, pp. 123-8, 1989.
- [22] Molina.Rafael, *EJCMO*, vol. 1, no. 2, pp. 25-32, 2009.
- [23] Yamaguchi.K., Abe.K., Kameya.T., Adachi.I., Taguchi.S., Otsubo.K. and Yanaihara.N, *Cancer Res*, vol. 43, pp. 3932-9, 1983.

- [24] Rafael.M., Xavier.F. and Josep.A, *Clin Biochem*, vol. 37, pp. 505-511, 2004.
- [25] Dumesny.C., Patel.O., Lachal.S., Giraud.A., Baldwin.G. and Shulkes.A, *Endocrinology*, vol. 147, pp. 502-509, 2006.
- [26] McDonald.T.J., Nilsson.G., Vagne.M., Ghatei.M., Bloom.S.R. and Mutt.V, *Gut*, vol. 19, pp. 767-774, 1978.
- [27] "UniProt," [Online]. Available: <http://www.uniprot.org/uniprot/P07492#P07492>. [Accessed 15 02 2013].
- [28] Ray.S., Reddy.P.J., Jain.R., Gollapalli.K., Moiyadi.A. and Srivastava.S, *Proteomics*, vol. 11, pp. 2139-2161, 2011.
- [29] DeBock.M., DeSeny.D., Meuwis.M-A., Servais.A-C., Minh.T., Closset.J., Chapelle.J-P., Louis.E., Malaise.M., Merville.M-P. and Fillet.M, *Talanta*, vol. 82, pp. 245-254, 2010.
- [30] Capriotti.A, Caruso.G., Cavaliere.C., Piovesana.S., Samperi.R. and Lagana.A, *Anal. Chim. Acta*, vol. 740, pp. 58-65, 2012.
- [31] Chertov.O., Biragyn.A., Kwak.L.W., Simpson.J.T., Boronina.T., Hoang.V.M., Prieto.D.A., Conrads.T.P., Veenstra.T.D. and Fisher.R.J, *Proteomics*, vol. 4, pp. 1195-1203, 2004.
- [32] Zheng.X., Baker.H. and Hancock.W.S, *J. Chromatogr. A*, vol. 1120, pp. 173-184, 2006.
- [33] Tirumalai.R.S., Chan.K.C., Prieto.D.A., Issaq.H.J., Conrads.T.P. and Veenstra.T.D, *Mol. Cell. Proteomics*, vol. 2, pp. 1096-1103, 2003.
- [34] Koomen.J.M., Li.D., Xiao.L.C., Liu.T.C., Coombes.K.R., Abbruzzese.J. and Kobayashi.R.J, *Proteome Res*, vol. 4, pp. 972-981, 2005.
- [35] Hu.L., Boos.K.S., Ye.M., Wu.R. and Zou.H, *J. Chromatogr. A*, vol. 1216, pp. 5377-5384, 2009.
- [36] Tian.R., Zhang.H., Ye.M., Jiang.X., Hu.L., Li.X., Bao.X. and Zou.H, *Angew. Chem. Int. Ed*, vol. 46, pp. 962-965, 2007.
- [37] Baumann.S., Ceglarek.U., Fiedler.G.M., Lembcke.J., Leichtle.A. and Thiery.J, *Clin. Chem*, vol. 51, pp. 973-980, 2005.
- [38] Marshall.J., Jankowski.A., Furesz.S., Kireeva.I., Barker.L., Dombrovsky.M., Zhu.W., Jacks.K., Ingratta.L., Bruin.J., Kristensen.E., Zhang.R., Stanton.E., Takahashi.M. and Jackowski.G, *J. Proteome Res*, vol. 3, pp. 364-382, 2004.
- [39] Gong.Y., Li.X., Yang.B., Ying.W., Li.D., Zhang.Y., Dai.S., Cai.Y., Wang.J., He.F. and Qian.X, *J. Proteome Res*, vol. 5, pp. 1379-1387, 2006.
- [40] Pieper.R., Su.Q., Gatlin.C.L., Huang.S.T., Anderson.N.L. and Steiner.S, *Proteomics*, vol. 3, pp. 422-432, 2003.
- [41] Brand.J., Haslberger.T., Zolg.W., Pestlin.G. and Palme.S, *Proteomics*, vol. 6, pp. 3236-3242, 2006.
- [42] Sennels.L., Salek.M., Lomas.L., Boschetti.E., Righetti.P.G. and Rappsilber.J, *J. Proteome Res*, vol. 6, pp. 4055-4062, 2007.
- [43] Luchini.A., Geho.D.H., Bishop.B., Tran.D., Xia.C., Dufour.R.L., Jones.C.D., Espina.V., Patanarut.A., Zhou.W., Ross.M.M., Tessitore.A., Petricoin.E.F. and Liotta.L.A, *Nano Lett*, vol. 8, pp. 350-361, 2008.
- [44] Rainczuk.A., Meehan.K., Steer.D.L., Stanton.P.G., Robertson.D.M. and Stephens.A.N, *Proteomics*, vol. 10, pp. 332-336, 2010.
- [45] Zhao.Y., Giorgianni.F., Desiderio.D.M., Fang.B. and Beranova-Giorgianni.S, *Anal Chem*, vol. 77, pp. 5324-5331, 2005.

- [46] Hamdan.Mohmoud, *Cancer biomarkers : analytical techniques for discovery*, New Jersey: John Wiley & Sons, 2007.
- [47] Lilley.K.S. and Friedman.D.B, *Expert Rev Proteomics*, vol. 1, pp. 401-409, 2004.
- [48] Jain.Kewal.K, *The Handbook of Biomarkers*, New York: Springer, 2010.
- [49] Aebersold.R. and Mann.M, *Nature*, vol. 422, pp. 198-207, 2003.
- [50] Winther.B., Moi.P., Nordlund.M., Lunder.N., Paus.E. and R. E, *J.Chromatogr.B*, vol. 877, pp. 1359-1365, 2009.
- [51] Nordlund.M.S., Warren.D.J., Nustad.K., Bjerner.J. and Paus.E, *Clin.Chem*, vol. 54, pp. 919-922, 2008.
- [52] Winther.B. and Reubsæet.L, *J.Sep.Sci*, vol. 30, pp. 234-240, 2007.
- [53] Winther.B., Moi.P., Paus.E. and Reubsæet.L, *J.Sep.Sci*, vol. 30, pp. 2638-2646, 2007.
- [54] Winther.B., Nordlund.M., Paus.E., Reubsæet.L. and Grønhaug.H, *J.Sep.Sci*, Vols. 2937-2943, p. 32, 2009.
- [55] Torsetnes.S., Nordlund.M., Paus.E., Halvorsen.G. and Reubsæet.L, *J. Proteome Res*, vol. 12, no. 1, pp. 412-420, 2013.
- [56] Kempe.Henrik, *Advances in Separation Science, Doctoral Thesis, Department of Analytical Chemistry*, Stockholm: Stockholm University, 2007.
- [57] Komiyama.M., Takeuchi.T., Mukawa.T. and Asanuma.H, *Molecular Imprinting From Fundamentals to Applications*, Weinheim: Wiley-VCH, 2003.
- [58] Magnani.John.L, "Discovery Medicine," [Online]. Available: <http://www.discoverymedicine.com/John-L-Magnani/2009/12/03/glycomimetic-drugs-a-new-source-of-therapeutic-opportunities/>. [Accessed 25 08 2013].
- [59] Helling.S., Shinde.S., Brosseron.F., Schnabel.A., Müller.T., Meyer.H., Marcus.K. and Sellergren.B, *Anal.Chem*, vol. 83, pp. 1862-1865, 2011.
- [60] Ambrosini.S., Shinde.S., DeLorenzi.E. and Sellergren.B, *Analyst*, vol. 137, pp. 249-254, 2012.
- [61] Wulff.G. and Sarhan.A, *Angew. Chem., Int. Ed. Engl*, vol. 11, no. 4, p. 341, 1972.
- [62] Arshady.R. and Mosbach.K., *Macromol. Chem*, vol. 182, p. 687, 1981.
- [63] Kugimiya.A. and Takeuchi.T, *Analyt.Sci*, vol. 15, pp. 29-33, 1999.
- [64] Sellergren.B. and Andresson.L, *J.Org.Chem*, vol. 55, pp. 3381-3383, 1990.
- [65] Whitcombe.M., Rodriguez.M., Villar.P. and Vulfson.E, *J.Am.Chem.Soc*, vol. 117, pp. 7105-7111, 1995.
- [66] Alexander.C., Andersson.H., Andersson.L.I., Ansell.R.J., Kirsch.N., Nicholls.I.A., O'Mahony.J. and Whitcombe.M.J, *J.Mol.Recognit*, vol. 19, pp. 106-180, 2006.
- [67] "Starlettime," [Online]. Available: <http://www.starlettime.com/stelle-della-musica/mcihael-jackson-propofol/>. [Accessed 11 12 2013].
- [68] Hong.C-C., Chang.P-H., Lin.C-C. and Hong.C-L, *Biosens.Bioelectron*, vol. 25, pp. 2058-2064, 2010.
- [69] Hong.C-C., Lin.C-C., Hong.C-L. and Chang.P-H, *Biomed Microdevices*, vol. 14, pp. 435-441, 2012.
- [70] Marty.J. and Mauzac.M, *Adv Polym Sci*, vol. 172, pp. 1-35, 2005.
- [71] Cormack.P. and Elorza.A, *J. Chromatogr. B*, vol. 804, pp. 173-182, 2004.
- [72] Vasapollo.G., DelSole.R., Mergola.L., Lazzoi.M., Scardino.A., Scorrano.S. and Mele. G, *Int.J.Mol.Sci*, vol. 12, pp. 5908-5945, 2011.
- [73] Cheong.W., Yang.S. and Faiz.A, *J.Sep.Sci*, vol. 36, no. 3, pp. 609-628, 2012.

- [74] Biffis.A., Dvorakova.G. and Falcimaigne-Cordin.A, *Top Curr Chem*, vol. 325, pp. 29-82, 2011.
- [75] Lanza.L. and Sellergren.B, *Macromol. Rapid Commun*, vol. 25, pp. 59-68, 2004.
- [76] Boonen.K., Landuyt.B., Baggerman.G., Husson.S.J., Huybrechts.J. and Schoofs.L, *J.Sep.Sci*, vol. 31, p. 427, 2008.
- [77] Andersson.L., Müller.R. and Mosbach.K, *Macromol. Rapid Commun*, vol. 17, pp. 65-71, 1996.
- [78] Rachkov.A. and Norihiko.M, *Biochim.Biophys.Acta*, vol. 1544, pp. 255-266, 2001.
- [79] Zheng.C., Liu.Z-S., Gao.R-Y. and Zhang.Y-K, *Chin.J.Chem.*, vol. 26, pp. 1857-1862, 2008.
- [80] Kempe.M. and Mosbach.K, *J.Chromatogr.A*, vol. 691, pp. 317-323, 1995.
- [81] Nicholls.I, Ramström.O. and Mosbach.K, *J.Chromatogr.A*, vol. 691, pp. 349-353, 1995.
- [82] Hart.B.R. and Shea.K.J, *J.Am.Chem.Soc*, vol. 123, pp. 2072-2073, 2001.
- [83] Kempe.Maria, *Lett Pept Sci*, vol. 7, pp. 27-33, 2000.
- [84] Kempe.M, *Anal.Chem*, vol. 68, p. 1958, 1996.
- [85] Hart.B.R. and Shea.K.J, *Macromolecules*, vol. 35, p. 6192, 2002.
- [86] Titirici.M.M. and Sellergren.B., *Anal.Bioanal.Chem*, vol. 378, p. 1913, 2004.
- [87] Klein.J., Whitcombe.M., Mulholland.F. and Vulfson.E, *Angew.Chem.,Int.Ed*, vol. 38, no. 13/14, pp. 2057-2060, 1999.
- [88] Yoshimatsu.K., LeJeune.J., Spivak.D.A. and Ye.L, *Analyst*, vol. 134, pp. 719-724, 2009.
- [89] Kanoh.H., Honda.K., Simizu.S., Muroi.M. and Osada.H, *Angew.Chem.Int.Ed*, vol. 44, pp. 3559-3562, 2005.
- [90] Tomizaki.K., Usui.K. and Mihara.H, *ChemBioChem*, vol. 6, pp. 782-799, 2005.
- [91] Michaud.G.A, Salcius.M., Zhou.F., Bangham.R., Bonin.J., Guo.H., Snyder.M., Predki.P.F. and Schweitzer.B.I, *Nat.Biotechnol*, vol. 21, pp. 1509-1512, 2003.
- [92] Zheng.C., Liu.Z., Gao.R., Zhang.L. and Zhang.Y, *Anal Bioanal Chem*, vol. 388, pp. 1137-1145, 2007.
- [93] Hawkinsa.D., Derek.S. and Reddya.S, *Anal.Chim.Acta*, vol. 542, pp. 61-65, 2005.
- [94] Stevenson.D, *TrAC*, vol. 18, pp. 154-158, 1999.
- [95] Ramström.O., Ye.L. and Gustavsson.R.E, *Chromatographia*, vol. 48, no. 3/4, pp. 197-202, 1998.
- [96] Rechichi.A., Cristallini.C., Vitale.U., Ciardelli.G., Barbani.N., Vozzi.G. and Giusti.P, *J.Cell.Mol.Med*, vol. 11, no. 6, pp. 1367-1376, 2007.
- [97] Hoshino.Y., Kodama.T., Okahata.Y. and Shea.K.J, *J.Am.Chem.Soc*, vol. 130, pp. 15242-15243, 2008.
- [98] Rachkov.A. and Minoura.N, *J.Chromatogr.A*, vol. 889, pp. 111-118, 2000.
- [99] Song.S., Shirasaka.K., Katayama.M., Nagaoka.S., Yoshihara.S., Osawa.T., Sumaoka.J., Asanuma.H. and Komiyama.M, *Macromolecules*, vol. 40, pp. 3530-3532, 2007.
- [100] Yilmaz.E., Haupt.K. and Moshach.K, *Angew Chem.Int Ed*, vol. 39, no. 2, pp. 2115-2118, 2000.
- [101] Titirici.M.M., Hall.A. and Sellergren.B, *Chem.Mater*, vol. 14, pp. 21-23, 2002.
- [102] Lindemann.Patrick, Protein Capture with Hierarchical Imprinted Polymer Microspheres Msc thesis at Technische Universität Dortmund, 2012.

- [103] Aureliano.C.S.A, Development of hierarchically imprinted mesoporous polymer beads for biologically active compounds, PhD thesis at Technische Universität Dortmund, 2010.
- [104] Rachkov.A. and Minoura.N, *J.Chromatogr A*, vol. 889, pp. 111-118, 2000.
- [105] Rachkov.A., Hu.M., Bulgarevich.E., Matsumoto.T. and Minoura.N, *Anal Chim Acta*, vol. 504, pp. 191-197, 2004.
- [106] Emgenbroich.M., Borrelli.C., Shinde.S., Lazraq.I., Vilela.F., Hall.A.J. and Oxelbark.J, *Chem.Eur.J*, vol. 14, pp. 9516-9529, 2008.
- [107] Janiak.D. and Kofinas.P, *Anal Bioanal Chem*, vol. 389, pp. 399-404, 2007.
- [108] Urraca.J, Aureliano.C, Schillinger.E., Esselmann.H., Wiltfang.J. and Sellergren.B, *J. Am.Chem.Soc*, vol. 133, pp. 9220-9223, 2011.
- [109] Sibrian-Vaquez.M. and Spivak.D.A, *J.Am.Chem.Soc*, vol. 126, pp. 7827-7833, 2007.
- [110] LeJeune.J. and Spivak.D.A, *Anal.Bioanal.Chem*, vol. 389, p. 433, 2007.
- [111] Subrahmanyam.S., Piletsky.S., Piletska.E., Chen.B., Karim.K. and Turner.A, *Biosens. Bioelectron*, vol. 16, pp. 631-637, 2001.
- [112] Chianella.I., Karim.K., Piletska.E., Preston.C. and Piletsky.S, *Anal.Chim.Acta*, vol. 559, pp. 73-78, 2006.
- [113] Chianella.I., Lotierzo.M., Piletsky.S., Tothill.E and Chen.B, *Anal Chem*, vol. 74, pp. 1288-1293, 2002.
- [114] Tamayo.F., Turiel.E. and Martin-Esteban.A, *J.Chromatogr.A*, vol. 1152, pp. 32-40, 2007.
- [115] Lanza.F. and Sellergren.B, *Anal Chem*, vol. 71, pp. 2092-2096, 1999.
- [116] Takeuchi.T., Fukuma.D. and Matsui.J, *Anal Chem*, vol. 71, pp. 285-290, 1999.
- [117] Batra.D. and Shea.K, *Curr.Opin.Chem.Biol*, vol. 7, pp. 434-442, 2003.
- [118] Takeuchi.T., Seko.A., Matsui.J. and Mukawa.T, *Instrum Sci Technol*, vol. 29, pp. 1-9, 2001.
- [119] Lanza.F., Hall.A.J., Sellergren.B., Bereczki.A., Horvai.G., Bayoudh.S., Cormack.P. and Sherrington.D.C, *Anal Chim Acta*, vol. 435, pp. 91-106, 2001.
- [120] Ferrer.I., Lanza.F., Tolokan.A., Horvath.V., Sellergren.B., Horvai.G. and Barcelo.D, *Anal Chem*, vol. 72, pp. 3934-3941, 2000.
- [121] Dirion.B., Lanza.F., Sellergren.B., Chassaing.C., Venn.R. and Berggren.C, *Chromatographia*, vol. 56, pp. 237-241, 2002.
- [122] Quaglia.M., Chenon.K., Hall.A.J., DeLorenzi.E. and Sellergren.B, *J Am Chem Soc*, vol. 123, pp. 2146-2154, 2001.
- [123] Zhu.Q.Z., Haupt.K., Knopp.D. and Niessner.R, *Anal Chim Acta*, vol. 468, pp. 217-227, 2002.

Chapter 2

Characterization techniques

2.1 Morphology, physical and chemical polymer characterization

2.1.1 Elemental analysis

Analyses for carbon, hydrogen and nitrogen (CHN) were determined at the Department of Organic Chemistry; Johannes Gutenberg University of Mainz using a Heraeus Elemental Analyzer CHN-O-Rapid (Elemental-Analysis system, GmbH).

Elemental analysis also provides information on the efficiency of the silica removal process and the polymerization step. Thus, agreement between theoretical C, H and N contents based on the monomer ratios in the pre-polymerization mixture and the measured values indicated that the monomers were randomly incorporated in the material.

About 10 mg of dried sample was submitted for elemental analysis. The experimental values obtained in this way were compared with the theoretical values calculated through given as follows:

$$\% X = M_{w(X)} \left(\frac{\sum_{j=1}^k N_{j,X} \cdot n_j}{\sum_{j=1}^k n_j M_{w(j)}} \right) \times 100 \quad \text{Eq. 2.1}$$

Where, X is the C , H , or N elements, $M_{w(X)}$ is the molecular weight of element X , n_j is the mole percentage of compound j , and $N_{j,X}$ and $M_{w(j)}$ are the number of X atoms and molecular weight of the compound j , respectively.

To calculate the percentage of each element in the polymer, we then need to consider all sources of each element.

2.1.2 Fourier-Transform infrared spectrometer

All samples were measured on a TENSOR 27 Fourier-Transform infrared spectrometer (*FT-IR*) from Bruker with a platinum ATR moiety. This instrument allows direct measurement of solids and solutions without any sample preparation.

2.1.3 Thermoporometry

Thermoporometry is a technique that allows the study of pore structures of materials in the liquid state by using differential scanning calorimeter (DSC) [1] [2]. The principle of the method is based on the lowering of the triple point temperature of a liquid filling a porous material. The phase transitions (crystallization or melting) for a liquid confined within a pore are observed to shift to lower temperatures that are determined by pore size. This difference in transition temperature, ΔT , between confined and bulk solvent can be detected calorimetrically by DSC. The DSC measurements were performed on DSC Q200 apparatus (TA Instruments) in nitrogen atmosphere. Samples of about 1–2 mg immersed in the 2–10 μL of solvent were put in hermetic aluminum pans. The samples were quenched at $-60\text{ }^\circ\text{C}$ at $5\text{ }^\circ\text{C}/\text{min}$ scanning rate and measured their melting behavior of solvent. The measurements were performed at least triplicates.

2.1.3.1 Pore diameter

From DSC curves $\Delta T = T - T_0$ was calculated, T_0 being the melting point of the pure acetonitrile = $-46 \pm 0.3\text{ }^\circ\text{C}$. Linear regression yields the following numerical expression for acetonitrile. The ΔT valued substituted in following equation and calculated the radius of the pore.

$$D_p (\text{\AA}) = -\frac{309}{\Delta T} + 13 \quad \text{Eq. 2.2}$$

The value 13\AA represents the thickness of the solvent layer remaining adsorbed on the internal pore surface (non-freezable solvent) [1].

2.1.3.2 Pore volume measurement

Total pore volume V_p (e.g., cm^3 pore per gram porous solid) is another important parameter for characterizing porous materials. A simple calculation of V_p can be obtained from a single thermoporometry heating experiment using.

$$V_p = \frac{\Delta H_{pore}}{\Delta H_{tot}} \frac{C_{liq}}{C_{solid} \rho_{liq}} \quad \text{Eq. 2.3}$$

Where a known mass of liquid C_{liq} , of density ρ_{liq} , is added to a known mass of porous solid C_{solid} . The pore melt area, ΔH_{pore} , and combined pore and excess melt peak areas, ΔH_{total} , are determined from the DSC melt endotherms, and their ratio is related to the fraction of liquid contained in the pores. The expression assumes a temperature-independent heat of fusion ΔH and liquid density, as well as a sufficient separation of the pore and excess melt peaks to independently integrate their areas. It is also assumed that all of the liquid has frozen during the initial quench cooling step and melts during heating, i.e., the contribution of the thin liquid layer adjacent to pore walls, and other non-frozen liquid, is negligible [2].

2.1.3.3 Surface area

Once you know the pore diameter and pore volume of the material it is easy to calculate the surface area of the materials using wheeler equation [3].

$$\text{Surface area } (S_A) = 4000 \times \frac{V_p}{D_p} \quad \text{Eq. 2.4}$$

Where, V_p = pore volume, D_p = pore diameter

2.1.4 Scanning electron microscopy (SEM)

SEM was provided at the Department of Biochemical and Chemical Engineering, TU Dortmund. The SEM pictures were recorded on a Hitachi H-S4500 FEG in secondary electron mode with an acceleration voltage of 1 kV. The samples were deposited on holders with carbon foil.

2.1.5 Thermogravimetric analysis

Thermogravimetric analysis (TGA) was carried out using a TGAQ50 (TA instruments, Eschborn, Germany). The sample (~ 10-15 mg) was placed in a platinum pan, which is suspended in a sensitive balance together with the reference pan. The sample was then heated, in a furnace, with at a rate of 10 or 20°C/min, under N_2 atmosphere.

This analysis is a thermal method that involves the measurement of weight loss as a function of temperature or time. The weight of the sample is plotted against temperature (as example Figure 4.8) or time to illustrate thermal transitions in the material – such as loss of solvent and

plasticizers in polymers, water of hydration in inorganic materials, and, finally, decomposition of the material.

In this work, TGA analysis were carried out in order to gather thermal stability information of the materials prepared.

2.1.6 Nitrogen adsorption

Nitrogen sorption measurements were performed on a Quantachrome Nova 4000e (Quantachrome Corporation, Boynton Beach, FL) automatic adsorption instrument. Prior to measurements, 100-150 mg of the samples was heated at 40-60°C under high vacuum (10-5 Pa) for at least 12 hours. The specific surface areas (S_A) were evaluated using the BET method, the specific pore volumes (V_p) following the Gurvitch method and the average pore diameter (D_p) using the BJH theory applied to the desorption branch of the isotherm [4].

2.2 Chromatographic conditions for the analysis

2.2.1 HPLC-UV

The HPLC measurements were carried out on Hewlett-Packard 1100 instruments (Agilent Technology, Waldbronn, Germany). Chromatographic separation of the peptides was performed on an Luna C18 (155 mm× 4.6mm I.D., 5µm) HPLC column protected by an RP18 guard column (4.0mm×3.0mm I.D., 5µm), both from Phenomenex (Torrance, CA,USA).

A gradient program was used with the mobile phase, combining solvent A (H₂O/MeOH (80:20) (0.1% TFA)) and solvent B (MeOH/H₂O (80:20) (0.1% TFA)) as follows: 60% B, (20 min). The flow rate was constant to 1 mL/min. Column temperature was kept at room temperature. The injection volume was 100 µL and all the compounds eluted within 16 min. The diode array detector wavelength was set at 205 nm all peptides. Quantification was performed using external calibration peak area measurements. Linear calibration graphs were obtained in the 1.5–50 mg/L range for all the peptides ($r^2 > 0.999$).

2.2.2 LC-MS/MS analysis

The chromatographic system consisted of an Ultimate 3000 systems pump, a WPS3000RS autosampler and a Ultimate 3000 flow manager. The LC system was controlled by Chromeleon v. 6.80 SR6 (all Dionex corp. Sunnyvale, CA, USA). Chromatographic separation was carried out on a Aquasil C18 Guard Cartridge column with average pore size

of 100 Å, particle diameter of 5 µm and column dimensions of 10 mm × 1 mm i.d., and Aquasil C18 analytical column with average pore size of 100 Å, particle diameter of 3 µm and column dimensions of 50 mm × 1 mm i.d. (both guard and analytical column: Thermo Scientific, Rockford, IL, USA).

The injection volume was 20 µL and the flow rate 40 µL/min during all analyses. A gradient elution was performed using the following conditions: mobile phase (A) consisted of 20 mM formic acid and ACN (99:1) and mobile phase (B) of 20 mM formic acid and ACN (1:99). The composition was changed as follows: 100 % of mobile phase A was kept constant for 1 min and then a linear gradient was run up from 0 to 85% mobile phase B in 29 min. A program, for wash and equilibration of the column, was executed after each analysis with injection of 10 µL mobile phase A. The column was then washed with 90 % mobile phase B for at least 3 column volumes and regenerated with 100 % mobile phase A for at least 10 column volumes.

A TSQ Quantum Access MS-detector (Thermo Scientific) was used as mass spectrometer. Data acquisition and processing was carried by Xcalibur™ version 2.0.7 software (Thermo Scientific). The mass spectrometer was operated in the positive ionization mode with an ESI as interface. The peptides were detected in the multi reaction monitoring (MRM) mode. The following transitions were monitored 408.2→272.6, 544.4 for LSAPGSQR and 485.8→630.3, 743.4 and 489.9→638.3, 751.4 for NLLGLIEAK.

2.3 Binding experiments

2.3.1 Single point rebinding

The binding properties were assessed using batch equilibrium partitioning experiments. A small amount of polymer ($m_{polymer}$) is allowed to equilibrate for 24h in a solution of the target analyte. The supernatant solutions were analyzed using a Hewlett-Packard HP 1100 instrument (Agilent Technologies, Waldbronn, Germany) equipped with a UV detector, an autosampler and a commercially available column (Phenomenex Luna C-18, 125×4.6 mm).

The results of these experiments are expected to provide information on the nature of the imprinted sites. Two values were calculated to evaluate the MIPs. The binding capacity (Q) is defined as µmol of substrate bound per 1 g of polymers, and calculated by the change of NLLGLIEAK concentration after and before adsorption.

The amount of NLLGLIEAK bound to MIP and NIP were tested under the same conditions by the following formula:

$$Q_{bound} = \frac{(C_{initial} - C_{free}) \cdot V_T}{m_{polymer}} \quad \text{Eq. 2.5}$$

Where $m_{polymer}$ is the mass of polymer (g), V_T (L) is the total volume of the target analyte solution, $C_{initial}$ (mg/L) is the initial target analyte concentration, C_{free} (mg/L) is the final target analyte concentration in the supernatant

And the imprinting factor (IF) was calculated as the ratio $IF = \frac{Q_{MIP}}{Q_{NIP}}$ When an $IF > 1$ indicates that an imprinting effect exists.

2.3.2 Determination of the binding capacity

Adsorption isotherms can yield important information concerning binding energies, modes of binding and site distributions in the interactions of small molecule ligands with receptors. In the batch rebinding studies, a soluble ligand interacts with the binding sites in a solid adsorbent, i.e. the MIP or NIP. The adsorption isotherms are then simply plots of equilibrium concentration of bound ligand versus concentration of free ligand [5].

The isotherms can be fitted using various models depending on the range of concentrations investigated and the heterogeneity of the binding sites [6]. Due to the properties of the MIPs investigated in this work, and the low concentrations used in the rebinding studies only the Freundlich model has been used to fit the isotherms,

$$B = aF^m \quad \text{Eq. 2.6}$$

Where B is the concentration of bound ligand, F the concentration of free ligand and a and m the parameters describing the power function. The parameter m is of particular importance since it represents the heterogeneity index of the polymer. This parameter ranges from 1 (homogeneous samples) to 0 (heterogeneous samples). Moreover, with the use of a and m it is possible to characterize the affinity distribution of the polymer by calculating the average affinity constant, K , and the average number of binding sites, N , as described in [5].

$$K = \left(\frac{m}{m-1} \right) \frac{K_1^{1-m} - K_2^{1-m}}{K_1^{-m} - K_2^{-m}} \quad \text{Eq. 2.7}$$

$$N = a(1-m^2)(K_1^{-m} - K_2^{-m}) \quad \text{Eq. 2.8}$$

Where K_1 and K_2 that can be calculated from the experimental maximum and minimum free analyte concentrations (F_{\min} and F_{\max}) and the relationships $K_1 = K_{\min} = 1/F_{\max}$ and $K_2 = K_{\max} = 1/F_{\min}$.

Bibliography

- [1] Rampey.A.M., Umpleby.R.J., Rushton.G.T., Iseman.J., Shah.R.N. and Shimizu.K.D, *Anal.Chem*, vol. 76, no. 4, pp. 1123-1133, 2004.
- [2] Yan.M. and Ramström.O, *Molecularly Imprinted Materials: Science and Technology*, New York: Marcel Dekker, 2005.
- [3] Wulff.M, *Thermochimica Acta*, vol. 419, pp. 291-294, 2004.
- [4] Landry.M.R, *Thermochimica Acta*, vol. 433, pp. 27-50, 2005.
- [5] Wheeler.A, *Catalysis*, New York: Reinhold Pub.Corp, 1955.
- [6] Aureliano.C.S.A, *Development of hierarchically imprinted mesoporous polymer beads for biologically active compounds*, PhD thesis at Technische Universität Dortmund, 2010.

Chapter 3

Mini-molecularly imprinted polymers libraries for targeting NLLGLIEAK

3.1 Abstract

Three libraries of molecularly imprinted polymers (MIPs) at mini-scale (mini-MIPs) for the peptide NLLGLIEAK have been prepared using high throughput synthesis (HTS). The imprinted and their corresponding non-imprinted polymers have been prepared using bulk polymerization. The target peptide, NLLGLIEAK is found in zwitterions form in aqueous solvent, which should carry two positive and two negative charges in neutral buffers. Due to this character it was decided to attempt two different imprinting approaches targeting either the amino groups by H-NLLGLIEAK-NH₂ (T1) and H-NLLGLIEAK-OEt (T3) or the carboxylic acid groups by Z-NLLGLIEA-Nle-OH (T2).

The effects of monomers, crosslinkers, porogens, and templates on adsorption selectivity for NLLGLIEAK were investigated and optimized. The first library (Library 1) was made to optimize the monomer-composition and the amount of crosslinker; based on these results, the second library (Library 2) was prepared in order to further make sure the effect of crosslinkers type and monomers on the affinity of polymer in addition to that, the functional monomer N-3, 5-bis (trifluoromethyl)-phenyl-N'-4-vinylphenylurea (TFU) is used to form a stronger bond with deprotonated carboxylic acid of half library. The third Library (Library 3) was prepared to evaluate the best template, the best porogen and the best level of crosslinking in N-(2-aminoethyl) methacrylamide hydrochloride/divinylbenzene (EAMA/DVB) system for successful imprinting.

The binding affinities of the polymers from the libraries were investigated by static binding experiments and in the solid phase extraction mode (SPE). The optimized polymer was prepared by using H-NLLGLIEAK-OEt (T3), EAMA and DVB as template, monomer and

crosslinker, respectively. The optimum molar ratio of the latter was found to be 0.04/4.74/24. The resulting molecularly imprinted polymer has shown capability of selectively binding the NLLGLIEAK in aqueous media. Therefore, this composition was used to prepare MIPs in a scaled-up reaction, as will be shown in Chapter 4.

3.2 Introduction

Design of a new MIP system suitable for a specific template molecule often requires a lot of time and work for synthesis, changing various experimental parameters, washing and testing, until finding the optimal conditions.

A large number of polymers are then needed to be synthesized. Therefore, combinatorial chemistry has been recently adopted in order to accelerate the optimization of MIPs to attain the desired performance [1] [2]. Sellergren [2] introduced a high-throughput synthesis and screening (HTS) system in a 96-well plate format that allows rapid optimization and fine tuning of the molecular recognition properties of MIPs library by the use of filter plates for rapid template removal and a multifunctional plate reader with a parallel analysis of every polymer.

The main object of this work is to find a specific molecularly imprinted polymer to NLLGLIEAK. With this purpose a design of a library was developed and the most relevant parameters involved in the specific recognition of were optimized such as monomers, crosslinkers, porogens and the ratio of every compound involved.

By reducing the batch size of conventional imprinting, the rapid synthesis and screening of a large variety of MIPs becomes possible. Thus, significant time saving can be made by preparing only 50 mg of imprinted polymer (mini-MIPs) on the bottom of small vials or of 96-well plates. By preparing a library of mini-MIPs, different parameters can be studied like incorporation of different monomers, different crosslinkers as well as the crosslinking-level and the porogen.

3.3 Methodology of polymer design

The molecular imprinting approach has recently been applied for the construction of peptide receptors. In this case, the approach involves formation of a complex between functional monomers and the target molecule (template/analyte) in an appropriate solution, and cross-links the complex by polymerization process. Following the removal of the template by

washing, binding sites (imprints) are left within the polymer with a structure, which is complementary to the template molecule [3] [4]. In theory, MIPs can be prepared for any kind of substance including drugs [5], nucleic acids [6], proteins [7], peptide [8] [9] and cells [10]. Design and synthesis of artificial receptor molecules have been a central research area for understanding the molecular recognition phenomena in biological systems and for developing novel materials mimicking biological functions usable in analytical application [11]. A key in this development is the identification and optimization of the main factors affecting structure and molecular recognition properties of the material. There are several important points to consider when designing an imprinted polymer. Obviously, one of the essential parameters is the capacity for specific interactions between the functional monomers and the template. Not only does one need to choose the appropriate monomer type, the monomer to template ratio must also be optimized. A ratio too small will not create enough binding sites, while a ratio too high may increase non specific adsorption. Another important consideration is the type and amount of crosslinking in comparison to the functional monomers. An optimization of these parameters can be achieved by scaling down the molecularly imprinted polymer (MIP) synthesis. This allows rapid screening for the recognition properties of large numbers of materials (mini-MIPs).

Synthetic polymers capable of binding NLLGLIEAK were selectively prepared by molecular imprinting. A combinatorial approach was employed using an automated polymer preparation system for optimization of different parameters.

We here reported three libraries which have been prepared using a down-scaled polymer synthesis. The first library (Library 1) was made to optimize the monomer-composition and the amount of crosslinkers; based on these results, the second library (Library 2) was prepared in order to further make sure the effect of crosslinkers type and monomers on the affinity of polymer, in addition to that, the functional monomer TFU is used to form a stronger bond with deprotonated carboxylic acid of half library. The third Library (Library 3) was prepared to evaluate the best template, the best porogen and the best level of crosslinking in EAMA/DVB system for successful imprinting.

3.4 Template, monomer, and crosslinker

Template

In most cases, the template is the target molecule that is to be selectively retained by MIP. For expensive templates, in case of problems with the solubility or insufficient template removal, a structural analog can be used as template for the synthesis in order to decrease the cost of the material. This dummy molecule must be similar to the target analyte in terms of shape, size and functionalities. The resulting MIP should have the ability to bind the target analyte. The dummy approach is also used to avoid the risk of residual template leaking from the polymer and causing erroneous results, particularly in molecularly imprinted solid phase extraction (MISPE) applied to the trace determination of compounds [12].

The MIPs developed in this work were designed aiming at the selective binding of trace amounts of the peptide NLLGLIEAK (Figure 3.1), in buffered media, mimicking the working conditions in serum for analyzing the protein ProGRP.

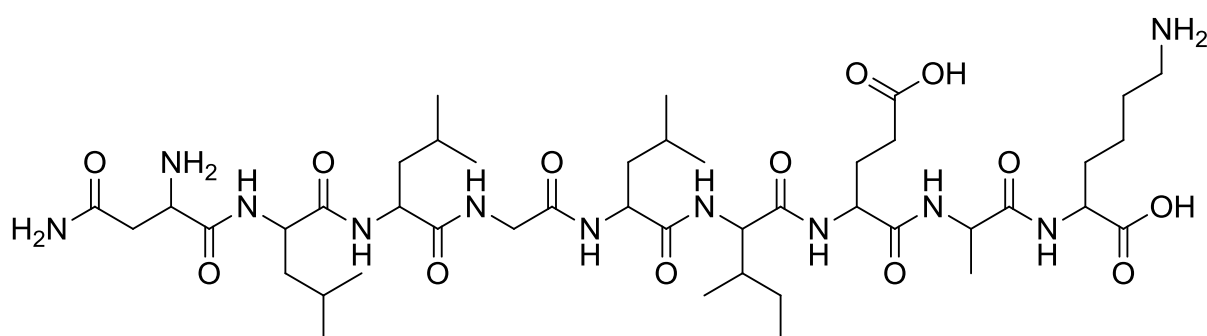


Figure 3.1: Chemical structures of the target peptide (NLLGLIEAK).

The target peptide, NLLGLIEAK is found in zwitterions form in aqueous solvent, which should carry two positive and two negative charges in neutral buffers. NLLGLIEAK has 9 amino acids of which K is basic. The E is acidic and N is polar, while the other amino acids are hydrophobic. Moreover contains a hydrophobic part sequence near the N-terminus and a more hydrophilic C-terminus.

In most cases, the template is the target molecule that is to be selectively retained by MIP. However sometimes in order to avoid problems associated to the use of the template molecule as toxicity, high costs and bleeding effect (especially in analysis where the LOD is extremely low, and MIPs are applied to the trace determination of compounds) [12], a structural analogue can be used as template for the synthesis of the MIP. This dummy molecule must be

similar to the target analyte in terms of shape, size and functionalities. Thus, the resulting MIP should have the ability to bind the target analyte.

Due to the ampholytic character it was decided to attempt two different imprinting approaches targeting either the amino groups by H-NLLGLIEAK-NH₂ (T1) and H-NLLGLIEAK-OEt (T3) or the carboxylic acid groups by Z-NLLGLIEA-Nle-OH (T2).

The design of T1 and T3 was based on structural analogy (crossreactivity) with the target peptide and solubility in imprinting solvents.

The T2 was chosen based on the expected solubility and affinity for the EAMA monomers (see below). The T2 solubility should be enhanced by removal of the basic side chain at the C-terminus, since these compete for the negative carboxyl groups. Therefore a near isosteric norleucine (Nle) was replacing the C-terminal Lysine and the N-terminus was benzyloxycarbonyl (Z) protected.

As can be seen in Table 3.1, the target peptide and templates are all amphiphilic molecules, *i.e.* they have some hydrophilic and some hydrophobic parts, with a net zero or unit negative charge.

Table 3.1: The templates used in the libraries of imprinted polymers for the peptide NLLGLIEAK

Peptide (Abbreviation)	Chemical Formula	Mwt	pI [§]	Charge	Hydrophobicity		Sequence Composition			
					pH 2.0	pH 6.8	Acidic	Neutral	Basic	Hydrophobic
H- NLLGLIEAK- NH₂ (T1)	C ₄₄ H ₈₀ N ₁₂ O ₁₂	969.21	10.28	+1	41.4	38.3	11.1	22.2	11.1	55.5
Z-NLLGLIEA- Nle-OH (T2)	C ₅₂ H ₈₄ N ₁₀ O ₁₅	1089.27	7.95	-2	51.7	46.0	12.5	25.0	0	62.5
H- NLLGLIEAK- OEt (T3)	C ₄₆ H ₈₃ N ₁₁ O ₁₃	998.24	10.28	+1	41.4	38.3	11.1	22.2	11.1	55.5
NLLGLIEAK (T)	C ₄₄ H ₇₉ N ₁₁ O ₁₃	970.24	6.99	0	41.9	38.3	11.1	22.2	11.1	55.5

[§] Isoelectric point

There are two major points to consider in the choice of the template: the template needs to have a reasonable solubility in the polymerization mixture and it should be able to form a stable complex with the monomers before polymerization.

The range of solvents that can be used with peptide templates is limited due to their low solubility in hydrophobic solvents [13]. The solubility of templates in various organic solvents to form 8.0 mg/mL has been evaluated using the polymerization protocol to test whether these templates were suitable for imprinting or not. The solubility of the templates

was checked as shown in Table 3.2. The templates were shown to be soluble in DMSO, DMF, MeOH and ACN/MeOH (1:1) at the high concentration levels necessary for imprinting. Whilst ACN is the most common solvent for preparing MIPs, it was not capable of dissolving the templates at 8.0 mg/mL, hence an ACN mixture with MeOH, DMF and DMSO in addition to pure DMSO were chosen as binary solvent for preparing the libraries.

Table 3.2: Templates solubility tests.

Template	Solvent	mg/mL	Note
T1	DMSO	166.7	Soluble
T1	DMF	18.0	Soluble
T1	MeOH	11.0	Soluble
T1	ACN/MeOH (1:1)	9.0	Soluble
T1	Toluene	7.3	Soluble
T1	THF	1.6	Cloudy, precipitated
T1	ACN	1.0	Cloudy, precipitated
T2	DMSO	22.0	Slightly soluble
T3	DMSO	250.0	Soluble

Monomers

A different library of functional monomers was selected for all possible interactions with the template. It is clearly very important to match the functionality of the template with the functionality of the functional monomer in a complementary fashion (e.g. H-bond donor with H-bond acceptor) in order to maximize the complex formation and thus the imprinting effect. The correct arrangement of functional monomers around the target molecule is one of the most important aspects of this technique. When designing an imprinting procedure, the choice of functional monomers is usually based on complementarity. For example, if the target molecule is a basic compound, the functional monomers should be acidic or if the target is a hydrogen bond donor, the functional monomer should be a hydrogen-bond acceptor.

Eight functional monomers were chosen with respect to the nature of the template. These included monomers for hydrogen bonding; neutral and acidic monomers (HEMA, TFU, MAA and TFMAA) as well as basic and cationic monomers (DEAEMA, 4-VPy, and EAMA) are targeting the peptide backbone and the C-terminal carboxylic acid. The urea monomer in particular is capable of forming strong, directed hydrogen bonds in polar media. The most successful monomer combinations will be taken as starting point for further screening experiments (i.e. optimization of crosslinker and/or porogen) (Figure 3.2).

The most widely applied functional monomer in non-covalent molecular imprinting is MAA. It has been shown to interact via ionic interactions with amines on the print molecules and via

hydrogen bonds with amides, carbamates and carboxyls on the print molecules [14]. The introduction of 4-VPy as a functional monomer in non-covalent molecular imprinting made ionic interactions between the recognition sites of the polymers and print molecules containing the carboxyl group possible [14]. TFMAA for targeting basic amino acid K while the basic monomer DEAEMA for targeting the acidic amino acid E. HEMA can be used with templates that are insoluble in non polar organic solvents or the polymers that can work in aqueous media, since HEMA contains a hydrophilic OH-group give the polymer matrix the possibility to swell in aqueous media [15].

The cationic EAMA monomer and the DVB crosslinker are targeting the hydrophobic amino acids.

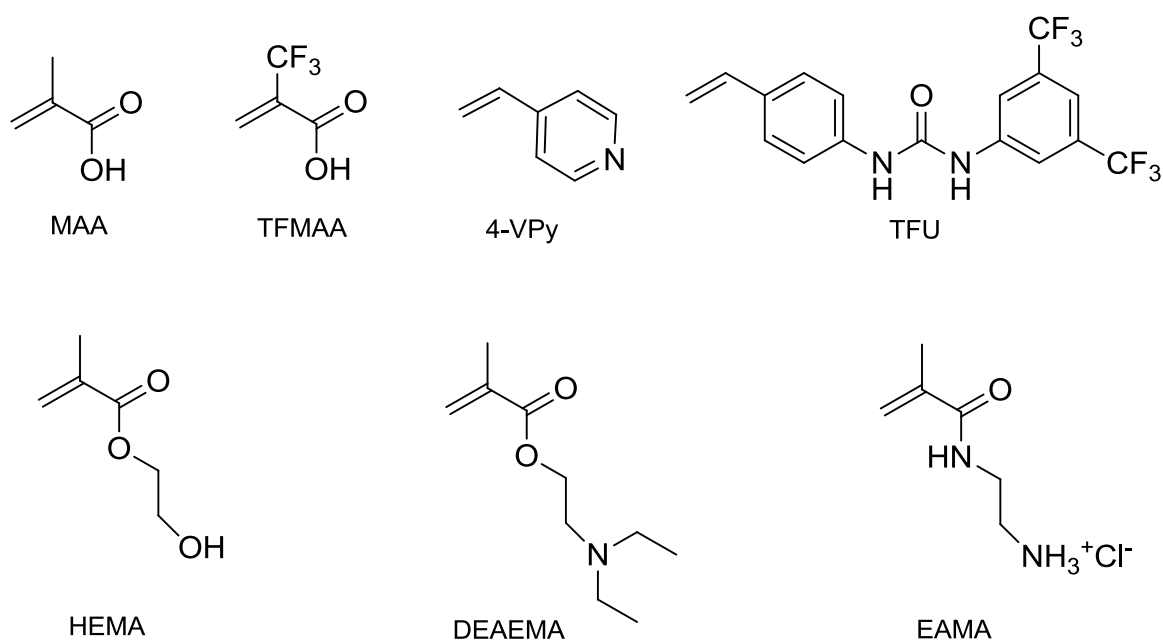


Figure 3.2: Chemical structures of the functional monomers used in the libraries of imprinted polymers for the **NLLGLIEAK**, MAA: methacrylic acid; TFMAA: trifluoro methacrylic acid; 4-VPy: 4 vinylpyridine; TFU: N-3,5-bis(trifluoromethyl)-phenyl-N'-4-vinylphenylurea. HEMA: 2-hydroxyethyl methacrylate; DEAEMA: diethylaminoethyl methacrylate; EAMA: N-(2-aminoethyl) methacrylamide hydrochloride.

Crosslinkers

Several molecules containing two or more polymerizable groups have been used as cross-linking monomers in molecular imprinting. The purpose of the crosslinker is to control the morphology of the polymer matrix, whether it is gel-type, macroporous or a micro-gel powder, to stabilize the imprinted binding site and to support the mechanical stability to the polymer matrix [16]. The selectivity is greatly influenced by the kind and amount of cross-linking agent used in the synthesis of the imprinted polymer. However, in a well known and common recipe the molar ratio between template, functional monomer and the crosslinker is 1:4:20 [17] which can be varied from one system to another. In this study, three crosslinker percentages were studied, 41% and 71% in library 1, 71% in library 2 and 71%, 83% in library 3.

Thus, in order to investigate the influence of crosslinker on the target affinity, the crosslinkers, shown in Figure 3.3, were selected for the imprinting of the NLLGLIEAK and ranged in polarity from polar (PETRA, NOBE), moderately polar (EDMA) to apolar (DVB).

The EDMA is among the most commonly used crosslinkers for methacrylate based systems. PETRA is a trifunctional polar crosslinker and it would give hydrophilic surface properties to the polymer and thereby reduce non-specific hydrophobic binding in aqueous systems. This crosslinker has shown to be superior to EDMA-based polymers for the extraction of caffeic acid [18] and riboflavin [19] from water-based samples.

NOBE was found to be capable to form hydrogen bonding in the absence of any other functional monomer; the amide functionality interacts sufficiently with most templates, with the only exception of amines, to afford molecular recognition without the need of introducing any other functional monomer [20].

On the other hand, DVB lacks the hydrogen bonding and can only establish $\pi - \pi$ interactions with the template and it is known to enhance the rigidity of the polymer chains [18].

Mini-molecularly imprinted polymers libraries for targeting NLLGLIEAK

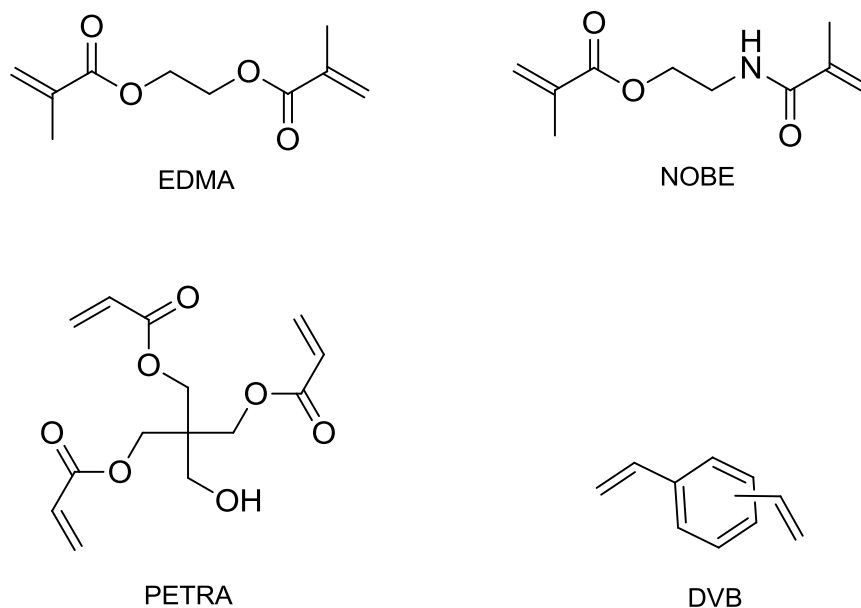


Figure 3.3: Chemical structures of the crosslinking agents used in the libraries of imprinted polymers for the NLLGLIEAK, EDMA: ethylene glycol dimethylacrylate; NOBE: N, O-bismethacryloyl ethanolamine; PETRA: pentaerythritol triacrylate; DVB: divinylbenzene.

Solvents as porogen

In principle, the choice of solvents depends on the polarity and solubility of the template, the monomer, the crosslinker and the initiator. Solvents provide the porous structure of the imprinted polymers, for this reason it is common to refer to the solvents as the porogen. The porogen has multiple roles; it influences the type and the strength of the interactions occurring in the prepolymerization mixture before polymerization. The interactions are strongly dependent on the polarity and the dissociating power of the solvent. In the example of a MIP composed of EDMA and MAA, polymerized around atrazine, the best performance was obtained with fairly apolar solvents such as toluene and dichloromethane [21]. This helps to control the physical state (morphology, pore size distribution, pore structure, swellability and toughness) for instance, the use of acetonitrile as solvent in acrylate networks leads to a more macroporous structure than chloroform [22].

The solvents applied for the polymerization in this work were chosen due to the nature of the templates and monomers solubility, ACN/MeOH (1:1), and ACN/DMF (1:1), were used for preparing library 1 and library 2, respectively. And ACN/DMSO (1:1) and DMSO were used for preparing library 3.

3.5 High Throughput Screening

Facing the challenge of designing and synthesizing a molecularly imprinted polymer, one needs to consider many variables affecting the material structure and molecular recognition properties. These variables can be the nature of template, the type and concentration of functional monomer, crosslinker or solvent of the polymerization. This can be achieved by scaling down the synthesis of the molecularly imprinted polymer to about 50 mg of material (mini-MIPs) at the bottom of small vials or wells of 96-well plates, which offer the opportunity of in situ batch rebinding evaluation.

In the present study, a semi automated liquid-handling robot was used for the rapid dispensing of monomers, crosslinkers, templates, solvents and initiators into the reaction vessels of a 96-well plate (Figure 3.4).

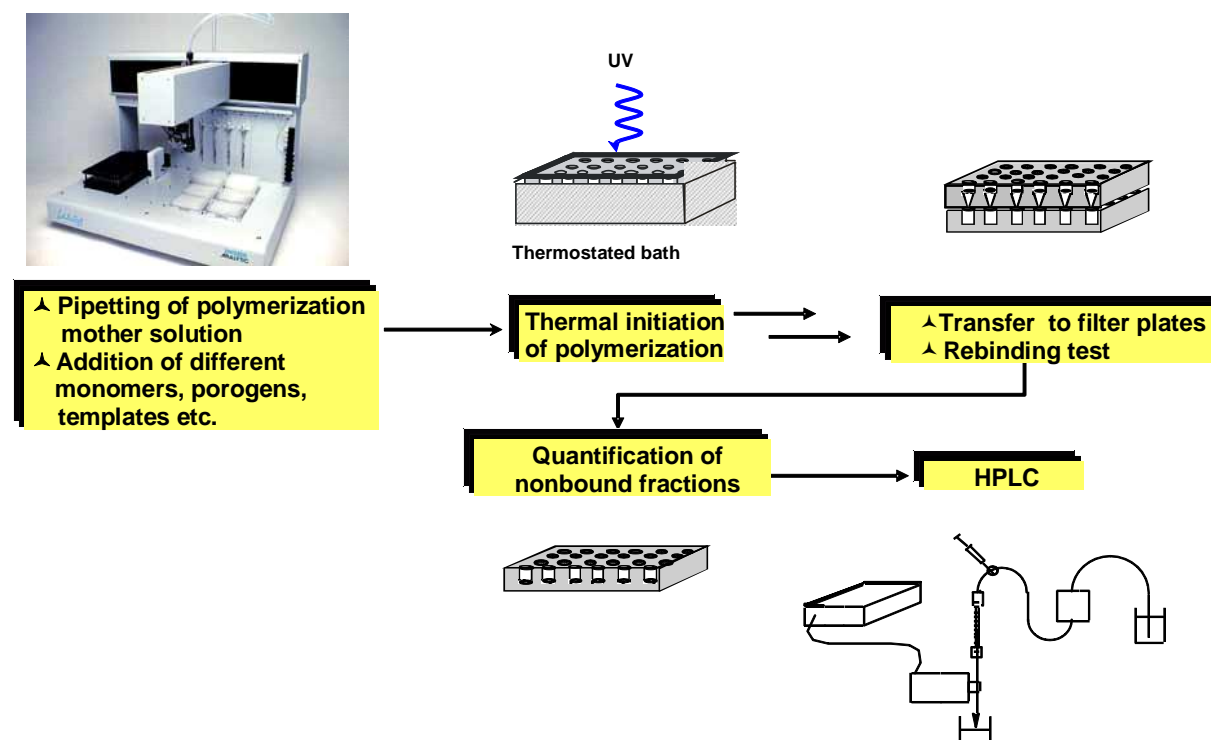


Figure 3.4: Schematic representation of the mini-MIPs library synthesis and evaluation [2]

Three libraries of 96 polymers each were synthesized by thermal polymerization at 40°C and the obtained polymers were transferred to a filter plate for testing. The rebinding capacity was then evaluated in the batch mode by quantifying the non-bound fractions of the template at equilibrium using HPLC measurements. Figure 3.5 shows an example of 96-well library before washing and grinding and after washing the template.

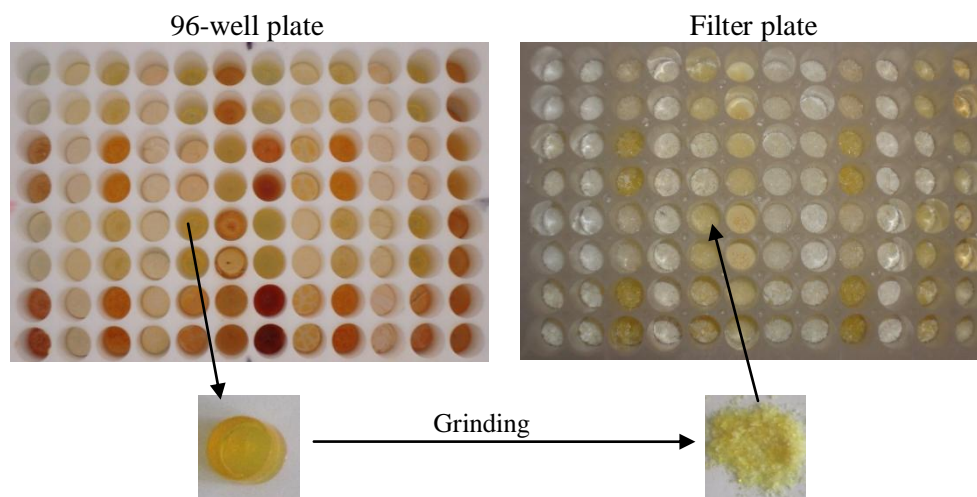


Figure 3.5: Left Top: Photograph showing the 96-well plate before washing. Right Top: Photograph showing filter plate after washing. Bottom: Photograph illustrating grinding the polymer and transferred to filter plate.

Although this combinatorial approach provided an improved method over the conventional trial-and-error approach in developing selective MIPs, the researcher noted that because of the slow HPLC for the binding studies, the process was still time consuming and did not allow for the development of a high throughput combinatorial library [23] [24].

To combat this problem, Takeuchi et al. [25] attempted to develop a faster screening method that would allow evaluation of binding capacity by fluorescence measurements using a microplate reader. But the drawback of this method needs a non-volatile porogen and a fluorescent analyte.

Also we noticed few drawbacks of combinatorial approach:

1. Occurrence of large error from the small scale preparation (e.g. 50 mg) of polymers. For instance from pipette and balance measurements.
2. The process is tedious and time-consuming. The particles obtained after grinding and sieving results in the different particle sizes and morphology.
3. Consumes longer time for the template removal and also high vacuum sometime destroys the wall of the 96 filter plate.
4. If the particles are not dried enough; this will lead to the larger error in the rebinding calculation.

The other way round the most privilege of using mini-scale is:

1. Saving the time by quick preparing 96 polymers to study different parameters.

2. Consumes less amount of peptide template (e.g. 50 mg) to prepare one library, especially the peptide price is costly.

3.6 Design and synthesis

3.6.1 Library 1

A first screening to select the functional monomers, crosslinker type and ratio was carried out in library 1. This library included 6 different monomers (MAA, TFMAA, 4-PV_y, HEMA, DEAEMA, and TFU) and three different crosslinkers (EDMA, PETRA and NOBE). ACN/MeOH (1:1) was used as a porogen. They were used in developing NLLGLIEAK responsive MIPs using H-NLLGLIEAK-NH₂ as template for preparing imprinted and their corresponding nonimprinted polymers.

The designed compositions of Library 1 are described in Table 3.3. Columns 1-3, 7-9 correspond to the NIPs and columns 4-6, 10-12 correspond to the MIPs. Rows A-F (1-6) were synthesized using a lower crosslinking level (T1/FM/CL, 0.04/14/10), Rows A-F (7-12) were synthesized using a higher crosslinking level using the molar ratio of T1/FM/CL (0.04/7/17). When the HEMA was added to MAA as a co-monomer the molar ratio changed to (T1/MAA/HEMA/CL, 0.04/7/7/10) in case low crosslinking level and to (T1/MAA/HEMA/CL, 0.04/3.5/3.5/17) in case higher crosslinking level.

Rows G and H correspond to polymers prepared with 71% crosslinkers using MAA, DEAEMA, and 4-VPy using the molar ratio of T1/FM/CL (0.04/7/17) (G1 to H6) and TFU and pentamethyl piperidine (PMP) (1 equivalent to the template) was added to same monomer (G7-H12) as a co-monomer using the molar ratio of (T1/TFU/FM/CL, 0.04/0.04/7/17).

The functional monomer TFU is known to form a stronger bond with anions. Therefore, PMP was added to the pre-polymerization solutions in rows G7 to H12 for the deprotonation of the carboxylic acid of the template.

The composition of each mini-MIP with lower crosslinking level (41%) was: template (0.8 μmol), functional monomer (280 μmol) and crosslinker (200 μmol). While the higher crosslinking level (71%) was: template (0.8 μmol), functional monomer (140 μmol), and crosslinker (340 μmol). The non-imprinted polymers were made in the same manner with the omission of the template molecule.

Mini-molecularly imprinted polymers libraries for targeting NLLGLIEAK

Table 3.3: Design of the library 1: Columns 1-3, 7-9 correspond to the NIPs and 4-6, 10-12 correspond to the MIPs with different crosslinkers type EDMA, PETRA, and NOBE. Columns 1 to 6 with 41% crosslinkers while columns 7 to 12 with 71% crosslinkers. Rows G and H correspond to polymers prepared with 71% crosslinkers using MAA, DEAEMA, and 4-VPy (G1 to H6) and same monomer with TFU (G7-H12).

Library 1	41 %CL						71 %CL					
	NIP			MIP			NIP			MIP		
	1	2	3	4	5	6	7	8	9	10	11	12
A	EDMA	EDMA	EDMA	EDMA	EDMA	EDMA	EDMA	EDMA	EDMA	EDMA	EDMA	EDMA
B	MAA	MAA-HEMA	TFMAA	MAA	MAA-HEMA	TFMAA	MAA	MAA-HEMA	TFMAA	MAA	MAA-HEMA	TFMAA
C	PETRA	PETRA	PETRA	PETRA	PETRA	PETRA	PETRA	PETRA	PETRA	PETRA	PETRA	PETRA
D	MAA	MAA-HEMA	TFMAA	MAA	MAA-HEMA	TFMAA	MAA	MAA-HEMA	TFMAA	MAA	MAA-HEMA	TFMAA
E	NOBE	NOBE	NOBE	NOBE	NOBE	NOBE	NOBE	NOBE	NOBE	NOBE	NOBE	NOBE
F	MAA	MAA-HEMA	TFMAA	MAA	MAA-HEMA	TFMAA	MAA	MAA-HEMA	TFMAA	MAA	MAA-HEMA	TFMAA
G	EDMA	EDMA	EDMA	EDMA	EDMA	EDMA	EDMA	EDMA	EDMA	EDMA	EDMA	EDMA
H	MAA	DEAEMA	4-VPy	MAA	DEAEMA	4-VPy	MAA-TFU	DEAEMA-TFU	4-VPy-TFU	MAA-TFU	DEAEMA-U	4-VPy-TFU
	MAA	DEAEMA	4-VPy	MAA	DEAEMA	4-VPy	MAA-TFU	DEAEMA-TFU	4-VPy-TFU	MAA-TFU	DEAEMA-TFU	4-VPy-TFU

3.6.2 Library 2

The main difference between the first and the second library (see Table 3.4) was the use of ACN/DMF (1:1) as a porogen and the addition of the TFU monomer to half of the polymers in an equimolar ratio to the template, changing the final ratios of T1/TFU/FM/CL to 0.04/0.04/7/17. TFU and PMP (1 equivalent to the template) was added assuming it to engage in binary hydrogen bonding with the peptide carboxylate groups which would be favored by the use of a less polar solvent as porogen. In addition to that, the monomer EAMA and DVB crosslinker were used.

The designed compositions of Library 2 are described in Table 3.4. Columns 1-3, 7-9 correspond to the NIPs and columns 4-6, 10-12 correspond to the MIPs. Columns (4-6) were synthesized using crosslinking level (T1/FM/CL, 0.04/7/17), when TFU was added to columns (10-12) as a co-monomer the molar ratio changed to (T1/TFU/FM/CL, 0.04/0.04/7/17). And when the HEMA was added to TFMAA as a co-monomer the molar ratio changed to (T1/TFMAA/HEMA/CL, 0.04/3.5/3.5/17).

The composition of each mini-MIP was: template (0.8 μmol); functional monomer (140 μmol); crosslinker (340 μmol). The non-imprinted polymers were made in the same manner with the omission of the template molecule.

Table 3.4: Design of the library 2: Columns 1-3, 7-9 correspond to the NIPs and 4-6, 10-12 the MIPs with different crosslinkers type EDMA, PETRA, and DVB. Columns 7 to 12 correspond to polymers prepared with addition TFU monomer. Each column represents polymers prepared using identical functional monomers as indicated.

	NIP			MIP			NIP			MIP		
Library 2	1	2	3	4	5	6	7	8	9	10	11	12
A	EDMA	EDMA	PETRA	EDMA	EDMA	PETRA	EDMA	EDMA	PETRA	EDMA	EDMA	PETRA
	MAA	TFMAA	TFMAA	MAA	TFMAA	TFMAA	MAA-TFU	TFMAA-TFU	TFMAA-TFU	MAA-TFU	TFMAA-TFU	TFMAA-TFU
B	EDMA	EDMA	PETRA	EDMA	EDMA	PETRA	EDMA	EDMA	PETRA	EDMA	EDMA	PETRA
	MAA	TFMAA	TFMAA	MAA	TFMAA	TFMAA	MAA-TFU	TFMAA-TFU	TFMAA-TFU	MAA-TFU	TFMAA-TFU	TFMAA-TFU
C	EDMA	EDMA	PETRA	EDMA	EDMA	PETRA	EDMA	EDMA	PETRA	EDMA	EDMA	PETRA
	DEAEMA	4-VPy	DEAEMA	DEAEMA	4-VPy	DEAEMA	DEAEMA-TFU	4-VPy-TFU	DEAEMA-TFU	DEAEMA-TFU	4-VPy-TFU	DEAEMA-TFU
D	EDMA	EDMA	PETRA	EDMA	EDMA	PETRA	EDMA	EDMA	PETRA	EDMA	EDMA	PETRA
	DEAEMA	4-VPy	DEAEMA	DEAEMA	4-VPy	DEAEMA	DEAEMA-TFU	4-VPy-TFU	DEAEMA-TFU	DEAEMA-TFU	4-VPy-TFU	DEAEMA-TFU
E	DVB	DVB	DVB	DVB	DVB	DVB	DVB	DVB	DVB	DVB	DVB	DVB
	MAA	TFMAA	EAMA	MAA	TFMAA	EAMA	MAA-TFU	TFMAA-TFU	EAMA-TFU	MAA-TFU	TFMAA-TFU	EAMA-TFU
F	DVB	DVB	DVB	DVB	DVB	DVB	DVB	DVB	DVB	DVB	DVB	DVB
	MAA	TFMAA	EAMA	MAA	TFMAA	EAMA	MAA-TFU	TFMAA-TFU	EAMA-TFU	MAA-TFU	TFMAA-TFU	EAMA-TFU
G	DVB	DVB	DVB	DVB	DVB	DVB	DVB	DVB	DVB	DVB	DVB	DVB
	DEAEMA	4-VPy	TFMAA-HEMA	DEAEMA	4-VPy	TFMAA-HEMA	DEAEMA-TFU	4-VPy-TFU	TFMAA-HEMA-TFU	DEAEMA-TFU	4-VPy-TFU	TFMAA-HEMA-TFU
H	DVB	DVB	DVB	DVB	DVB	DVB	DVB	DVB	DVB	DVB	DVB	DVB
	DEAEMA	4-VPy	TFMAA-HEMA	DEAEMA	4-VPy	TFMAA-HEMA	DEAEMA-TFU	4-VPy-TFU	TFMAA-HEMA-TFU	DEAEMA-TFU	4-VPy-TFU	TFMAA-HEMA-TFU

In Both libraries a semi automated liquid-handling robot was used for rapid dispersion of monomers, template, solvent and initiator into the reaction vessels of a 96 well plate allowing the preparation of a library of 96 polymer, each about 50 mg, in 24 hour. Stock solutions and volumes dispensing from each stock solution of template, monomer, crosslinker, and initiator were initially prepared as shown in Table 3.12 (L1) and Table 3.13 (L2) in the experimental part of this chapter.

For comparison, NIPs (non-imprinted polymers without template) were made following the same procedure as for the MIPs and were prepared at the same time. In principle, the NIP is entirely analogous to the MIP except that there is no binding site within its porous structure. The NIP can therefore be used a benchmark for assessing the selectivity of the MIP such as recovery and breakthrough as reported in published paper.

3.6.3 Library 3

The purpose of library 3 was to evaluate the best template, the best porogen and the best level of crosslinking for successful imprinting. All polymers were made using DVB as crosslinkers, EAMA as monomer and one of the three templates T1, T2 and T3 was used to prepare the library. Thereby, T1, T2, and T3 corresponded to the N- or C-protected target sequences described in 3.4. The designed composition of library 3 is described in Table 3.5. The library can be divided into three subgroups, each containing one NIP and three MIPs imprinted with T1, T2 or T3, respectively. The first subgroup (polymers 1-4) was prepared by using ACN/

Mini-molecularly imprinted polymers libraries for targeting NLLGLIEAK

DMSO (1:1) as porogen while the other two subgroups were prepared in pure DMSO in order to improve the solubility and study the effect of porogen. Each polymer of the first two subgroups (P1-P8) was synthesized using the same molar ratio of Tx/FM/CL (0.04/7/17). The polymers of the third subgroup (P9-P12) were synthesized using a higher crosslinking level (T1/FM1/CL, 0.04/4.74/24).

The composition of each mini-MIP with lower crosslinking level (P1-P8) was: template (1.6 μmol), functional monomer (280 μmol), and crosslinker (670 μmol); and of mini-MIPs with higher crosslinking level (P9-P12) was: template (1.6 μmol), functional monomer (190 μmol) and crosslinker (960 μmol). The non-imprinted polymers were made in the same manner with the omission of the template molecule.

Stock solutions and volumes dispensing from each stock solution of template, monomer, crosslinker, and initiator were initially prepared as shown in Table 3.14 in the experimental part of this chapter.

Table 3.5: Design of the library 3.

Library 3	Template	Functional Monomer	Crosslinker	Porogen	T/FM/CL [§]
P1	T1	EAMA	DVB	DMSO/ACN	0.04/7/17
P2	T2	EAMA	DVB	DMSO/ACN	0.04/7/17
P3	T3	EAMA	DVB	DMSO/ACN	0.04/7/17
P4	-	EAMA	DVB	DMSO/ACN	-/7/17
P5	T1	EAMA	DVB	DMSO	0.04/7/17
P6	T2	EAMA	DVB	DMSO	0.04/7/17
P7	T3	EAMA	DVB	DMSO	0.04/7/17
P8	-	EAMA	DVB	DMSO	-/7/17
P9	T1	EAMA	DVB	DMSO	0.04/4.74/24
P10	T2	EAMA	DVB	DMSO	0.04/4.74/24
P11	T3	EAMA	DVB	DMSO	0.04/4.74/24
P12	-	EAMA	DVB	DMSO	-/4.74/24

[§] molar ratio

3.7 Results and Discussion

Preparation of MIP for peptide recognition is challenging as relatively few reports can be found in the literature. From the practical understanding of MIP development, a number of rules of thumb have emerged in the literatures that are helpful when developing particular MIPs. The synthesis of efficient MIPs requires the optimization of certain parameters by using HTS, different libraries can be prepared and different parameters can be studied.

3.7.1 Library 1

3.7.1.1 Rebinding results

The functional monomer is a very important parameter of any imprinting protocol. Therefore the main purpose followed by library 1 was focused on the search for a reasonably good combination of monomers to target the main functionalities of the given template. A porogen, ACN/MeOH (1:1) was capable of dissolving all the components used as polymerization diluent and EDMA, PETRA, and NOBE were the first choice of crosslinkers for this library. The most successful monomer combinations will be taken as starting points for other screening libraries.

The resulting polymers were evaluated according to their binding features in an equilibrium rebinding test. The percentage of template bound from the original amount of template in the solution was as a parameter to evaluate the goodness of the polymer. The binding percentage in Table 3.6 show that both EDMA and PETRA have high binding percentages which range between 40-90% in case of 71% crosslinker percentage ratio, while ranges between 10-60 % in case of 41% crosslinker percentage ratio. NOBE shows the binding percentage between 0-30 % in all cases except TFMAA-NOBE which was between 30-40%. Polymers prepared with MAA and basic monomer DEAEMA and 4-VPy with EDMA and NOBE crosslinker show low binding percentage and there is no difference in case with or without TFU monomer.

Since the uptake of template is depended on the amount of polymer used, dividing through the polymer mass converts is necessary to compare the ability of retention form every polymer. Table 3.7 shows the results from the same library in binding capacity scale, which is the amount bound per gram of polymer.

Mini-molecularly imprinted polymers libraries for targeting NLLGLIEAK

Table 3.6: Binding percentage for library 1 in HEPES buffer (0.1 M, pH 7.5) with NLLGLIEAK.

Library 1	41 %CL						71 %CL					
	NIP			MIP			NIP			MIP		
	1	2	3	4	5	6	7	8	9	10	11	12
A	EDMA	EDMA	EDMA									
B	EDMA	EDMA	EDMA									
C	PETRA	PETRA	PETRA									
D	PETRA	PETRA	PETRA									
E	NOBE	NOBE	NOBE									
F	NOBE	NOBE	NOBE									
G	EDMA	EDMA	EDMA									
H	NOBE	NOBE	NOBE									
	0-10%	10-20%	20-30%	30-40%	40-50%	50-60%	60-70%	70-80%	80-90%	90-100%		

Table 3.7: Capacity scale based on uptake data in Table 3.6.

Library 1	41 %CL						71 %CL					
	NIP			MIP			NIP			MIP		
	1	2	3	4	5	6	7	8	9	10	11	12
A	EDMA	EDMA	EDMA	EDMA	EDMA	EDMA	EDMA	EDMA	EDMA	EDMA	EDMA	EDMA
B	EDMA	EDMA	EDMA	EDMA	EDMA	EDMA	EDMA	EDMA	EDMA	EDMA	EDMA	EDMA
C	PETRA	PETRA	PETRA	PETRA	PETRA	PETRA	PETRA	PETRA	PETRA	PETRA	PETRA	PETRA
D	PETRA	PETRA	PETRA	PETRA	PETRA	PETRA	PETRA	PETRA	PETRA	PETRA	PETRA	PETRA
E	NOBE	NOBE	NOBE	NOBE	NOBE	NOBE	NOBE	NOBE	NOBE	NOBE	NOBE	NOBE
F	NOBE	NOBE	NOBE	NOBE	NOBE	NOBE	NOBE	NOBE	NOBE	NOBE	NOBE	NOBE
G	EDMA	EDMA	EDMA	EDMA	EDMA	EDMA	EDMA	EDMA	EDMA	EDMA	EDMA	EDMA
H	NOBE	NOBE	NOBE	NOBE	NOBE	NOBE	NOBE	NOBE	NOBE	NOBE	NOBE	NOBE
	0-0.07 $\mu\text{mol/g}$	0.07-0.14 $\mu\text{mol/g}$	0.14-0.21 $\mu\text{mol/g}$	0.21-0.28 $\mu\text{mol/g}$	0.28-0.35 $\mu\text{mol/g}$	0.35-0.42 $\mu\text{mol/g}$	0.42-0.49 $\mu\text{mol/g}$	0.49-0.56 $\mu\text{mol/g}$	0.56-0.63 $\mu\text{mol/g}$	0.63-0.70 $\mu\text{mol/g}$		

The rebinding results are plotted in more details in Figure 3.6 A. It shows that the rebinding capacity of polymers prepared with EDMA and PETRA is higher than that of ones prepared with NOBE. Moreover, when comparing the binding properties of the polymers made with MAA, MAA-HEMA, and TFMAA, a difference in binding capacity can be observed with increasing monomer acidity TFMAA > MAA > MAA-HEMA. However, the combination of these two monomers did not improve the binding capacity, but instead decreased the non-specific interaction in aqueous media because the hydroxyl groups of HEMA give a hydrophilic character to the polymer matrix [15].

Besides the capacity, the specificity of the binding also is an important factor. Therefore, the imprinting factors (IFs) were calculated and are also shown in Figure 3.6 B. It was found that

the imprinting factor for these polymers is around 1 (MIP and NIP bind the same amount of template) but the imprinting factor (IF) of polymers with EDMA is higher than of ones with PETRA.

Moreover, the binding properties of the polymers made with EDMA were compared at different levels of crosslinker 41% and 71%. No obvious effect was observed for different crosslinker percentages. In several single cases, MIPs made of 71% crosslinker percentage did have a better imprinting effect than others.

Some conclusions can be derived from results above. Some monomers seemed good candidates for T1: MIPs made of DEAEMA-EDMA, MAA-TFU-EDMA, and 4-VPy-TFU-EDMA, where the IF was 1.76, 1.23, and 1.65, respectively.

This result allows us to think about that a stable template: FM interaction is formed in the prepolymerization solution and the crosslinker ratio 71% was kept for the next assays.

Finally, in order to further make sure the effect of crosslinker type and monomer on the affinity of polymer, another library (Library 2) was prepared by using EDMA, PETRA, and DVB as crosslinker and DEAEMA, MAA, TFMAA, 4-VPy, EAMA, HEMA and TFU as monomers.

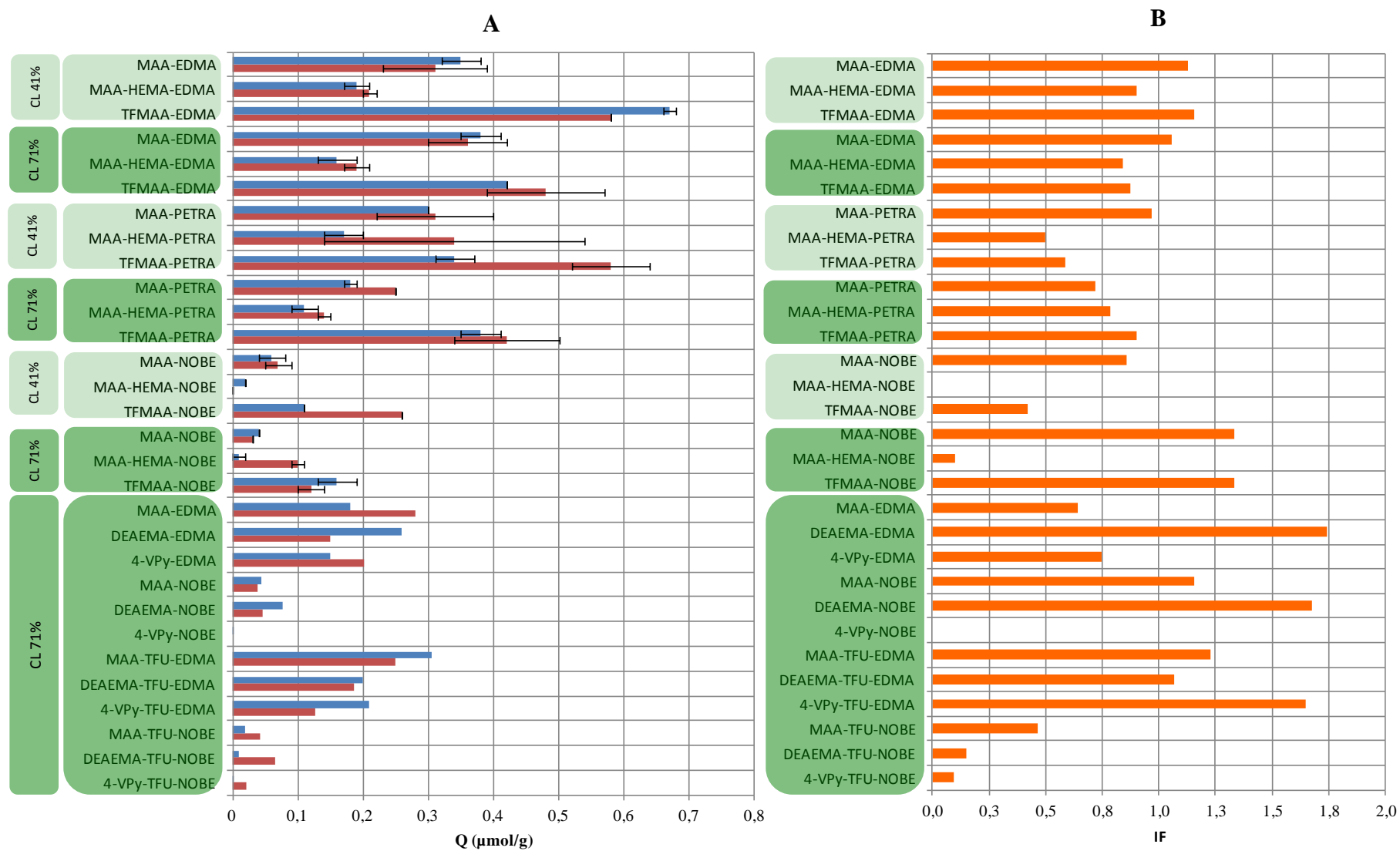


Figure 3.6: Binding capacity (A) and imprinting factors (B) for library 1 (■ MIP ■ NIP)

3.7.2 Library 2

3.7.2.1 Rebinding in dependence of the pH

In library 2, the rebinding test was done at pH 7.0 and pH 10.0. The latter pH was aimed in particular at study of the binding between the deprotonated carboxylic acid and TFU monomer, which was added to the right half of the plate. Binding percent and binding capacity results for both pH-values are shown in Table 3.8. As we have seen the results are reproducible and the binding percent higher than 50% in most cases. The final results are plotted in Figure 3.7 and Figure 3.8.

When we compared with the results for the both pH-values a general increase in binding for most of the polymers can be observed but without changing of IF. This means that the binding between template and TFU monomer is mainly of an unspecific nature.

In order to have a more detailed comparison of the different rebinding tests, the results were compared for the different crosslinkers separately.

EDMA Polymers

As it can be observed in Figure 3.7 and Figure 3.8, acidic monomer TFMAA and MAA showed higher binding capacity than basic monomer DEAEMA and 4-VPy. Moreover these polymers showed no significant change either in cases with TFU monomer or changing pH.

While by changing the pH from 7 to 10 no improvement of the IF was shown and it was around 1.

PETRA Polymers

For the DEAEMA polymer it can be observed in Figure 3.7 that the binding capacity was two times higher than TFMAA polymer. Interestingly, the binding capacity of TFMAA increased two times in pH 10. But the results showed no significant change of IF by changing the pH from 7 to 10, or with and without TFU monomer.

DVB Polymers

For the DVB polymers, in Figure 3.7 it can be observed that the binding capacity was increased in general, except in case of TFMAA at both pH. In comparison with EDMA the binding capacity of monomers MAA, DEMEA and 4-VPy was increased 2, 2.5 and 5 times.

Polymers EAMA-DVB, DEAMA-DVB, and TFMAA-HEMA-DVB showed higher binding and also a slightly higher IF. The imprinting factor of EAMA-DVB at pH 7 was 2.38 but decreased to 1.02 at pH 10. On the other hand DEAEMA-DVB showed 2.40 IF at pH 10 in

comparison to pH 7, where it was 1.32. But the imprinting factor of TFMAA-HEMA-DVB improved significantly at both pH (pH 7: 2.28, pH 10: 1.49) which is very promising for cross-selectivity applications. While by adding TFU monomer to second part of the library no improvement of binding capacity or IF was showed.

In all these cases it is illustrated that the crosslinker plays a very important role; the benzene ring in DVB may provide additional π - π interactions with the hydrophobic moiety of NLLGLIEAK, which will improve the MIP's binding performance in aqueous solvents, based on the before mentioned observations about the binding ability and the IF values the most promising polymers (EAMA-DVB, DEAEMA-DVB, TFMAA-HEMA-DVB).

For library 2 these polymers were selected and a molecularly imprinted solid phase extraction (MISPE) experiment was carried out over to for further comparison of their affinities and selectivities. The basic monomer DEAEMA provides ionic interaction especially at high pH. EAMA is cationic monomers which provide with DVB a cationic and hydrophobic interaction with NLLGLIEAK. An acidic functional monomer, TFMAA, was used to provide hydrogen bond interactions with C-terminal of NLLGLIEAK.

Table 3.8: Rebinding test for library 2. A: Binding percentage at pH 7, B: Capacity scale at pH 7 (HEPES buffer (0.1 M)), C: Binding percentage at pH 10, D: Capacity scale at pH 10 (NH₄Cl, NH₄OH buffer) with NLLGLIEAK.

A		NIP			MIP			NIP			MIP		
Library 2	1	2	3	4	5	6	7	8	9	10	11	12	
A	EDMA	EDMA	PETRA	EDMA	EDMA	PETRA	EDMA	EDMA	PETRA	EDMA	EDMA	PETRA	
B	MAA	TFMAA	TFMAA	MAA	TFMAA	TFMAA	MAA-TFU	TFMAA-TFU	TFMAA-TFU	MAA-TFU	TFMAA-TFU	TFMAA-TFU	
C	EDMA	EDMA	PETRA	EDMA	EDMA	PETRA	EDMA	EDMA	PETRA	EDMA	EDMA	PETRA	
D	DEAEMA	4-VPy	DEAEMA	DEAEMA	4-VPy	TFMAA	DEAEMA-TFU	4-VPy-TFU	DEAEMA-TFU	DEAEMA-TFU	4-VPy-TFU	DEAEMA-TFU	
E	DVB	DVB	DVB	DVB	DVB	DVB	DVB	DVB	DVB	DVB	DVB	DVB	
F	MAA	TFMAA	EAMA	MAA	MAA-HEMA	TFMAA	MAA-TFU	TFMAA-TFU	EAMA-TFU	MAA-TFU	TFMAA-TFU	EAMA-TFU	
G	DVB	DVB	DVB	DVB	DVB	DVB	DVB	DVB	DVB	DVB	DVB	DVB	
H	DEAEMA	4-VPy	TFMAA-HEMA	MAA	DEAEMA	4-VPy	DEAEMA-TFU	4-VPy-TFU	TFMAA-HEMA-TFU	DEAEMA-TFU	4-VPy-TFU	TFMAA-HEMA-TFU	
	0-10%	10-20%	20-30%	30-40%	40-50%	50-60%	60-70%	70-80%	80-90%	90-100%			
B		NIP			MIP			NIP			MIP		
Library 2	1	2	3	4	5	6	7	8	9	10	11	12	
A	EDMA	EDMA	PETRA	EDMA	EDMA	PETRA	EDMA	EDMA	PETRA	EDMA	EDMA	PETRA	
B	MAA	TFMAA	TFMAA	MAA	TFMAA	TFMAA	MAA-TFU	TFMAA-TFU	TFMAA-TFU	MAA-TFU	TFMAA-TFU	TFMAA-TFU	
C	EDMA	EDMA	PETRA	EDMA	EDMA	PETRA	EDMA	EDMA	PETRA	EDMA	EDMA	PETRA	
D	DEAEMA	4-VPy	DEAEMA	DEAEMA	4-VPy	TFMAA	DEAEMA-TFU	4-VPy-TFU	DEAEMA-TFU	DEAEMA-TFU	4-VPy-TFU	DEAEMA-TFU	
E	DVB	DVB	DVB	DVB	DVB	DVB	DVB	DVB	DVB	DVB	DVB	DVB	
F	MAA	TFMAA	EAMA	MAA	MAA-HEMA	TFMAA	MAA-TFU	TFMAA-TFU	EAMA-TFU	MAA-TFU	TFMAA-TFU	EAMA-TFU	
G	DVB	DVB	DVB	DVB	DVB	DVB	DVB	DVB	DVB	DVB	DVB	DVB	
H	DEAEMA	4-VPy	TFMAA-HEMA	MAA	DEAEMA	4-VPy	DEAEMA-TFU	4-VPy-TFU	TFMAA-HEMA-TFU	DEAEMA-TFU	4-VPy-TFU	TFMAA-HEMA-TFU	
	0-0.07 μmol/g	0.07-0.14 μmol/g	0.14-0.21 μmol/g	0.21-0.28 μmol/g	0.28-0.35 μmol/g	0.35-0.42 μmol/g	0.42-0.49 μmol/g	0.49-0.56 μmol/g	0.56-0.63 μmol/g	0.63-0.70 μmol/g			
C		NIP			MIP			NIP			MIP		
Library 2	1	2	3	4	5	6	7	8	9	10	11	12	
A	EDMA	EDMA	PETRA	EDMA	EDMA	PETRA	EDMA	EDMA	PETRA	EDMA	EDMA	PETRA	
B	MAA	TFMAA	TFMAA	MAA	TFMAA	TFMAA	MAA-TFU	TFMAA-TFU	TFMAA-TFU	MAA-TFU	TFMAA-TFU	TFMAA-TFU	
C	EDMA	EDMA	PETRA	EDMA	EDMA	PETRA	EDMA	EDMA	PETRA	EDMA	EDMA	PETRA	
D	DEAEMA	4-VPy	DEAEMA	DEAEMA	4-VPy	TFMAA	DEAEMA-TFU	4-VPy-TFU	DEAEMA-TFU	DEAEMA-TFU	4-VPy-TFU	DEAEMA-TFU	
E	DVB	DVB	DVB	DVB	DVB	DVB	DVB	DVB	DVB	DVB	DVB	DVB	
F	MAA	TFMAA	EAMA	MAA	MAA-HEMA	TFMAA	MAA-TFU	TFMAA-TFU	EAMA-TFU	MAA-TFU	TFMAA-TFU	EAMA-TFU	
G	DVB	DVB	DVB	DVB	DVB	DVB	DVB	DVB	DVB	DVB	DVB	DVB	
H	DEAEMA	4-VPy	TFMAA-HEMA	MAA	DEAEMA	4-VPy	DEAEMA-TFU	4-VPy-TFU	TFMAA-HEMA-TFU	DEAEMA-TFU	4-VPy-TFU	TFMAA-HEMA-TFU	
	0-10%	10-20%	20-30%	30-40%	40-50%	50-60%	60-70%	70-80%	80-90%	90-100%			
D		NIP			MIP			NIP			MIP		
Library 2	1	2	3	4	5	6	7	8	9	10	11	12	
A	EDMA	EDMA	PETRA	EDMA	EDMA	PETRA	EDMA	EDMA	PETRA	EDMA	EDMA	PETRA	
B	MAA	TFMAA	TFMAA	MAA	TFMAA	TFMAA	MAA-TFU	TFMAA-TFU	TFMAA-TFU	MAA-TFU	TFMAA-TFU	TFMAA-TFU	
C	EDMA	EDMA	PETRA	EDMA	EDMA	PETRA	EDMA	EDMA	PETRA	EDMA	EDMA	PETRA	
D	DEAEMA	4-VPy	DEAEMA	DEAEMA	4-VPy	TFMAA	DEAEMA-TFU	4-VPy-TFU	DEAEMA-TFU	DEAEMA-TFU	4-VPy-TFU	DEAEMA-TFU	
E	DVB	DVB	DVB	DVB	DVB	DVB	DVB	DVB	DVB	DVB	DVB	DVB	
F	MAA	TFMAA	EAMA	MAA	MAA-HEMA	TFMAA	MAA-TFU	TFMAA-TFU	EAMA-TFU	MAA-TFU	TFMAA-TFU	EAMA-TFU	
G	DVB	DVB	DVB	DVB	DVB	DVB	DVB	DVB	DVB	DVB	DVB	DVB	
H	DEAEMA	4-VPy	TFMAA-HEMA	MAA	DEAEMA	4-VPy	DEAEMA-TFU	4-VPy-TFU	TFMAA-HEMA-TFU	DEAEMA-TFU	4-VPy-TFU	TFMAA-HEMA-TFU	
	0-0.07 μmol/g	0.07-0.14 μmol/g	0.14-0.21 μmol/g	0.21-0.28 μmol/g	0.28-0.35 μmol/g	0.35-0.42 μmol/g	0.42-0.49 μmol/g	0.49-0.56 μmol/g	0.56-0.63 μmol/g	0.63-0.70 μmol/g			

Mini-molecularly imprinted polymers libraries for targeting NLLGLEAK

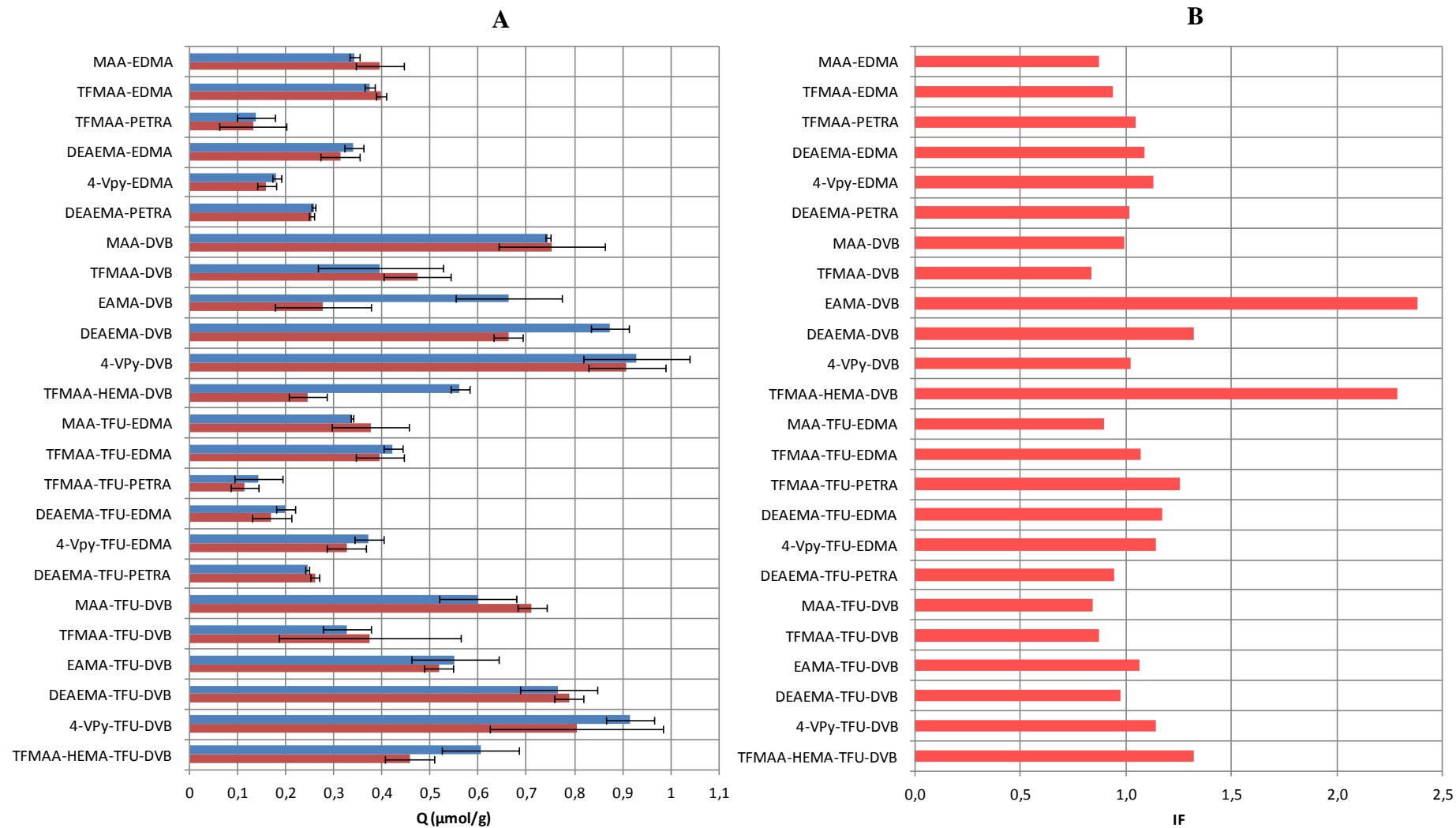


Figure 3.7: Binding capacity (A) and imprinting factors (B) for library 2 at pH 7. (■ MIP ■ NIP)

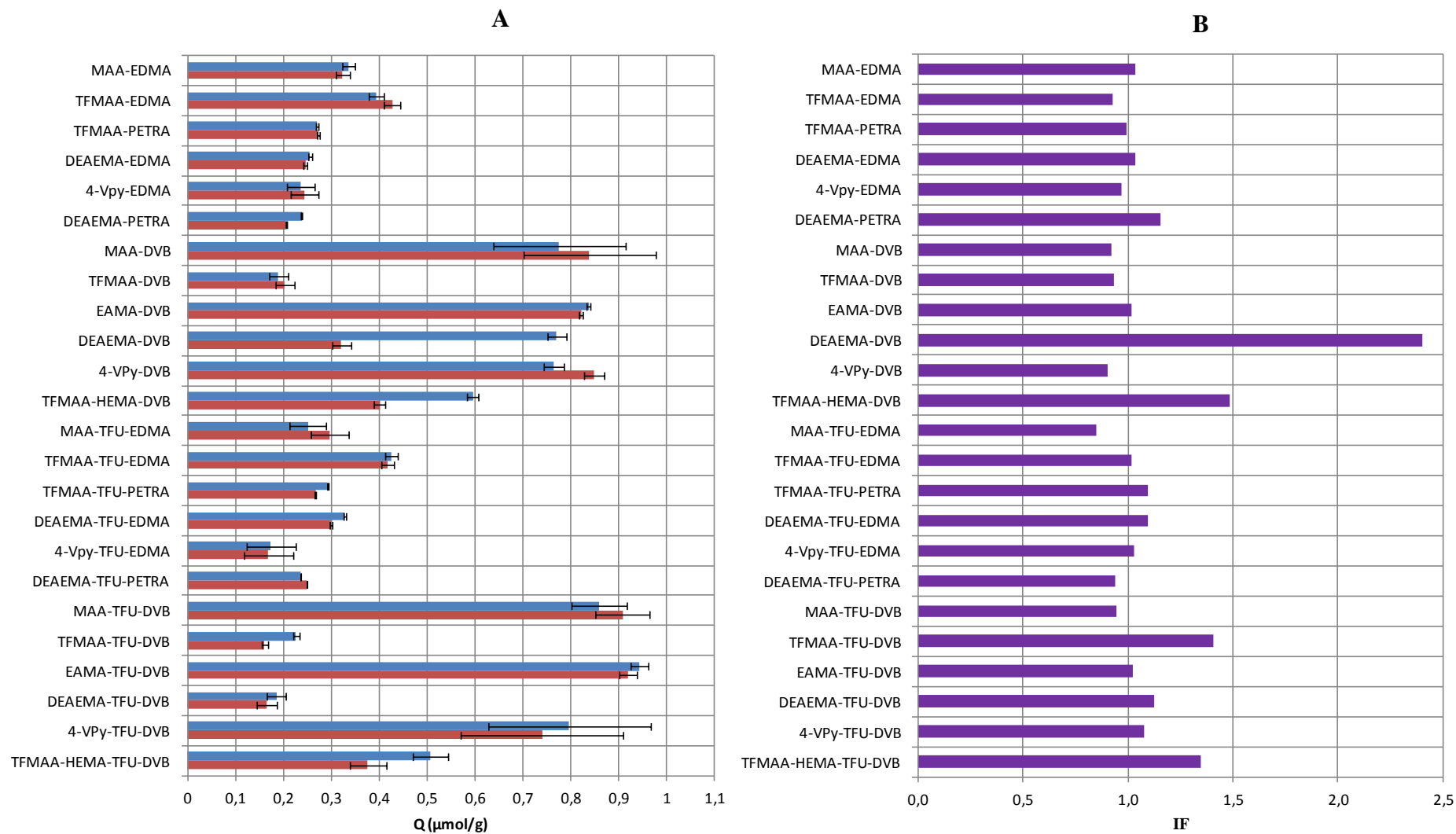


Figure 3.8: Binding capacity (A) and imprinting factors (B) for library 2 at pH 10. (■ MIP ■ NIP)

3.7.2.2 Molecularly imprinted solid phase extraction (MISPE)

Finally, based on the aforementioned observations about the binding ability and the IF values the most promising polymers (DEAEMA-DVB, EAMA-DVB, TFMAA-HEMA-DVB) from library 2 were selected and a solid-phase extraction (SPE) experiment was carried out over to for further comparison of their affinities and selectivities. SPE consists of a loading step, and an elution step followed by measurement of the amount of peptide in elution. Figure 3.9 shows the recovery of the NLLGLIEAK in the elution MeOH/TFA (98:2) after sample loading in HEPES buffer (N-2-hydroxyethylpiperazine-N'-2-ethanesulfonic acid) (pH 7.5) (24 mg/L).

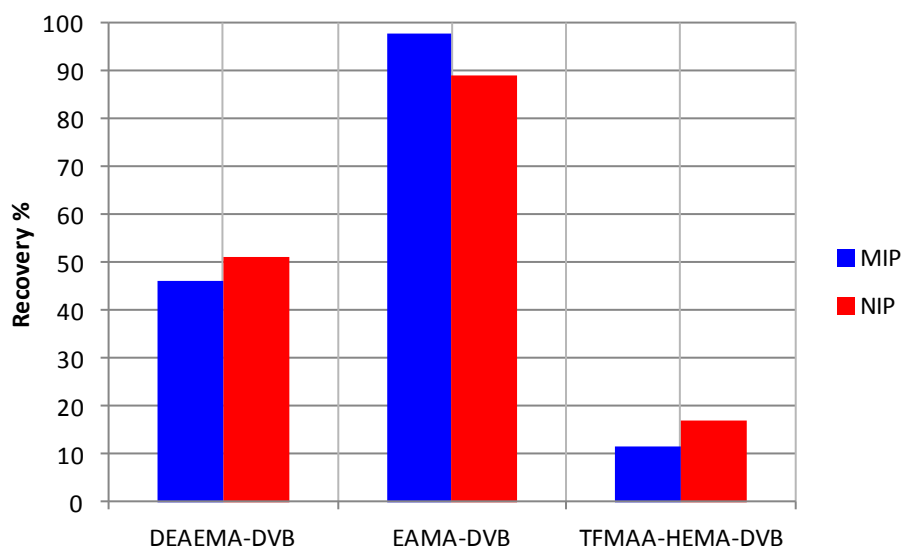


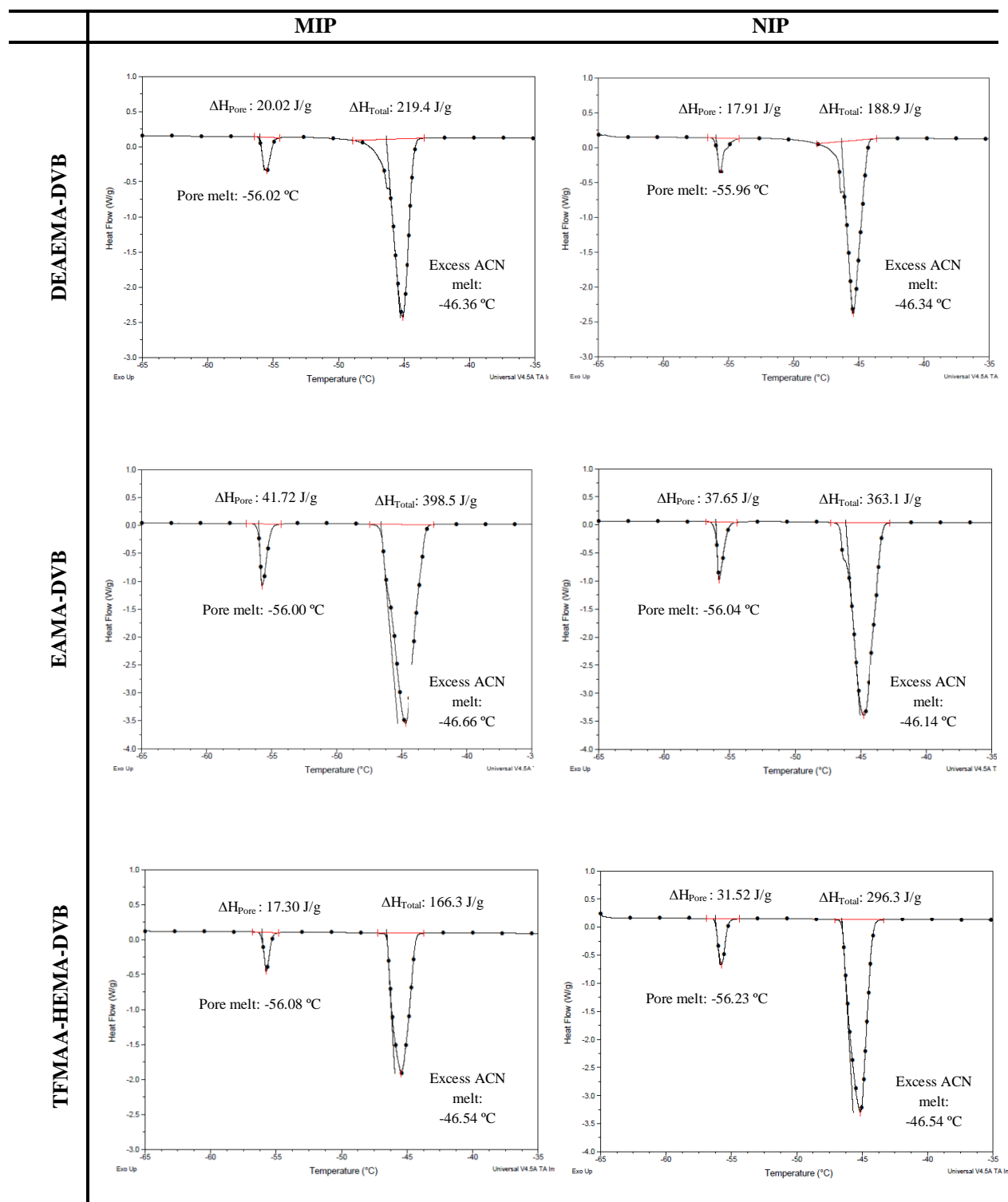
Figure 3.9: Recovery of NLLGLIEAK after loading 1 mL of an aqueous sample of the peptide (24 mg/L) in HEPES buffer (0.1 M, pH 7.5) onto T1 imprinted polymers (20 mg) selected from L2. The loading equilibration time was one hour. The elution was performed by percolating 0.5 mL of MeOH/TFA (98:2).

The best results were obtained for the EAMA-DVB polymer by which around 95% of NLLGLIEAK was retained. This is because the EAMA is cationic monomers which provide with DVB a cationic and hydrophobic interaction with NLLGLIEAK in aqueous media. While recovery of the other polymers was in the range between 10-50 % because depend on non covalent template-monomer interactions which reduce in aqueous media.

3.7.2.3 Thermoporometry

The specific surface area, total pore volume and average pore diameter for the DEAEMA-DVB, EAMA-DVB, and TFMAA-HEMA-DVB were determined by differential scanning calorimeter (DSC) (Figure 3.10) and details are listed in Table 3.9. Table 3.9 showed that

EAMA-DVB polymer has a two times higher surface area and pore volume ($60 \text{ m}^2/\text{g}$, $0.7 \text{ cm}^3/\text{g}$, respectively) compared to DEAEMA-DVB and TFMAA-HEMA-DVB polymer, ($28 \text{ m}^2/\text{g}$, $0.3 \text{ cm}^3/\text{g}$ for both polymer, respectively) while these parameters were slightly the same in the case of corresponding NIP polymer. This clearly suggests that the influence of EAMA monomer on polymer morphology.



Mini-molecularly imprinted polymers libraries for targeting NLLGLIEAK

Figure 3.10: DSC curves for the melting of acetonitrile in the DEAEMA-DVB, EAMA-DVB, and TFMAA-HEMA-DVB polymers. The polymers were frozen by rapidly quenching to $-60\text{ }^{\circ}\text{C}$ and the heating curves shows pore melt and excess melt.

Table 3.9: Physical properties of imprinted and non-imprinted polymers. The DSC average pore diameter (D_p), specific pore volume (V_p), and specific surface area (S_A), were determined.

Polymer	D_p (nm)	V_p (cm^3/g)	S_A (m^2/g)
DEAEMA-DVB-MIP	4.50	0.33	28.98
DEAEMA-DVB-NIP	4.51	0.34	30.02
EAMA-DVB-MIP	4.61	0.70	60.58
EAMA-DVB-NIP	4.42	0.65	58.63
TFMAA-HEMA-DVB-MIP	4.54	0.32	28.55
TFMAA-HEMA-DVB-NIP	4.49	0.41	36.46

3.7.2.4 SEM images

The SEM images show appreciable differences in the morphology of the polymers. In general, there are some differences between the surface morphology of the MIP and NIP, though both have rough surfaces, and the MIP seemed denser with few pores.

Meanwhile, the surface morphologies of EAMA-DVB seemed denser with more and larger-dimension of the pore and bigger volume rough structure than that of DEAEMA-DVB or TFMAA-HEMA-DVB. It was found in Figure 3.10 and Figure 3.11 that the analyte binding capacity and chemical as well as thermal capacities were directly dependent on the characteristics of their surface morphology. The more porosity and more open structure speed-up the mass transfer rate of the releasing and rebinding of the template [26].

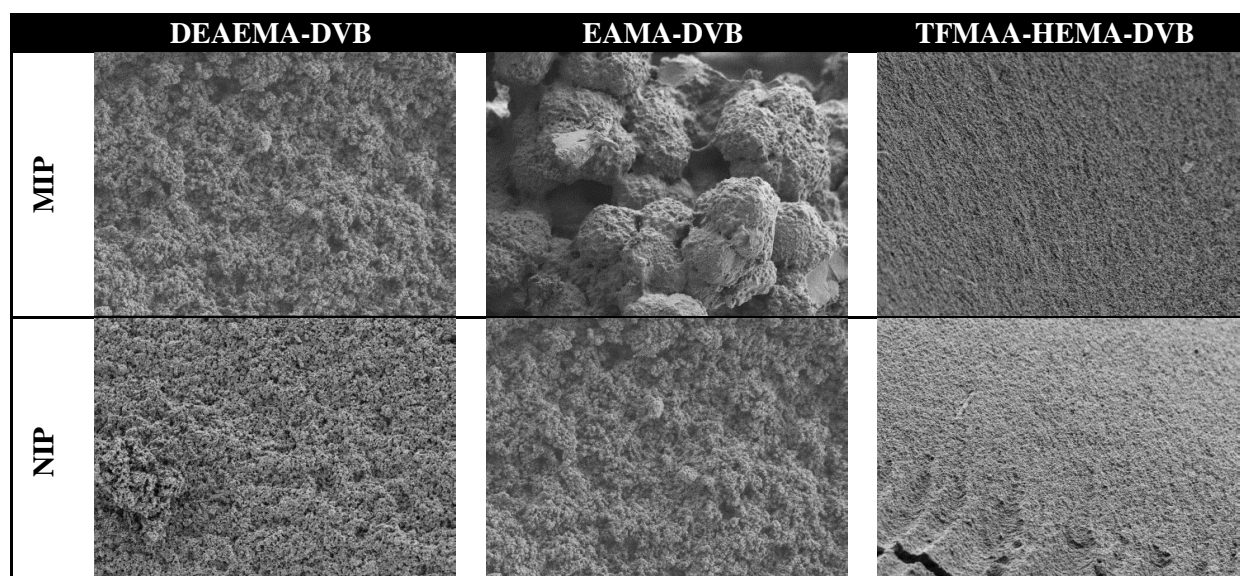


Figure 3.11: Scanning electron micrographs of imprinted and non-imprinted polymers. 2000 X magnification.

In the end EAMA monomer and DVB crosslinker are promising candidates, so in the next library other parameters like porogen, DVB ratio and deferent templates were further explored.

3.7.3 Library 3

3.7.3.1 Rebinding results

Based on above discussion, in this library we focused on further EDMA-DVB polymer. By studying different parameters like templates, crosslinker ratio and porogens one can improve the imprinting effect in order to get a balance between good capacity and imprinting factors. Polymers were prepared with the formulations as shown in Table 3.5.

The rebinding results plotted in Figure 3.12 show that the rebinding capacity for P1-P4 is lower by half than P5-P8. Two set of polymers were prepared with same molar ratio (0.04/7/17) but with different porogen in the first set was ACN/DMSO (1:1) while in the second one was DMSO only. As mentioned in the introduction part the solvent role effect in morphology of polymers thus this porogen was used to prepare P9-12 with changing molar ratio to (0.04/4.74/24) to decrease template/monomer ratio and increase the monomer solubility. In the end the binding capacity was the same in both sets. This indicates that porogen DMSO is a main parameter by increasing the porosity within polymer network, thus increasing binding capacity. P9-P12 polymers were tested in more details by MISPE.

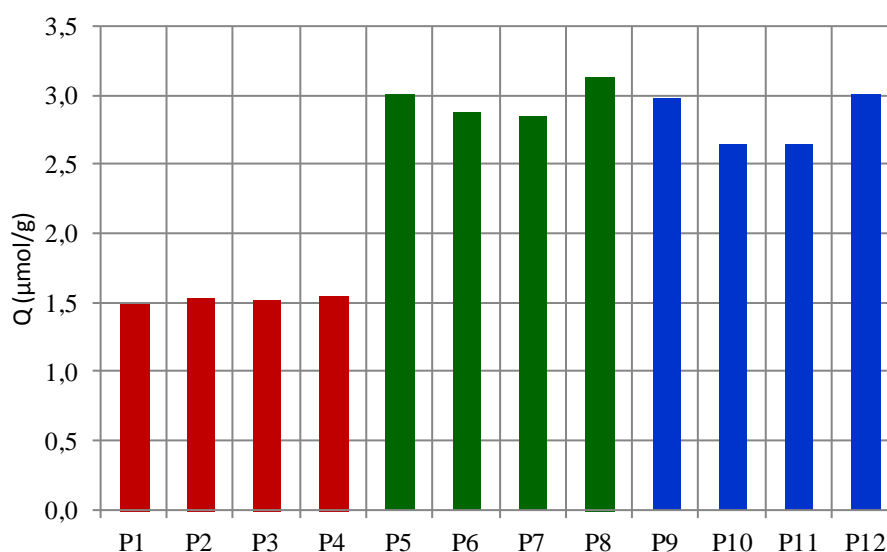


Figure 3.12: Binding capacity of library 3. HEPES buffer (0.1 M, pH 7.5) with NLLGLIEAK.

3.7.3.2 Molecularly imprinted solid phase extraction (MISPE)

To investigate the selectivity of the NLLGLIEAK imprinted polymer, three polymers with different templates were investigated (P9-P12) including H-NLLGLIEAK-NH₂ (T1), Z-NLLGLIEA-Nle-OH (T2), H-NLLGLIEAK-OEt (T3) and P12 prepared without template. 1 mL of a solution containing 25 mg/L NLLGLIEAK (HEPES, 0.1 M, pH 7.5) was loaded onto the cartridges, which were subsequently washed with 0.5 mL of different ratio of ACN in water to elute the non-specifically retained compounds. Finally, the elution was performed by passing a 0.5 mL MeOH/TFA (98:2).

As we can see in Figure 3.13, P11 shows less breakthrough and higher recovery comparing to other polymers, this means that the C-protecting group of the template is the most important factor as well as monomer and crosslinker. If we look at Table 3.2 again, the solubility of T1, T2, and T3 was 166.7, 22.0, and 250 mg/mL respectively. This means that the C-protecting group improves the template solubility (T3) and can make a strong complex with EAMA monomer in prepolymerization.

3.7.3.3 Selectivity test

At last, the selectivity of the P11 cartridge was evaluated by using standard mixture of other peptides with similar size but different chemical structure, FGGF, DRVYIHPF, GMLVGGVV, and NLLGLIEAK. As shown in Table 3.10 the properties of these peptides range from low to high molecular weight also the hydrophobicity scale is in between 23 to 50. For this purpose 1 mL of 25 mg/L standard mixture was percolated onto the P11/P12 cartridges under the MISPE conditions. The results are shown in Figure 3.14 clearly indicate that the P11 material was able to discriminate between target peptide and the rest of studied peptides. In the loading step, the MIP cartridge retains 73% of NLLGLIEAK, while the NIP cartridge retains only 53%. After a washing step, 64% of the loaded peptide was recovered in the elution fraction from the MIP and in 48% from the NIP, showing the high selectivity of the P11 for NLLGLIEAK. In case of the other peptides, the amount of peptide in the flow through was in the range between 35-55% and in the range 25-35% in the elution step. Based on these results, it is demonstrated that the EAMA-DVB polymer can be very useful as stationary phases for MISPE procedure.

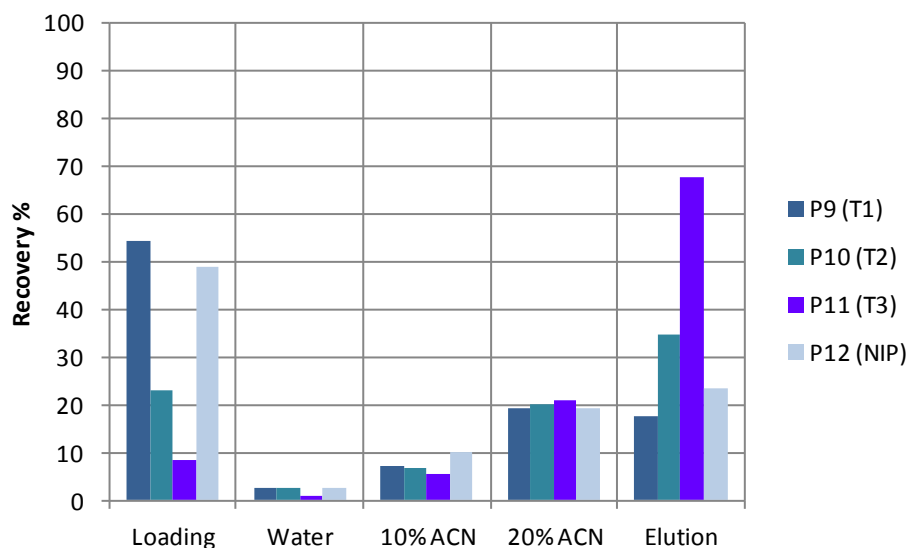


Figure 3.13: Recovery of NLLGLIEAK in the fractions collected after loading 1 mL of an aqueous sample of the peptide (25 mg/L) in HEPES buffer (0.1 M, pH 7.5) on Library 3 through P9-P12 polymers followed by percolation of 0.5 mL of ACN/H₂O wash solutions as indicated and elution in 0.5 mL of MeOH/TFA (98:2). The loading equilibration time was one hour.

Table 3.10: Peptide property functions.

Peptide	Chemical Formula	Mwt	pI [§]	Charge	Hydrophobicity		Sequence Composition			
					pH 2.0	pH 6.8	Acidic	Neutral	Basic	Hydrophobic
FGGF	C ₂₂ H ₂₆ N ₄ O ₅	426.49	6.09	0	46.0	48.5	0	50	0	50
DRVYIHPF	C ₅₀ H ₇₁ N ₁₃ O ₁₂	1046.23	7.95	1 ⁺	23.5	28.5	12.5	12.5	25	50
GMLVGGVV	C ₃₂ H ₅₈ N ₈ O ₉ S	730.98	9.09	0	51.4	50.2	0	37.5	0	62.5
NLLGLIEAK	C ₄₄ H ₇₉ N ₁₁ O ₁₃	970.24	6.99	0	41.9	38.3	11.1	22.2	11.1	55.5

[§] Isoelectric point

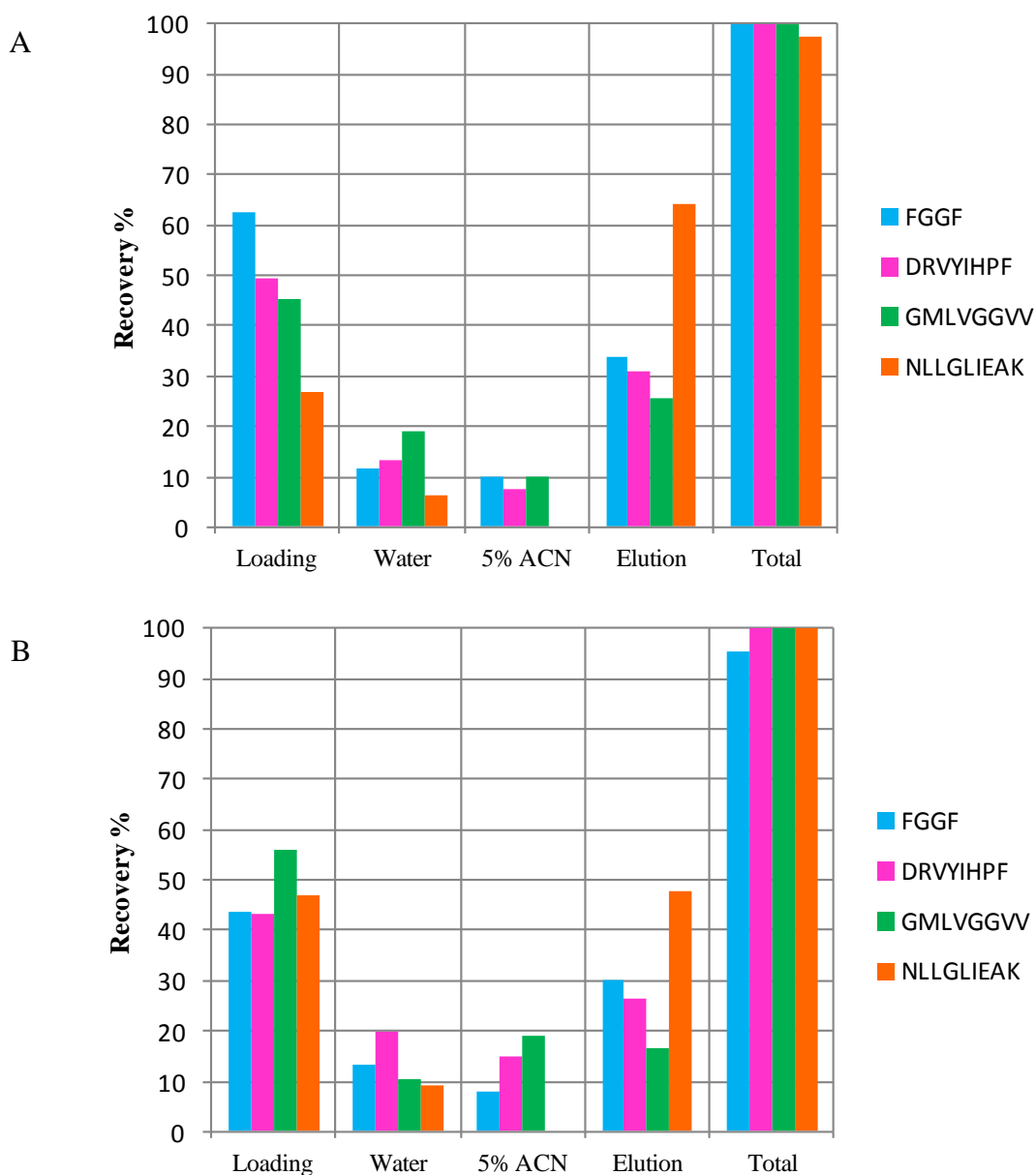
Mini-molecularly imprinted polymers libraries for targeting **NLLGLIEAK**

Figure 3.14: Peptide recoveries in the fractions collected after loading 1 mL of an aqueous sample of the indicated peptides (25 mg/L in HEPES buffer (0.1 M, pH 7.5) on P11 (A) and P12 (B) followed by percolation of 0.5 mL of wash solutions as indicated and elution in 0.5 mL of MeOH/TFA (98:2). The loading equilibration time was one hour.

3.7.4 Polymers morphology: TFMAA as a model

Scanning electron microscopy (SEM) can give information about the morphology and surface texture of the materials. In this work are presented several polymers that were prepared using the bulk polymerization method, but under different synthesis conditions, i.e. different monomers, crosslinkers type and ratio, as well as porogens. This produced polymers with different structural conformations and characteristics (hardness, porosity, stiffness, loading capacity, strength etc.). The SEM was used to examine these polymers morphologically.

The analyte binding capacity, binding specificity and chemical as well as thermal capacities of these polymers are likely to depend on the characteristics of their surface morphology [26].

In this chapter, TFMAA was selected as a model to study the morphology of polymers because it's a common monomer used in combination all crosslinkers in both libraries (1 and 2). Table 3.11 shows the properties of TFMAA polymers which were selected for library 1 and library 2 to study the effect of polymerization condition on the morphology of polymers.

Table 3.11: Selected TFMAA polymer form library 1 and library 2 for morphology study.

#	Library #	Polymer composition	CL %	T/FM/CL [§]	Porogen
A	1	NIP-TFMAA-EDMA	41	-/14/10	ACN/MeOH (1:1)
B	1	MIP-TFMAA-EDMA	41	0.04/14/10	ACN/MeOH (1:1)
C	1	NIP-TFMAA-EDMA	71	-/7/17	ACN/MeOH (1:1)
D	1	MIP-TFMAA-EDMA	71	0.04/7/17	ACN/MeOH (1:1)
E	1	MIP-TFMAA-PETRA	71	0.04/7/17	ACN/MeOH (1:1)
F	1	MIP-TFMAA-NOBE	71	0.04/7/17	ACN/MeOH (1:1)
G	2	MIP-TFMAA-EDMA	71	0.04/7/17	ACN/DMF (1:1)
H	2	MIP-TFMAA-PETRA	71	0.04/7/17	ACN/DMF (1:1)
I	2	MIP-TFMAA-DVB	71	0.04/7/17	ACN/DMF (1:1)

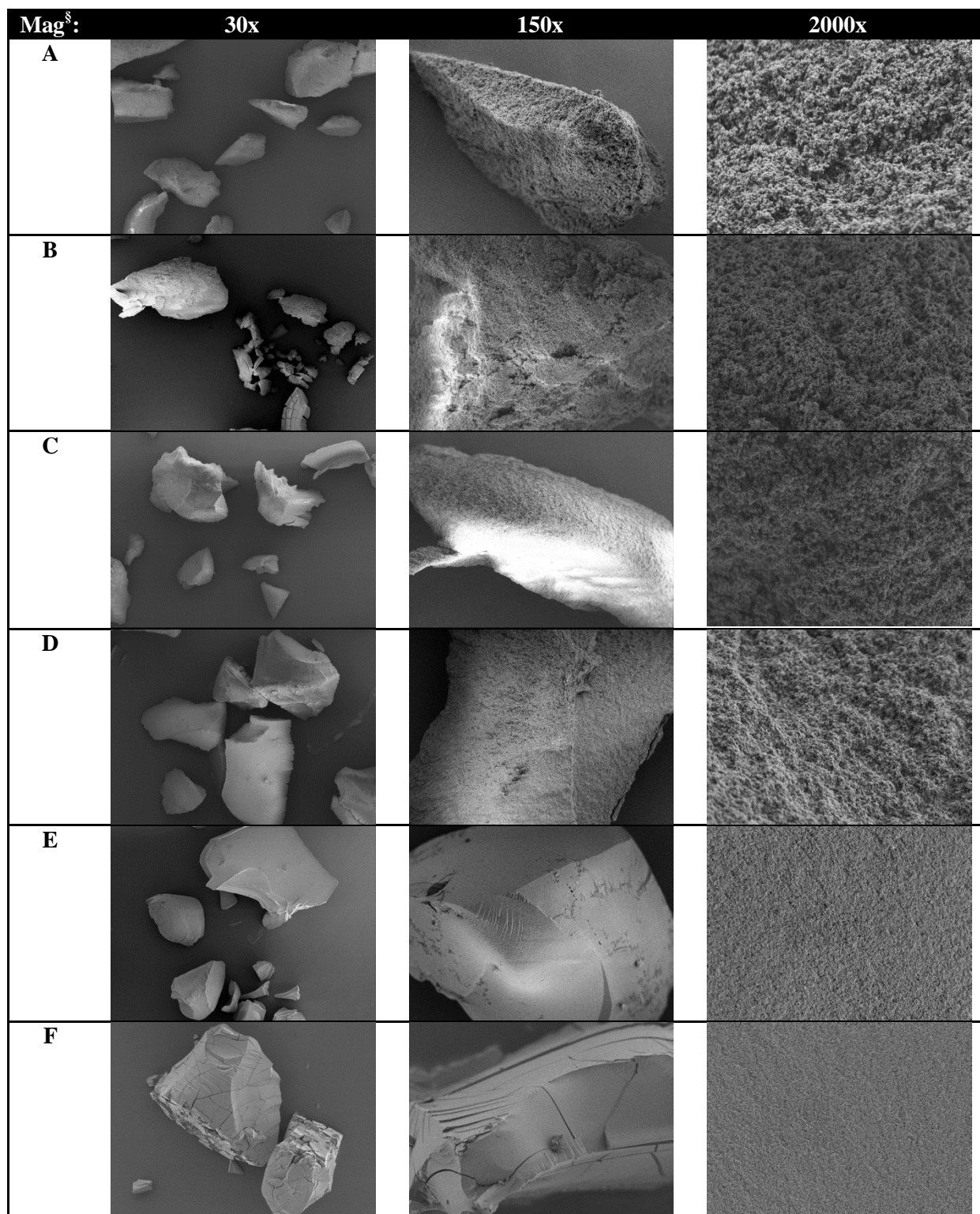
[§] molar ratio

The SEM was employed to observe the surface of the particles prepared from TFMAA. Library1: [A-B] NIP/MIP EDMA (41%); [C-D] NIP/MIP EDMA (71%); [E] MIP PETRA; [F] MIP NOBE; and Library 2 [G] MIP EDMA; [H] MIP PETRA; [I] MIP DVB. The obtained micrographs are presented in Figure 3.15 at different magnifications.

Figure 3.15 (A-D) showing the SEM images of NIP and MIP at two crosslinker percentages 41% and 71%. We can see that all of the polymers (A-D) showed an irregular, rough surface and that the morphologies of crosslinker percentages were quite similar. As also observed (Figure 3.15(A-D)), the spectrum of NIP is almost the same as that of MIP. This indicates that

Mini-molecularly imprinted polymers libraries for targeting NLLGLIEAK

almost all templates are removed from the MIP. Depending on these results we will study only the morphology of MIP in the following SEM images.



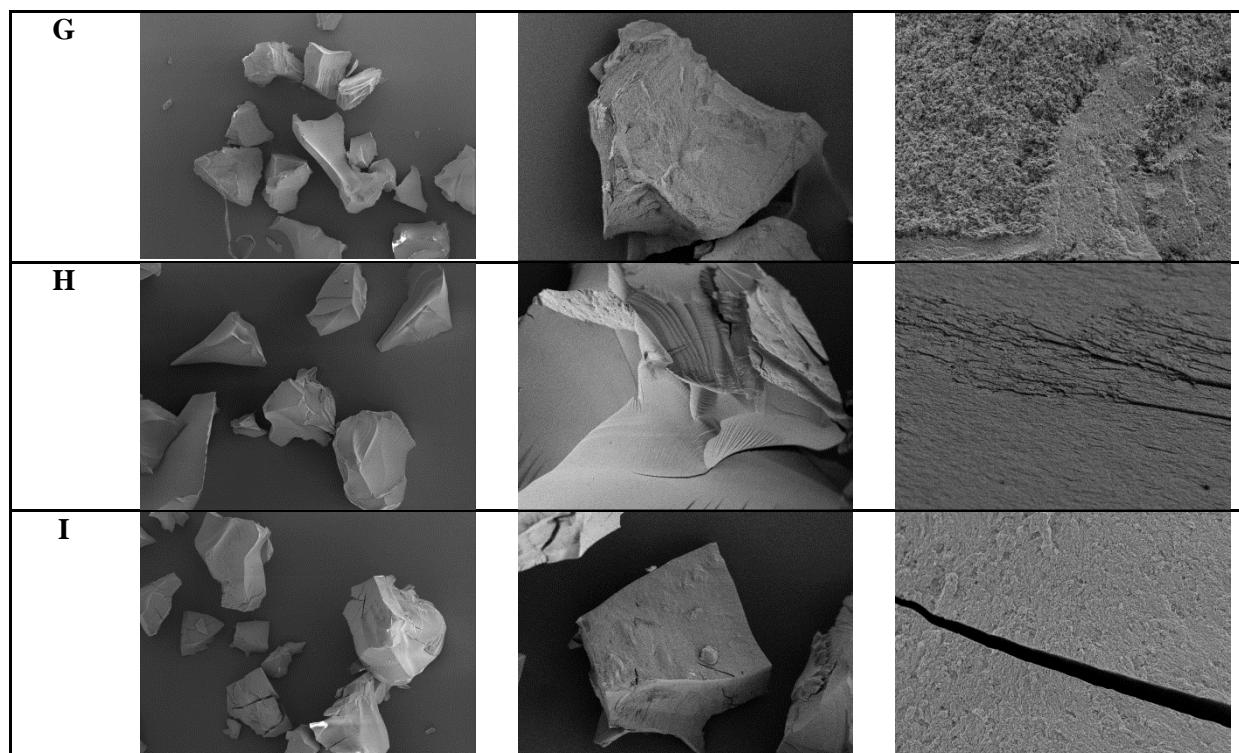


Figure 3.15: Scanning electron micrographs of TFMAA polymers, more detailed see (Table 3.11).

[§]Mag: magnification

Meanwhile, the surface morphologies of MIPs prepared in different crosslinkers were studied in Figure 3.15 (D-F). We analyzed three polymers synthesized from TFMAA and three different crosslinkers: EDMA (Figure 3.15D), PETRA (Figure 3.15E), and NOBE (Figure 3.15F). The images show the influence of the crosslinker on morphology of the polymers. The surface of EDMA has a lot of small pores. When compared to PETRA and NOBE, the latter feature increasingly smoother surfaces. On other hand, the binding capacities of crosslinkers EDMA, PETRA, NOBE (0.50, 0.40, and 0.15, respectively) decrease in the same order. Whether the latter is an effect of polymer porosity cannot be answered based on dry state porosity data. For this information about the swollen state porosity is required.

Next the effect of the porogen on the polymer morphology was studied. Polymers in Figure 3.15 (G-H and D-E) were all synthesized using the same polymerization conditions except using DMF as co-porogen instead of MeOH. We can see that there were no substantial differences in the morphology at least in the TFMAA system.

The morphology of polymer prepared with DVB show relatively smooth surface, while the binding capacity was a little higher (0.4 $\mu\text{mol/g}$) if it was compared to other (same

morphology) PETRA and NOBE. This fact could explain by $\pi - \pi$ interaction on the surface of polymer and the hydrophobic template.

3.8 Experimental

3.8.1 Chemical and reagents

The peptide H-NLLGLIEAK-NH₂ (T1), Z-NLLGLIEA-Nle-OH (T2), H-NLLGLIEAK-OEt (T3), FGGF, and GMLVGGVV were purchased from Genscript (Piscataway, NJ, USA), DRVYIHPF were purchased from Calbiochem-Merck, (Darmstadt, Germany). The target nona-peptide NLLGLIEAK was synthesized in the group of Prof. Dr. Thomas Schrader (University Duisburg-Essen, Germany) with a purity above 95% on a microwave peptide synthesizer from CEM (Carolina, USA). Dry acetonitrile (ACN), methanol (MeOH), dimethylformamide (DMF), and dimethylsulfoxide (DMSO) were purchased from Acros Organics (Geel, Belgium). Nitrogen (4.6) was purchased from Air Liquide (Düsseldorf, Germany). HPLC grade acetonitrile and methanol were purchased from Merck KGaA (Darmstadt, Germany), and HPLC water was purified using a Milli-Q system (Millipore, Bedford, MA). Trifluoroacetic acid and hydrochloric acid were purchased from Sigma-Aldrich Chemical Co (Deisenhofen, Germany). Pentaerythritol triacrylate (PETRA), N-(2-aminoethyl) methacrylamide hydrochloride (EAMA), and diethylaminoethyl methacrylate (DEAEMA) came from Polysciences, Inc. (Eppelheim, Germany). Ammonium chloride-ammonium hydroxide buffer solution (NH₄Cl, NH₄OH), Methacrylic acid (MAA), 2-hydroxyethyl methacrylate (HEMA), 4-Vinylpyridine (4-VPy), divinylbenzene (DVB), ethylene glycol dimethacrylate (EDMA), and N-2-hydroxyethylpiperazine-N'-2-ethanesulfonic acid (HEPES) were purchased from Sigma-Aldrich Chemie GmbH (Taufkirchen, Germany) and purified prior to use as follows: DVB and MAA was distilled under reduced pressure (~8x10⁻⁵ bar); EDMA was washed consecutively with 10% NaOH, water, and brine and then dried over MgSO₄, filtered, and distilled under reduced pressure prior to use. All other reagents were used as received. The initiator 2, 2'-azobis(2,4-dimethylvaleronitrile) (ABDV) was purchased from Wako Specialty Chemicals (Neuss, Germany), and used without further purification.

The monomer N-3, 5-bis (trifluoromethyl)-phenyl-N'-4-vinylphenylurea (TFU) [27], as well as the crosslinker N, O-bismethacryloyl ethanolamine (NOBE) [28] were synthesized previously in our group according to the literature protocols.

All porogens were kept under nitrogen atmosphere over molecular sieves and were used without further purification.

3.8.2 Apparatus

The 96-well PTFE microtitre plate and PTFE coated closures were obtained from Radleys (Shire Hill, Saffron Walden, Essex, UK). The 0.45 μm Captiva 96-wellfilter and chemically resistant PTFE microtitre plates were obtained from Varian Deutschland GmbH (Darmstadt, Germany).

The HPLC measurements were carried out on Hewlett-Packard 1100 instruments (Agilent Technology, Waldbronn, Germany) that consisted of a quaternary pump, an autosampler and a diode array detector. For pipetting of the polymer solutions, a 4-port liquid sample handler LISSY from Zinsser Analytic (Frankfurt, Germany), equipped with Zinsser WinLissy software, was used. The pipetting of washing solutions and the preparation of monomer solutions was performed with Eppendorf Research Pro 8-manifold pipettes (Eppendorf AG, Hamburg, Germany).

3.8.3 Synthesis

The polymers of libraries were prepared using the monomers and crosslinkers shown in Figure 3.2 and Figure 3.3, respectively. For Library 1 and 2 the MIPs were prepared using the H-NLLGLIEAK-NH₂ (T1) as template and ACN/MeOH (1:1) and ACN/DMF (1:1) as porogen, respectively. While for Library 3 the H-NLLGLIEAK-NH₂ (T1), Z-NLLGLIEA-Nle-OH (T2), and H-NLLGLIEAK-OEt (T3) was used as template and ACN/DMSO (1:1), DMSO as porogen.

3.8.3.1 Library 1

In **Library 1** the composition of each mini-MIP (Columns 4-6, 10-12) is reported in Table 3.3, where the mini-NIPs (Columns 1-3, 7-9) have the same composition except for the template.

Due to the solubility limitation of T1 in ACN, T1 was first deposited in the plate by pipetting a solution in dry MeOH. The solvent was left evaporating in fume hood overnight prior to proceeding with the library preparation. The molar ratios were as follows: T1/FM/CL (0.04/14/10) in rows A4-A6 to rows F4-F6, and T1/FM/CL (0.04/7/17) in rows A10-A12 to F10-F12. Rows G4-G6 to rows H4-H6 has molar ratios T1/FM/CL (0.04/7/17). The urea monomer and PMP were added (1 equivalent to the template) to rows G10-G12 and rows H10-H12 where the molar ratio was T1/TFU/FM/CL (0.04/0.04/7/17).

The stock solutions concentrations and volumes pipetted were calculated in order to obtain the final molar ratios for a template amount of 0.8 μmol and a total volume of porogen of 180 μL per well (Table 3.12). ACN/MeOH (1:1) was used as porogens due to poor solubility of template and some monomers in ACN. Prior to preparation of the stock solutions the porogens were purged with nitrogen for 30 min. A stock solution of each of the components used in the polymers formulations was prepared, except for urea monomer and T1, which the stock solutions were prepared in MeOH and exact volume was transferred directly to the respective wells to get after evaporation the amount which was needed.

The solutions were dispensed into a 96-well PTFE microtitre plate and the plate sealed with a PTFE coated silicon septum. Each pipetting step was accompanied by degassing with argon for 5 seconds. The polymerization was initiated thermally at 40°C and after 24h the polymers were cured at 60°C for 24 hour. The plates were then placed in the vacuum oven at 50°C for 24h to remove the porogen. After the drying step, each polymer was weighed, transferred to a 96-well filter plate and crushed.

Table 3.12: Stock solution preparation for template, functional monomers, initiator, and crosslinkers for library 1.

Reagent	Amount		Solvent	Volume (μL)	Volume used in each well (μL)
	41 %	71%			
T1	38 mg	38 mg	MeOH	7500	150
MAA	712 μL	356 μL	ACN/ MeOH (1:1)	1800	60
TFMAA	1176 mg	588 mg	ACN/ MeOH (1:1)	1800	60
MAA/HEMA	356/509(μL)	178/255 (μL)	ACN/ MeOH (1:1)	1800	60
4-VPy	-	453 μL	ACN/ MeOH (1:1)	1800	60
DEAEMA	-	843 μL	ACN/ MeOH (1:1)	1800	60
TFU	-	7.49 mg	MeOH	750	30
EDMA	943 μL	1603 μL	ACN/ MeOH (1:1)	2250	90
PETRA	1491 mg	2535 mg	ACN/ MeOH (1:1)	2250	90
NOBE	986.2 mg	1676 mg	ACN/ MeOH (1:1)	2250	90
ABDV	167 mg	167 mg	ACN/ MeOH (1:1)	4200	30

3.8.3.2 Library 2

In **Library 2** the composition of each mini-MIP (columns 4-6, 10-12) is reported in Table 3.4, where the mini-NIPs (columns 1-3, 7-9) have the same composition except for the template. The molar ratios were as follows: T1/FM/CL (0.04/7/17). The main difference between columns 1-6 and columns 7-12 was the use of the urea monomer to all the polymers in a molar ratio of T1/TFU/FM/CL to 0.04/0.04/7/17/. The stock solutions concentrations and volumes pipetted were calculated in order to obtain the final molar ratios for a template amount of 0.8 μmol and a total volume of porogen of 180 μL per well. ACN/DFM (1:1) was used as porogens due to poor solubility of template and some monomers in ACN. Prior to

Mini-molecularly imprinted polymers libraries for targeting NLLGLIEAK

preparation of the stock solutions the porogens were purged with nitrogen for 30 min. A stock solution of each of the components used in the polymers formulations was prepared, except for urea monomer and T1, which the stock solutions were prepared in MeOH and exact volume was transferred directly to the respective wells to get after evaporation the amount which was needed. Table 3.13 illustrating the volumes used from each stock solution.

Table 3.13: Stock solution for template, functional monomer, initiator, and crosslinker for library 2.

Reagent	Amount	Solvent	Volume (μL)	Volume used in each well (μL)
T1	38 mg	MeOH	7500	150
MAA	356 μL	ACN/ DMF (1:1)	1800	60
TFMAA	588 mg	ACN/ DMF (1:1)	1800	60
TFMAA/HEMA	119/85	ACN/ DMF (1:1)	600	60
4-VPy	302 μL	ACN/ DMF (1:1)	1200	60
DEAEMA	843 μL	ACN/ DMF (1:1)	1800	60
TFU	15 mg	MeOH	750	15
EAMA	230 mg	ACN/ DMF (1:1)	600	90
EDMA	1603 μL	ACN/ DMF (1:1)	2250	90
PETRA	1014 mg	ACN/ DMF (1:1)	900	90
DVB	1453 μL	ACN/ DMF (1:1)	2700	90
ABDV	167 mg	ACN/ DMF (1:1)	4200	30

The solutions were dispensed into a 96-well PTFE microtitre plate and the plate sealed with a PTFE coated silicon septum. Each pipetting step was accompanied by degassing with argon for 5 seconds. The polymerization was initiated thermally at 40°C and after 24 hour the polymers were cured at 60°C for 24 hour. The plates were then placed in the vacuum oven at 50°C for 24 hour to remove the porogen. After the drying step, each polymer was crushed, weighed, and transferred to a 96-well filter plate.

3.8.3.3 Library 3

In **Library 3** herein, a set of polymers were imprinted using three template T1, T2, and T3 the composition of each polymers (P1-P12) is reported in Table 3.5.

P1-P8

In HPLC vials, DVB (670 μmol), the functional monomer (280 μmol), the template T1, T2, and T3 (1.6 μmol), and the initiator (6 μmol , 1% w/w) was mixed in 200 μL of the porogen ACN: DMSO (1:1). The molar ratios were as follows: T1/FM/CL (0.04/7/17).

P9-P12

In HPLC vials DVB (960 μmol), the functional monomer (189.6 μmol), the template T1, T2, and T3 (1.6 μmol), and the initiator (6 μmol , 1% w/w) was mixed in 200 μL of the porogen DMSO. The molar ratios were as follows: T1/FM/CL (0.04/4.74/24).

The polymerization mixture was then degassed with nitrogen for 3 min and closed. The polymerization was initiated thermally at 45°C and after 24 hour the polymers were cured at 60°C for 24 hour. The vials were then placed in the vacuum oven at 50°C for 24h to remove the porogen. After the drying step, each polymer was crushed, weighed, and transferred to a 96-well filter plate. The reference (none imprinted) polymer was prepared similarly as above only in the absence of the template molecule. Table 3.14 illustrating the volumes used from each stock solution.

Table 3.14: Stock solution for template, functional monomer, initiator, and crosslinker for and volumes used for the preparation of the polymers library 3 in each well (μL).

P1-P8	Amount	Solvent	Volume (μL)	Volume used in each well (μL)
T1	5 mg	ACN/ DMSO (1:1)	65	20
T2	6 mg	ACN/ DMSO (1:1)	80	20
T3	5 mg	ACN/ DMSO (1:1)	65	20
EAMA	460 mg	ACN/ DMSO (1:1)	1200	60
DVB	1367 μL	ACN/ DMSO (1:1)	900	90
ABDV	83 mg	ACN/ DMSO (1:1)	1200	30
P9-P12	Amount	Solvent	Volume (μL)	Volume used in each well (μL)
T1	5 mg	DMSO	65	20
T2	6 mg	DMSO	80	20
T3	5 mg	DMSO	65	20
EAMA	156 mg	DMSO	600	60
DVB	680 μL	DMSO	450	90
ABDV	83 mg	DMSO	1200	30

3.8.4 Template extraction

After polymerization the polymers were transferred to a 96-well filter plate. The template and the unreacted monomers and crosslinker were extracted by consecutive washing steps, using 0.5 mL x 50 of MeOH (per well), 0.5 mL x 50 of MeOH/TFA (99:1), 0.5 mL x 25 of 10 mL MeOH and 0.5 mL x 50 of water until the template could no longer be detected in the washing solution, by RP-HPLC.

3.8.5 Single point rebinding

To obtain information on the existence of imprinted sites, equilibrium rebinding experiments were carried out with the total amount of mass obtained for each polymer.

Library 1 and Library 2

0.8 mL of an aqueous solution (0.1 M HEPES buffer pH=7.5, or NH₄Cl, NH₄OH buffer pH=10 (L2)) with a concentration of 100 mg/L NLLGLIEAK was loaded in each well. MIP and NIP samples with mass 30-100 mg were weighed out and added to the 0.8 mL aliquot of NLLGLIEAK solution in filter plate then the filter plate was sealed on top and bottom with PTFE-coated silicon closures.

Library 3

0.8 mL of an aqueous solution (0.1 M HEPES buffer pH=7.5) with a concentration of 50 mg/L NLLGLIEAK was loaded in each well. MIP and NIP samples with mass 10 mg were weighed out and added to the 0.8 mL aliquot of NLLGLIEAK solution in filter plate then the filter plate was sealed on top and bottom with PTFE-coated silicon closures.

After the solutions were incubated in the plates for 24 hours, the closures were removed and the solutions were filtered under vacuum into microplates, from which samples were taken for subsequent measurements.

The supernatants were injected into the HPLC for analysis. Two values were calculated to evaluate the MIPs.

3.8.6 Molecularly imprinted solid phase extraction (MISPE)

Solid phase extraction was carried out with a peristaltic pump. The cartridges were prepared by packing 20 mg of the dry polymer into 1 mL empty syringe (Braun, Germany) between two polyethylene frits. Prior to the extraction, a conditioning was carried out with 1 mL of MeOH/TFA (98:2) and 1 mL of MeOH followed by 1 mL water. For method evaluation, 1 mL of a solution containing 24 mg/L NLLGLIEAK in HEPES buffer (0.1 M pH 7.5) was loaded onto the cartridges, which were subsequent washed with 0.5 mL of different ratio of ACN in water to eluate the non specifically retained compounds. Finally, the elution was performed by passing a 0.5 mL of MeOH/TFA (98:2). The eluted fractions were collected and diluted with 0.5 mL H₂O and injected to HPLC-UV.

3.8.7 Selectivity test

The selectivity test was carried out using standard mixture of a peptide mixture (25 mg/L, 0.1 M HEPES, pH 7.5) containing FGGF, DRVYIHPF, GMLVGGVV, and NLLGLIEAK. 1 mL of standard mixture was loaded to MIP/NIP cartridges, washed with 0.5 mL H₂O and H₂O/ACN (95:5) followed by elution with 0.5 mL of MeOH/TFA (98:2). The elution fraction was diluted with 0.5 mL H₂O and analyzed by HPLC-UV according to section 2.2.1.

Bibliography

- [1] Lanza.F. and Sellergren.B, *Anal.Chem*, vol. 71, pp. 2092-2096, 1999.
- [2] Dirion.B., Cobb.Z., Schillinger.E., Andersson.I.L. and Sellergren.B, *J.Am.Chem.Soc*, vol. 125, no. 49, pp. 15101-15109, 2003.
- [3] Sellergren.B, MOLECULARLY IMPRINTED POLYMERS Man-made mimics of antibodies and their applications in analytical chemistry, Amsterdam: Elsevier, 2001.
- [4] Vasapollo.G., Sole.R.I, Mergola.L., Lazzoi.M, Scardino.A., Scorrano.A. and Mele.G, *Int.J.Mol.Sci*, vol. 12, pp. 5908-5945, 2011.
- [5] Hung.C-Y., Huang.Y-T., Huang.H-H. and Hwang.C-C, *J.App.Polym.Sci*, vol. 101, pp. 2972-2979, 2006.
- [6] Sreenivasan.K, *Reactive & Functional Polymers*, vol. 67, pp. 859-864, 2007.
- [7] Nicholas.T., Christopher.J., Keith.B., Christopher.Ar., Vladimir.H. and David.B, *Biotechnol.Prog*, vol. 22, pp. 1474-1489, 2006.
- [8] Hoshino.Y., Kodama.T., Okahata.Y. and Shea.K, *J.Am.Chem.Soc*, vol. 130, pp. 15242-15243, 2008.
- [9] Urraca.J., Aureliano.C., Schillinger.E., Esselmann.H., Wiltfang.J. and Sellergren.B, *J.Am.Chem.Soc*, vol. 133, pp. 9220-9223, 2011.
- [10] Hoshino.Y., Koide.H., Urakami.T., Kanazawa.H., Kodama.T., Oku.N. and Shea.K, *J.Am.Chem.Soc*, vol. 132, pp. 6644-6645, 2010.
- [11] Toshifumi.T., Daigo.F. and Jun.M., *Anal Chem*, vol. 71, pp. 285-290, 1999.
- [12] Dirion.B., Lanza.F., Sellergren.B., Chassaing.C., Venn.R. and Berggren.C., *Chromatographia*, vol. 56, p. 237, 2002.
- [13] Tothill.E.Ibtisam, "Peptides as Molecular Receptors," in *Recognition Receptors in Biosensors*, New York, Springer, 2009, pp. 249-274.
- [14] Kempe.M. and Mosbach.K, *J. Chromatogr. A*, vol. 691, pp. 317-323, 1995.
- [15] Takeuchi.A. and Kugimiya.T, *Anal Sci*, vol. 15, pp. 29-33, 1999.
- [16] Cormack.P.A.G. and Elorza.Z, *J.Chromatogr B*, vol. 804, pp. 173-182, 2004.
- [17] Sellergren.B., Ekberg.B. and Mosbach.K, *J.Chromatogr*, vol. 347, no. 1, pp. 1-10, 1985.
- [18] Michailof.C., Manesiotis.P. and Panayiotou.C, *J.Chromatogr.A*, vol. 1182, pp. 25-33, 2008.
- [19] Manesiotis.P., Hall.A., Courtois.J., Irgum.K. and Sellergren.B, *Angew.Chem.Int.Ed*, vol. 44, pp. 3902-3906, 2005.
- [20] Sibrian-Vazquez.M. and Spivak.D.A, *J.Org.Chem*, vol. 68, p. 9604, 2003.
- [21] Matsui.J., Kubo.H. and Takeuchi.T, *Aval Sci*, vol. 14, p. 699, 1998.
- [22] Sellergren.B. and Shea.K, *J.Chromatogr A*, vol. 635, pp. 31-49, 1993.
- [23] Takeuchi.T., Fukuma.D. and Matsui.J, *Anal Chem*, vol. 71, pp. 285-290, 1999.
- [24] Takeuchi.T., Fukuma.D., Matsui.J. and Mukawa.T, *Chem Lett*, vol. 1, pp. 530-531, 2001.
- [25] Takeuchi.T., Seko.A., Matsui.J. and Mukawa.T, *Iinstrum Sci Technol*, vol. 29, pp. 1-9, 2001.
- [26] Gonzalez.G., Hernando.P. and Alegria.J.S., *Anal Chim Acta*, vol. 557, pp. 179-183, 2006.
- [27] Hall.A.J., Manesiotis.P., Emgenbroich.M., Quaglia.M., DeLorenzi.E. and Sellergren.B, *J.Org.Chem*, vol. 70, no. 5, pp. 1762-1736, 2005.

- [28] Sibrian-Vazquez.M. and Spivak.D.A, *Macromolecules*, vol. 36, no. 14, pp. 5105-5113, 2003.

Chapter 4

Scaling up MIP for selective extraction of NLLGLIEAK from digestion of ProGRP in biological samples

4.1 Abstract

The early diagnosis of biomarker is crucial for patient survival and successful prognosis of the disease, and for this reason sensitive and specific methods are required for early cancer diagnosis. However, common techniques for separation and concentrating biomarker are not optimal from the viewpoints of sensitivity and selectivity because analyzing these biomarkers from a small amount of serum is difficult due to the complexity of the sample and low levels of these biomarkers.

Pro-gastrin releasing peptide (ProGRP) is used as a specific diagnostic marker for small cell lung cancer (SCLC). The object of this work has been developing a solid phase extraction method for the detection and quantification of ProGRP in human serum using molecularly imprinted polymers.

Various parameters affecting the extraction efficiency of the polymer have been evaluated to achieve the selective preconcentration of the NLLGLIEAK from aqueous samples and to reduce nonspecific interactions. The imprinted polymer was evaluated for use as a SPE sorbent, in tests with aqueous standards; by comparing recovery data obtained using the imprinted form of the polymer and a non-imprinted form (NIP). Extraction from the aqueous solutions resulted in more than 80 % recovery. A range of linearity for NLLGLIEAK between 1.5 and 50 mg/mL was obtained by loading 1 mL aqueous sample spiked with NLLGLIEAK at different concentrations in HEPES buffer of pH 7.0. The intra-day coefficient of variation (CV) and inter-day CV was below 7%. The optimized procedure has been successfully applied to the extraction and clean-up NLLGLIEAK from digest ProGRP with recoveries of

75%. The MIP format showed excellent affinity and selectivity to NLLGLIEAK and was therefore suitable for the application in SPE.

4.2 Introduction

The most important application area of molecular imprinting in the analytical separation field is probably solid phase extraction (SPE). The technique has been referred to as either MIP-SPE or MISPE and has recently been reviewed [1] [2] [3]. Examples of the most recent are: Pichon et al. [4], reviewed sample treatment using MIPs; Yan et al. [5], reviewed the main aspects involved in the synthesis of MIPs; Haginaka [6] recently reviewed monolithic imprinted materials and some examples of how these could be applied; and Caro et al. [7], reviewed the extraction of the analytes of interest from environmental and biological samples.

The first application of MISPE was presented by Sellergren in 1994 [8]. An MIP with selective extraction of pentamidine (Figure 4.1), a drug used to treat AIDS-related pneumonia from human urine. The pentamidine-imprinted materials were prepared using methacrylic acid as the monomer and ethylene dimethacrylate as the crosslinker by *in situ* polymerization in a chromatographic column coupled with a simple HPLC system and enabled selective extraction and concentration of pentamidine in biological fluids. A Urine sample was spiked with pentamidine and the MIP based extraction resulted in a clean extract and enrichment of the sample to a level where direct detection could be achieved. The MIP-based SPE yielded a clean extract and enrichment of the sample enabling direct detection.

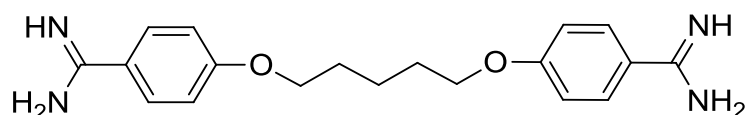


Figure 4.1: Pentamidine.

As shown in Figure 4.2 (A), obtained from Scopus, July 2013, there is an increase in the literature on this topic demonstrated by the increasing number of hits on “*Molecularly Imprinting Polymer*” and hits on “*Solid Phase Extraction*” in literature searches [9].

For example in 2012 (Figure 4.2 B), MISPE procedures have been extensively reported in the areas of environmental and food samples, while a small number of studies have dealt with drug, biological and other real samples.

Table 4.1 lists exemplified applications of MISPE to the extraction of analytes (Figure 4.3) in different matrices. Most of the MIPs used in MISPE procedures were prepared by the noncovalent imprinting technique and bulk polymerization method, and most of the MISPE procedures were carried out in the off-line mode for extracting analytes from different matrices, such as environmental (river water, sea, and soil), food (milk, egg), biological fluids (urine, serum, and plasma), and plant samples.

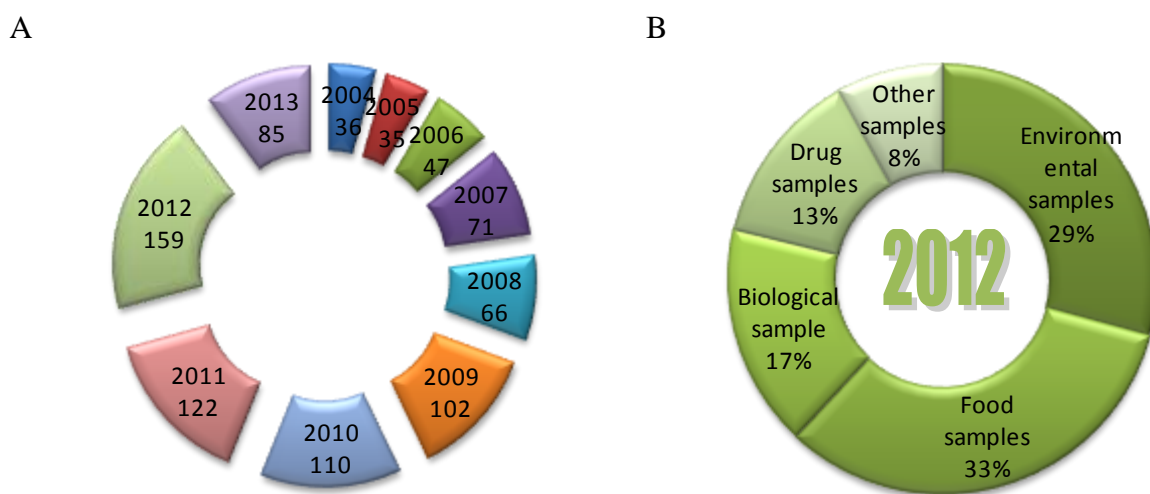


Figure 4.2: Original papers on MISPE application published since 2004. The numbers of paper were obtained from Scopus database during 2004-2013, searched by using “**Molecularly Imprinting Polymer AND Solid Phase Extraction**” as keywords (A) and then 2012 manually selected according to the MISPE application to the real samples (B).

Table 4.1: Selected application example of MISPE technique.

Analyte	Template	Matrix	Polymer system	Amount of MIP	Sample pretreatment	Washing step	Elution step	Detection technique	Ref
Melamine	Melamine	Milk	MAA/EDMA/ EtOH: H ₂ O (3:1)	100 mg	Precipitation with ACN	H ₂ O, MeOH	MeOH/NH ₄ OH (98:2)	HPLC-UV	[10]
Ibuprofen	Ibuprofen	River water	4-VPy/EDMA/Toluene	200 mg	pH adjustment (3)	CH ₂ Cl ₂	ACN/AA (99:1)	HPLC-UV	[11]
Fenitrothion	Fenitrothion	Tomato	MAA/EDMA/Toluene	200 mg	Extraction with NaCl/Acetone/ CH ₂ Cl ₂	Buffer pH 7/ACN (6:4)	ACN/AA (9:1)	HPLC- DAD	[12]
Testosterone	1,2,3,4-tetra- O-acetyl-b- glucuronic acid	Urine	TFU/PETRA/ACN	30 mg	Filtration and addition NaN ₃ (0.1% w/v)	ACN/H ₂ O/AA (97.99:1:0.01,)	ACN/AA (99:1)	HPLC-UV	[13]
Ropivacaine	Structural analog of Ropivacaine	Plasma	MAA/EDMA/Toluene	15 mg	Diluted with citrate buffer pH 5, containing 10% EtOH and 0.1% Tween 20	MeOH/H ₂ O (80:20) EtOH/ACN (1:9)	H ₂ O/ACN/FA (85:14:1)	LC-MS	[14]
AB1-40, AB1-42	AcGGVVIA AcGGVVIA ⁻ ⁺ TBA	Serum	TFU/EAMA/DVB/ DMSO TFU/EAMA/DVB/ ACN:DMSO (65:35)	25 mg	Diluted with GuHCl, 4 M	ACN/H ₂ O (95:5)	MeOH/TFA (95:5)	HPLC-UV, urea-SDS- PAGE	[15]

Table 4.1: continuo

Nitroimidazole	Structural analog of Nitroimidazole	Egg	MAA/DVB/CHCl ₃	25 mg	Diluted with H ₂ O, and Precipitation with ACN	H ₂ O, Hexane	ACN/H ₂ O/AA (6:4:0.5)	LC-ESIMS/MS	[16]
Cholesterol	Cholesterol	Cheese	MAA/EDMA/CHCl ₃	500 mg	Extraction with ACN	ACN/H ₂ O (70:30)	50 °C ACN	HPLC-UV	[17]
Mycophenolae mofetil	Mycophenolae mofetil	Plasma	4-VPy/EDMA/ACN: Toluene (7:3)	200 mg	Precipitation with ACN	H ₂ O, MeOH/H ₂ O (25:75), MeOH	MeOH/AA (8:2)	HPLC-UV	[18]
17β-Estradiol	17β-Estradiol	Fish	MAA/EDMA/ACN	300 mg	Extraction with ACN	ACN/H ₂ O (4:6)	MeOH/AA (99:1)	HPLC-UV	[19]
Caffeine	Caffeine	Plasma, Cola	MAA/EDMA/ACN	200 mg	Precipitation with ACN, and diluted with H ₂ O	ACN/TEA (99:1)	ACN/AA (99:1)	HPLC-UV	[20]
Nicotine, Cotinine	Nicotine	Hair	MAA/EDMA/CH ₂ Cl ₂	200 mg	Washed with CH ₂ Cl ₂ and diluted with alkaline buffer pH 10	Alkaline buffer pH 10 (C ₂ H ₃ O ₂ NH ₄ ⁻ NH ₃)	ACN/H ₂ O/TFA (95:2.5:2.5)	HPLC-PDA	[21]

AA: acetic acid; DMSO: dimethylsulphoxide; DVB: divinylbenzene; EAMA: N-(2-aminoethyl) methacrylamide hydrochloride; EDMA: ethylene glycol dimethylacrylate; EtOH: ethanol; FA: formic acid; GuHCl: Guanidinium chloride; MAA: methacrylic acid; PDA: photo-diode array detector; PETRA: pentaerythritol triacrylate; TBA: tetrabutylammonium; TEA: triethylamine; TFA: trifluoroacetic acid; TFU: N-3, 5-bis (trifluoromethyl)-phenyl-N'-4-vinylphenylurea; Tween 20: polyoxyethylene (20) sorbitan monolaurate; 4-VPy: 4-vinylpyridine.

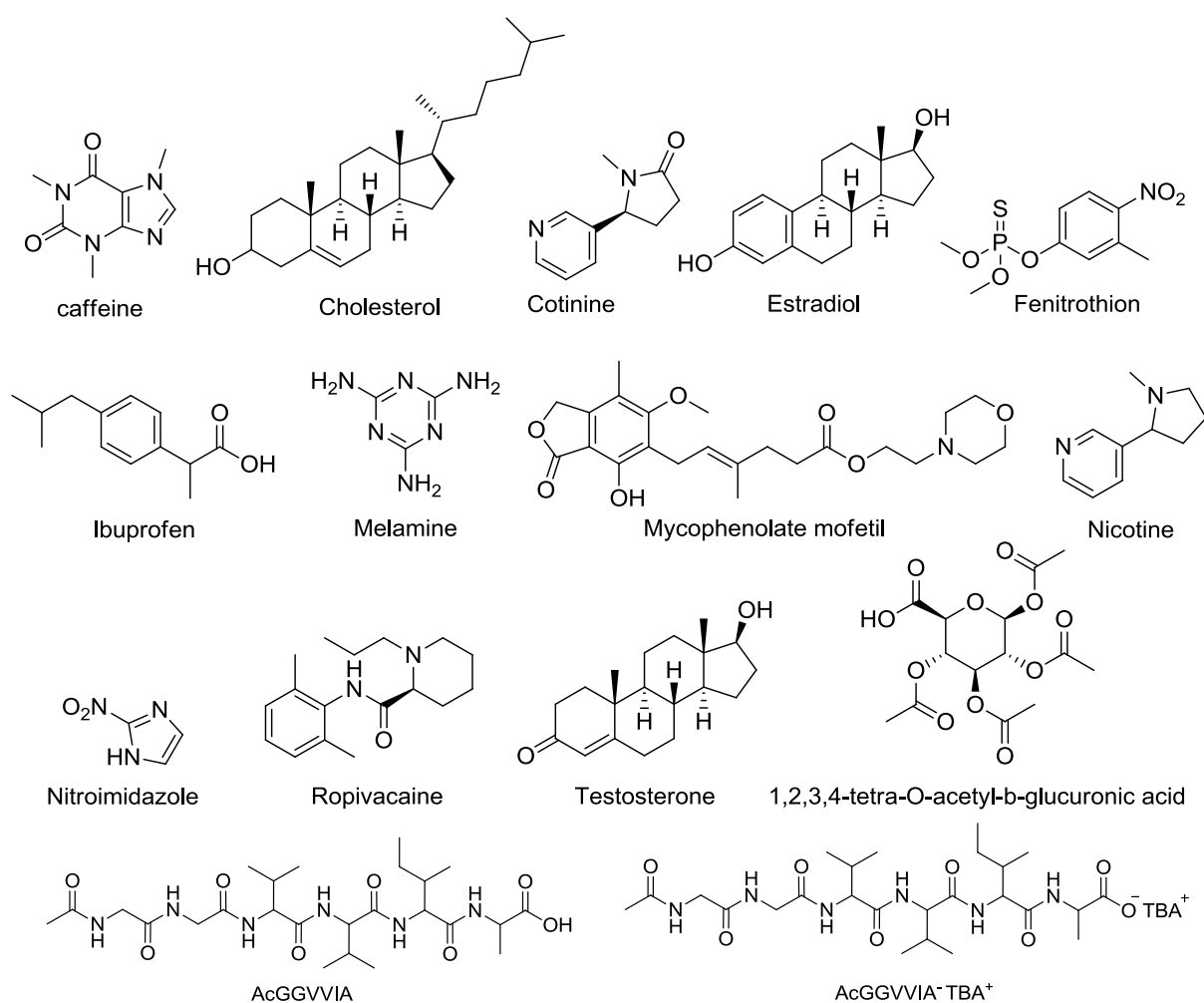


Figure 4.3: Chemical structures of analytes and template used in the MISPE protocols reported in Table 4.1.

The MISPE cartridges work in a similar way to the conventional SPE procedure except that the usual stationary phases are replaced with the imprinted polymer. Consequently, MISPE involves conditioning, sample loading, washing and elution steps. The adsorption of the analytes onto an MISPE sorbent may be either due to non-selective interactions, as with conventional reversed phase materials (C8, C18 etc.), or to selective interactions of the template or related analytes with the polymer matrix [2].

MISPE can be based on selective adsorption [22] [23], as can be expected in the extraction of analytes in media of low polarity, the example include a step where the sample is modified or extracted with organic solvents prior to application. It has been shown that the ideal solvent for selective rebinding to the imprints is often the same as the porogen [24] [25]. Or non-selective adsorption [26] [27], when the samples (e. g. biological and environmental samples)

are directly applied to the cartridge, extensive non-selective adsorption to the polymer surface generally occurs. The MIP sorbent works here as a conventional reversed phase or an ion-exchange SPE sorbent during the loading step. Furthermore, the non-selective adsorption can be converted to selective adsorption by washing the cartridge with carefully chosen solutions capable of disrupting only the non-specific interaction of the matrix components with polymer matrix.

Commonly, if the sample is loaded on the MIP in a low- polarity solvent, a selective loading step can be achieved, in which only the target analyte is selectively retained on the MIP while the sample matrix is non-retained. If the analyte of interest is presented in an aqueous medium, the analyte and other interfering compounds are retained non- specifically on the polymer. Consequently, to achieve a selective extraction, a clean-up step with an organic solvent is introduced prior to the elution step.

It is important to underline the fact that MIPs are not essentially selective. Therefore optimisation of the extraction steps is required, especially the washing and elution steps, in terms of solvent composition, pH and ionic strength.

Theoretically, the best results expected when using MISPE correspond to the achievement of a recovery close to 100% on the MIP with no retention on the NIP after percolating real samples containing the target analytes.

Due to their advantages, including high selectivity, stability, reusability, simplicity and low cost of preparation, MIPs are successfully used as sorbents for cleaning up and selectively enriching analytes from different real samples, such as environmental, biological, food, drug and other real samples.

Today there are already MISPE cartridges commercially available for selective extraction of several molecules (i.e. Nitroimidazoles, triazines, riboflavine) [28].

However, there are still some features that need to be improved most of the MISPE-related papers published just describe the use of different templates for different applications, and only few of them propose new alternatives to minimize the inherent drawbacks of the preparation and use of MIPs (i.e. template bleeding, tedious synthesis procedure etc.) [29].

The MIPs used for SPE are mainly prepared by the noncovalent-imprinting technique, which gives low yields of specific binding sites, resulting in low sample load capacity and high non-specific binding. Therefore, one goal in particular is to prepare MIPs with homogeneous

binding sites by developing new MIP synthesis methods. Another problem of the present MISPE methods is the difficulty in removing 100% of the whole template analyte molecule, typically, a few percent (< 5% or so) remains in the polymer matrix [30].

The problem is usually that large amounts of template (mg levels) are used to prepare the polymer but individual samples may contain only a few pg-ng of analyte, which can seriously interfere with the quantification of trace compound in complex samples. The “dummy” imprinting technique can prevent the bleeding of target analyte, but the selectivity of such MIPs is usually reduced to some extent [31].

Besides considerations of capacity, heterogeneous binding sites and template leakage, one further area of fundamental importance that has to be addressed is that of direct loading of the aqueous sample.

During percolation of the water sample, the analyte cannot be retained by the selective polar interactions that are developed in the solvent of synthesis (especially by hydrogen bonds that are too weak in aqueous medium). The retention mainly occurs by nonselective hydrophobic interactions with the polymeric matrix [32].

Often it is easier to optimize for selective binding using organic solvents than aqueous buffers. Therefore, many studies have used a water-to-solvent switch on-column, which removes contaminants by both aqueous and solvent washes, prior to selective elution using a solvent containing acid or base [15]. The purpose is to first quantitatively trap the analyte from the aqueous sample using both selective imprint binding and non-specific adsorption, and then change to an organic solvent in which the imprints bind the analyte in a highly selective manner, and in which non-specific MIP-analyte adsorption is weak or absent.

The selection of washing and elution steps is crucial for optimisation of selectivity when developing a MIP-based extraction procedure. With many procedures it has been found that optimum selectivity is found if the solvent in which the polymer was formed is used for retention and elution studies [31].

However, when these requirements are fulfilled, the MISPE can be widespread used in the near future.

4.3 Results and Discussion

4.3.1 Polymer synthesis

The ratio and the selection of the template, functional monomer, crosslinker and porogen have previously been described in Chapter 3. The porogen DMSO was chosen for the polymerization reaction because the solubility of the template molecule (T3) was moderated in this solvent. In comparison with DMSO, the solubility of T3 was poorer than in less polar and non-polar organic solvents (e.g., acetonitrile and dichloromethane). In spite of to be a polar organic solvent in comparison to acetonitrile or dichloromethane, DMSO still can render hydrogen bounds strong enough.

The functional monomer EAMA, which may form cationic bonding to T3, was selected as the functional monomer in the MIP preparation. In order to form an ionic complex between the functional monomer and the template was necessary the previous deprotonation of the carboxylic acid group of the template. With this purpose a stoichiometric amount of the base PMP respect to the T3 was added before the addition of the EAMA monomer.

The template contains several functional groups that may form hydrogen bonds, ionic and hydrophobic interactions with the functional monomer, EAMA and the crosslinker DVB. A possible cavity formed in the polymer is presented in Figure 4.4.

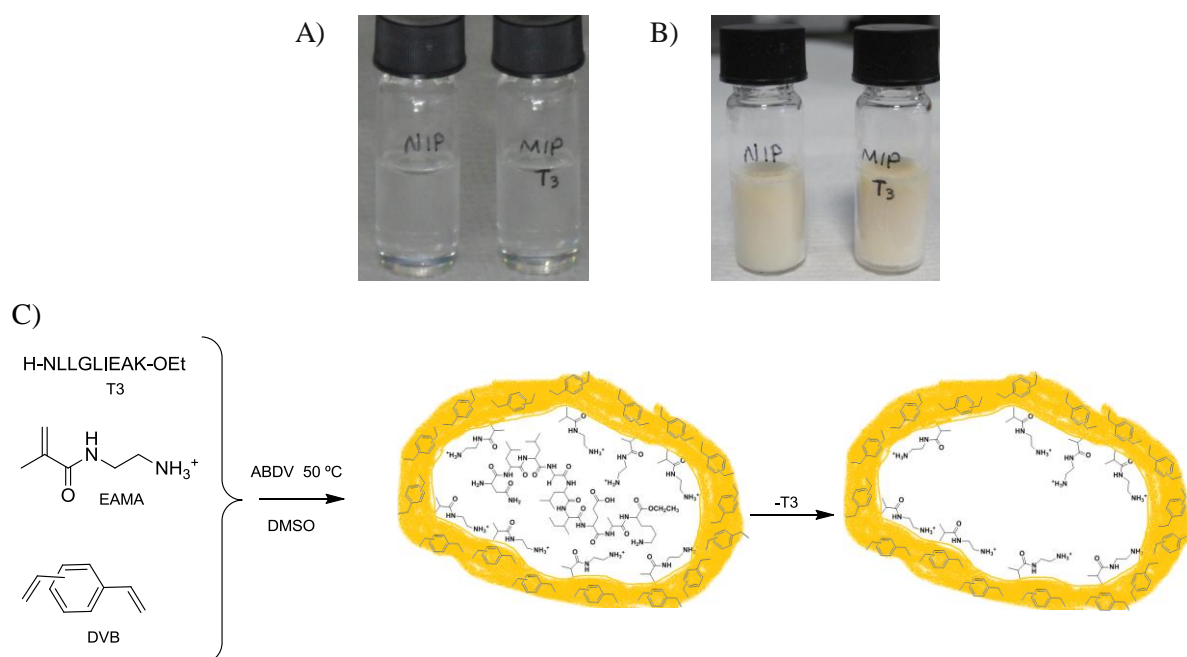


Figure 4.4: Photograph of large scaling of polymer synthesis. Before polymerization (A), after polymerization (B), and synthetic procedure for MIP preparation and hypothetical structure of the imprinted binding site (C).

4.3.2 Morphology, physical and chemical polymer characterization

4.3.2.1 Elemental analysis

Elemental analysis data for MIP and NIP are given in Table 4.2. The theoretical values were calculated through Eq.2.1 and were compared with experimental values. Nonetheless, the elemental analysis values for C, H and N differ from calculated ones. Since the C/N for both polymers, i.e. MIP and NIP are in good agreement to the theoretical values; the difference can be associated to the polymerization yield. From these results and taking in account that all the nitrogen present in the polymer will come from the presence of the functional monomer (the crosslinker does not bear nitrogen), we can conclude that all functional monomer involved in the polymerization process has been incorporated properly to the polymer matrix (experimental values are similar than the theoretical one). Moreover from these results it is also observed that similar results are obtained for MIP and NIP that shows the template molecule has been extracted efficiently from the polymer matrix in the imprinted material.

Table 4.2: Elemental analysis of MIP, NIP and theoretical values.

Sample	%C	%H	%N	C/N
MIP	79.75	8.75	3.13	25.47
NIP	80.11	8.87	3.30	24.27
Calculated by Eq.2.1	82.57	7.79	3.40	24.28

4.3.2.2 Infrared spectroscopy

In order to confirm the results obtained from the elemental analysis a confirmatory test of the structure of the polymer was achieved by FT-IR. After extraction of the template molecule FT-IR spectra were carried out for the imprinted and the non imprinted material. Figure 4.5 illustrate the FT-IR spectrum of MIP and NIP materials. In this spectrum, the absorption peak at 2981 cm^{-1} and 2889 cm^{-1} representing the C–H of the alkanes and aromatic group respectively, C=O stretching vibrations at 1630 cm^{-1} (amide bond related to EAMA). The band 3400 cm^{-1} (N–H), the peak 1155 cm^{-1} (C–N stretch) and its peak at 1510 cm^{-1} (N–H bending) indicate the amine group of the EAMA monomer in the final polymer. From these results can be extracted that both MIP and NIP had the similar composition in terms of chemical structure.

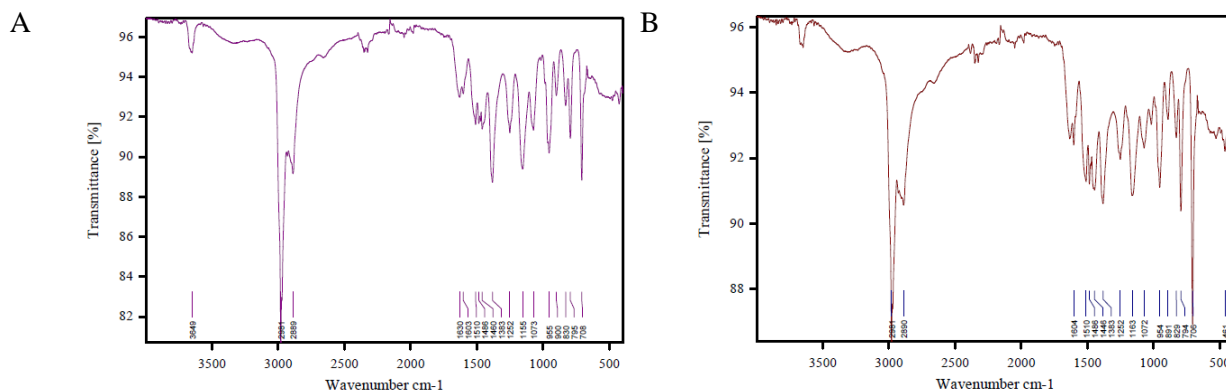


Figure 4.5: FT-IR spectra of (A) MIP and (B) NIP.

4.3.2.3 Microscopy SEM

The irregular bulk imprinted polymer in particle size 25-36 μm was studied by scanning electron microscopy (SEM). The representative picture of MIP and NIP is shown in Figure 4.6 at different magnifications. We can see that the polymers showed an irregular, rough surface and, there are some differences between the surface morphology of the MIP and NIP, looking at a higher magnification we clearly observed the presence of sporadic macro-pores and the MIP seemed denser with few pores comparing with NIP. Although slight changes in morphology of imprinted polymers were observed by some authors [33] [34], these findings should be interpreted with caution to consider effect of factors such as type of porogen and template removal condition. Considering the same conditions for preparation of NIP and MIP, this difference in morphology could be attributed to presence of template molecules during preparing MIP.

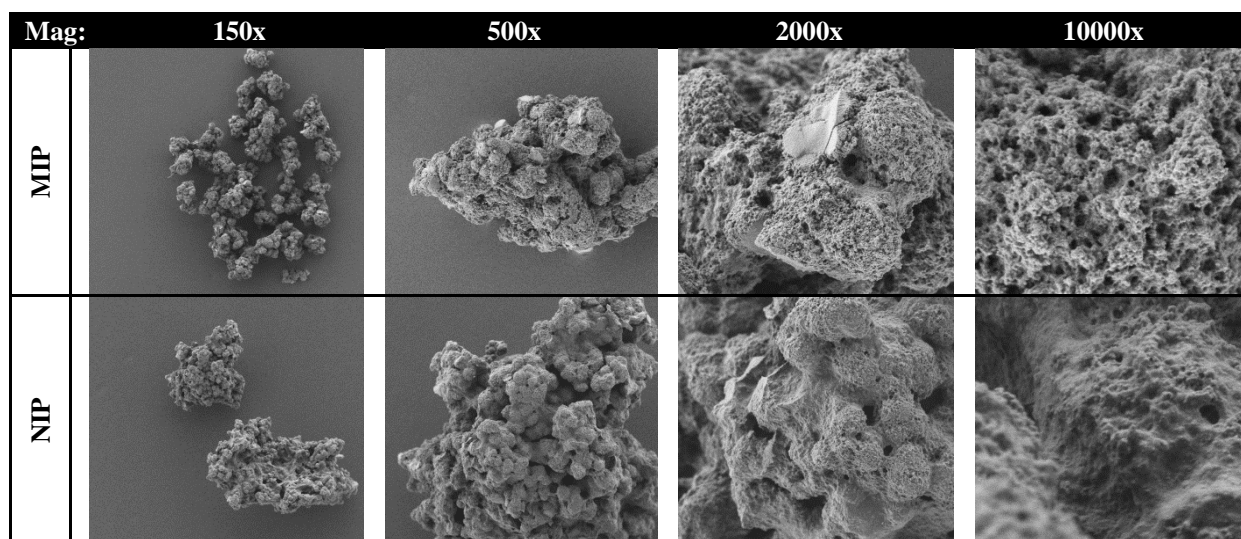


Figure 4.6: Scanning electron microscopy (SEM) picture of MIP and NIP (particle size: 25-36 μm) at different magnifications.

4.3.2.4 Thermoporometry

The porous properties of material (average pore diameter (D_p), specific pore volume (V_p), and specific surface area (S_A)) were determined by DSC (Figure 4.7) and details are reported in experimental procedure (2.1.3). Table 4.3 shows that the polymers exhibited mesoporous morphology with surface area $75 \text{ m}^2/\text{g}$ and average pore diameters of roughly at 4 nm. These morphologies of MIP and NIP were the same, indicative that presence of the template had no a major effect on porosity of the imprinted material.

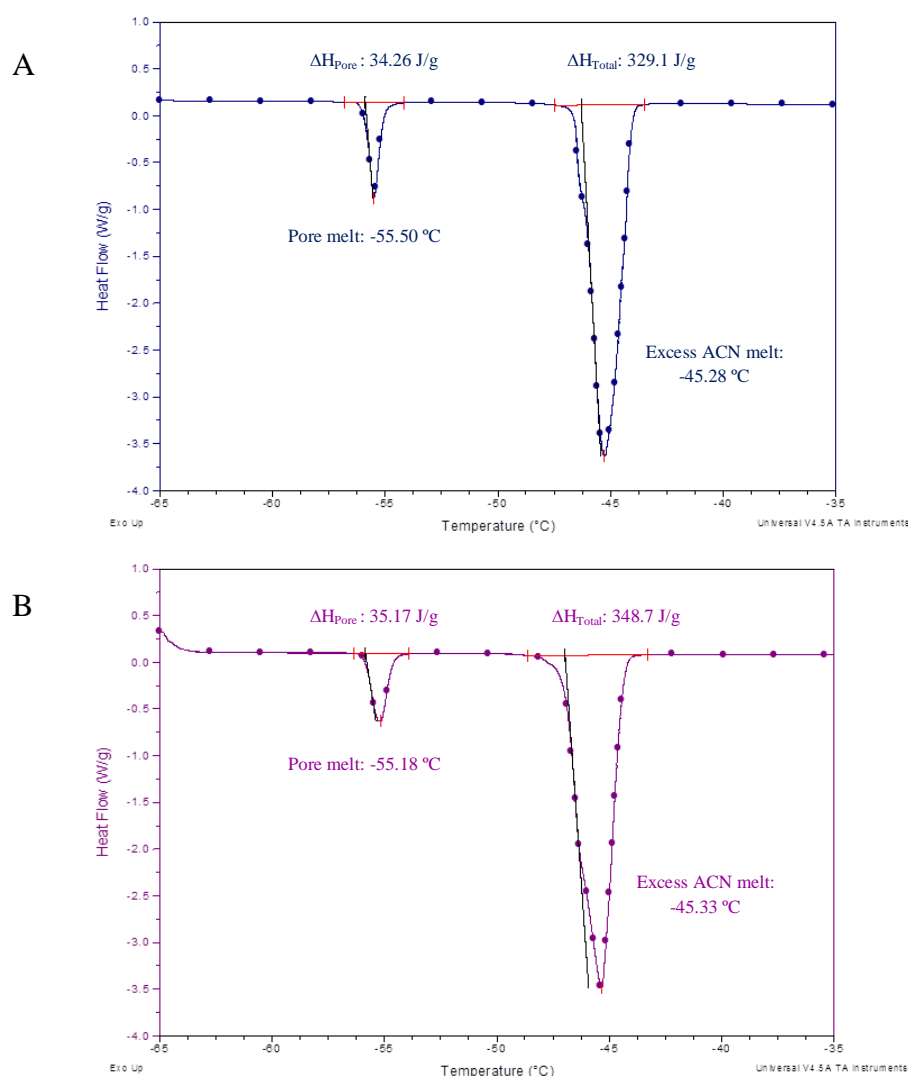


Figure 4.7: DSC curves for the melting of acetonitrile in (A) MIP and (B) NIP. The sample was frozen by rapidly quenching to $-60 \text{ }^\circ\text{C}$. The heating curves shows pore melt and excess melt.

Table 4.3: Properties of MIP and NIP measured by Thermoporometry.

Polymer	Dp ± STD (nm)	Vp ± STD(cm ³ /g)	S _A ± STD (m ² /g)
MIP	4.62 ± 0.07	0.85 ± 0.18	73.83 ± 16.54
NIP	4.65 ± 0.10	0.88 ± 0.12	75.89 ± 9.61

4.3.2.5 Thermogravimetric analysis

The thermal stability of the polymers was measured by thermo-gravimetric analysis (TGA). The measurement was conducted at 30 °C to 800 °C at a constant heating rate 10 °C/min in N₂ atmosphere. Figure 4.8 demonstrates the thermo-gravimetric analysis (TGA) and corresponding differential thermogravimetry (DTG) curves of MIP and NIP with the raise of temperature. Both of the polymers were showed two step of degradation (290 °C and 450 °C). This phenomenon could be explained by different thermal stability of copolymer segments (EAMA vs DVB). Comparison of first derivative curves of both polymers, the MIP start degradation at 380 °C is higher than NIP (350 °C).

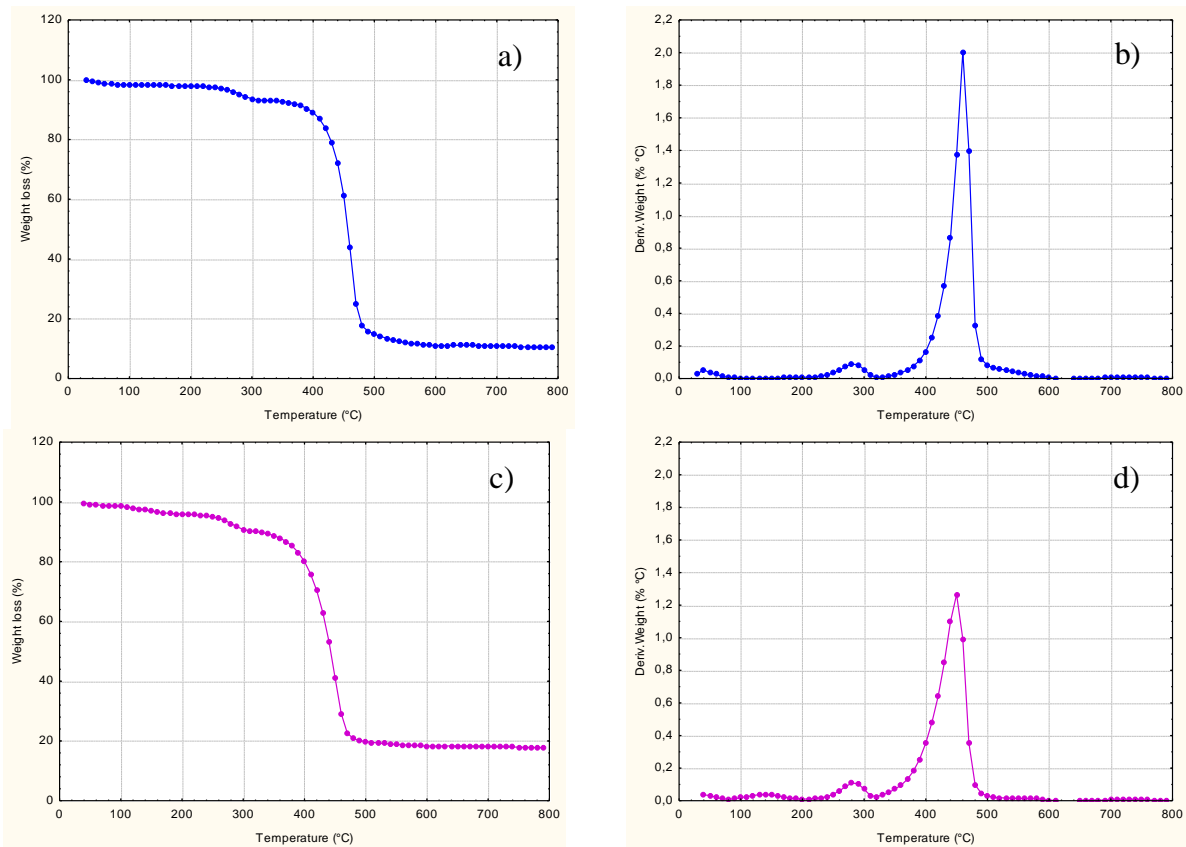


Figure 4.8: TGA and DTG curves of MIP (a, b), NIP (c, d).

This phenomenon could be explained that the thermal degradation of functional groups on backbone of NIP is adjacent in polymeric network. Therefore, they can degrade easier. On the other hand, in presence of template (imprinting effect) leads to more dispersion of functional monomers groups, which require more energy (heat) to overcome the polymer chain network. Based on these observations, presence of the template is able to change the stability of polymeric network and degradation profile of the imprinted polymer.

4.3.2.6 Determination of binding site distributions and affinities

Theoretically, the efficiency of the MIP-based SPE materials should display, apart from high affinity and selectivity, appreciable binding capacities for the analyte of interest. If these requirements are fulfilled, the MISPE procedure can be performed with rather small amounts of polymer, allowing the reduction, or even suppression, of nonselective adsorption effects.

The experimental binding data obtained for the polymers are shown on Figure 4.9 and Table 4.4. The values corresponding to the total number of binding sites as well as the affinity constant are markedly higher for the imprinted polymer compared to the non-imprinted polymer. The binding capacity of MIP3 ($N_{\text{MIP}}: 14 \pm 1$ ($\mu\text{mol/g}$)), exceeded with more than 4 fold that of the NIP ($N_{\text{NIP}}: 3.2 \pm 0.5$ ($\mu\text{mol/g}$)). Likewise the average affinity ($K_{\text{MIP}}: 29 \pm 2$ ($\times 10^{-1} \text{ mM}^{-1}$)), was nearly six-fold higher than that of the NIP ($K_{\text{NIP}}: 4.8 \pm 0.5$ ($\times 10^{-1} \text{ mM}^{-1}$)) in the measured concentration range. Thus it is demonstrated that the template plays a very important role in the recognition creating well defined cavities that offer very high affinity to the peptide.

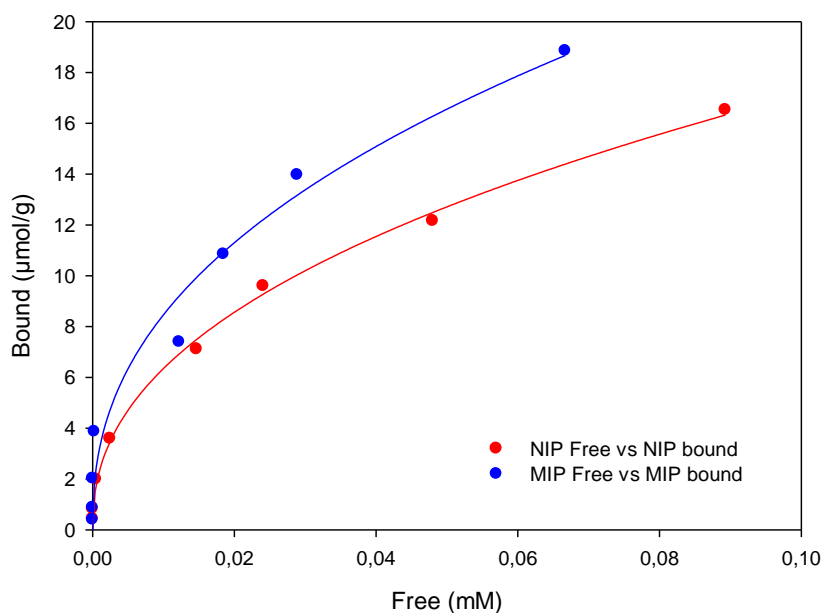


Figure 4.9: Equilibrium binding isotherms for the uptake of NLLGLIEAK by MIPs (blue line) and NIP (red line) in HEPES (0.1 M, pH 7)/ACN(95:5). Free = concentration of the free solute, Bound = specific amount of bound solute.

Table 4.4: Freundlich fitting parameters, obtained with the experimental binding data of target peptide towards the imprinted (MIP) and non-imprinted polymer (NIP).

Isotherm model	Affinity constant, K (mM^{-1}) $\times 10^{-1}$	Total number of binding sites N ($\mu\text{mol/g}$)	Heterogeneity parameter, m	Binding capacity, a ($\mu\text{mol/g}$ (mol^{-1}) m)	Regression coefficient, r^2
Freundlich MIP	29 ± 2	14 ± 4	0.42 ± 0.05	59 ± 4	0.98
Freundlich NIP	4.8 ± 0.5	3.2 ± 0.5	0.43 ± 0.03	46 ± 5	0.99

4.3.3 Optimization of MISPE procedure

The factors evaluated to establish the optimum conditions for the SPE procedure include the study of the composition and volume of the eluting solvent, the composition of the washing solvent, and cross-reactivity to the NLLGLIEAK.

Since the prepared MIPs were intended to be used for extracting NLLGLIEAK from human serum, their selectivity and recognition mechanisms were further evaluated under aqueous conditions. As already mentioned, several problems are related to this issue. Since the polymer backbone is of hydrophobic nature there is a problem with wettability of the surface and transport to the imprints in these conditions. Another problem related to these conditions is that the polar interactions, e.g. hydrogen bonds, formed in the pre-polymerization complex

are weakened by the presence of the polar and aqueous solvent. Extracting aqueous samples often leads to most of the adsorption to the polymer surface being of nonselective nature. However, this non-selective adsorption can be disrupted and transformed to selective adsorption to the imprints by carefully choosing the washing protocol.

The analyte contains several functional groups that may form hydrogen bonds, cationic and hydrophobic interactions with the functional monomer used, EAMA and the crosslinker, DVB. Since hydrogen bonding is weak in aqueous environment these non-selective interactions were interrupted when the MISPE cartridges were washed with water. However, the retention to the imprints was still strong under these conditions, probably due to a combination of several hydrogen bonds, steric factors and ionic interactions between the functionality of the analyte and the monomer.

The testing of the selective binding of NLLGLIEAK to the MIP was carried out off-line using MISPE cartridges that were manually packed in house with the imprinted material.

The selectivity of the MIP, or confirmation of the establishment of imprints, is often evaluated by comparing its retention parameters with those of a non-imprinted form of the polymer, NIP, synthesized in the same way, and often in parallel to the MIP, except for the addition of the template molecule.

Evaluating the elution solvent

The elution solvent was optimized in the first instance. The eluting step was optimized based on the principle of elution that the analytes could be eluted completely by a small volume (1–2 mL) of solvent. The strongest solvent (ability of the solvent to disrupt the interaction between the functional monomers and the analyte) is the one that uses less solvent volume. Therefore this one will be more concentrated in the resulting eluate. The addition of organic modifiers as acids to the elution solvent is usually [35] used due to help breaking the interactions between the polymers and the target analyte, upon protonation of the carboxylic acid(s) of the peptide. In order to optimize the elution solvent, 1 mL of 25 mg/L NLLGLIEAK, dissolved in HEPES buffer (0.1M, pH = 7.5), were percolated through the MIP cartridge. A stepwise gradient of 0.5 mL of 0.1 to 2 % trifluoroacetic acid (TFA) in MeOH was used for washing the MISPE (n=3) to select the optimised elution solvent for the extraction steps. The concentration of NLLGLIEAK was measured in each fraction.

Scaling up MIP for selective extraction of NLLGLIEAK

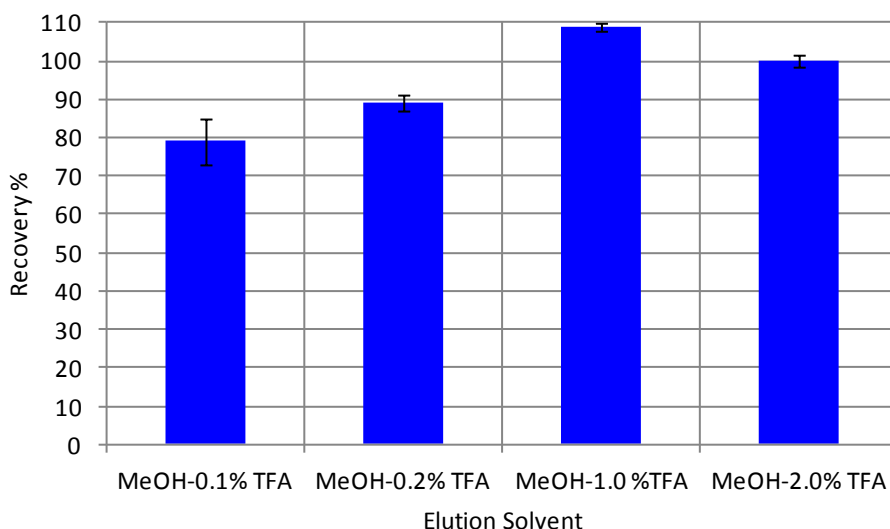


Figure 4.10: Recoveries obtained on the MIP after percolation of 1 mL of 25 mg/L NLLGLIEAK (HEPES, 0.1 M, pH 7.5), using 0.5 mL of different elution solvent.

As we have seen in Figure 4.10 the recoveries for NLLGLIEAK were increased with increasing acidic power. A quantitative extraction of the analyte is reached when one percent of TFA is used in the elution solvent. Nevertheless when the extraction procedure is achieved with real samples, other matrix component can interfere with this mechanism and make it less efficient. With the purpose and trying to assure that all the analyte will elute in these samples a final value of 2% TFA in methanol was selected as elution solvent.

Evaluating the washing solvent

Selectivity associated to an analytical method means that a specific method is suitable to determine the concentration of a particular analyte independently from the composition of the sample matrix, at least in a wide range of possible sample compositions and analyte concentrations.

In order to enhance the selectivity of MIP and decrease the cross-reactivity, the washing step was optimized. It is well known that the template could be retained on the MIP by selective and nonspecific interactions. Thus, a washing solution with moderate elution strength was used to damage the nonspecific interactions and to let the target peptide be retained by specific interactions [23]. In this experiment, MIP and NIP cartridges were preconditioned with 1 mL of MeOH, MeOH/H₂O (1:1), and followed by 1 mL of 25 mg/L NLLGLIEAK, (n=3) was passed through a cartridges and then washed with a stepwise gradient of 0 to 30 % acetonitrile in water was used for washing the cartridges. The recoveries of target peptide from the MIP and NIP are shown in Figure 4.11.

The results showed that when loading the NLLGLIEAK onto the polymer cartridges, approximately 17% breakthrough was detected from NIP cartridge whereas the MIP completely retained the peptide. Upon subsequent stepwise washes with water: ACN mixtures the NIP continued to release more peptide than the MIP. This is illustrated in Figure 4.11. This indicates that recognition occurs through a combination of hydrophobic and electrostatic interactions [14].

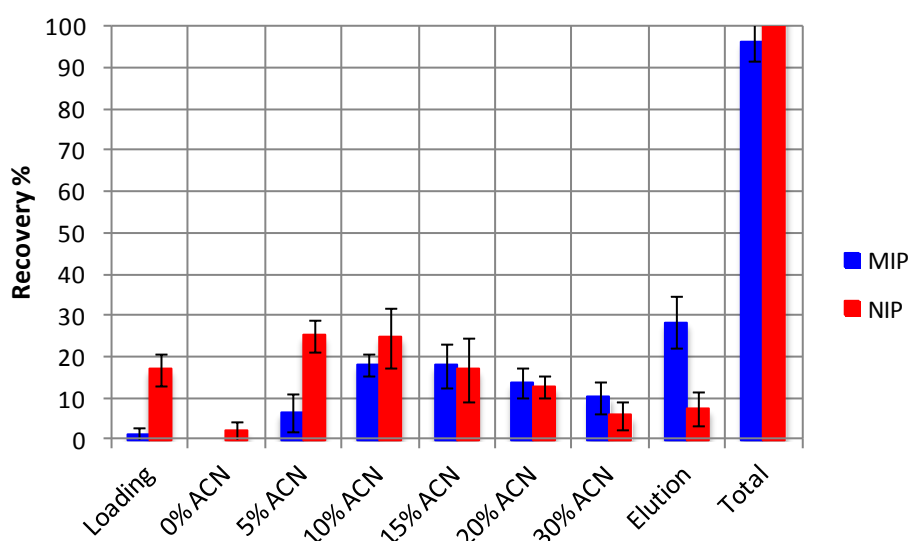


Figure 4.11: Recovery of NLLGLIEAK in the fractions collected after loading 1 mL of an aqueous sample of the peptide (25 mg/L) in HEPES buffer (0.1M, pH 7.5) on MIP and NIP followed by percolation of 0.5 mL of ACN/H₂O wash solutions as indicated and elution in 0.5 mL 0.5 mL of MeOH/TFA (98:2). The loading equilibration time was one hour. Columns represent three replicated and the error bars show the standard deviation.

After applying these conditions to MIP/NIP as shown in Figure 4.12 the high recovery of target peptide from the MIP arose from the excellent molecular recognition of the template molecule imparted by the imprinting process. Lower recoveries were obtained when the NIP was used as the extraction sorbent, as expected.

Consequently, 0.5 mL of H₂O/ACN (95:5) was investigated. This experiment showed that the selectivity of an MIP for an analyte depends on the careful choice of the extraction procedures as demonstrated in Figure 4.12 and Figure 4.13. In this regard, a washing step of 0.5 ml of H₂O/ACN (95:5) was added to the SPE protocol to “switch on” the molecularly selective retention mechanism of the MIP. The final optimized MISPE method is shown in Table 4.5.

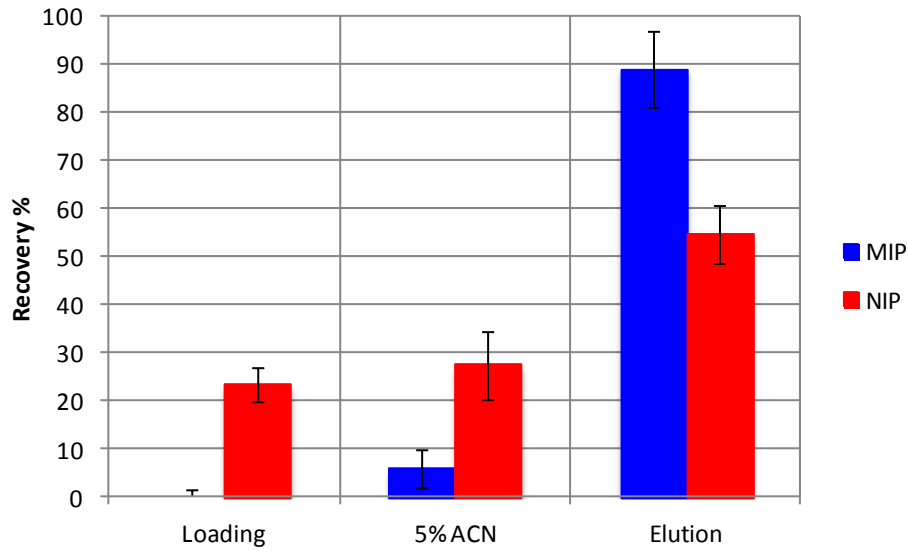


Figure 4.12: Recovery of NLLGLIEAK in each fraction using MIP and NIP, after percolation of 1 mL of 25 mg/L NLLGLIEAK (HEPES, 0.1 M, pH 7.5), washing with 0.5 mL of H₂O/ACN (95:5) and elution with 0.5 mL of MeOH/TFA (98:2). Columns represent three replicated and the error bars show the standard deviation.

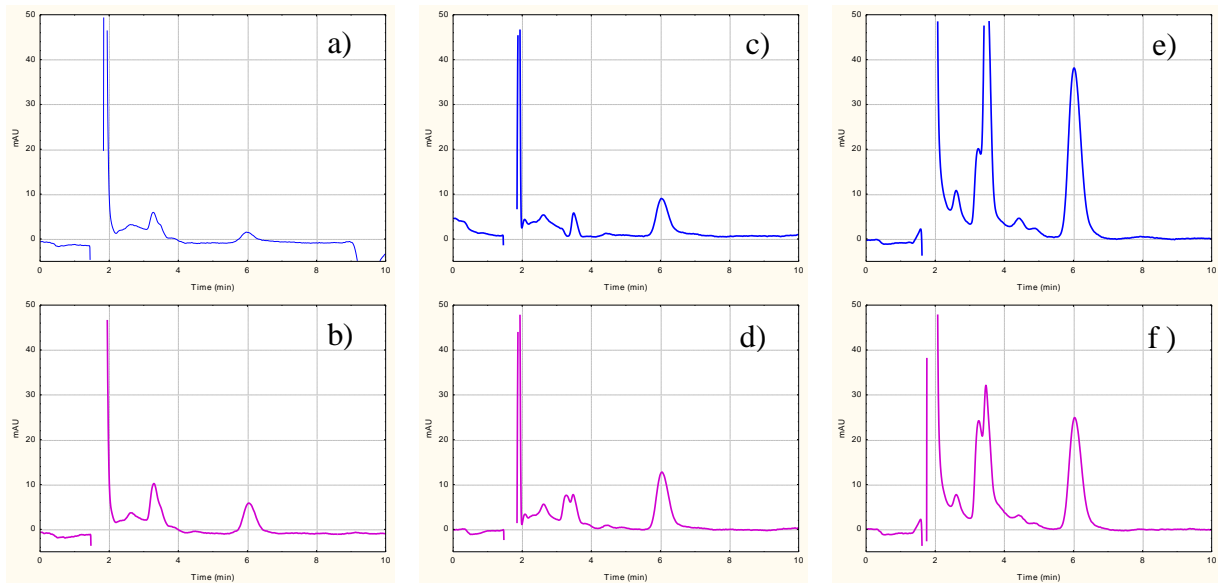


Figure 4.13: Chromatograms of loading, washing, and eluting fractions of spiked sample from MIP (a,c,e, respectively) and NIP (b,d,f, respectively) SPE cartridges. after percolation of 1 mL of 25 mg/L NLLGLIEAK (HEPES, 0.1 M, pH 7.5), washing with 0.5 mL of H₂O/ACN (95:5) and elution with 0.5 mL of MeOH/TFA (98:2).

Table 4.5: Optimised MISPE protocol for extraction of NLLGLIEAK from aqueous samples.

Parameter	Value
Load	1.0 mL (0.1 M HEPES, pH 7.5)
Wash	0.5 mL of H ₂ O/ACN (95:5)
Elution	0.5 mL of MeOH/TFA (98:2)
Flow rate	0.5 mL/min
Amount of polymer	20 mg

Analytical parameters

The intra- and inter-day precision study was performed using three different analyte concentrations. The analyses were carried out by repeating the SPE extraction using five replicates for intra-day precision and the same experiment was repeated for 3 separate days over a 1-week period for inter-day precision. NLLGLIEAK showed good precision for both intra-day and inter-day, with low relative standard deviation (RSD) as depicted in Table 4.6. Accuracy was assessed spiking the extract with three different levels of the analyte. The recovery values were between 81% and 87%, thus indicating the satisfactory accuracy of the method. Also the method is linear in range, 1.5-50 mg/L and limits of detection (LOD) and lower limit of quantification (LOQ) was 0.5, 1.6 mg/L, respectively. The analytical parameters summarized in Table 4.6 refers to the MISPE procedure after a determination of NLLGLIEAK by HPLC-UV. In other conditions using HPLC-MS-MS the determination of NLLGLIEAK in an adequate concentration range could be carried out.

Table 4.6: Analytical parameters of MISPE cartridge.

Validation parameters	
Linear range mg/L	1.5-50
Linearity	0.9962
Intra-assay precison (RSD,%) 9.70 mg/L (n=5)	6.2
Inter-assay precison (RSD,%) 4.85 mg/L (n=3)	5.7
9.70 mg/L (n=3)	5.9
19.40 mg/L (n=3)	7.4
Limit of detection mg/L	0.5
Limit of quantification mg/L	1.6
Accuracy (%Recovery) 4.85 mg/L (n=3)	87
9.70 mg/L (n=3)	85
19.40 mg/L (n=3)	81

4.3.4 Analysis spiked serum sample

Biological samples are challenging to extract since they contain many compounds that can be co-extracted simultaneously by the sorbent. As described above, the adsorption to the MIP in aqueous environment is often due to a non-selective interaction, which may be disrupted by a selective wash step. In the case of extraction from real sample matrix may also affect the selective rebinding to the imprints. It is therefore of great importance to investigate these effects in order to use the MIP most efficiently.

Digestion of ProGRP results in production of several peptides [36]. Among these NLLGLIEAK and LSAPGSQR which both are proteotypic. The chosen LC-MS/MS method was designed to specifically determine these two peptides. A typical chromatogram of these peptides is shown in Figure 4.14.

MISPE and NISPE of a digested ProGRP sample

To be able to monitor the behaviour of both NLLGLIEAK and LSAPGSQR on the MISPE and NISPE cartridges all flow-through fractions as well as the eluate were collected and analyzed on the LC-MS/MS.

Figure 4.15 shows the recovery of both NLLGLIEAK and LSAPGSQR in these fractions. The recovery was calculated in relation to the signals from the reference sample: $(\text{peptide intensity}_{\text{fraction}} / \text{peptide intensity}_{\text{reference}}) * 100 \%$. The flow through from the sample application shows a difference between the two cartridges. Hence whereas NLLGLIEAK was absent in the load and wash fractions after percolation through the MIP ca 15 % and 22% breakthrough respectively was observed after percolation through the NIP. Elution resulted in more than 60% recovery of NLLGLEIAK from the MIP while around 20 % was recovered from the NIP. The overall recovery in both cases was approx. 60 % implying that all NLLGLIEAK recovered after the MIP based extraction was recovered in the elution fraction – this in spite of loading a highly diverse peptide mixture on the column. Moreover, the fact that LSAPGSQR, was detectable in all collected fractions as well as in the elution step indicates that the MIP is selective for the target sequence. The total recovery of this peptide is comparable to that of NLLGLIEAK but it is clear that it is not specifically retained: most of the LSAPGSQR disappears in the during the washing step. The summary of analysis ProGRP sample is shown in Figure 4.16.

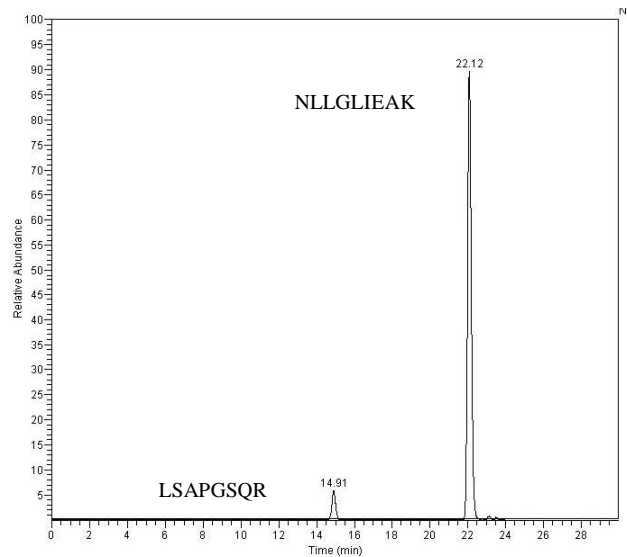


Figure 4.14: MS-extracted chromatogram of NLLGLIEAK (transition m/z 485.8→630.3, 743.4) and LSAPGSQR (transition m/z 408.2→282.6, 544.4) in an aquatic ProGRP digest sample.

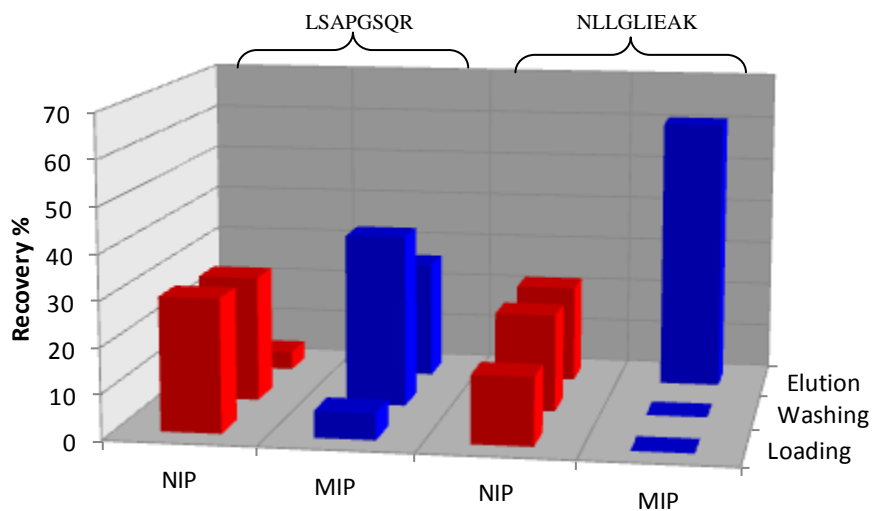


Figure 4.15: Recovery of NLLGLIEAK and LSAPGSQR in the fractions collected after loading 1 mL of 211 $\mu\text{g/L}$ digested ProGRP (ABC buffer (0.05M, pH 7.0) on MIP and NIP followed by percolation of 0.5 mL of $\text{H}_2\text{O}/\text{ACN}$ (95:5) and elution in 0.5 mL MeOH/TFA (98:2). The loading equilibration time was one hour.

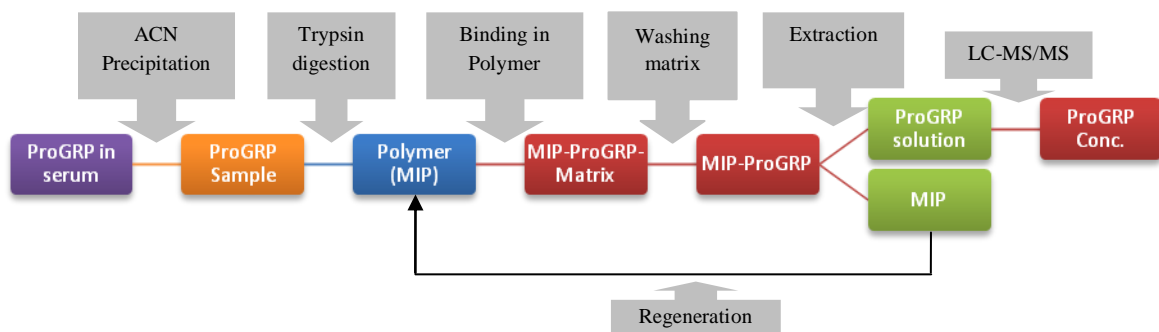


Figure 4.16: Flow chart for analysis ProGRP sample.

4.4 Experimental

4.4.1 Chemicals

The peptide H-NLLGLIEAK-OEt (T3) were purchased from Genscript (Piscataway, NJ, USA). The target nona-peptide NLLGLIEAK was synthesized in the group of Prof. Dr. Thomas Schrader (University Duisburg-Essen, Germany) with a purity above 95% on a microwave peptide synthesizer from CEM (Carolina, USA). Dry dimethylsulfoxide (DMSO) were purchased from Acros Organics (Geel, Belgium). Nitrogen (4.6) was purchased from Air Liquide (Düsseldorf, Germany). HPLC grade methanol (MeOH) and acetonitrile (ACN) were purchased from Merck KGaA (Darmstadt, Germany), and HPLC water was purified using a Milli-Q system (Millipore, Bedford, MA). Trifluoroacetic acid (TFA), hydrochloric acid (HCl), and pentamethyl piperidine (PMP) were purchased from Sigma-Aldrich Chemical Co (Deisenhofen, Germany). N-(2-aminoethyl) methacrylamide hydrochloride (EAMA) came from Polysciences, Inc. (Eppelheim, Germany). (N-2-hydroxyethylpiperazine-N'-2-ethanesulfonic acid) (HEPES) buffer and DVB were purchased from Sigma-Aldrich Chemie GmbH (Taufkirchen, Germany) and purified prior to use by distilled under reduced pressure ($\sim 8 \times 10^{-5}$ bar). The initiator 2, 2'-azobis (2, 4-dimethylvaleronitrile) (ABDV) was purchased from Wako Specialty Chemicals (Neuss, Germany) and used without further purification.

All porogen were kept under nitrogen atmosphere over molecular sieves and were used without further purification.

Recombinant ProGRP (31–98) were provided by Radiumhospitalet, Rikshospitalet Medical Centre (Oslo, Norway). Porcine TCPK treated Trypsin and ammonium bicarbonate (ABC) were purchased from Sigma-Aldrich (St. Louis, MO, USA), all other chemicals used were of analytical grade.

4.4.2 Polymer preparation

The molecularly imprinted polymer (MIP) pre-polymerization solution was prepared as follows: The template H-NLLGLIEAK-OEt (T3) (10 mg, 0.01 mmol) and the PMP (1.8 μ L, 0.01 mmol) were dissolved in 300 μ L DMSO in 4 mL HPLC vial. The mixture was left in contact for 15 minutes and then EAMA (195 mg, 1.18 mmol) and DMSO (1000 μ L), DVB (854 μ L, 6.0 mmol), ABDV (15 mg) were added and the solution purged with nitrogen for 5 min to remove dissolved oxygen. The vial was then sealed, and polymerization was allowed to proceed thermally in oven set at 50 °C for 24 hour and then at 60 °C for 24 hour.

The template molecule was removed through the following sequential washing steps: MeOH (100 mL), MeOH/0.1M HCl (90:10) (100 mL) and finally MeOH (100 mL). The MIP particles were allowed to equilibrate for *ca.* 6 h with each washing solution, after which the wash solution was decanted off. Thereafter, the resulting bulk polymers were grounded and sieved to a final size ranging between 25 and 50 μm . Prior to use, they were sedimented using MeOH/H₂O (80:20) in order to remove fine particles. A non-imprinted polymer was prepared in the same way, but in the absence of the template molecule.

4.4.3 Adsorption isotherms

Theoretically, the efficiency of the MIP-based SPE materials should display, apart from high affinity and selectivity, appreciable binding capacities for the analyte of interest. If these requirements are fulfilled, SPE can be performed with rather small amounts of polymer, allowing the reduction, or even suppression, of nonselective adsorption effects.

Adsorption isotherm studies were carried out using solvent mixture HEPES/ACN (95:5), 5 % v/v of acetonitrile was added in the incubation aqueous solvent to achieve effective particle sedimentation. For this purpose, 10 mg of dry polymer MIP and NIP were weighed and transferred to plate, and 0.8 mL of 5, 10, 25, 50, 100, 150, 200 and 300 μM of NLLGLIEAK (T) (0.1 M HEPES, pH 7.5) were added. The plate were sealed and incubated in shaker for 24 hour. a 0.8 mL aliquot of the supernatant was removed and placed into HPLC vial then analyzed for remaining free analyte concentration *F*.

The amount of bound analyte to the polymer (*B*) was calculated by subtracting the non-bound amount (*F*), from the initial target peptide concentration in the mixture. The binding experiments were carried out by duplicate.

All data was determined from average *B* and *F* values from duplicate analysis, which was then fitted to Freundlich model using Sigma plot software.

4.4.4 MISPE method development and optimization

To prepare the MISPE columns, 20 mg \pm 0.5 of MIP and NIP were weighed into 1.8 mL HPLC empty vial (Braun, Germany). The MIP and NIP in the HPLC vial were slurred with 2.0 mL Methanol and the slurry was transferred to the empty SPE cartridges (1mL, Varian, Gemany), were connected to a vacuum manifold and sedimented with application of vacuum, in order to ensure the particles were uniformly packed into the cartridges between two polyethylene frits with a pore size of 20 μm . The cartridges were subjected to vacuum for 30 s

before insertion of second frit on top of the sorbent beds. The cartridges were labeled for identification purposes. Figure 4.17 shows examples of SPE cartridges and peristaltic pump.

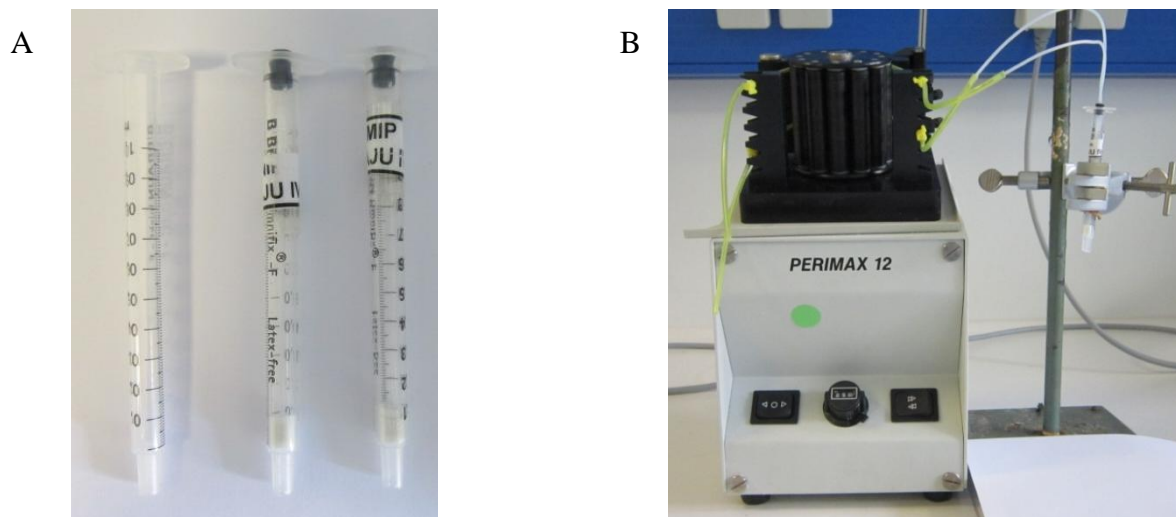


Figure 4.17: Examples of SPE cartridges (A), Peristaltic pump (B).

SPE experiments were performed offline using Peristaltic pump (Figure 4.17 (B)) at flow rate 0.5 mL/min. Analyte detection was performed at 205 nm. The optimised procedure for the SPE experiments comprised three steps: I) a loading step using aqueous solvent HEPES buffer 0.1 M, pH 7.5, II) a washing step were investigated by using different ratio of ACN (0-30%) in H₂O, and III) an elution step using a stronger eluent MeOH/TFA (98:2). And the percentage of target peptide removed from MIP/NIP in each step were analysed by HPLC-UV. After each run the columns were regenerated by a continuous washing with 1 mL of MeOH, MeOH/H₂O (1:1), and H₂O.

In order to evaluate intermediate precision (inter-day precision) and accuracy (intra-day precision), assays were performed by loading and extracting 9.70 mg/L five times on the same day and 4.85, 9.70, 19.40 mg/L five times over different days. The percentage relative standard deviations (RSD %) of the data thus obtained were calculated.

Accuracy was evaluated by means of recovery assays carried out by loading analyte corresponded to concentrations of 4.85, 9.70, and 19.40 mg/L. The mean recoveries of three times were then calculated.

Evaluation of the linearity was performed by loading 1 mL of NLLGLIEAK (T) with concentrations with 1.5, 5.0, 10.0, 25.0, and 50.0 mg/L.

The limit of detection (LOD) and the limit of quantification (LOQ) were the minimum detectable amounts of analyte spiked giving a signal-to-noise ratio of 3 or 10, respectively. The LOQ was 1.6 mg/L, whereas the LOD was 0.5 mg/L.

4.4.5 Digestion of ProGRP

Trypsin was weighed in and dissolved in fresh prepared 50 mM ammonium bicarbonate buffer at a concentration of 1 g/L. This was done immediately before use. The solution was kept on ice during all further steps.

A stock solution ProGRP with a concentration of 211 mg/L was diluted using fresh prepared ammonium bicarbonate buffer to a standard solution with a concentration of 211 µg/L. To 1 mL of this standard solution trypsin was added such that the enzyme:substrate ratio was 1:40. After mixing the sample was incubated over night at 37 °C to ensure maximal digestion. The next day possible trypsin activity was stopped by adding 10 µL formic acid. The resulting aliquot was either directly applied as sample on both MISPE and NISPE or used as reference sample to calculate the extraction recovery.

Bibliography

- [1] He.C., Long.Y., Pan.J., Li.K. and Liu.F, *J.Biochem.Biophys.Methods*, vol. 70, pp. 133-150, 2007.
- [2] Martina.L. and Pavel.J, *J.Sep.Sci*, vol. 32, 2009.
- [3] Sellergren.Börje, *Molecularly imprinted polymers man made mimics of antibodies and their applications in analytical chemistry*, Amsterdam: Elsevier, 2001.
- [4] Pichon.V. and Chapuis-Hugon.F, *Anal.Chim.Acta*, vol. 622, p. 48, 2008.
- [5] Yan.H.Y. and Row.K.H., *Int.Mol.Sci*, vol. 7, p. 155, 2006.
- [6] Haginaka.J, *J.Sep.Sci*, vol. 32, p. 1548, 2009.
- [7] Caro.E., Marce.R.M., Borrull.F., Cormack.P.A.G. and Sherrington.D.C., *Trends Anal. Chem*, vol. 25, p. 143, 2006.
- [8] Sellergren.B, *Anal.Chem*, vol. 66, pp. 1578-1582, 1994.
- [9] "Scopus," [Online]. Available: <http://www.scopus.com/home.url>. [Accessed 17 07 2013].
- [10] Yanga.H-H., Zhou.W-H., Guob.X-C., Chenb.F-R., Zhaob.H-Q., Linc.L-M. and Wang.X-R, *Talanta*, vol. 80, pp. 821-825, 2009.
- [11] Yanga.H-H., Zhou.W-H., Guob.X-C., Chenb.F-R., Zhaob.H-Q., Linc.L-M. and Wang.X-R, *J.Sep.Sci*, vol. 28, pp. 2080-2085, 2005.
- [12] DeBarros.L.A., Martins.I. and Rath.S, *Anal Bioanal Chem*, vol. 397, pp. 1355-1361, 2010.
- [13] Ambrosini.S., Shinde.S., DeLorenzi.E. and Sellergren.B, *Analyst*, vol. 137, pp. 249-254, 2012.
- [14] Cobb.Z. and Andersson.L, *Anal Bioanal Chem*, vol. 383, pp. 645-650, 2005.
- [15] Urraca.J, Aureliano.C, Schillinger.E., Esselmann.H., Wiltfanf.J. and Sellergren.B, *J.Am.Chem.Soc*, vol. 133, pp. 9220-9223, 2011.
- [16] Mohamed.R., Mottier.P., Treguier.L., Richoz-Payot.J., Yilmaz.E. and Tabet.J-C., *J.Agric.Food.Chem*, vol. 56, no. 10, pp. 3500-3508, 2008.
- [17] Puoci.F., Curcio.G., Iemma.F., Spizzirri.U.G. and Picci.N, *Food Chem*, vol. 106, pp. 836-842, 2008.
- [18] Yin.J., Wang.S., Yang.G., Yanga.G. and Chena.Y, *J.Chromatogr.B*, vol. 844, pp. 142-147, 2006.
- [19] Jiang.T., Zhao.L., Chu.B., Feng.Q., Yan.W. and Lin.J-M, *Talanta*, vol. 78, pp. 442-447, 2009.
- [20] Theodoridis.G. and Manesiotis.P, *J.Chromatogr.B*, vol. 844, pp. 142-147, 2006.
- [21] Yang.J., Hu.Y., Cai.J.B., S. Zhu.X.L., Hu.Y.Q. and Liang.F.X, *Food Chem Toxicol*, vol. 45, pp. 896-903, 2007.
- [22] Muldoon.M.T. and Stanker.L.H, *Anal.Chem*, vol. 69, p. 803, 1997.
- [23] Zander.A., Findlay.P., Renner.T., Sellergren.B. and Swietlow.A, *Anal.Chem*, vol. 70, p. 3304, 1998.
- [24] Muldoon.M.T. and Stanker.L.H, *Anal.Chem*, vol. 69, p. 803, 1997.
- [25] Stevenson.D, *Trends Anal.Chem*, vol. 18, p. 154, 1999.

- [26] Rashid.B.A., Briggs.R.J., Hay.J.N. and Stevenson.D, *Anal. Commun*, vol. 34, p. 303, 1997.
- [27] Berggren.C., Bayouhd.S., Sherrington.D. and Ensing.K.J, *J. Chromatogr.A*, vol. 889, p. 105, 2000.
- [28] “Sigmaaldrich,” [Online]. Available: <http://www.sigmaaldrich.com/analytical-chromatography/sample-preparation/spe/supelmip.html>. [Accessed 19 07 2013].
- [29] Tamayo.F.G., Turiel.E. and Martin-Esteban.A., *J.Chromatogr.A*, vol. 1152, pp. 32-40, 2007.
- [30] Cormack.P.A.G. and Mosbach.K., *React Func Polym*, vol. 41, pp. 115-124, 1999.
- [31] Stevenson.D, *Trends Anal. Chem*, vol. 18, no. 3, pp. 154-158, 1999.
- [32] Chapuis.F., Pichon.V. and Hennion.M-C., *LC GC Europe*, vol. 17, no. 7, pp. 408-417, 2004.
- [33] Gonzalez.P.G., Pilar.F.H. and Alegria.J.S., *Anal.Chem.Acta*, vol. 557, pp. 179-183, 2006.
- [34] Lulinski.P. and Maciejewska.D, *Mat Sci Eng C*, vol. 31, pp. 281-289, 2011.
- [35] Benito-Peña.E., Martins.S., Orellana.G. and Moreno-Bondi.M.C, *Anal. Bioanal.Chem*, vol. 393, p. 235, 2009.
- [36] Winther.B. and Reubsæet.J, *J.Sep.Sci*, vol. 30, pp. 234-240, 2007.

Chapter 5

Grafted Peptide imprinted films, design and development

5.1 Abstract

In this chapter we introduce a new method for designing and producing grafted molecularly imprinted polymers on activated silica surfaces for the NLLGLIEAK peptide chosen for ProGRP quantification. The synthetic materials are cheap and robust with affinity recognition sites.

The polymers were developed using the previously optimized monomers-crosslinker type and ratio. The polymers created by incubating prepolymerization solution with modified silica by 4-cyanopentanoic acid dithiobenzoate (CPDB).

The molecularly imprinted solid phase extraction (MISPE) optimization has been initially carried out off-line by investigating different conditioning, wash and elution solvents and by comparing recoveries from imprinted and non-imprinted polymers achieving different elution profiles. Increasing progressively sample complexity from digested ProGRP standard solution to fortified digested serum injection, the research will explore MIPs application in ProGRP analysis of complex clinical samples with the goal to achieve a sensitive, fast and cost-effective analytical tool for the early diagnosis of small cell lung cancer (SCLC).

5.2 Introduction

MIPs prepared by the conventional free radical polymerization (FRP) technique have some disadvantages such as low affinity binding, high diffusion barrier, low rate mass transfer.

The most drawbacks to conventional FRP are the lack of control over chain propagation and termination because of the very high reactivity of the radicals. This results in the formation of

polymer networks with heterogeneous structures [1] [2]. The presence of heterogeneity within the network structures of MIPs could have significant affects on the quality of the binding sites inside the networks, which might be responsible in a broad of binding sites and low affinity sites and low overall capacity [3].

Many polymerization methods have been employed to address the drawbacks generated from the above-mentioned MIP format. Surface imprinted polymer (SIP) via controlled/living radical polymerization is one of the most promising techniques and has been used to give hybrid materials with controlled shape and size [4] [5].

SIP has been prepared on silica gel [4] [5], organic polymers carrier [6], gold electrodes [7] [8], and capillary columns [9] [10] with molecularly imprinted technique, which offered rapid kinetics and site accessibility.

In fact, polymer/silica composites are the most commonly reported in the literature. They have received much attention in recent years and have been employed in a variety of applications.

The use of surface initiated controlled/living radical polymerization can control the structure of the resultant polymer shell through changes in grafting density, composition and molar mass for different types of organic polymers with varied structural design on the silica surfaces [11]. In general controlled/ living polymerization can be achieved by nitroxide-mediated processes (NMP), metal catalyzed atom transfer radical polymerization (ATRP) and degenerative transfer, e.g. reversible addition– fragmentation chain transfer (RAFT).

Among these techniques, reversible addition-fragmentation chain transfer (RAFT) polymerization, which was first reported by the group of Rizzardo in 1998 [12], is most promising. RAFT technique has the capability to control the polymerization of a wide variety of monomers.

5.3 Scope of the work and chemicals used

5.3.1 Templates and monomers

In 2011, 2012, Hallhali et al [13] [14] improved grafting technique for producing imprinted thin film on silica beads. The imprinted polymer showed high recognition and binding ability towards the template molecule. However, the scope of the study here presented focused only on proving that RAFT method can be used for imprinting peptides. Guided by this work,

which was performed in our laboratories, we decided to use the same protocol used by Hallhali et al. but we applied it to generate composite-MIPs potentially able to specifically bind the model NLLGLIEAK. With this goal, we selected the two templates (T1 and T2), with EAMA-DVB system.

To the best of our knowledge, this is the first time that RAFT method is used to produce such polymeric format. The resulting MIP composites have the advantages of more accessible binding sites and faster mass transfer compared to the MIPs prepared by conventional bulk polymerization techniques [15].

The resulting thin MIP film coated silica can be applied in solid-phase extraction, HPLC as well as in capillary electrochromatography [15].

5.3.2 RAFT mechanism

RAFT agents are organic compounds possessing a thiocarbonylthio moiety. The generic structures of RAFT agents employed in RAFT are shown below (Figure 5.1). The R group should be a good free radical leaving group, capable of reinitiating the radical polymerization process, whereas the Z group activates the C=S double bond towards radical addition and then stabilizes the resultant adduct radical.

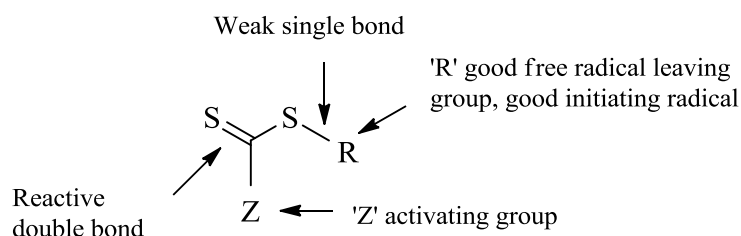


Figure 5.1: Generic structures of RAFT chain transfer agent.

In principle, the polymer obtained by RAFT polymerization is believed to involve a series of initiation, propagation and termination.

The mechanism is explained well with the help of Figure 5.2. After initiation, the primary propagating radical P_n^\bullet is added with the RAFT agent (1) to form an initial intermediate RAFT radical (2), and then it is followed by the fragmentation of RAFT radical (2) to get a new RAFT agent (3) and release an R^\bullet radical. Thereafter, the radical R^\bullet react with monomer to form a new propagating radical P_m^\bullet .

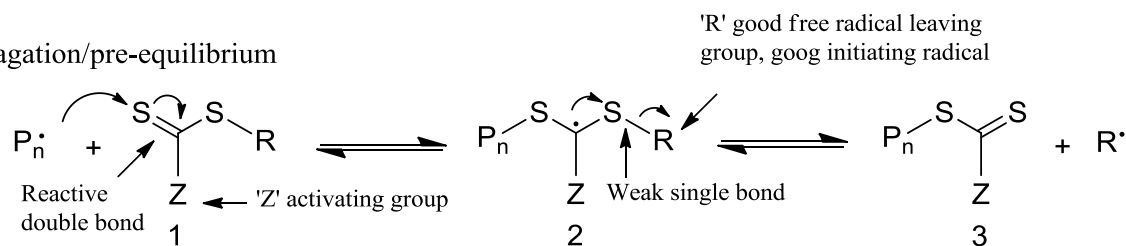
During the main equilibrium, a propagating radical reacts with the RAFT agent (3), forming a new dormant polymer (5). The polymer chain from the RAFT agent is released as a radical

capable of further growth, i.e. an active polymeric radical P_n^\bullet . The cycle of addition to the C=S bond, followed by fragmentation of a radical, continues until all monomer or initiator is consumed [16].

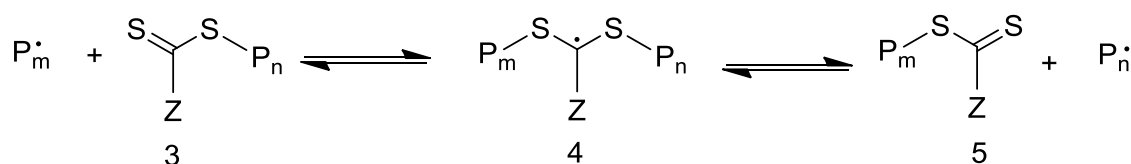
Initiation



Propagation/pre-equilibrium



Propagation/main equilibrium



Termination



Figure 5.2: Reaction scheme of RAFT polymerization adapted from [17]

RAFT has some advantages because: (1) it can be successfully carried out under a wide range of reaction conditions (bulk, solution, suspension, emulsion) and give polymers a with narrow molecular weight distribution (MWD), (2) it is applicable to a wide range of functionality in monomer types (e.g., OH, $-\text{COOH}$, $-\text{CONR}_2$, $-\text{NR}_2$, $-\text{SO}_3\text{Na}$) and (3) as the majority of chains in the product polymer possess the $\text{S}=\text{C}(\text{Z})\text{S}$ group the polymerization can be continued in the presence of a second monomer resulting in a block copolymer [18].

Due to these advantages, the RAFT technique has recently received substantial attention in the area of surface modification with polymers. Since the first report of applying this

technique to surface initiated graft polymerization on a solid surface in 2001 [19], the RAFT technique has been utilized in the surface modification of various substrates, including inorganic /organic particles [20] [21] [22], flat silicon wafers [23] [24], clay [25], flat gold surfaces [26] [27], glass slides [28], carbon nanotubes [29] [30] [31], cellulose [32] [33], and polymer films [34] [35] [36].

5.4 Silica support and modification

5.4.1 Immobilization of RAFT agent

The silica supports were modified with 3- aminopropyltriethoxysilane (APTS) as previously reported [37].

The Si-500 beads (average surface area: $S_A = 45 \text{ m}^2/\text{g}$; average pore volume: $V_p = 0.81 \text{ mL/g}$, average pore diameter: $D_p = 47.5 \text{ nm}$) was modified by grafting the 4-cyanopentanoic acid dithiobenzoate (CPDB) as illustrated in the Figure 5.3.

Grafting the photosensitive dithiobenzoate group on the silica surface allows the creation of radicals upon thermo initiation; these radicals can be used as starters of a graft copolymerization of functional monomers from the surface. Thus, by living radical polymerisation [34] it occurs the formation of a thin layer of covalently attached functional polymer covering the entire specific surface of the support material occurs. The resulting grafting modified silica was then subjected to N_2 sorption to ascertain the exact pore volume, surface area and diameter of the silica particles after modification. These values are critical in the calculation of the exact amounts of monomer, crosslinker and solvent to use during the subsequent polymerization to achieve a desired polymer thickness.

In Table 5.1 the Brunauer-Emmett-Teller (BET) method showed, as expected, an overall decrease in all the structural parameters when compared with the starting silica support (average surface area: $S_A = 37 \text{ m}^2/\text{g}$; average pore volume: $V_p = 0.424 \text{ mL/g}$, average pore diameter: $D_p = 32.26 \text{ nm}$), indicating the successful grafting of the RAFT with an initiator density of $(3.6 \text{ } \mu\text{mol}/\text{m}^2)$.

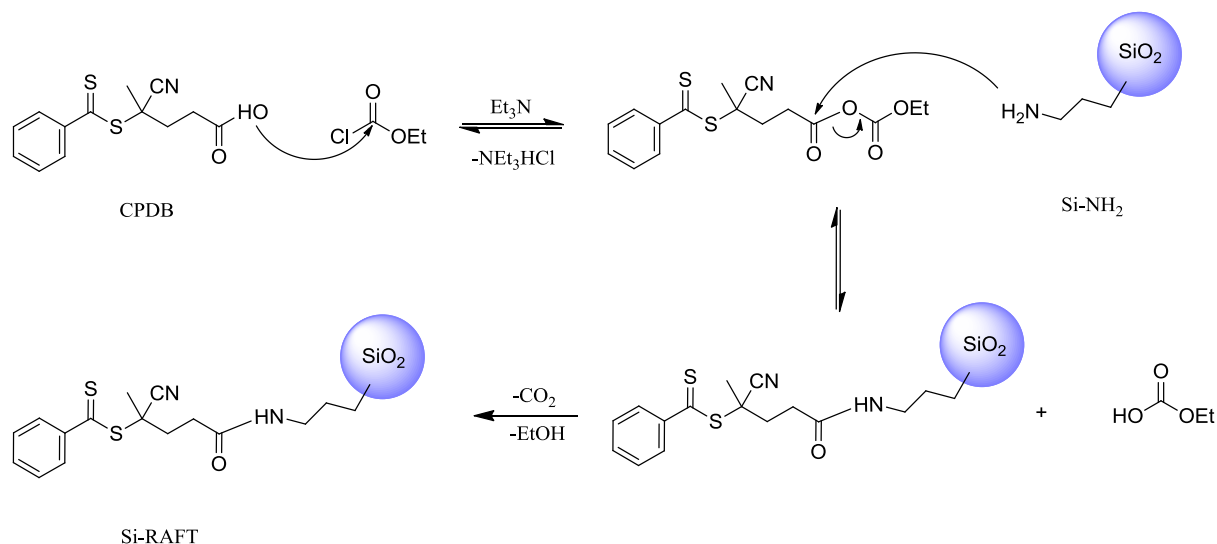


Figure 5.3: Reaction mechanism for the synthesis of functionalized RAFT.

Table 5.1: Physical characterization of composite materials

Modified support	Elemental Composition			S_A (m^2/g)	BET	
	% C	% N	% S		Vp (mL/g)	Dp (nm)
Si-500	1.80	0.80	—	45	47.50	0.810
Si-500-RAFT	3.25	0.24	1.10	37	32.26	0.424

5.4.2 Polymer synthesis

The ratio and the selection of the templates, functional monomer, crosslinker and porogen have been described in Table 5.2. The porogen DMSO was chosen to dissolve the templates and EAMA monomer in less amount and then diluted with ACN.

EAMA and DVB in previous chapters show a good combination with templates used in this work. To take advantage of the EAMA/DVB system, two templates T1 and T2 was used by RAFT polymerization method. A possible cavity formed in the polymer is presented in Figure 5.4.

Table 5.2: Composition of the polymers synthesized

Poymer	Template	Monomer	Crosslinker	ABDV	Si-RAFT	Molar ratio T/FM/CL	RAFT:ADVB ratio
P_{T1}	1.81 mg	EAMA (36 mg) 0.22 mmol	DVB (144 μ L) 1.10 mmol	37 mg (0.15 mmol)	1.0 g	0.03/3.93/20	1
P_{T2}	2.03 mg	EAMA (36 mg) 0.22 mmol	DVB (144 μ L) 1.10 mmol	37 mg (0.15 mmol)	1.0 g	0.03/3.93/20	1
P_{NIP}	—	EAMA (36 mg) 0.22 mmol	DVB (144 μ L) 1.10 mmol	37 mg (0.15 mmol)	1.0 g	—/3.93/20	1

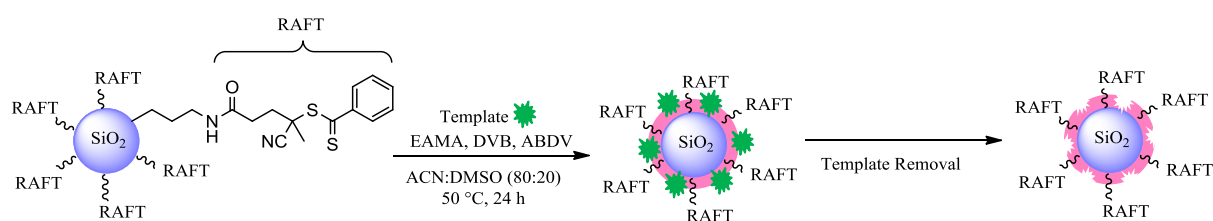


Figure 5.4: Procedure for preparation of MIP via RAFT modified silica for binding the T1 or T2, and hypothetical structure of the imprinted binding site.

5.5 Results and Discussion

5.5.1 Characterisation

After polymerization and template extraction, the particles were dried and subsequently characterised by elemental analysis, scanning electron microscopy (SEM), and thermogravimetric analysis (TGA).

5.5.1.1 Elemental analysis

Table 5.3 summarises the results obtained from the elemental analysis. All the composite materials contain sulfur in their composition, which support the living radical polymerization mechanism. Thus, dithiocarbamate molecules are attached at the end of the polymer chain. The calculated layer thickness from the % C using the equation mentioned below revealed values very close to the aimed 3 nm.

Table 5.3: Elemental composition of the prepared polymers

Polymer	C (%)	N (%)	S (%)	d [§] (nm)
P _{T1}	9.60	1.03	0.61	3.09
P _{T2}	9.63	0.94	0.61	3.10
P _{NIP}	9.60	0.95	0.59	3.09

[§]The average thickness (d) of the grafted polymer films was estimated based on the carbon content as $d = ((mc \times Mw) / (Mc \times \rho \times S_A)) \times 10^3$, where $mc = \%C / (100 - ((\%C \times Mw) / Mc))$ = weight of carbon of the grafted polymer per gram of bare silica support, Mw = weighted average molecular weight of the grafted polymer assuming stoichiometric incorporation of reactive monomers, Mc = weighted average molecular weight of the carbon fraction of the grafted polymer ρ = weighted average density of monomers (g/mL) and S_A = specific surface area of the bare silica support (m²/g) [38].

5.5.1.2 Thermogravimetric analysis TGA

The TGA profiles showed similar decomposition steps upon heating for all the materials, these decompositions start at around 200 °C to end at around 680 °C, which corresponds to the decomposition temperature of the polymeric material. Heating above 680 °C leaves only the silica. Figure 5.5 demonstrates the (TGA) curves of RAFT agent, P_{T1}, P_{T2}, and P_{NIP}. All polymers were showed mass weight loss around 17% but if substrate it from the mass weight loss of RAFT agent 7% we will get 10 %. This mean it is difficult to achieve high monomer conversion in EAMA-DVB system even after preparing the polymers many times. Since this

is the first time to use EAMA-DVB system in RAFT techniques, it looks the RAFT agent CPDB not totally suitable with this system.

Further, from TGA data, the thickness of the grafted polymer film, d (nm) inside the solid silica support was calculated as shown in Table 5.4 and the values agree elemental analysis method as shown in Table 5.3 with from both methods are the same.

Table 5.4: Mass loss and calculated film thickness

Polymer	Weight loss %	d^{\S} (nm)
RAFT	7.34	1.29
P _{T1}	17.88	3.73
P _{T2}	17.58	3.65
P _{NIP}	16.32	3.31

[§]The average thickness (d) of the grafted polymer films was extracted from the equation: $d = ((\Delta m \times \rho) / S_A) \times 10^3$, where Δm = weight of the grafted polymer per gram of bare silica support, ρ = weighted average density of monomers (g/mL) and S_A = specific surface area of the bare silica support (m²/g) [38].

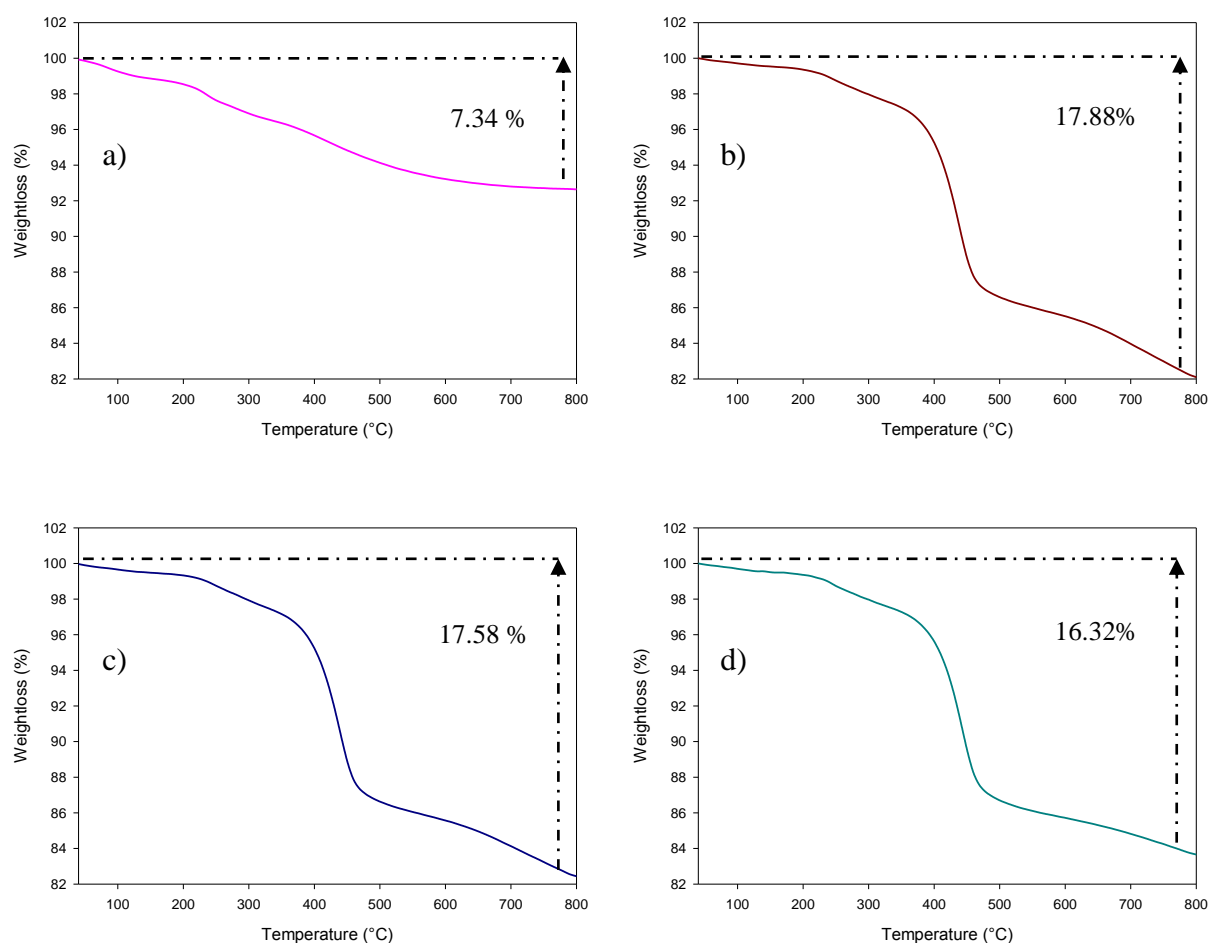


Figure 5.5: TGA curves of Si-RAFT (a), P_{T1} (b), P_{T2} (c), P_{NIP} (d)

5.5.1.3 Microscopy SEM

Scanning electron microscopy (Figure 5.6) indicates the successful formation of the graft polymer inside the pores. No agglomeration is observed also in the case of smaller particles. The P_{NIP} shows a relatively smooth surface. However, there are obviously some holes existing within the P_{T2} and P_{T1} . These strongly indicate that an imprint was formed within the MIP. As also observed, the spectrum of MIPs is almost the same as that of NIP. This indicates that almost all templates are removed from the precursor, which presents a convenience for further study.

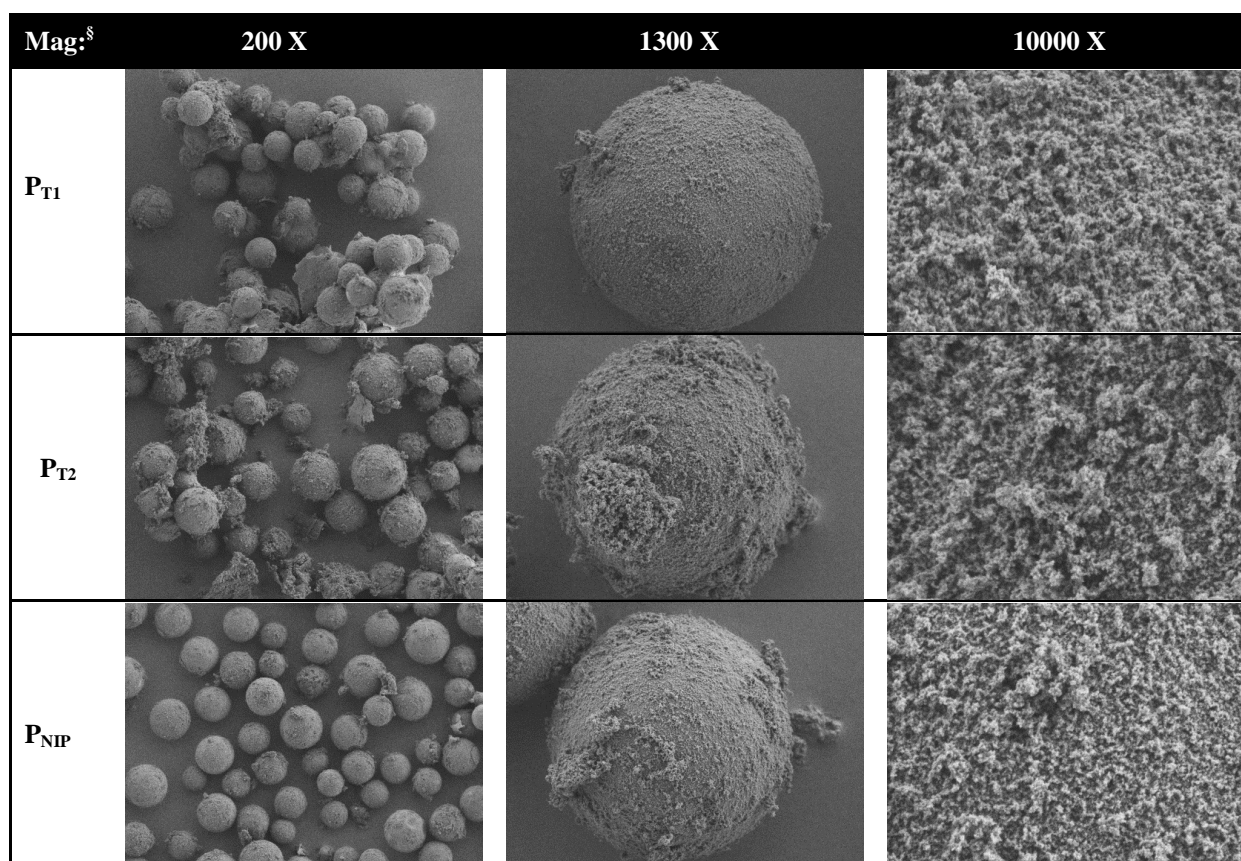


Figure 5.6: Scanning electron microscopy (SEM) picture of P_{T1} , P_{T2} and P_{NIP} at different magnifications. § Mag: Magnification

5.5.2 Molecularly imprinted solid phase extraction (MISPE)

The objective of this task was to develop an MISPE method capable of selectively enriching low concentrations of NLLGLIEAK in presence of digestion ProGRP biomarker. MISPE consists of a loading step, a washing step to remove unspecifically bound peptide by using different ratio of ACN (0-30%) in H₂O, and an elution step done by 0.5 mL of MeOH/TFA (98:2). The direct injection of MISPE eluent in the HPLC column gave rise to a significant peak desorption in the chromatographic separation, even if smaller sample volumes were injected into the column. This behavior was attributed to the higher elution strength of the eluent to respect to the mobile phase. One way to avoid this problem would be to evaporate the organic solvent and reconstitute the extract in the mobile phase. However to avoid stability problems of the peptides under these conditions, a dilution with 0.5 mL of H₂O was added.

It has been described before for other similar compounds that the non specific interactions between the analytes and the imprinted polymer can be minimized in presence of mixtures ACN/H₂O. With this purpose different proportion of ACN/H₂O were tested using a fix volume of 0.5 mL, loading a fix concentration of 10 mg/L of NLLGLIEAK to the imprinted and non imprinted polymer. The results are summarized in Figure 5.7.

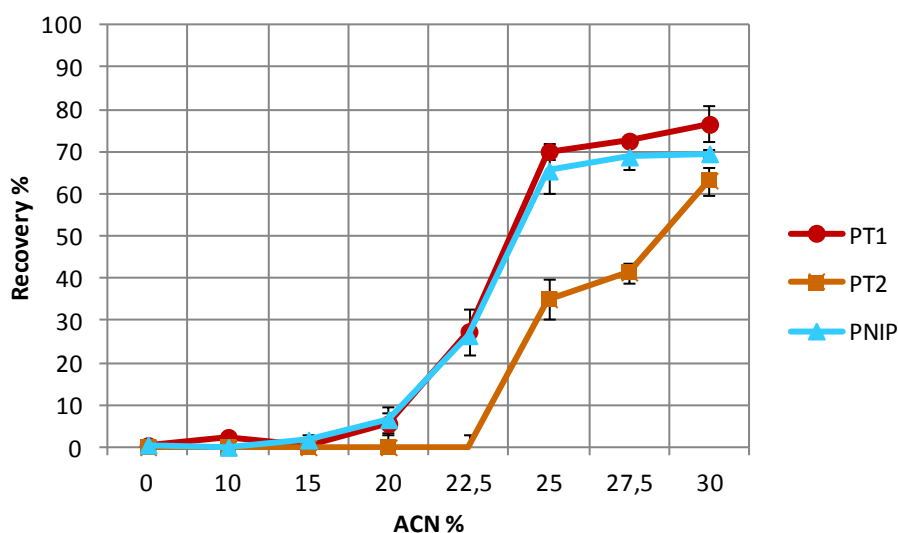


Figure 5.7: Recoveries obtained on the P_{T1}, P_{T2} and P_{NIP} after percolation of 1 mL of 10 mg/L NLLGLIEAK (HEPES, 0.1 M, pH 7.5), using 0.5 mL of different washing solvent and elution with 0.5 mL of MeOH/TFA (98:2).

As shown in Figure 5.7 that the use of a mixture ACN/H₂O (22.5:77.5) allowed recoveries with a big difference for both polymers. The MIP polymer (P_{T2}) rebind 100 % of peptide

comparing to P_{T1} and P_{NIP} which was around 74 % for both of them ($n=2$). On the other hand, the differences between these polymers decrease until to be non significance at 30% ACN.

Thus it is explored a strong imprinting effect in the P_{T2} comparing to P_{T1} when these conditions are used. In conclusion a volume of 0.5 mL using ACN/ H₂O (22.5:77.5) was selected for the washing step.

5.5.3 Determination of the binding capacity of the polymers

The binding properties of the P_{T2} and P_{NIP} polymers were assessed by equilibrium analysis. A rebinding test was carried out using NLLGLIEAK in mixture of ACN/HEPES (5:95) (0.1 M, pH 7.1) with a concentration range from 0.005 to 0.2 mM. The addition of small amounts of organic solvents such ethanol or acetonitrile in the adsorption assay may suppress the hydrophobic nonspecific binding leading to better substrate recognition into the imprinted cavities based upon other weak noncovalent forces.

The binding parameters of NLLGLIEAK to both the imprinted (P_{T2}) and non-imprinted polymer (P_{NIP}) were accurately modeled using the Freundlich isotherm (FI). As shown in Figure 5.8 and as detailed in Table 5.5, the binding isotherms generated for the P_{T2} and P_{NIP} were well fit by the Freundlich model (regression coefficient, $r^2 \sim 0.90$). The imprinted beads exhibited higher adsorption of NLLGLIEAK than their corresponding blank polymers over 24 hour times; thus, an imprinting effect was shown, where the P_{T2} was able to capture the guest molecule more strongly than the NIPs. This was attributed to the multiply noncovalent interactions and shape complementarity formed during the monomer-template complex formation, which allowed the formation of tailor-made cavities for the target substrate. The binding observed in the presence of NIPs was attributed to the nonspecific interactions between the side chains of the target peptide and randomly distributed functionalities on the backbone of the polymer.

The physical constants a and m are obtained directly from Eq.2.6. The polymers have the same heterogeneity index (m) which is in more heterogeneous ($m=0$) than homogeneous ($m=1$). The affinity constant (K) and total number of sites (N) were calculated with Eq. 2.7-2.8.

The total number of sites (N) P_{T2} ($N: 59 \pm 4$ ($\mu\text{mol/g}$)), is higher than that for the corresponding P_{NIP} ($N: 4.1 \pm 0.4$ ($\mu\text{mol/g}$)). The same occurs for the affinity constant (K) that is also higher for the MIPs in the measured concentration range ($K: 14 \pm 1$ ($\times 10^{-1}$ mM^{-1})), than in P_{NIP} ($K: 0.6 \pm 0.1$ ($\times 10^{-1}$ mM^{-1})). Thus it is demonstrated that the template displays a

very important role in the recognition creating well defined cavities that offer very high affinity to the peptide.

From the Freundlich isotherm affinity distribution analysis, it can be concluded that every MIP containing the template it was synthesized with the C-terminal is able to recognize that fragment better than another, demonstrating the imprinting effect for each polymer.

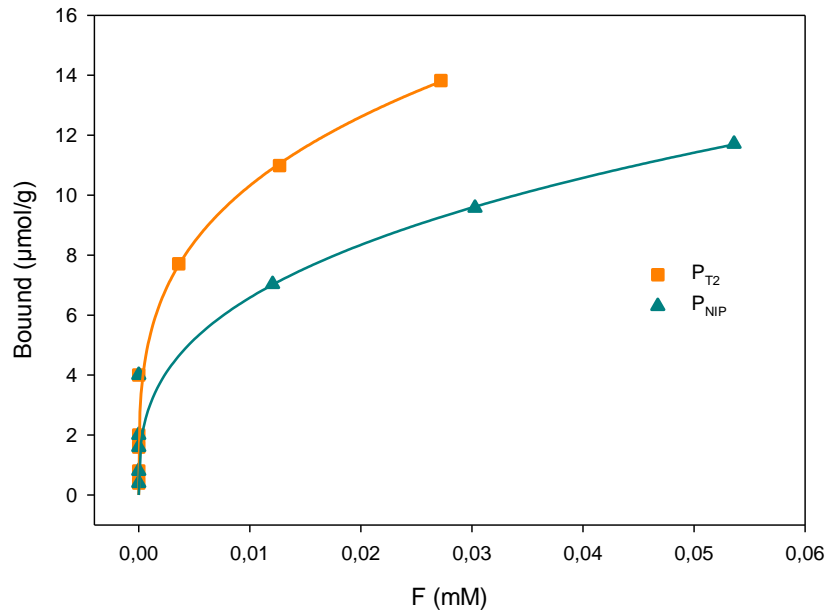


Figure 5.8: Freundlich fitting isotherm for P_{T2} and P_{NIP}. Each data represents the average of two replicate measurements with a coefficient of variation in the range of 0-0.3%.

Table 5.5: Freundlich fitting parameters, obtained with the experimental binding data of NLLGLIEAK towards the P_{T2} and P_{NIP}. Each data represents the average of two replicate measurements with a coefficient of variation in the range of 0-0.3%.

Isotherm model	Affinity constant, $K(\text{mM}^{-1}) \times 10^{-1}$	Total number of binding sites N ($\mu\text{mol/g}$)	Heterogeneity parameter, m	Binding capacity, a ($\mu\text{mol/g} (\text{mol}^{-1})^m$)	Regression coefficient, r^2
Freundlich P_{T2}	14 ± 1	59 ± 4	0.29 ± 0.03	39 ± 4	0.93
Freundlich P_{NIP}	0.6 ± 0.1	4.1 ± 0.4	0.34 ± 0.06	31 ± 5	0.91

5.5.4 MISPE and NISPE of a digested ProGRP sample

These polymers (P_{T2} and P_{NIP}) have been sent to Prof Reubsaet group (Department Of Pharmaceutical Chemistry School of Pharmacy, University of Oslo) to test real samples.

Rossetti et al [39] has been optimized MISPE protocol by using 3 x 0.5 mL of ACN/H₂O (7.5:92.5) to wash non-specific interaction and 0.5 mL of ACN/H₂O/FA (80:17:3) to elute the NLLGLIEA[K-¹³C₆¹⁵N₂]. As show in Figure 5.9 no the flow through from the sample application on P_{T2} or P_{NIP} . During the washing steps showed 52% elution of NLLGLIEA[K-¹³C₆¹⁵N₂] from the P_{T2} while around 82 % flowed through the P_{NIP} . In elution step more than 46% of the NLLGLIEA[K-¹³C₆¹⁵N₂] was recovered from the P_{T2} while around 17 % was recovered from the P_{NIP} .

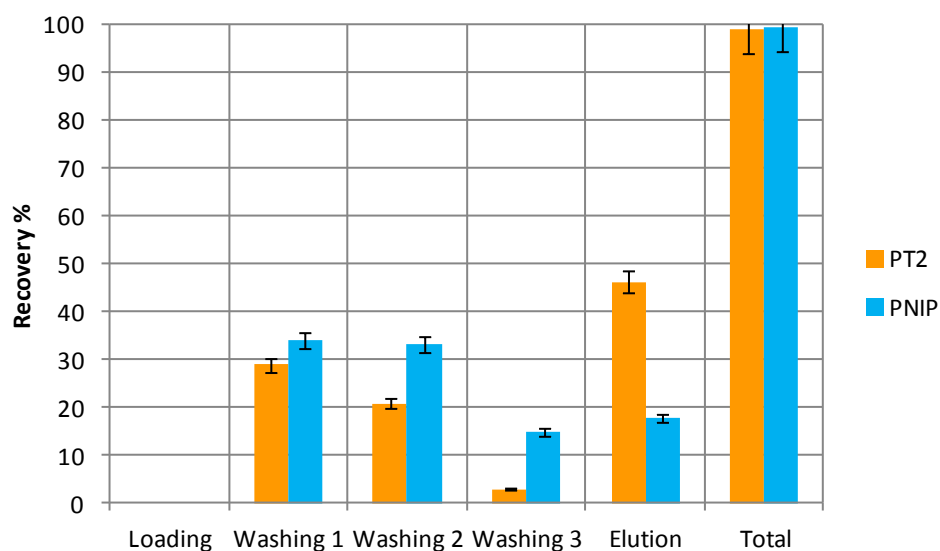


Figure 5.9: Recovery of NLLGLIEA[K-¹³C₆¹⁵N₂] in each fraction using P_{T2} and P_{NIP} , after percolation of 0.5 mL of 1 nM of NLLGLIEA[K-¹³C₆¹⁵N₂] (ABC buffer, 0.04M, pH 7.0), washing with 3x 0.5 mL of H₂O/ACN (92.5: 7.5) and elution with 0.5 mL of ACN/H₂O/FA (80:17:3). Columns represent two duplicated and the error bars show the standard deviation.

Finally this protocol was testing with digested ProGRP as shown in Figure 5.10 giving the same elution profile as the one achieved by Figure 5.9 and giving the same recovery around 56% from the P_{T2} while around 27 % was recovered from the P_{NIP} .

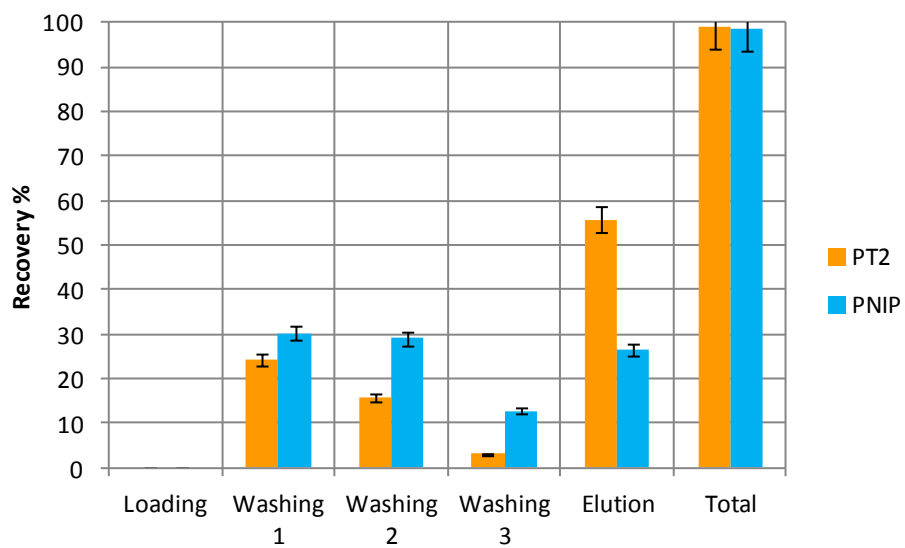


Figure 5.10: Recovery of digested of ProGRP in each fraction using P_{T2} and P_{NIP} , after percolation of 1.0 mL of 1 digestion buffer (ABC buffer, 0.04M, pH 7.0), washing with 3x 0.5 mL of H_2O/ACN (92.5: 7.5) and elution with 0.5 mL of $ACN/H_2O/FA$ (80:17:3). Columns represent two duplicated and the error bars show the standard deviation.

5.6 Experimental

5.6.1 Chemicals

The peptide H-NLLGLIEAK-NH₂ (T1), Z-NLLGLIEA-Nle-OH (T2), were purchased from Genscript (Piscataway, NJ, USA). The target nona-peptide NLLGLIEAK was synthesized in the group of Prof. Dr. Thomas Schrader (University Duisburg-Essen, Germany) with a purity above 95% on a microwave peptide synthesizer from CEM (Carolina, USA). Dry acetonitrile (ACN), methanol (MeOH), tetrahydrofuran (THF), ethanol (EtOH) and dimethylsulfoxide (DMSO) were purchased from Acros Organics (Geel, Belgium). Toluene (dry) was purchased from Fluka (Deisenhofen, Germany). Nitrogen (4.6) was purchased from Air Liquide (Düsseldorf, Germany). HPLC grade acetonitrile and methanol were purchased from Merck KGaA (Darmstadt, Germany), and HPLC water was purified using a Milli-Q system (Millipore, Bedford, MA). N-(2-aminoethyl) methacrylamide hydrochloride (EAMA) came from Polysciences, Inc. (Eppelheim, Germany). Trifluoroacetic acid (TFA), hydrochloric acid (HCl), (N-2-hydroxyethylpiperazine-N'-2-ethanesulfonic acid) buffer (HEPES) and divinylbenzene (DVB) were purchased from Sigma-Aldrich Chemical Co (Taufkirchen, Germany). All other reagents were used as received. The initiator 2, 2'-azobis (2, 4-dimethylvaleronitrile) (ABDV) was purchased from Wako Specialty Chemicals (Neuss, Germany) and used without further purification. All porogen were kept under nitrogen atmosphere over molecular sieves and were used without further purification.

For the RAFT immobilization macroporous beads (Si500) (30 nm average particle size) with a surface area (S_A) of 45 m²/g, an average pore diameter (D_p) of 0.81 nm and a pore volume (V_p) of 47.5 mL/g purchased from Fuji Silysia, Japan. The RAFT agent 4-cyanopentanoic acid dithiobenzoate (CPDB) was purchased from Stream Chemicals, Germany. 3-aminopropyltriethoxysilane (APTS), triethylamine (TEA), and ethyl chloroformate (ECF) come from Aldrich, (Steinheim, Germany).

Standard solution of NLLGLIEA[K-¹³C₆¹⁵N₂] AQUA Peptide with purity above 95% and was purchased from Sigma-Aldrich Chemical Co (Stockholm, Sweden) was diluted according to the Custom AQUA Peptides Storage and Handling Guidelines by Sigma-Aldrich and stored at -20°C. Ammonium bicarbonate (ABC), polyethylene glycols (PEG 20000) and formic acid (FA) were purchased from Sigma-Aldrich Chemical Co (Stockholm, Sweden)

5.6.2 Silica surface activation

In order to convert the surface siloxane bonds (Si-O-Si) generated during the calcinations step of the silica synthesis into silanol groups (Si-OH) which will then react with the 3-aminopropyltriethoxysilane (APTS). This was accomplished through treatment with hydrochloric acid (17% aq.sol), which converted the siloxane bonds into silanol groups according to Figure 5.11. Thus 300 mL of 17 % HCl were poured into a 500 mL three-necked round bottom flask, using a funnel. The round bottom flask was equipped with a condenser and an overhead stirrer. Silica rehydroxylation (20 g) was added in small portions while stirring.

The flask was placed in an oil-bath (electronic-thermometer; 150°C; heater: 200°C) and the suspension was subsequently refluxed for 24h. After cooling the silica was filtrated and washed with water (4 x 100 mL) and MeOH (6 x 100 mL). The silica was then dried in the vacuum oven at 80 °C for 3 h and at 150 °C overnight.

The amount of silanol groups per unit of surface can be considered as a physicochemical constant independent of the silica type, thus it was assumed that fully hydroxylated silica contains around 8 $\mu\text{mol}/\text{m}^2$ of silanol groups [40].

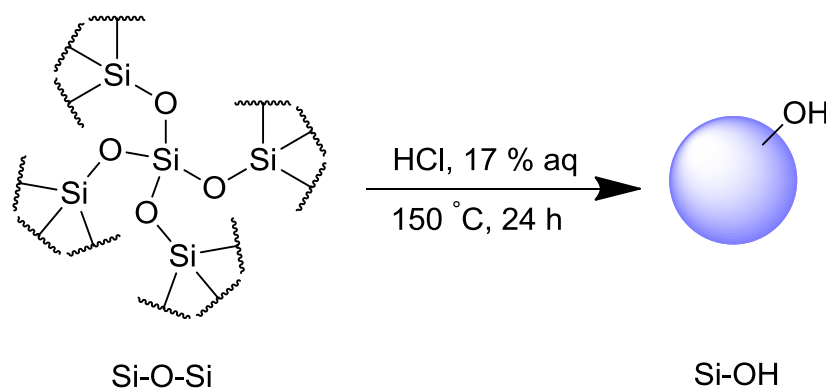


Figure 5.11:Rehydroxylation of siloxane groups.

5.6.3 Amino modified silica surface

Amino modified silica (Si-NH₂) is the solid support chosen for the coupling of RAFT agent. This modification can be achieved by using 3-aminopropyltriethoxysilane (APTS) as shown in Figure 5.12.

In 250 mL three-necked round-bottom flasks equipped with a condenser, an overhead stirrer and a dropping funnel, 20 g of previously rehydroxylised silica were suspended in 200 mL dry

toluene and the flask was connected to a N_2 stream. The whole system was flushed with N_2 . According to the number of silanol groups on the silica surface ($8 \mu\text{mol}/\text{m}^2$) the appropriate amounts of APTS (16.8 mmol, 3.73 g), were added to the mixture and refluxed overnight at 110°C . The products were filtered through glass funnels and washed with $2 \times 50 \text{ mL}$ of toluene and $2 \times 50 \text{ mL}$ of MeOH. The products were dried in a vacuum oven at 40°C for 24h. 6.1 g APTS modified silica have been obtained.

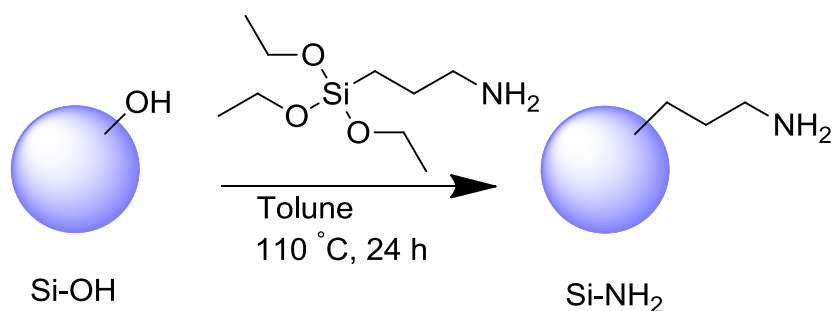


Figure 5.12: Functionalisation of silica surface with APTS.

5.6.4 Immobilization of RAFT agent

In a three-necked round bottom flask (250 mL), equipped with a dropping funnel, an overhead stirrer and an ethanol thermometer, 200 mL of dry THF was introduced, and the flask purged with nitrogen. 1.395g (4.99 mmol) of 4-cyanopentanoic acid dithiobenzoate, 543mg (5.00 mmol) ethylchloroformate and 506 mg (5.00 mmol) triethylamine were consecutively added. The mixture was then cooled at -78°C using a liquid-nitrogen-ethanol bath. After stirring for 30 min, a 25g of Si-NH_2 was added to the mixture and the suspension was stirred for 3h at -78°C and then for 4 h at -10°C . The product was then filtered, washed with THF and MeOH and dried under vacuum at room temperature. RAFT immobilization reaction is illustrated in Figure 5.13. The surface density of RAFT agent calculated based on % mass loss by TGA was $3.32 \mu\text{mol}/\text{m}^2$ [41].

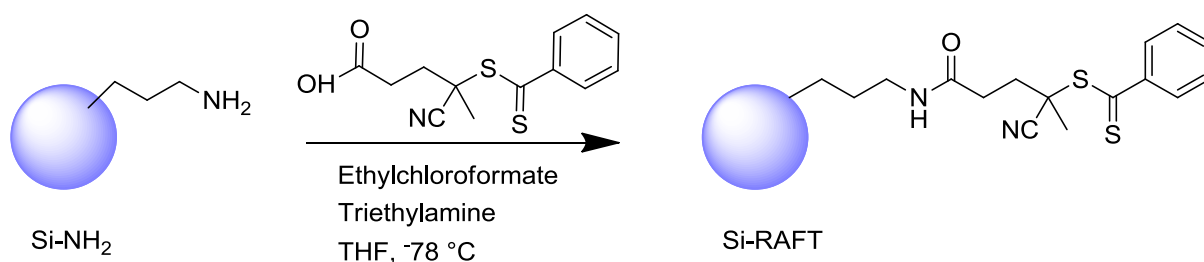


Figure 5.13: Immobilization of RAFT agent on silica surface.

5.6.5 Preparation procedure

Polymerizations were performed by incubating 1.0 g of Si-RAFT with the exact amount of monomers dissolved in 20 mL of dry solvent ACN/DMSO (80:20) the applied volume will coat the available surface with a polymeric film thickness of ca. 3 nm. Thus, prepolymerization solutions with the composition and the molar ratios showed in the Table 5.2 were used to generate the MIP-composite materials. The solution was transferred to a glass tube, cooled to $0\text{ }^\circ\text{C}$ and purged with N_2 three times by freez-thaw and finally added initiator ABDV (37 mg) with high vacuum system. The glass tube was then sealed and polymerization initiated thermally by placing the tube in incubator set at $50\text{ }^\circ\text{C}$. Polymerization was allowed to proceed at this temperature for 24 hour.

The template molecule was removed through the following sequential washing steps: MeOH (100 mL), MeOH/0.1M HCl (90:10) (100 mL) and finally MeOH (100 mL). A non-imprinted polymer was prepared in the same way, but in the absence of the template molecule. Figure 5.14 show a photograph of polymer before and after synthesis, and after washing.

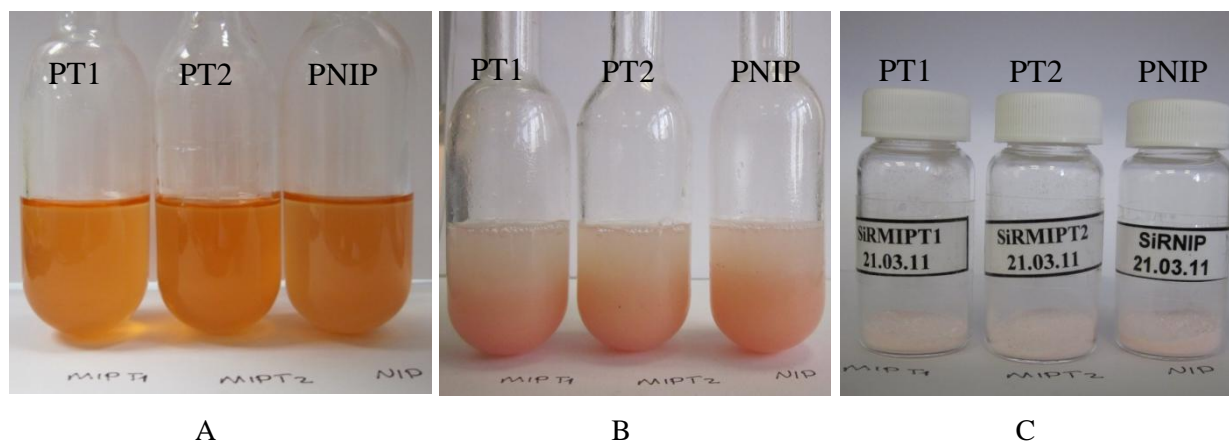


Figure 5.14: Photograph of RAFT polymer synthesis. Before polymerization (A), after polymerization (B), and after washing and drying (C).

5.6.6 Adsorption isotherms

The polymer particles (10mg) were mixed with 0.8 mL in ACN/HEPES (5:95) (0.1 M, pH 7.1) containing different amounts of NLLGLIEAK (0.005–0.2 mM) and the mixtures were incubated for 24 hour at room temperature. After incubation, the supernatant was collected and injected into the HPLC using the gradient program described in section 2.2.1. The amount of bound analyte to the polymer (B) was calculated by subtracting the nonbounded amount (F), from the initial NLLGLIEAK concentration in the mixture. The binding experiments were carried out by duplicate.

5.6.7 Optimization of MISPE Procedure

Solid-phase extraction cartridges, with a 1 mL volume, were packed with 20 mg of imprinted or the corresponding nonimprinted polymers. The cartridges were equilibrated with 5 mL of HEPES buffer (0.1 M, pH 7.1) and the sample containing the peptide, dissolved in HEPES buffer (0.1 M, pH 7.1) was percolated at a constant flow rate of 0.5 mL/min with the aid of a peristaltic pump. The cartridges were washed with 0.5 mL of different ratio of ACN (0-30%) in water to elude the none specifically retained compounds. Finally the peptides were eluted with 0.5 mL of a solution of MeOH/TFA (98:2). The eluates from the cartridges columns were diluted with 0.5 mL H₂O and directly injected into the HPLC system for analysis. The cartridges were reconditioned with 2 mL of MeOH and HEPES (0.1 M, pH 7.1) before a new application.

5.6.8 MISPE protocol for NLLGLIEA[K-¹³C₆¹⁵N₂]

After activation and condition steps with 1 mL of MeOH and 1 mL of ABC 50 mM, the MISPE and NISPE cartridges were loaded with 0.5 mL of standard solution with a concentration of 1nM. Each cartridge was subsequently washed with 3 x 0.5 mL of H₂O/ACN (92.5: 7.5). Elution was achieved by 0.5 mL of ACN/H₂O/FA (80:17:3). Before the LC-MS analysis dilution 1:10 with a solution of polyethylene glycols (PEG 20000) 0.001% acidified with 0.1% FA was performed

Bibliography

- [1] Wang.A and Zhu.S, *Polym Eng Sci*, vol. 45, pp. 720-727, 2005.
- [2] Chen.Y., Kele.M., Sajonz.P., Sellergren.B. and Guiochon.G, *Anal.Chem*, vol. 79, pp. 928-938, 1999.
- [3] Zimmerman.S.C. and Lemcoff.N.G, *Chem.Commun*, pp. 5-14, 2004.
- [4] Sulitzky.C., Rückert.B., Hall.A.J., Lanza.F., Unger.K. and Sellergren.B, *Macromolecules* , vol. 35, pp. 79-91, 2002.
- [5] Rückert.B., Hall.A.J. and Sellergren.B, *J.Mater.Chem*, vol. 12, pp. 2275-2280, 2002.
- [6] Kato.M., Kamigaito.M., Sawamoto.M. and Higashimura.T, *Macromolecules* , vol. 28, pp. 1721-1723, 1995.
- [7] Panasyuk.T.L., Mirsky.V.M., Piletsky.S.A. and Wolfbeis.O.S, *Anal.Chem*, vol. 71, pp. 4609-4613, 1999.
- [8] Gong.J., Gong.F., Zeng.G., Shen.G. and Yu.R, *Talanta*, vol. 61, pp. 447-453, 2003.
- [9] Schweitz.L, *Anal. Chem*, vol. 74, pp. 1192-1196, 2002.
- [10] Turiel.E. and Martin-Esteban.A, *Anal.Bioanal.Chem*, vol. 378, pp. 1876-1886, 2004.
- [11] Matyjaszewski.K, *Controlled Radical Polymerization*, Washington DC: American Chemical Society, 1997.
- [12] Chiefari.J., Chong.Y.K., Ercole.F., Krstina.J., Jeffery.J., Le.T.P.T., Mayadunne.R.T.A., Meijs.G.F., Moad.C.L., Moad.G., Rizzardo.E. and Thang.S, *Macromolecules*, vol. 31, pp. 5559-5562, 1998.
- [13] Halhalli.M., Aureliano.C., Schillinger.E., Sulitzky.C., Titirici.M. and Sellergren.B, *Polym.Chem*, vol. 3, pp. 1033-1042, 2012.
- [14] Halhalli.M., Aureliano.C., Schillinger.E. and Sellergren.B, *Chem.Mater*, vol. 24, pp. 2909-2919, 2012.
- [15] Li.Yong., Zhou.Wen-Hui., Yang.Huang-Hao. and Wang.Xiao-Ru, *Talanta*, vol. 79, pp. 141-145, 2009.
- [16] Lu.C.H., Zhou.W.H., Han.B., Yang.H.H., Chen.X. and Wang.X.R, *Anal.Chem*, vol. 79, pp. 5457-5461, 2007.
- [17] Moad.G., Rizzardo.E. and Thang.S.H, *Aust.J.Chem*, vol. 58, pp. 379-410, 2005.
- [18] Radhakrishnan.B., Ranjan.R. and Brittain.W.J, *Soft Matter*, vol. 2, pp. 386-396, 2006.
- [19] Tsujii.Y., Ejaz.M., Sato.K., Goto.A. and Fukuda.T, *Macromolecules*, vol. 34, no. 26, pp. 8872-8878, 2001.
- [20] Titirici.M.M. and Sellergren.B, *Chem.Mater*, vol. 18, no. 7, pp. 1773-1779, 2006.
- [21] Joso.R., Stenzel.M.H., Davis.T.P., Barner-Kowollik.C. and Barner.L, *Aust.J.Chem*, vol. 58, no. 6, pp. 468-471, 2005.
- [22] Nguyen.D.H. and Vana.P, *Polym.Adv.Technol*, vol. 17, no. 9-10, pp. 625-633, 2006.
- [23] Peng.Q., Lai.D., Kang.E. and Neoh.K, *Macromolecules*, vol. 39, no. 16, pp. 5577-5582, 2006.
- [24] Xu.F.J., Kang.E.T. and Neoh.K.G, *J.Mater.Chem*, vol. 16, no. 28, pp. 2948-2952, 2006.
- [25] Salem.N. and Shipp.D.A, *Polymer*, vol. 46, no. 19, pp. 8573-8581, 2005.

- [26] Sumerlin.B., Lowe.A., Stroud.P., Zhang.P., Urban.M. and McCormick.C, *Langmuir*, vol. 19, no. 14, pp. 5559-5562, 2003.
- [27] Duwez.A.S., Guillet.P., Colard.C., Gohy.J.F. and Fustin.C.A, *Macromolecules*, vol. 39, no. 8, pp. 2729-2731, 2006.
- [28] Pirri.G., Chiari.M., Damin.F. and Meo.A, *Anal.Chem*, vol. 78, no. 9, pp. 3118-3124, 2006.
- [29] Hong.C.Y., You.Y.Z. and Pan.C.Y, *Chem.Mater*, vol. 17, no. 9, pp. 2247-2254, 2005.
- [30] Xu.G.Y., Wu.W.T., Wang.Y.S., Pang.W.M., Zhu.Q.R., Wang.P.H. and You.Y.Z, *Polymer*, vol. 47, no. 16, pp. 5909-5918, 2006.
- [31] You.Y.Z., Hong.C.Y. and Pan.C.Y, *Nanotechnology*, vol. 17, no. 9, pp. 2350-2354, 2006.
- [32] Roy.D., Guthrie.J.T. and Perrier.S, *Aust.J.Chem*, vol. 59, no. 10, pp. 737-741.
- [33] Roy.D, *Aust.J.Chem*, vol. 59, no. 3, pp. 229-229, 2006.
- [34] Wang.Y.H., Kobayashi.T. and Fujii.N, *J.Chem.Tech.Biotech*, vol. 70, p. 355, 1997.
- [35] Yu.W.H., Kang.E.T. and Neoh.K.G, *Langmuir*, vol. 21, no. 1, pp. 450-456, 2005.
- [36] Yoshikawa.C., Goto.A., Tsujii.Y., Fukuda.T., Yamamoto.K. and Kishida.A, *Macromolecules*, vol. 38, no. 11, pp. 4604-4610, 2005.
- [37] Titirici.M.M., Hall.A.J. and Sellergren.B, *Chem.Mater*, vol. 15, pp. 822-824, 2003.
- [38] Titirici.M.M., Dissertation, Universität Dortmund, 2005.
- [39] Rossetti.C., Abdel-Qader.A., Sellergren.B. and Reubsaet.L, *submitted*, 2014.
- [40] Vansant.E.F., VanDerVoort.P. and Vrancken.K.C, "Chapter 4 - Quantification of the silanol number," in *Studies in Surface Science and Catalysis*, vol. 93, Elsevier, 1995, pp. 79-91 Volume 93.
- [41] Halhalli.M, Functional Porous Polymer Beads Nanostructured by Imprinting, Layer by Layer Grafting and Templated Synthesis, PhD thesis at Technische Universität Dortmund, 2012.

Chapter 6

Conclusions

In this work the development of new molecularly imprinted polymers (MIPs) for the selective extraction of NLLGLIEAK from the small cell lung cancer biomarker ProGRP is successfully achieved.

The analysis of compounds present at low levels is often not straight-forward. Especially the trace analysis of biomarker in the presence of far higher concentrations of pharmaceutically active compounds is a demanding task.

In chapter 3, traditional bulk polymerization was applied in order to produce three libraries of mini-MIPs, from which the best monomer, crosslinker and porogen were identified. By preparing mini-MIP libraries for the screening of various templates, monomers, crosslinkers and porogen, one of the essential parameters is the capacity for specific interactions between the functional monomers and templates. Not only does one need to choose the appropriate monomer type, the monomer to template ratio must also be optimized. A ratio too small will not create enough binding sites while a ratio too high may create nonspecific adsorption. In library 2 EAMA show promising results then was selected for further optimization. Another important consideration is the type and amount of crosslinker DVB showed to be a better crosslinker than other crosslinkers for the imprinting of the NLLGLIEAK. Furthermore, based on the specific binding ability of EAMA-DVB system, the third library was run to optimize DVB percentage, EAMA/template interaction in addition to porogen.

The goal was to find a polymer that, as stationary phase, would retain and resolve the NLLGLIEAK by specific binding sites.

From the results presented in this chapter, it could be concluded that T3-EAMA-DVB (P11) with molar ratio 0.04/4.74/24 is a promising polymer and could be scaled up and tested for analysis of ProGRP spiked sample.

Combinatorial approach provided an improved method over the conventional trial-and-error approach in developing selective MIPs. However the need of the evaluation by HPLC-UV for the binding studies, made the process was still time-consuming, especially when a lot of parameters were involved in the combinatorial library [1] [2].

The results presented in chapter 4 showed that the MIP is capable of strong binding to NLLGLIEAK under aqueous conditions. Various parameters affecting the extraction efficiency of the polymer have been evaluated to achieve the selective preconcentration of the NLLGLIEAK from aqueous samples and to reduce nonspecific interactions. The experimental binding data obtained for the polymers shows the total number of binding sites as well as the affinity constant are markedly higher for the imprinted polymer compared to the non-imprinted polymer. The binding capacity of MIP3 ($N_{\text{MIP}}: 14 \pm 1$ ($\mu\text{mol/g}$)), exceeded with more than 4 fold that of the NIP ($N_{\text{NIP}}: 3.2 \pm 0.5$ ($\mu\text{mol/g}$)). Likewise the weighted average affinity ($K_{\text{MIP}}: 29 \pm 2$ ($\times 10^{-1} \text{ mM}^{-1}$)), was nearly six-fold higher than that of the NIP ($K_{\text{NIP}}: 4.8 \pm 0.5$ ($\times 10^{-1} \text{ mM}^{-1}$)) in the measured concentration range.

The imprinted polymer was evaluated for use as a SPE sorbent, in tests with aqueous standards; by comparing recovery data obtained using the imprinted form of the polymer and a non-imprinted form (NIP). Extraction from the aqueous solutions resulted in more than 80 % recovery. A range of linearity for NLLGLIEAK between 1.5 and 50 mg/mL was obtained by loading 1 mL aqueous sample spiked with NLLGLIEAK at different concentrations in HEPES buffer of pH 7.0. The intra- and inter-day precision was below 7%. This investigation under the optimal conditions showed a specific recognition of NLLGLIEAK from the mixture of NLLGLIEAK and LSAPGSQR in human serum sample.

In chapter 5, a simple and effective method was developed to prepare silica surface-imprinted polymer with uniform morphology and controllable layer thickness by transfer the bulk composite to RAFT polymerization. Two series of polymers have been designed to circumvent the two main limits of MIPs, namely the insolubility of hydrophobic templates in the organic solvents (ACN) traditionally used during polymerization, and the non-selective binding that arises when the MIPs are applied to aqueous samples. It has been demonstrated that the templates play very important role for producing selective binding sites. Furthermore, by taking the advantage of RAFT method the RAFT polymers show some attractive characteristics, such as uniform morphology, higher binding capacity and the same film thickness required (3 nm). The scanning electron micrographs indicated absence of agglomeration. During the initial stage it has been necessary to carry out a preliminary SPE characterization of all the RAFT polymers to select the best MIPs for the further experiments. These experiments led to an understanding of the behavior of these stationary phases and allowed to find the media in which the imprinted receptors display their best specificity. PT2 turned out to display the highest selectivity and affinity of the phases tested and was thus selected for further tests. These results gave furthermore evidence that recognition of the

NLLGLIEAK is dependent on the structure of the template and it is due to the formation of specific imprinted binding sites against the NLLGLIEAK moiety of the molecule have shown a high selective retention. So PT2 have been selected as the best imprinted materials. These results give evidence that recognition of the NLLGLIEAK is dependent from the structure of the template and it is due to the formation of specific imprinted binding sites against the NLLGLIEAK moiety of the molecule.

Not surprisingly the values corresponding to the total number of binding sites as well as the affinity constant are higher for the imprinted polymer compared to the non-imprinted polymer. The binding capacity of P_{PT2} (N_{PT2} : 59 ± 4 ($\mu\text{mol/g}$)), exceeded with more than 12 fold that of the NIP (N_{NIP} : 4.1 ± 0.4 ($\mu\text{mol/g}$)). The same occurs for affinity constant (K) (K_{PT2} : 14 ± 1 ($\times 10^{-1} \text{ mM}^{-1}$)), was nearly 23 fold higher than that of the NIP (K_{NIP} : 0.6 ± 0.1 ($\times 10^{-1} \text{ mM}^{-1}$)) in the measured concentration range.

In the final experimental phase of this project, the suitability of the developed MIPs as SPE packing has been demonstrated. A SPE cartridge was packed with PT2 (and NIP, as control) and employed to accomplish the molecularly imprinted solid phase extraction (MISPE) of NLLGLIEAK from ProGRP digested samples. The MISPE protocol was first optimized in artificial sample where the MIP cartridge efficiently captured the NLLGLIEAK with a recovery of 45% (RSD= 5%, n=2), whilst on NIP was 18 % (RSD= 5%, n=2).

Based on these results, the MISPE protocol has been successfully used for in the analysis of the target peptide in digested ProGRP samples. The results showed the same recovery as previously obtained, which appears to be a really promising SPE sorbent.

The optimized MISPE was successfully used to develop an implemented a protocol offering enhanced target clean-up and enrichment. This promises to cut detection limits in real sample analysis and thereby to offer a new rugged diagnostic tool.

Such phases would fill a void in the proteomics sample pretreatment tool box by allowing peptide capture and release under conditions compatible with LCMS mobile phase media and hence on-line LCMS formats. Contrasting with immunobased methods, MIPs are furthermore robust and available for a fraction of the cost of biological receptors.

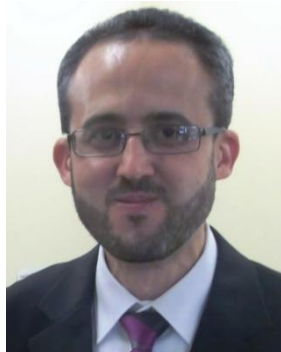
The obtained results may prove useful in: (i) Develop ELISA kit by using MIP as antibody in clinical application. (ii) Preparing biosensor to monitor NLLGLIEAK in routine clinical work. Obviously they are also useful for use of MIP as sorbent for SPE prior to MS or fluorescence based detection.

Further optimization of the MIP synthesis like nanoparticles, reversible addition-fragmentation chain transfers (RAFT) or printing ProGRP may improve the capacity of the MISPE column and consequently allow lower concentrations to be determined.

Bibliography

- [1] Takeuchi.T., Fukuma.D. and Matsui.J, *Anal Chem*, vol. 71, pp. 285-290, 1999.
- [2] Takeuchi.T., Fukuma.D., Matsui.J. and Mukawa.T, *Chem Lett*, vol. 1, pp. 530-531, 2001.

Curriculum Vitae



Personal information

Surname / First name	Abdel Qader, Abed
Address	Planetenfeldstr.45, 44149, Dortmund, Germany.
E-mail(s)	abed.abdelqader@hotmail.com
Nationality	Jordanian
Date and Place of birth	18 th February 1976, Benghazi-Libya
Social State	Married

Scientific experience

Dates	01/10/2008-18/06/2014
Occupation or position held	PhD position at the Institut für Umweltforschung (INFU), University of Dortmund under the supervision of Prof. Dr. Börje Sellergren with the topic: “Imprinted Polymers for Affinity based Extractions of a Peptidic Biomarker from Protein Digests”
Applied Techniques	Synthesis, characterization and evaluation of molecularly imprinted polymers, Silica templated polymerization, Hierarchical imprinting, Grafting techniques, Elemental analysis, FTIR spectroscopy, optical microscopy, SEM, TGA/DSC, Nitrogen Adsorption, HPLC, MISPE, Binding Studies.
Main activities and responsibilities	My duties consist in: carrying on experimental work in order to synthesize and characterize smart systems for selectively targeting of molecules of biological interest; writing periodic reports about my work in progress; attending meetings of review and conferences with oral or poster presentations; supervising the work of under graduated students; spending work-periods at partner-universities.
Dates	01/01/2005-31/12/2007
Occupation or position held	Researcher fellow at Environmental Chemistry and Ecotoxicology Department, Faculty of Biology Chemistry and Earth Sciences, University of Bayreuth, Germany
Applied Techniques	Application and Technical Services of Preparative Capillary Gas Chromatography (PCGC). Sampling and Analysis of Organic and Inorganic Pollutants in Water, Air, Soil and Biological Samples. Applications of Gas Chromatography with Different Detectors (GC/FID, GC/MS, and GC/ECD), two dimensional GC, Accelerator mass spectrometry (AMS), and Isotope measurement.
Main activities and responsibilities	I joined the “On-line Hyphenation of Gas Chromatography to Accelerator Mass Spectrometry AMS „ project, aimed to develop a method for the ¹² C/ ¹³ C/ ¹⁴ C–isotope ratio determination of organic environmental trace chemicals in the microgram range and to apply it to trichloroacetic acid (TCA) occurring in rain water and soil, in order to be able to differentiate between the natural and anthropogenic origin of such compounds. This is of importance in many other such cases, e.g. for various environmental halocarbons or nitrophenols. After enrichment, the TCA in the soil extracts was separated by two-dimensional preparative gas chromatography, pure TCA-OMe was collected;

	combusted to CO ₂ and the ¹² C/ ¹⁴ C isotope ratio was determined by AMS.
Dates	01/03/2003-30/09/2004
Occupation or position held	Researcher at Pharmaceutical Research Unit, Royal Scientific Society, Jordan
Main activities and responsibilities	The aim of my work was preparing biological samples and analysis by HPLC-UV. Optimisation HPLC method for different drugs.
Dates	Jan 2003 – Jun 2003
Occupation or position held	Teacher (chemistry), secondary school, Jordan.
Dates	Oct 1999- Jul 2002
Occupation or position held	M.Sc position at Chemistry Department, Faculty of Science, University of Jordan, Jordan under the supervision of Prof. Dr. Manar Fayyad and Dr. Abbas Al-Omari with the topic: “The Effect of Bromide ion on Trihalomethane Formation in King Abdullah Canal and Zai Drinking Water Treatment Plant”
Dates	Oct 2000 – Sep 2002
Occupation or position held	Teaching: General Chemistry, Analytical Chemistry, and Organic Chemistry Laboratories, Chemistry Department, University of Jordan.
Dates	Oct 1998 – Apr 1999
Occupation or position held	Research assistant in analytical laboratory (Oil Shale), Al al-Bayt University, Jordan.

Education and training

Dates	2002
Title of qualification awarded	Master Degree in Chemistry (M.Sc)
Name and type of organisation providing education and training	University of Jordan (Jordan)
Dates	1999
Title of qualification awarded	Bachelor of Chemistry (B.Sc)
Name and type of organisation providing education and training	Al al-Bayt University (Jordan)
Dates	1994
Title of qualification awarded	Certificate of Secondary School, June 1993
Name and type of organisation providing education and training	Ministry of Education, Jordan
Level in national or international classification	High School Diploma

Personal skills

Mother tongue(s)	Arabic
Other language (s)	English, excellent reading, writing and verbal German, basic reading, writing and verbal (level B1)

Technical skills and competences

Good capacity to organize and lead work-projects and to guide under-graduated students and colleagues of work; high ability in giving clear and satisfactory scientific and technical explanations concerning my work-projects or about subjects and issues of my competences.

Theoretical knowledge and practical experience in: Technology of Molecularly Imprinting Polymers; Synthesis of polymers; characterization of polymers: **UV VIS** and **FT-IR spectroscopies**, **¹H and ¹³C NMR**: Varian 300 Hz, 400 Hz and 500 Hz, **GC**: Shimadzu, **Automated Robot for Polymerisation**, Optical Microscopy, **DSC** (differential scanning calorimetry): Perkin Elmer, **HPLC**:

	Agilent. Experience in MALDI-TOFMS (matrix-assisted laser desorption ionization time-of-flight mass spectrometry), Thermal analysis (TGA and DSC), SEM (scanning electron microscope), TEM (transmission electron microscope). Ability to write technical reports and updates concerning any kind of work in progress.
Computer skills and competences	Microsoft Office Package, Paint ShopPro, Chem 3D, Autoflex II (Software for MALDI-TOF MS Equipment); Safire-TECAN (Software for UV Reader equip); Omnic (Software for IR instrument); Agilent (Software for HPLC).
Member	Member of the Royal Society of Chemistry, 2006-present. Member of Molecular Imprinting Polymer Society, 2009-present.
Manuscripts under preparations	Peptide imprinted receptors for the determination of the small cell lung cancer associated biomarker progastrin releasing peptide. Abed Abdel Qader, Javier Urraca, Silje Bøen Torsetnes, Finn Tønnesen, Léon Reubsæet, and Börje Sellergren (<i>submitted, 2014</i>). Grafted Peptide imprinted films, design and development for targeting NLLGLIEAK. Abed Abdel Qader, Rossetti.Cecilia, Léon Reubsæet, and Börje Sellergren (<i>Manuscript under preparation</i>). Molecular Imprinted Polymers as new tools in Small Cell Lung Cancer diagnosis. Cecilia Rossetti, Trine Halvorsen, Abed Abdel Qader , Börje Sellergren and Léon Reubsæet (<i>Manuscript under preparation</i>)
Publications	
2011	Mathematical Modeling of Trihalomethane. The Effect of Bromide ion on Trihalomethane Formation in Zai Drinking Water Treatment Plant. Abed Abdel Qader , Abbas Al-Omari, Manar Fayyad, ISBN 978-3-8443-8140-5 (Book Published by LAP Lambert Academic Publishing GmbH & Co. KG (www.lap-publishing.com)) July 2011. (https://www.lap-publishing.com/catalog/details/store/es/book/978-3-8443-8140-5/mathematical-modeling-of-trihalomethane?search=Abed)
2006	Mathematical modeling of the different trihalomethane species for Zai Water Treatment Plant. Abdel Qader, A, Abbas Al-Omari, and Manar Fayyad, <i>Dirasat</i> , 2006, 33, 103-114.
2006	Modeling of Trihalomethane formation in Jabal Amman Drinking Water Network Abed Abdel Qader , Abbass Al-Omari, and Manar Fayyad, <i>Dirasat, Pure Sciences</i> , 2006, Volume 33, No.1,
2004	Modeling trihalomethane formation for Jabal Amman water supply in Jordan. Al-Omari, A., Fayyad, M., Abdel Qader, A , <i>Journal of Environmental Modeling and Assessment</i> . 2004, 9, 245-252.
Conferences	
2013	Molecular Imprinted Polymers as new tools in Small Cell Lung Cancer diagnosis. Cecilia Rossetti, Trine Halvorsen, Abed Abdel Qader, Börje Sellergren, Léon Reubsæet. 39th International Symposium on High Performance Liquid Phase Separations and Related Techniques, HPLC2013, 16 th -20 th June 2013, The Netherlands.
	Molecular Imprinted Polymers as new tools in Small Cell Lung Cancer diagnosis. Cecilia Rossetti, Trine Halvorsen, Abed Abdel Qader, Börje Sellergren, Léon Reubsæet. Graduate Student Symposium on Molecular Imprinting, Queen's University, Belfast, 15 th -17 th August 2013, United Kingdom.
2012	MIPs for extracting peptidic disease biomarkers in blood and other matrices. Abdel Qadar A. ,

- Modry A., Halhalli M.R., Aureliano C.A., Urraca J., and Sellergren B. 7th International conference on Molecularly Imprinted Polymers-Science and technology, MIP2012 Paris, 27th-30th August 2012, France.
- A versatile method to prepare RAFT anchored thin film imprinted polymer micro and nanobeads.** Halhalli M.R., Mohammadi R, Urraca J, Kadirvel P., Dirkmann M, **Abdel Qader A.**, Fritz E., Sulc R., and Sellergren B. 7th International conference on Molecularly Imprinted Polymers-Science and technology, MIP2012 Paris, 27th-30th August 2012, France.
- 2011 **Imprinted polymers for affinity based extractions of biomarker and pathogenic peptides from blood serum.** **Abdel Qader A**, Urraca J,Aureliano C, Sellergren B, 4. Tag der Chemie, TU Dortmund, 4 February 2011.
- 2010 **Molecularly imprinted polymers for the analysis of biomarker and pathogenic peptides in blood plasma and other matrices.** J. L. Urraca, C. S. A. Aureliano, **A. Abdel Qader**, S. Shinde, E. Schillinger, B. Sellergren, *3rd EuCheMS Chemistry Congress 2010*, Nuremberg, Germany, 29 Aug-02 Sept.
- Imprinted blood plasma and other matrices.** J. L. Urraca, C. S. A. Aureliano, **A. Abdel Qader**, S. Shinde, E. Schillinger, B. Sellergren, MIP2010, New Orleans, USA, 09-12 Aug.
- Preparation of Small-Scale Molecularly Imprinted Polymers (Mini-MIPs) for recognition of the digest peptide product NLLGLIEAK from the SCLC biomarker ProGRP.** **Abdel Qader A**, Urraca J, Schillinger E, Sellergren B, 3. Tag der Chemie, TU Dortmund, 5 February 2010.
- Preparation of Small-Scale Molecularly Imprinted Polymers (Mini-MIPs) for recognition of the digest peptide product NLLGLIEAK from the SCLC biomarker ProGRP.** **Abdel Qader A**, Urraca J, Schillinger E, Sellergren B, 3. Tag der Chemie, TU Dortmund, 5 February 2010.
- 2009 **Imprinted polymers for recognition of the digest peptide product NLLGLIEAK from the SCLC biomarker ProGRP.** **Abdel Qader A** and Sellergren B. 2 Tag der Chemie, TU Dortmund, 5 February 2009.